Order Number 9315515

The uses and limitations of fractal geometry in digital terrain modelling

Xia, Zong-Guo, Ph.D.

City University of New York, 1993

U·M·I
300 N. Zeeb Rd.
Ann Arbor, MI 48106

THE USES AND LIMITATIONS OF FRACTAL GEOMETRY IN DIGITAL TERRAIN MODELLING

by

Zong-Guo Xia

A dissertation submitted to the Graduate Faculty in Earth and Environmental Sciences in partial fulfillment of the requirements for the degree of Doctor of Philosophy, The City University of New York.

1993

This manuscript has been read and accepted for the Graduate Faculty in Earth and Environmental Sciences in satisfaction of the dissertation requirement for the degree of Doctor of Philosophy.

1-27-93
Date

Keith C Clarke
Professor Keith C. Clarke
Chair of the Examining Committee

1/28/93
Date

Daniel Habib
Professor Daniel Habib
Executive Officer

Members of the Supervisory Committee

Professor Keith C. Clarke

Professor Somdev Bhattacharji

Professor David Mark

(Abstract)

THE USES AND LIMITATIONS OF FRACTAL GEOMETRY IN DIGITAL TERRAIN MODELLING

by

Zong-Guo Xia

Advisor: Professor Keith C. Clarke

In this study, fractal concepts and techniques are tested using nearly 200 DEMs produced by the USGS. The specific objectives include (1) an examination of statistical self-similarity of topographic data; (2) an evaluation of three most commonly used methods for estimating the fractal dimension of topographic surfaces; (3) a preliminary test of using fractal parameters to characterize various landforms and to delineate landform regions; and (4) an examination of the relationships between fractal parameters and geomorphic variables affecting landform characteristics.

The analysis of the computational results has led to the following conclusions: (1) the fractal model fits certain types of terrain surface better than others, and topography is only self-similar within quite limited scale ranges and in certain direction(s); (2) the fractal dimension of landforms varies within a wide range, the fractal dimension used to produce realistic-looking synthetic terrain (D = 2.2) only represents some special type of terrain surface, and a D value of 2.5 obtained by some early researchers is merely a result of artificial agglomeration of diversified terrain surfaces; (3) most DEMs from the mountain regions can be easily separated from those of plains or plateaus, and the fractal parameters of adjacent physiographic provinces are significantly different so that fractal segmentation of landform regions appears possible; (4) fractal parameters reflect well the effects of lithology, geological structure, and the stage of landform evolution on landform characteristics, but no clear relationship between fractal parameters and climate was identified possibly due to the relatively coarse resolu-

tion of the data; and (5) the variogram method is the most suitable method for estimating the fractal dimension of topographic profiles or surfaces, the box-counting method also produces reasonable results when careful consideration is given to the selection of the maximum cell size, the contour interval and the minimum r-squared value, and the walking dividers method can not be easily applied to self-affine fractals such as topographic profiles.

ACKNOWLEDGEMENTS

First of all, I wish to express my deep appreciation to my advisor, Professor Keith C. Clarke. He has not only acted as an extremely helpful advisor but also as a close friend. His tireless quest for new territories of scientific research has kept me in close touch with the frontiers of research in the geosciences, not only in the areas of fractal research, but also in the areas of analytical cartography and spatial information systems. I have truly enjoyed many stimulating discussions with him and benefited from them tremendously. He also taught me how to program in C and helped me debug computer programs on numerous occasions. I am particularly impressed by his always-ready-mode for helping his students. His hearty encouragement, kind understanding and generous support have been so critical to the successful completion of my academic program at the City University of New York.

I would also like to thank Professor David Mark in the Department of Geography at the State University of New York at Buffalo for serving on my supervisory committee. As one of the pioneers of fractal research in terrain modelling, he has given many insightful suggestions. Cordial thanks are also due to Professor Somdev Bhattacharji for his helpful advice on my dissertation research, my overall graduate program, my professional career and life in general. In addition, I wish to thank my office-mate, Reese Plews, whose friendship has made my stay in New York City a quite pleasant experience, and Anthony Grande and Thomas Walter for their constant support during my study and teaching at Hunter College.

Finally, I want to thank my wife, Li Song, for her kind understanding and thoughtful care and my son, Arthur Song Xia, for bringing some truly joyful chaos into my life and for providing enduring inspiration for continuing success in my professional career.

TABLE OF CONTENTS

LIST OF TABLES

LIST OF FIGURES

Chapter 1 INTRODUCTION

Lines, squares, circles, ellipses, triangles, planes, cubes, spheres, and cones are familiar shapes of classical geometry. They represent a powerful abstraction of the man-made world, and once inspired an influential philosophy of Platonic harmony. Euclid devised from them a geometry which has lasted two millennia. Artists found an ideal beauty in them, and Ptolemaic astronomers built a theory of the universe out of them.

For understanding the complexity of the natural world, however, these geometric objects turn out to be elements of an overly simplistic and inadequate model. A more accurate and precise description of natural shapes requires the concepts and techniques of fractal geometry.

Fractal geometry is a new branch of mathematics that specifically deals with the quantitative description, modelling and analysis of highly irregular and fragmented geometrical objects or spatial and temporal patterns of measurable features, processes and phenomena. Since such shapes are ubiquitous in the natural world, fractal geometry is commonly reputed to be the geometry of nature. It is undoubtedly one of the major developments of twentieth century mathematics. To many people, fractal geometry is "*a lingua franca for all of science*" and "*the greatest idea since calculus*" (see Krantz, 1989, p.13). Since the first book on fractals in English was published by Benoit B. Mandelbrot in 1977, this field of mathematics has blossomed tremendously during the past fifteen years. Most important of all, fractal geometry provided an indispensable mathematical language for the development of the theory of chaos, which is considered by some as one of the three greatest discoveries of twentieth century science, comparable to the theory of relativity and quantum mechanics (Gleick, 1987, p.6). For example, Gerd Binnig, winner of the Nobel Prize for Physics, stated,

> "*Research in chaos ------ the most interesting current area of research that there is. I am convinced that chaos research will bring about a*

> *revolution in the natural sciences similar to that produced by quantum mechanics*" (see Peitgen et al., 1992a, p.vii).

Fractal concepts, techniques, and applications have become central issues in most of the natural science disciplines, including physics (Shlesinger et al., 1984; Pietronero and Tosatti, 1986; Pynn and Skjeltorp, 1985; Stanley and Ostrowsky, 1986, 1989; Pynn and Riste, 1987; Pietronero, 1989; and Aharony and Feder, 1990), chemistry (Avnir, 1989), biology (West, 1990; and Rigaut, 1991), geology (Turcotte, 1989, 1992; Middleton, 1991; Barton and LaPointe, 1992; and Snow and Mayer, 1992), geophysics (Scholz and Mandelbrot, 1991), geography (Burrough, 1984, 1985, 1989; Buttenfield, 1985; Goodchild and Mark, 1987; Unwin, 1989; and Lam and DeCola, 1992), astronomy (Heck and Perdang, 1991), meteorology (Schertzer and Lovejoy, 1991), and materials science (Mandelbrot and Passoja, 1984; Laibowitz et al., 1985; Schaefer et al., 1986; Hurd et al., 1987; Weitz et al., 1988; and Kaufman et al., 1989). The wide and far-reaching significance of fractal geometry to the entire scientific community is perhaps no less than that of quantum theory to physicists, the theory of evolution to biologists, and the theory of plate tectonics to the earth scientists. Furthermore, fractals have stimulated strong interest from graphic designers and filmmakers because of their ability to create new and exciting shapes and artificial but seemingly realistic worlds (Peitgen and Richter, 1986; and Peitgen and Saupe, 1988). Today, as Unwin (1989, p.163) remarked, "*Wherever you look in both the sciences and the graphic arts the word 'fractal' seems to be all the rage ...*"

Fractal geometry has also made an irrefutable impact on orthodox mathematics. It has revived a long considered dead subject of geometry and caused a return of geometry in the frontiers of mathematics (Falconer, 1985, 1990; Devaney and Keen, 1989; Edgar, 1990; Cherbit, 1991a; and Wicks, 1991). Fractals currently dominate certain research areas in geometric topology and are coming into prominence in the study of Kleinian groups and hyperbolic geometry (Cannon, 1984, p.118). The computer rendering of fractals has caused the rebirth of experimental mathematics (Barnsley,

1989; Becker and Dorfler, 1989; Devaney, 1990; and Mandelbrot, 1992). In fact, the development of fractal geometry has been so rapid and its acceptance has been so widespread that they have caused great fear and insuppressible uneasiness among some orthodox mathematicians. For example, Krantz (1989, p.13) warned us that "*now there is a mathematical development that threatens to dwarf all others for its potential publicity value: the theory of fractals.*"

In addition, fractal geometry has helped reconnect pure mathematical research both with the natural sciences and with computing. Man has always been confronted with a world filled with seemingly complex, irregular shapes and random fluctuations. In the quest for understanding, mathematics and natural sciences have progressed by concentrating on the simplest of natural systems. In this process, mathematicians and scientists gradually moved away from the direct experience of nature and from each other. Over the centuries, we have reached a point at which some mathematicians can proudly declare to the world that they have never done nor would they ever do anything that scientists in other fields would care about and find use for (see Krantz, 1989). With the advent of fractal geometry, the quest for scientific understanding and the emphasis on the relevance of scientific research to the society have brought us back to the everyday natural world and significantly improved the communications between different fields of scientific inquiry.

Terrain features such as coastlines, topographic profiles, and surfaces were among the first natural geometrical shapes Mandelbrot (1967b, 1975c, 1977) used to develop his theory of fractal geometry. The realistic-looking simulations of mountains and lunar landscape produced by Mandelbrot (1977, 1983) and his co-worker, Richard Voss, and the successful rendering of fictional worlds by Fournier et al. (1982a) seem to suggest that the underlying fractal models have grasped some of the essential geometric elements of natural landforms. On the other hand, the lack of accurate characterization of geometric form of topography has long hampered our efforts in identifying spatial regularities of geomorphological features and modelling the processes that

have sculptured the earth's surface into diversified landforms. As a result, terrain scientists were among the first to adopt the fractal concepts and techniques in their work. A large number of studies have been carried out to test the validity of the fractal model in describing topographic features and to explore the possibility of using the concept of fractal dimension to characterize various types of landform. A general review of the applications of fractal geometry in terrain characterization and terrain simulation is given in Chapter 3.

Despite the unambiguous popularity of fractals among terrain scientists, many previous studies were plagued by procedural problems, resulting in a state of great confusion on the potential value of fractal geometry in the science of landforms. There is still a great deal to be learned. First of all, to what degree the fractal model is applicable to terrain features is still quite obscure. Different authors have expressed contrasting views on the validity of fractal concepts in describing landforms. Part of the reason is that many of the earlier conclusions were based on empirical testing with extremely limited terrain data. Furthermore, different algorithms have been used for estimating the fractal dimension of contour lines, topographic profiles, and terrain surfaces. These algorithms often produced significantly different results for the same data sets. Some methods have been obviously extended beyond their limits of applicability. Certain results were based on erroneous mathematical formulations. On the other hand, relatively few comparative studies have been carried out to systematically calibrate different algorithms and to uncover the physical significance of the model parameters. Thus, there is no reliable ground for choosing a particular method over others. All these problems related to the computational procedures greatly complicate the discussions on the applicability of fractal geometry to terrain features. In addition, relatively little research has been carried out to explore the wide range of geomorphological problems and the ways in which fractal concepts and techniques can be applied. Finally, how efficient fractal parameters are in characterizing landforms and in modelling geomorphological processes in comparison with traditional geomorphometric

parameters is yet to be evaluated. The present research was designed to address some of these issues.

The specific objectives of this study include (1) an examination of the validity of the fundamental assumption of statistical self-similarity of fractal geometry as applied to topographic data; (2) an evaluation of some of the most commonly used methods for estimating the fractal dimension of topographic surfaces; (3) the characterization of various landforms using fractal parameters and the exploration of the possibility of using fractal parameters as a basis for delineating physiographic regions; and (4) the study of the relationships between fractal parameters and the controlling factors of landform characteristics, such as rock type, prominence of geological structure, stage of fluvial erosion, and climate or type of geomorphological processes.

The results presented in the following chapters are based on the study of 191 Digital Elevation Models (DEMs) obtained from the U. S. Geological Survey (USGS). Figure 1.1 shows the geographic locations of these selected DEMs. The boundaries of physiographic provinces are adopted from Fenneman (1946). Table 1.1 lists the names of these DEMs and provides some other pertinent information. All DEMs are digital representation of the USGS 1:24,000 scale topographic maps and have a ground resolution of 30 meters. These DEMs were produced by one of the following four methods: (1) the Gestalt Photo Mapper II (GPM), a highly automated photogrammetric system designed to produce orthophotos, digital terrain data, and contours in subunits called patches; (2) manual profiling (MP) from photogrammetric stereomodels using stereoplotters equipped with three-axis electronic digital profile recording modules, by scanning stereomodels along successive terrain profiles; (3) interpolation of the elevations from stereomodel digitized contours, derived from stereoplotters equipped with three-axis digital recording modules used for compilation of 7.5-minute topographic quadrangle maps; and (4) interpolation from Digital Line Graph (DLG) hypsography and hydrography data, collected using scanners, manual digitizers, and automated line followers.

Figure 1.1 Geographic Locations of the DEMs Used in the Present Study. Dash lines are boundaries of major physiographic provinces of Fenneman (1946).

Table 1.1 DIGITAL ELEVATION MODELS SELECTED FOR FRACTAL ANALYSIS

NAME OF TOPO QUAD	PHYSIOGRAPHIC PROVINCE	DEM SIZE	RELIEF	GENERATION METHOD	QUALITY
Barbara, MS	Coastal Plain	390X390	94	MP	good
Barlow, KY-IL	Coastal Plain	361X361	174	DCAS	excellent
Coharie NW, NC	Coastal Plain	368X368	61	GPM	fair
Coharie SE, NC	Coastal Plain	368X368	58	GPM	fair
Coharie SW, NC	Coastal Plain	369X369	69	GPM	fair
Dobbersville, NC	Coastal Plain	367X367	60	GPM	fair
Falson, NC	Coastal Plain	368X368	65	GPM	fair
Grantham, NC	Coastal Plain	367X367	63	MP	good
Horn Lake SW, MS	Coastal Plain	369X369	433	MP	fair
Newton Grove North, NC	Coastal Plain	367X367	57	GPM	fair
Calahain, NC	Piedmont	375X375	134	GPM	good
Central, NC	Piedmont	376X376	321	GPM	excellent
Church Road, VA	Piedmont	358X358	74	GPM	good
Cleveland, NC	Piedmont	375X375	83	GPM	excellent
Cool Springs, NC	Piedmont	375X375	98	GPM	good
Harmony, NC	Piedmont	375X375	60	GPM	good
Shepherds, NC	Piedmont	377X377	103	GPM	good
Statesville East, NC	Piedmont	375X375	87	GPM	good
Statesville West, NC	Piedmont	376X376	122	GPM	good
Troutman, NC	Piedmont	377X377	83	GPM	excellent
Prentiss, NC	Blue Ridge	369X369	999	GPM	good
Shining Rock, NC	Blue Ridge	371X371	1225	GPM	excellent
Mt. Le Conte, TN	Blue Ridge	366X366	1604	GPM	excellent
Smokemont, NC	Blue Ridge	368X368	995	GPM	excellent
Aughwick, PA	Valley & Ridge	340X340	473	GPM	excellent
Baker, WV	Valley & Ridge	349X349	564	GPM	excellent
Blain, PA	Valley & Ridge	342X342	465	GPM	excellent
Blair Mills, PA	Valley & Ridge	341X341	487	GPM	excellent
Burem, TN	Valley & Ridge	365X365	273	GPM	excellent
Camelot, TN	Valley & Ridge	364X364	443	GPM	excellent
Duffield, VA	Valley & Ridge	364X364	574	GPM	excellent
Kyles Ford, VA	Valley & Ridge	364X364	442	GPM	excellent
Looneys Gap, TN	Valley & Ridge	364X364	387	GPM	excellent
McCoysville, PA	Valley & Ridge	341X341	525	GPM	excellent
Plum Grove, VA	Valley & Ridge	365X365	395	GPM	excellent
Rio, WV	Valley & Ridge	349X349	504	GPM	excellent
Stickleyville, VA	Valley & Ridge	364X364	613	GPM	excellent
Stony Point, TN	Valley & Ridge	366X366	346	GPM	excellent
Wardensville, WV	Valley & Ridge	348X348	588	GPM	excellent
Yellow Springs, WV	Valley & Ridge	348X348	417	GPM	excellent
Arena, NY	Appalachian Plateaus	343X343	707	GPM	excellent
Broad Bottom, KY	Appalachian Plateaus	361X361	1317	GPM	excellent
Cameron, PA	Appalachian Plateaus	334X334	437	GPM	excellent
Downsville, NY	Appalachian Plateaus	345X345	513	GPM	excellent
Emporium, PA	Appalachian Plateaus	333X333	412	GPM	good
Fayetteville, WV	Appalachian Plateaus	365X365	481	GPM	excellent
First Fork, PA	Appalachian Plateaus	334X334	475	GPM	good
Fishs Eddy, NY	Appalachian Plateaus	344X344	424	GPM	excellent
Fleischmanns, NY	Appalachian Plateaus	342X342	604	GPM	excellent
Hancock, NY	Appalachian Plateaus	344X344	365	GPM	excellent
Harold, KY	Appalachian Plateaus	360X360	335	GPM	good
Horton, NY	Appalachian Plateaus	345X345	433	GPM	excellent
Hunter, NY	Appalachian Plateaus	339X339	773	GPM	good
Keating Summit, PA	Appalachian Plateaus	333X333	351	GPM	good
Lancer, KY	Appalachian Plateaus	359X359	282	MP	excellent
Lee Fire Tower, PA	Appalachian Plateaus	335X335	468	GPM	good
Lewbeach, NY	Appalachian Plateaus	344X344	529	GPM	excellent
Lexington, NY	Appalachian Plateaus	341X341	786	GPM	excellent
Livingston Manor, NY	Appalachian Plateaus	344X344	407	GPM	excellent
Long Eddy, PA	Appalachian Plateaus	345X345	319	GPM	excellent
Margaretville, NY	Appalachian Plateaus	342X342	586	GPM	excellent
Marshlands, PA	Appalachian Plateaus	334X334	369	GPM	good
Martin, KY	Appalachian Plateaus	360X360	306	MP	excellent
Mc Dowell, KY	Appalachian Plateaus	360X360	449	GPM	excellent

Table 1.1 continued.

NAME OF TOPO QUAD	PHYSIOGRAPHIC PROVINCE	DEM SIZE	RELIEF	GENERATION METHOD	QUALITY
Pikeville, KY	Appalachian Plateaus	361X361	439	GPM	excellent
Prestonburg, KY	Appalachian Plateaus	359X359	259	MP	excellent
Roscoe, NY	Appalachian Plateaus	345X345	415	GPM	excellent
Seager, NY	Appalachian Plateaus	343X343	698	GPM	excellent
Thomas, KY	Appalachian Plateaus	360X360	308	GPM	excellent
Wayland, KY	Appalachian Plateaus	360X360	342	GMP	excellent
West Kill, NY	Appalachian Plateaus	341X341	683	GPM	excellent
Wharton, PA	Appalachian Plateaus	333X333	431	GPM	excellent
Whitwell, TN	Appalachian Plateaus	373X373	499	GPM	excellent
Chatham, NJ	New England	349X349	141	GPM	good
Hancock, MA	New England	333X333	544	GPM	excellent
Lyndonville SE, VT	New England	316X316	338	GPM	good
Pound Ridge, CT	New England	342X342	195	GPM	fair
Roselle, NJ	New England	349X349	175	GPM	fair
Mammoth Cave, KY	Interior Low Plateaus	365X365	169	MP	good
Park City, KY	Interior Low Plateaus	366X366	155	MP	good
Rhoda, KY	Interior Low Plateaus	366X366	157	MP	fair
Smiths Grove, KY	Interior Low Plateaus	366X366	131	MP	good
Williams, IN	Interior Low Plateaus	361X361	132	GPM	excellent
Bartlett, KS-MO	Central Lowland	360X360	61	MP	fair
Chetopa, KS-MO	Central Lowland	361X361	37	MP	fair
Harvey, IA	Central Lowland	349X349	66	MP	excellent
Labette, KS-MO	Central Lowland	360X360	46	MP	fair
Leighton, IA	Central Lowland	348X348	67	MP	good
Missouri Valley NW, NE	Central Lowland	332X332	110	MP	fair
Oswego, KS-MO	Central Lowland	360X360	49	MP	fair
Paxton NW, IL	Central Lowland	348X348	40	DCAS	excellent
Paxton SE (Gifford), IL	Central Lowland	348X348	42	DCAS	excellent
Paxton SW (Rantoul), IL	Central Lowland	348X348	38	DCAS	excellent
Pella, IA	Central Lowland	348X348	66	MP	excellent
Peoria, IA	Central Lowland	347X347	61	MP	good
Bar C Bar Ranch, NM	Great Plains	385X385	103	MP	fair
Derrick Draw, NM	Great Plains	385X385	82	MP	fair
Dexter East, NM	Great Plains	385X385	76	MP	fair
Double Mill Draw NE, TX	Great Plains	390X390	82	GPM	fair
Double Mill Draw NW, TX	Great Plains	389X389	76	GPM	fair
Double Mill Draw SE, TX	Great Plains	391X391	68	GPM	fair
Forks Ranch, MT	Great Plains	320X320	161	GPM	fair
Fort Hood, TX	Great Plains	392X392	135	MP	excellent
Holmes Ranch, MT	Great Plains	319X319	234	GPM	good
Hot Springs, SD	Great Plains	329X329	380	GPM	excellent
Indio Hill, TX	Great Plains	390X390	70	GPM	fair
North Fort Hood, TX	Great Plains	391X391	127	MP	good
North Loup Hord, NE	Great Plains	347X347	110	MP	good
Pine Butte School, MT	Great Plains	319X319	212	GPM	excellent
Post Oak Mountain, TX	Great Plains	392X392	141	MP	good
Shell Mountains, TX	Great Plains	392X392	153	MP	excellent
Bowen Mountain, CO	Southern Rocky Mtns.	350X350	1054	MP	excellent
Granby, CO	Southern Rocky Mtns.	350X350	562	MP	excellent
Grand Lake, CO	Southern Rocky Mtns.	350X350	1268	GPM	excellent
Isolation Peak, CO	Southern Rocky Mtns.	351X351	1331	MP	excellent
Mc Henrys Peak, CO	Southern Rocky Mtns.	350X350	1441	MP	excellent
Monarch Lake, CO	Southern Rocky Mtns.	352X352	1558	MP	excellent
Shadow Mountain, CO	Southern Rocky Mtns.	351X351	1207	MP	good
Strawberry Lake, CO	Southern Rocky Mtns.	351X351	829	GPM	excellent
Trail Mountain, CO	Southern Rocky Mtns.	350X350	793	GPM	excellent
Big Horn, WY	Middle Rocky Mountains	319X319	360	MP	good
Flaming Gorge, UT	Middle Rocky Mountains	344X344	514	CTOG	excellent
Pat O'Hara Mtn., WY	Middle Rocky Mountains	321X321	1431	MP	excellent
Atlanta West, ID	Northern Rocky Mtns.	325X325	1189	CTOG	excellent
Bata Mountain, MT	Northern Rocky Mtns.	304X304	941	MP	good
Belmont Point, MT	Northern Rocky Mtns.	302X302	785	GPM	excellent
Belmore Sloughs, MT	Northern Rocky Mtns.	300X300	1104	GPM	excellent
Cedar Lake, MT	Northern Rocky Mtns.	296X296	1132	GPM	excellent
Chief Mountain, MT	Northern Rocky Mtns.	290X290	1313	MP	good
Condon, MT	Northern Rocky Mtns.	299X299	1567	GPM	excellent

Table 1.1 continued.

NAME OF TOPO QUAD	PHYSIOGRAPHIC PROVINCE	DEM SIZE	RELIEF	GENERATION METHOD	QUALITY
Crimson Peak, MT	Northern Rocky Mtns.	302X302	1181	MP	excellent
Elevation Mountain, MT	Northern Rocky Mtns.	305X305	899	MP	good
Gold Creek Peak, MT	Northern Rocky Mtns.	301X301	840	MP	excellent
Gray Wolf Lake, MT	Northern Rocky Mtns.	299X299	1282	MP	excellent
Hemlock Lake, MT	Northern Rocky Mtns.	299X299	1328	GPM	excellent
Holland Peak, MT	Northern Rocky Mtns.	300X300	1359	GPM	excellent
Lake Inez, CO	Northern Rocky Mtns.	301X301	1222	MP	excellent
Lake Marshall, MT	Northern Rocky Mtns.	301X301	894	GPM	excellent
Morrell Lake, MT	Northern Rocky Mtns.	301X301	1220	GPM	good
Morrell Mountain, MT	Northern Rocky Mtns.	303X303	1071	GPM	excellent
Peck Lake, MT	Northern Rocky Mtns.	298X298	994	GPM	excellent
Porcupine Creek, MT	Northern Rocky Mtns.	296X296	969	GPM	excellent
Priest Lake NE, ID	Northern Rocky Mtns.	306X306	1236	MP	excellent
Salmon Lake, MT	Northern Rocky Mtns.	303X303	506	GPM	excellent
Seeley Lake East, MT	Northern Rocky Mtns.	302X302	961	GPM	excellent
Seeley Lake West, MT	Northern Rocky Mtns.	302X302	488	GPM	excellent
Upper Jocko Lake, MT	Northern Rocky Mtns.	301X301	954	GPM	excellent
Wapiti Lake, MT	Northern Rocky Mtns.	301X301	894	MP	excellent
Woodworth, MT	Northern Rocky Mtns.	304X304	520	GPM	excellent
Yew Creek, MT	Northern Rocky Mtns.	295X295	856	GPM	excellent
Wilcox, WA	Columbia Plateaus	315X315	218	MP	fair
Yakima East, WA	Columbia Plateaus	305X305	347	MP	excellent
Anvil Points, CO	Colorado Plateaus	344X344	1123	MP	excellent
Greasewood Canyon, CO	Colorado Plateaus	359X359	384	GPM	excellent
Moccasin Mesa, CO	Colorado Plateaus	358X358	643	MP	excellent
Moqui Canyon, CO	Colorado Plateaus	359X359	523	GPM	excellent
Wetherill Mesa, CO	Colorado Plateaus	359X359	601	MP	excellent
Zion National Park NE, UT	Colorado Plateaus	360X360	921	MP	excellent
Adel, OR	Basin and Range	329X329	716	MP	excellent
Buffalo Springs NW, NV	Basin and Range	351X351	1317	MP	excellent
Buffalo Springs SW, NV	Basin and Range	352X352	917	MP	excellent
Cain Mountain NE, NV	Basin and Range	352X352	942	MP	excellent
Cain Mountain NW, NV	Basin and Range	351X351	696	MP	excellent
Cain Mountain SE, NV	Basin and Range	352X352	1262	MP	excellent
Cain Mountain SW, NV	Basin and Range	352X352	438	MP	excellent
Calderwood Resevoir, OR	Basin and Range	329X329	347	MP	excellent
Coleman Lake, OR	Basin and Range	331X331	481	MP	excellent
Collins Rim, OR	Basin and Range	330X330	651	MP	excellent
Cortez NE, NV	Basin and Range	353X353	4419	DCAS	excellent
Cortez NW, NV	Basin and Range	353X353	1953	DCAS	excellent
Cortez SE, NV	Basin and Range	353X353	2601	DCAS	excellent
Cortez SW, NV	Basin and Range	353X353	3038	DCAS	excellent
Crump Lake, OR	Basin and Range	329X329	441	MP	excellent
Drake Peak, OR	Basin and Range	328X328	882	MP	excellent
Fencemaker NE, NV	Basin and Range	351X351	776	MP	excellent
Fencemaker SE, NV	Basin and Range	351X351	1265	MP	excellent
Glamis SE, CA	Basin and Range	382X382	113	MP	fair
Kyle Hot Springs NE, NV	Basin and Range	349X349	935	MP	excellent
Kyle Hot Springs SE, NV	Basin and Range	350X350	1221	MP	excellent
May Lake, OR	Basin and Range	330X330	526	MP	good
Mt. Moses NW, NV	Basin and Range	352X352	124	MP	excellent
Mt. Moses SW, NV	Basin and Range	353X353	983	MP	excellent
Mt. Tobin NE, NV	Basin and Range	350X350	1432	MP	excellent
Mt. Tobin NW, NV	Basin and Range	350X350	818	MP	excellent
Mt. Tobin SW, NV	Basin and Range	350X350	970	MP	excellent
Priday Resevoir, OR	Basin and Range	329X329	742	MP	excellent
Sage Hen Butte, OR	Basin and Range	330X330	417	MP	excellent
Mt. Langley, CA	Cascade-Sierra Mountains	368X368	2770	MP	excellent
Mount Tom, CA	Cascade-Sierra Mountains	361X361	2009	MP	excellent
Yosemite NW, CA	Cascade-Sierra Mountains	355X355	1725	MP	excellent
Pacifico Mountain, CA	Pacific Border	378X378	1195	GPM	excellent

*** excellent ------ without any obvious error
good ------ with only minor identifiable error
fair ------ with major error but deemed usable
poor ------ with serious error and excluded from fractal analysis (not included in this table)

Chapter 2 THE HISTORY OF FRACTAL GEOMETRY

2.1 Introduction

Although fractal geometry as a systematic subject dates from 1975 when the first book on fractals, **"Les Objets Fractals: Forme, Hasard et Dimension,"** was published by Benoit B. Mandelbrot, many of its tools and concepts and a number of geometric shapes now recognized as fractals have been known for a long time. Fractal geometry was born belatedly as a result of the crisis in mathematics that was begun in 1875 when Paul DuBois Reymond first reported on a continuous nondifferentiable function constructed by Karl Weierstrass in 1861, a crisis which lasted approximately to 1925 (see Hahn, 1956, p.1959; and Mandelbrot, 1983, p.4). This chapter traces the development of fractal geometry from unorthodox construction of "pathological" mathematical structures to a full-fledged subject and highlights some of the major events in the history of fractal geometry.

This chapter is largely based on a collection of historical notes written by Mandelbrot and others, which are scattered in the fractal literature. A systematic study of the history of fractal geometry gives one a proper perspective on the evolution of fractal ideas, on the direct relevance of fractal concepts and techniques to the subjects of other scientific disciplines, and on the reason for the immense success of this newly emerged branch of mathematics. It also provides an overview of fractal applications in various fields and helps identify a collection of important references on fractals. Mandelbrot (see Peitgen et al., 1991, p.xi) reported that some people thought that fractal geometry must have been around almost forever, like counting, and he must have lived long ago. This recount of fractal history can certainly serve as a reminder of its extremely recent origin.

The development of fractal geometry can be roughly divided into three different stages: (1) fractal ideas before Mandelbrot, (2) the stage of systematic development

and organization of fractal concepts, models and techniques, and (3) the stage of proliferative applications. Mandelbrot (1983) provided the biographical sketches of some precursors of fractal ideas. Later, in a forward he wrote for the book **"The Science of Fractal Images"** edited by Heinz-Otto Peitgen and Dietmar Saupe, Mandelbrot (1988a) described the early contributions by Henri Poincare, R. Robert Fricke, Felix Klein, and Maurits C. Escher. Jones (1991) has also given a detailed account of some of the most important discoveries made before Mandelbrot. The development during the second stage is well documented in Albers and Alexanderson (1985), which was based on an interview with Mandelbrot by Anthony Barcellos, and Mandelbrot (1988a, 1991).

2.2 The First Stage: Fractal Ideas before Mandelbrot

The first stage of fractal history involved the construction of highly irregular shapes by mathematicians such as Georg Cantor (1883), Giuseppe Peano (1890), David Hilbert (1891), Eliakim Hastings Moore (1900), Henri Leon Lebesgue (1903), William F. Osgood (1903), Helge von Koch (1904), Ernesto Cesaro (1905), and Waclaw Sierpinski (1915, 1916), which were meant to defy the behavioral precepts of classic Euclidean geometry. Some of their famous creations include the Cantor dust, the Peano curve, and the Koch curve, which were later transformed into innovative mathematical models of objects, phenomena, and processes of the real world (Mandelbrot, 1983). Traditional mathematicians regarded these unorthodox creations as "psychotic" and "pathological" and described them as a "gallery of monsters", kin to the cubist painting and atonal music that were upsetting the established standards of taste in the world of arts at about the same time. Many mathematicians refused to deal with these highly irregular shapes at all. Even the great analyst Charles Hermite once wrote to Thomas Stieltjes of "*turning away in fear and horror from this lamentable plague of functions with no derivatives*" (Hermite and Stieltjes, 1905, vol. II, p.318). On the other hand, the mathematicians who created the "monsters" regarded them as important in demon-

strating that the world of pure mathematics contained a richness of possibilities going far beyond the simple structures that they saw in nature. In many ways, twentieth-century mathematics flowered in the belief that it had transcended completely the limitations imposed by its natural origins. However, as Freeman Dyson (1978, p.678) commented,

> "*now, ..., we see that nature has played a joke on the mathematicians. The 19th-century mathematicians may have been lacking in imagination, but nature was not. The same pathological structures that the mathematicians invented to break loose from 19th-century naturalism turn out to be inherent in familiar objects all around us in nature.*"

Having once discovered these "monsters" and congratulated themselves on a "creativity superior to nature," the mathematicians could imagine no use for, or interest in, these creations by natural scientists and soon banished these "pathological beasts" to a mathematical zoo. Nevertheless, a few mavericks continued their efforts in taming these classical monsters and constructing other highly irregular curves (for example, Pepper, 1928; and Kline, 1945). Most importantly, Felix Hausdorff (1919) and Abram Samoilovitch Besicovitch (1929, 1934a, 1934b, 1934c, 1937, 1968) proposed a new type of dimensioning in which a curve could have a fractional dimension, not just an integer one. Recursive techniques and iterated expressions were also discovered that could describe curves that have fractional dimensions. However, lacking the tools of modern computers to help visualize these strange and often complex functions, identify their relevance to the real world problems, and stimulate the thinking of most imaginative mathematical minds, not much progress was made in studying these mathematical structures.

2.3 The Second Stage: Systematic Organization of Concepts and Techniques

The second stage was begun in the early 1950s. This was the stage of systematic organization of fractal concepts, models and techniques, and of gradual development of its theoretical foundations. It involved essentially the work of one man, Benoit B. Mandelbrot, a Polish-born French mathematician, now working at the IBM Thomas J.

Watson Research Center located in Yorktown Heights, New York. According to Mandelbrot (1991, p.4; also see Albers and Alexanderson, 1985, p.212), his lifetime involvement in fractal research was triggered in 1951 by accident. One day, he went for a chat with his uncle (Szolem Mandelbrojt, a prominent professional mathematician, the successor of Hadamard and a colleague of Lebesgue). When he was about to leave, his uncle retrieved a book review by Joseph L. Walsh (1949), a Harvard mathematics professor and the former president of the American Mathematical Society from the wastebasket for him as a light reading on the Paris subway. The book review was on the empirical regularity of word frequencies recognized by George Kingsley Zipf (1949), a statistical human ecologist and a Lecturer at Harvard for twenty years. The remarkable finding is that in any reasonably sized sample of an individual's writing the product of the frequency (f) of any word and its rank (r) in terms of frequency is always approximately constant. In other words, the relation between r and f takes the form

$$f \propto 1/r.$$

This relation was established by analyzing numerous samples in different languages and by studying English writings of diversified styles. Quite possibly, it was the final comment by Walsh which stimulated the ambition of the young and energetic Mandelbrot. After enumerating many unsolved problems suggested by Zipf's work, Walsh (1949, p.58) commented, "*Opportunity is ripe for new Tycho Brahes, Keplers and Newtons!*" As he recalled years later (see Albers and Alexanderson, 1985, p.212), Mandelbrot felt at the time that to explain Zipf's law could be "*a golden opportunity of becoming the Kepler of mathematical linguistics.*" Mandelbrot (1991) remembers that when he was 20 years old, he told anyone who would listen that his ambition was to find a corner of science, not necessarily very extensive or even significant, of which he would know enough to be its Kepler or even its Newton. After reading Walsh's book review, he made the task of explaining Zipf's law his dissertation research at the

University of Paris, which he defended in December, 1952.

According to Mandelbrot (see Albers and Alexanderson, 1985, p.212), during the several years before and after he obtained his Ph. D. degree, he also developed an immense respect for the work of Norbert Wiener and John von Neumann. Having read Wiener's book **"Cybernetics"** and von Neumann and Morgenstern's **"Theory of Games and Economic Behavior,"** he felt that they were very precisely what he would emulate one day, a goal he accomplished about twenty years later. What impressed Mandelbrot was that "*each seemed to be a bold attempt to put together and develop a mathematical approach to a set of very old and very concrete problems that overlapped several disciplines*" (see Albers and Alexanderson, 1985, p.212). Whether such an evaluation was exactly what Mandelbrot had in mind at the time will probably never be known, which seems trivial in any event. Nevertheless, this statement describes precisely his own approach in developing the geometry of fractals.

With his knowledge on Zipf's law of linguistics, Mandelbrot became sensitive to analogous empirical regularities in diverse fields, beginning with economics. While reading Zipf's works, he became acquainted with Pareto's law of income distribution (Mandelbrot, 1960, 1961, 1962, 1963a). Later, when he was invited by Hendrik Houthakker, a Harvard economics professor, to give a talk, he saw on Professor Houthakker's blackboard a diagram similar to what he had encountered in the study of incomes (Albers and Alexanderson, 1985, p.214). On the ground that such geometric similarity was bound to be the visible symptom of an underlying similarity of structure, he inquired about the problem that had led to the diagram in question. He was told that it referred to the variation of eight years of cotton prices. He became fascinated with this subject and carried Houthakker's cotton data in a box of computer cards back to the IBM research center. He also sent to the Department of Agriculture in Washington, D. C., for more, dating back to 1900.

Economists generally assumed that the price changes of a commodity like cotton followed two different patterns at different time scales. On the one hand, the short term fluctuations would come randomly. On the other hand, the long term price changes would be driven steadily by deep macroeconomic forces such as the rise and fall of the New England textile industry, the opening of international trade routes, and the trends of war or economic recession, forces that should give way to understanding. However, this dichotomy had no place in the picture of reality that Mandelbrot was uncovering. Instead of separating short term changes from long term changes, he bound them together and identified a perfect symmetry of price changes across different time scales. He found that each particular price change was random and unpredictable. However, the sequence of changes was independent of scales: curves for daily price changes and monthly price changes matched extremely well. In fact, the degree of variation had remained constant over a tumultuous sixty-year period that saw two World Wars and the Great Depression. He soon came to distinguish two syndromes in price variation, sudden jumps and non-periodic "cycles", which he later denoted by the expressions "Noah and Joseph Effects". He showed that the stochastic process obtained via self-similarity could generate sample functions that were very rich in configurations and capable of accounting for a great part of observed price variation (Mandelbrot, 1963b, 1963c, 1966, 1967a).

Thereafter, he came upon a practical problem of intense concern to his corporate patron. Engineers were perplexed by the problem of noise in telephone lines used to transmit information from computer to computer. Electric current carries the information in discrete packets, and engineers knew that the stronger they made the current the better it would be at drowning out noise. But they discovered that some spontaneous noise could never be eliminated. Once in a while it would wipe out a piece of signal, creating an error. By talking to the engineers, Mandelbrot learned that the transmission noise comes in clusters and that the more closely you look at the clusters, the more complicated the patterns of errors become. He then argued that you could never find a

time during which errors were scattered continuously. Within any burst of errors, no matter how short, there would always be periods of completely error-free transmission. Furthermore, he discovered a consistent geometric relationship between the bursts of errors and the spaces of clean transmission. On scales of an hour or a second, the proportion of error-free periods to error-ridden periods remained constant. On the basis of these observations, he saw clearly the relevance of one of the mathematical monsters to the problem at hand. He used random forms of the Cantor set as a first approximation to represent these self-similar error patterns and adopted the concept of Hausdorff-Besicovitch dimension in their description (Berger and Mandelbrot, 1963; and Mandelbrot, 1965a). Mandelbrot became aware of the notion of Hausdorff-Besicovitch dimension through a friend he made while he was a research fellow at the Institute for Advanced Study in Princeton in 1953-1954, Henry McKean, Jr., who was writing his thesis on the Hausdorff-Besicovitch dimension of certain probabilistic sets at the time.

Mandelbrot's description had practical implications for scientists trying to decide between different strategies of controlling error. In particular, it meant that, instead of trying to increase signal strength to drown out more and more noise, engineers should settle for a modest signal, accept the inevitability of errors and use a strategy of redundancy to catch and correct them. Mandelbrot' work also changed the way IBM's engineers thought about the cause of noise and made them realize that the noise would never be explained on the basis of specific local events.

Upon seeing the facts about turbulence at a seminar Robert Stewart gave at Harvard in the fall of 1963, Mandelbrot found it obvious that his methods could be translated wholesale into these new terms (see Albers and Alexanderson, 1985, p.218). Then, he tried to explain the validity of the translation, which led him to conjecture that turbulence represented a singularity in the flow of fluids, and that this singularity was concentrated on a fractal (Mandelbrot, 1974, 1975a). However, this was an entirely new approach to the problem at the time. For many years it was viewed as

exotic and even bizarre, and it took ten years for the results of his study to be published other than in abstracts or via allusions.

Although by then Mandelbrot was convinced that he had identified a fundamental structure of nature, his message was not getting through well enough to satisfy his ambition. While encountering unvarying resistance to his increasingly unified approach and in particular to his use of Hausdorff dimension as a concrete notion, he wished and set out to search for a simpler illustration. He stumbled upon coastlines, introduced another monster curve, the Koch snowflake curve, as a crude model, and proposed that the irregularity of a coastline could be measured by its Hausdorff dimension (Mandelbrot, 1967b). Mandelbrot's analysis of the coastline problem further heightened his confidence in his gradually emerging new geometry and acted as a turning point in his thinking since this was the first application of his geometry in describing familiar features found in nature. He wrote: "*Thus, the so far esoteric concept of 'random figure of fractional dimension' is shown to have simple and concrete applications and great usefulness*" (Mandelbrot, 1967b, p.636). Since then, he went on practicing his geometry in a very strong and intense fashion and made great effort to bring geometry and the study of nature back together.

While at Harvard, through Professor Harold A. Thomas, Jr., Mandelbrot also became aware of the work of Harold Edwin Hurst (1951, 1955) on the fluctuations in the yearly discharge and flood level of the Nile River. The purpose of Hurst's studies was to determine the size of reservoirs required in the Great Lakes of the Nile Basin for meeting water shortages that might occur during a century. He examined long-period records of natural events, including river discharges, rainfall, temperature, annual growth rings of trees, and annual deposits of clay in lakes in search for an answer. In analysing his data, he devised a statistic R, which is the range from maximum to minimum of the curve obtained by sequentially plotting the cumulative totals of the departures from the mean of the annual discharges over a certain period. This range is the storage required to maintain the mean discharge over the period. He

examined the dependence of R upon the number of years of observation (N). For reasons of convenience, he divided R by the standard deviation of observations (S) and plotted log (R/S) against log (N). His results show that log (R/S) is a linear function of log (N) and can be expressed as

$$\log (R/S) = K \log (N / 2)$$

where K is the slope of the line of best fit. The values of K for different phenomena vary from 0.46 to 0.96, with a mean value of 0.729. This means that R/S increases more rapidly with N in the case of natural phenomena than in the case of chance events for which K = 1/2. This relationship has been variously referred to as the "Hurst law", the "Hurst effect", or the "Hurst phenomenon" (Klemes, 1974; Potter, 1976; Mandelbrot, 1983; and Kirkby, 1987). On the basis of similar descriptions in the stories of Noah and Joseph of the Bible, Mandelbrot and Wallis (1968) coined the terms "Noah Effect" and "Joseph Effect" to designate the two facets of Hurst's observation. The Noah Effect refers to the fact that extreme precipitation can be very extreme indeed. The Joseph Effect designates the finding that a long period of unusual (high or low) precipitation can be extremely long.

Hurst's discovery posed a serious challenge to the conventional approaches in hydrological modelling. Traditional models of hydrology assume precipitation to be random and Gaussian with successive years' precipitations either mutually independent or with a short memory. "Independence" implies in particular that a large precipitation in one year has no "aftereffect" on the following years; "short memory" means that all aftereffects die out within a few years. "*We are, then, in one of those situations, so salutary to theoreticians, in which empirical discoveries stubbornly refuse to accord with theory*" (Lloyd, 1967). As such, the Hurst phenomenon has attracted much attention from hydrologists during the past forty years (Klemes, 1974; Potter, 1975, 1976; and Kirkby, 1987). "*To some it has become a puzzle to be explained, to others a feature to be reproduced by their models, and to others still, a ghost to be conjured*

away" (Klemes, 1974).

Challenged by Harold A. Thomas, Jr. to account for the Hurst phenomenon, Mandelbrot (1965b) conjectured that it was a symptom of scaling. A few years later, Mandelbrot and Wallis (1968, 1969a, 1969b, 1969c) published a series of papers to test the validity of Hurst's law and to introduce a family of self-similar models. Through extensive computer simulations on the sample behavior of fractional Brownian motions and of fractional Gaussian noise and analyses of large collection of hydrological and other geophysical records, they showed that the rescaled range R/S was a very robust statistic for testing the presence of noncyclic long run statistical dependence in records and, in cases where such dependence is present, for estimating its intensity. They also demonstrated that the self-similar models adequately account for the Noah and Joseph effects.

Mandelbrot's inquiry into the highly irregular also extends to the fractal treatment of galaxy clustering. He has shown that both the theories of the formation of stars and galaxies and the empirical data can be interpreted in terms of a scaling Cantor-like fractal dust. He argued that the distribution of galaxies and of stars includes a zone of self-similarity in which the fractal dimension satisfies $0 < D < 3$ and developed a random walk model and a trema model to mimic the distribution of mass in the Universe. His early results were summaried in a paper finished in 1971, which was submitted to several periodicals but repeatedly rejected. The results of his research were first published as part of his book on fractals in 1975.

By the middle 1970s, fractal geometry had gradually grown into maturity. In 1973, on a sabbatical leave in Paris, Mandelbrot was asked to lecture at the College de France. He considered this a golden opportunity to present a general manifesto and to explain how his different interests fit together. Preparing that talk made him aware that his work was already more complete and more homogeneous than he had himself known it to be. His talk was received with much praise and no hostility at all. To

denote his unified approach, he soon coined the term "fractal". Under the encouragement of his friends, he expanded his lecture notes into a short book, **"Les Objets Fractals: Forme, Hasard et Dimension,"** which was first published in 1975 and is now in its third edition. The publication of this book marked the change in his pursuit from the piecemeal approach to the unified approach and transformed his ideas from an oddity into a full-fledged geometry.

In 1976, after reading Hadamard's superb obituary of Poincare, Mandelbrot felt that his work should be extended beyond the linearly invariant fractals, to which he had restricted himself up to that point. Then, he set out to work on the limit sets of Kleinian groups and of groups based upon inversions. He first worked out an explicit construction algorithm for the self-inverse limit sets. A short step then brought him to some old work of his former teacher Gaston Julia, and of Pierre Fatou. A few months of work with complicated mapping had prepared him for a detailed study of iteration. He started with the simplest mapping, which is the second order polynomial. There is only one significant parameter involved, and to each parameter value corresponds a Julia set. He drew the set of parameter values such that the corresponding Julia set is not a "Fatou dust", but a connected "dragon". The set is so rich in substance, so simple to construct, and so visually appealing, to honor the contribution of its creator, it was later named "the Mandelbrot set" by two well-known mathematicians, Adrien Douady and John Hubbard (see Peitgen and Richter, 1986; and Mandelbrot, 1992, p.17).

2.4 The Third Stage: Diversified Applications

The third stage of fractal history follows the publication of the first English edition of Mandelbrot's book, **"Fractals: Form, Chance, and Dimension,"** which appeared in 1977. Although the theoretical development of fractal geometry continues, especially in the area of multifractals, and so does the controversy on the impact of fractal geometry on the subject of mathematics in particular and on the sciences in

general (see Krantz, 1989; and Mandelbrot 1989c), the third stage is largely characterized by the widespread applications of fractal geometry in almost every branch of natural sciences (La Brecque, 1986; Avnir, 1989; Kaye, 1989; Scholz and Mandelbrot, 1989; Fleischmann et al., 1990; Takayasu, 1990, Cherbit, 1991a; and Crilly et al., 1991). For Mandelbrot, this is the stage of glory and immense popularity, which forms a vivid contrast to the earlier stage of frustration and repeated rejection.

First of all, fractal geometry provided an indispensable mathematical language for the study of chaos (Fischer and Smith, 1985; Barnsley and Demko, 1986; Moon, 1987; Pike and Lugiato 1987; Stanley and Ostrowsky, 1989; Devaney, 1990; Bunde and Havlin, 1991; and Peitgen et al., 1992a, 1992b). Many patterns in dynamic systems with their complex boundaries between orderly and chaotic behavior, had unsuspected regularities that could only be described in terms of the relation of large scales to small scales. The structures that provided the key to nonlinear dynamics proved to be fractal. In addition, fractal geometry has become the dominant theme in many other areas of physics during the past ten years or so. Leo Kadanoff (1986, p.6), Nobel Laureate and Professor of Physics at the University of Chicago, reported that "*Physical Review Letters complains that every third submission seems to concern fractals in some way or another.*" Some of the results of fractal research in physics are presented in Pietronero and Tosatti (1986), Pynn and Skjeltorp (1985), Shlesinger et al. (1984), Stanley and Ostrowsky (1986), Jullien and Botet (1987), Pynn and Riste (1987), Pietronero (1989), Viczek (1989), and Aharony and Feder (1990). The impact of fractal geometry or its originator, Benoit B. Mandelbrot, on the subject of physics is clearly reflected in the title of a recent introductory text on theoretical physics by Stauffer and Stanley (1990), **"From Newton to Mandelbrot: A Primer in Theoretical Physics."**

Secondly, fractal geometry has been extensively used in the studies of materials. Some typical applications include the characterization of metal and catalyst surfaces, powders and aggregates, the study of the dynamic behavior of fractal materials, and

the evaluation of the effects of fractal characteristics on the properties of materials. For example, Avnir et al. (1984, 1985) used the concept of fractal dimension to describe quantitatively surface geometric irregularities of a wide variety of particulate materials at the molecular level. Kaye (1989) and his co-workers have made fractal analysis a standard procedure in fine particle characterization. Since 1984, there has been an annual symposium on fractal aspects of materials organized by the Materials Research Society (Mandelbrot and Passoja, 1984; Laibowitz et al., 1985; Schaefer et al., 1986; Hurd et al., 1987; Weitz et al., 1988; and Kaufman et al., 1989).

Thirdly, fractal geometry has spurred many new approaches and led to many new developments in the geosciences. For the purpose of this discussion, the geosciences include astronomy, geography, geology, geophysics, meteorology and oceanography (Turner, 1969). In developing his theories and testing his algorithms, Mandelbrot invoked numerous examples from geomorphology, astronomy, hydrology, and meteorology. Some of his most impressive and convincing computer simulations are images of clouds, coastlines, mountains, and lunar landscapes, which are the objects of the geosciences. Naturally, fractal concepts have had most direct appeal to many geoscientists and, at times, stirred up heated controversies and provoked harsh criticisms. When fractal geometry was finally becoming organized, geoscientists were among the earliest who found new applications in the areas of their research. Some of the earlier studies were reviewed by Burrough (1984, 1985, 1989), Buttenfield (1985), and Goodchild and Mark (1987). The results of some more recent studies are presented in Scholz and Mandelbrot (1989), Turcotte (1992), Unwin (1989), Snow and Mayer (1992), Lam and DeCola (1992), and Palaz and Sengupta (1992).

Some fractal studies in the geosciences are designed to duplicate Mandelbrot's results, to confirm his speculations, or to test the validity of his ideas, techniques and algorithms. Others are simply extensions of the research work initiated by Mandelbrot. Yet, many other studies are completely fresh or have shed new light on some of the traditional problems. Some of the important applications of fractal concepts in the

geosciences include (1) to describe the spatial distribution of galaxies and clusters of galaxies and to simulate the clustering processes (Efstathiou, 1984; Coleman, 1989; Heck and Perdang, 1991; Coleman and Pietronero, 1992; and Schramm and Luo, 1992), (2) to model clouds, rain, and other atmospheric fields (Lovejoy, 1982; Lovejoy and Mandelbrot, 1985; Lovejoy and Schertzer, 1986; Skoda, 1987; and Schertzer and Lovejoy, 1991), (3) to characterize the irregularities of the land surface and to reconstruct the ocean floor topography (Culling and Datko, 1987; Gilbert, 1989; Malinverno, 1989b; and Mareschal, 1989), (4) to differentiate different landform regions and to investigate geomorphological processes (Culling, 1986b, 1987, 1988, 1989; Goodchild, 1988; Klinkenberg, 1988; and Newman and Turcotte, 1990), (5) to model the spatial variability of soil properties (Burrough, 1981, 1983a, 1983b; Armstrong, 1986; Tyler and Wheatcraft, 1990a, 1990b; Bartoli et al., 1991; Rieu and Sposito, 1991a, 1991b; and Young and Crawford, 1991), (6) to analyze the changing patterns of urban land use and to simulate processes of urban growth (Arlinghaus, 1985; Batty, 1985, 1991a, 1991b; Batty and Longley, 1986, 1987a, 1987b, 1988; Arlinghaus and Arlinghaus, 1989; Batty et al., 1989; Longley and Batty, 1989a, 1989b; and Longley et al., 1990), (7) to improve the consistency of cartographic generalization and digital representation of terrain data and to increase the efficiency of spatial data storage (Dell'Orco and Ghiron, 1983; Goodchild and Grandfield, 1983; Muller, 1986, 1987; and Polidori et al., 1991), and (8) to enhance the visual quality of computer-generated maps (Dutton, 1981; Hill and Walker, 1982; and Armstrong and Hopkins, 1983). Applications of fractal concepts in terrain modelling will be reviewed in more detail in Chapter 3.

One branch of the geosciences, geology, is probably one of the disciplines in which fractals are most extensively used (Middleton, 1991; Turcotte, 1992; and Barton and LaPointe, 1992). In fact, fractal geometry has become so widely used in geology that it is practically impossible to list all relevant references here. Four hundred and forty-two titles were found under the key word "fractals" in GeoRef covering from 1980 to June of 1992 despite of its incompleteness. Most of these entries deal with

geological applications of fractal concepts and techniques. Some of the most common applications include (1) the quantitative description of irregular particles (Orford and Whalley, 1983) and pore space of sedimentary rocks (Katz and Thompson, 1985; Wong et al., 1986; Hansen et al., 1988; Krohn, 1988; Thompson et al., 1987; and Thompson, 1991), quasicrystal lattice (Peng, 1986a, 1986b) and disequilibrium mineral textures of igneous rocks (Fowler, 1990; and Fowler et al., 1989), (2) the characterization of irregularity of fault or joint surfaces (Brown and Scholz, 1985; Power et al., 1987; and Power and Tullis, 1991) or their linear traces (Aviles et al., 1987; Okubo and Aki, 1987; and Matsumoto et al., 1992), (3) the representation of spatial distribution of chemical elements in sediments (Block et al., 1991; and Bolviken et al., 1992), ore deposits (Carlson, 1991), porosity, permeability and oil reservoir heterogeneity of sedimentary rocks (Sen et al., 1981; Hewett, 1986; Ruffet et al., 1991; and Taggart and Salisch, 1991), fractures in rocks (Velde et al., 1990; Leary, 1991; Merceron and Velde, 1991; and Vignes-Adler et al., 1991), earthquakes (Kagan and Knopoff, 1980; Kagan, 1981; Geilikman et al., 1990; and Hirata and Imoto, 1991), hot spots (Jurdy and Stefanick, 1990), and volumetric inhomogeneities in the lithosphere (Wu and Aki, 1985; and Shapiro and Faizullin, 1992), (4) modelling of temporal distribution of geological events such as discontinuous sedimentation (Plotnick, 1986), population fluctuations of foraminifera through geological time (McKinney and Frederick, 1992), clustering of earthquakes (Smalley et al., 1987; and Kagan and Jackson, 1991), and eruptive activity of volcanoes (Dubois and Cheminee, 1991; and Sornette et al, 1991), (5) the description of size distribution of earthquakes (Turcotte, 1989, 1992), fault surfaces (king, 1983; Turcotte, 1986a; and Marrett and Allmendinger, 1992), ore deposits (Turcotte, 1986c), particles in fault gouge (Sammis et al., 1986; and Zhao et al., 1990) and a large number of other fragmented geological objects (Turcotte, 1986b), and (6) process modelling of mineral growth (Fowler, 1990), fluid transport in porous media (Williams and Dawe, 1986; and Lemaitre and Adler, 1990) or through rock joints (Brown, 1987a), faulting and earthquakes (Andrews, 1980; Aki, 1981; Kagan and Knopoff,

1981; King, 1983; Turcotte, 1986a; Huang and Turcotte, 1988; and Ito and Matsuzaki, 1990). The results of some of these studies and a large number of other fractal studies of geological features and processes are reviewed in Turcotte (1989, 1992).

Fractal applications in biology have been relatively rare (Rigaut, 1991). Nonetheless, the situation is gradually changing. For example, eight Ph. D. dissertations written by biology students from 1989 to 1991 involved fractal concepts and techniques, comparing to one between 1980 and 1984 and three between 1985 and 1988.

The earliest use of fractal concepts in biology appears to be that by Weibel (1979). Following his meeting with Mandelbrot, he announced his estimate of a fractal dimension of 2.17 for the alveolar surface of human lungs. Then, the first Ph. D. dissertation recorded in **"University Microfilms International Dissertation Abstracts,"** that involved the use of fractals, was written by a biology graduate student at the University of Kansas in 1980. Kukuk (1980) used fractal parameters to describe the foraging path of a particular species of fish under several experimental conditions simulated in the laboratory. Weibel and his coworkers (Paumgartner et al., 1981) examined the effect of resolution on the stereological estimation of surface and volume density of subcellular membrane systems and suggested to use the fractal technique to derive resolution correction factors to facilitating comparison of measurements made at different magnifications. Loehle (1983) suggested a wide range of possibilities for applying fractal concepts in biology, such as large-scale patterns of an ecological landscape, the branching structure of trees and shrubs, and the three-dimensional nature of a forest canopy. Morse et al. (1985) showed that transects across individual plants are fractal and examined the effect of the fractal nature of vegetation on the distribution of arthropod body lengths. Milne (1988) analyzed the fractal patterns in kilometers-wide ecological landscapes.

Several authors have studied the fractal geometry of human and animal organs. Barenblatt and Monin (1983) used similarity principles to compare respiratory

exchanges in pelagic animals and suggested that the oxygen-absorbing organs of pelagic animals could be represented as fractal surfaces. Lefevre and his collaborators (Lefevre, 1983; Lefevre and Barreto, 1983; and Lefevre et al., 1982, 1983) have proposed a remarkable model of the pulmonary vascular layer, based on fractal trees and a cost function. Both symmetric and asymmetric tree models were considered. Mandelbrot (1983) suggested that the convolutions of the brain and the physiology of the capillary circulation of blood can best be understood by means of fractal geometry. Referring to the fractal geometry of capillary networks, Mandelbrot (1983, p.149) wrote, "*Lebesgue-Osgood monsters are the very substance of our flesh.*" Rigaut and his coworkers (Rigaut, 1984, 1991; and Rigaut et al., 1983a, 1983b) carried out extensive empirical studies on the relationship between boundary lengths and resolution and developed a "semi-fractal" model for use in biometry. Cherbit (1991b) reported the use of fractal dimension in quantifying the complexity of glomerular basal membrane and in studying the effect of pulse-type perturbation (light pulses, thermal shocks, etc.) on the rate of growth of a culture.

Finally, fractal geometry has made a significant impact on computer imaging and visualization. Computer graphics has played an essential role both in the development and rapid acceptance of fractal geometry as a valid new discipline (Mandelbrot, 1977, 1983; Fournier et al., 1982a, 1982b; Norton, 1982; and Voss, 1988). The computer rendering of fractal shapes leaves no doubt of their relevance to nature. Conversely, fractal geometry now plays an important role in the rendering, modelling and animation of natural phenomena and phantasmic shapes in computer graphics (McDermott, 1983; Smith, 1984; Sorensen, 1984; Demko et al., 1985; Oppenheimer, 1986; Peitgen and Richter, 1986; Peitgen and Saupe, 1988; and Prusinkiewicz and Hanan, 1989). Fractals have also been used in the creation of phenomenally realistic landscapes, earthly and extraterrestrial, in special effects for movies (Batty, 1985; Dewdney, 1986; and McClure, 1985). For example, Pixar, formerly the Lucasfilm Computer Graphics Laboratory, has used techniques based on fractals to produce the landscape of the

Genesis planet in the movie **"Star Trek II: the Wrath of Khan"** and to create the outlines of the Death Star and of the continents and oceans on the moons of Endor in the hologram sequence in the briefing room in **"Return of the Jedi."** In fact, computer rendering of fractal objects has become a new art form. Fractal images have been put on display in museums. The exhibition **"Frontiers of Chaos: Images of Complex Dynamic Systems"** by Hartmut Jurgens, Heinz-Otto Peitgen, M. Prufer, P. H. Richter and Dietmar Saupe attracted more than 140,000 visitors at the London Museum of Science and since 1985 has traveled to more than 100 cities in more than 30 countries on all continents (Peitgen et al., 1992a, p.vii). Fractal postcards, fractal T-shirts, fractal mugs, and fractal calendars have also appeared in the market during the last a few years. Fractals have even entered the scenery of an imaginary planet in a science fiction novel by Allan Dean Foster (1985).

The phenomenal proliferation of fractal research is partially reflected in the rate of increase of Ph. D. dissertations written on the subject in the last twelve years. Figure 2.1 shows the number of dissertations for each year between 1980 and 1991, which have been recorded in the University Microfilm International's **"Dissertation Abstracts"** CD-ROM database. The rate of increase is clearly exponential. The decrease in 1991 is due to the fact that a large number of dissertations finished in that year are still waiting to be recorded. The same trend was also reflected in the number of publications using fractal geometry abstracted annually in the **Chemical Abstracts** (see Avnir, 1989, p.xvi) and in the number of publications on chaos (see Middleton, 1991).

Figure 2.2 shows the number of dissertations written in each year for different subject categories. By far, the largest number of studies and applications are in the natural sciences. Among the natural sciences, the physical sciences, which also include all branches of engineering, and the earth sciences make the most extensive use of fractal geometry in their research.

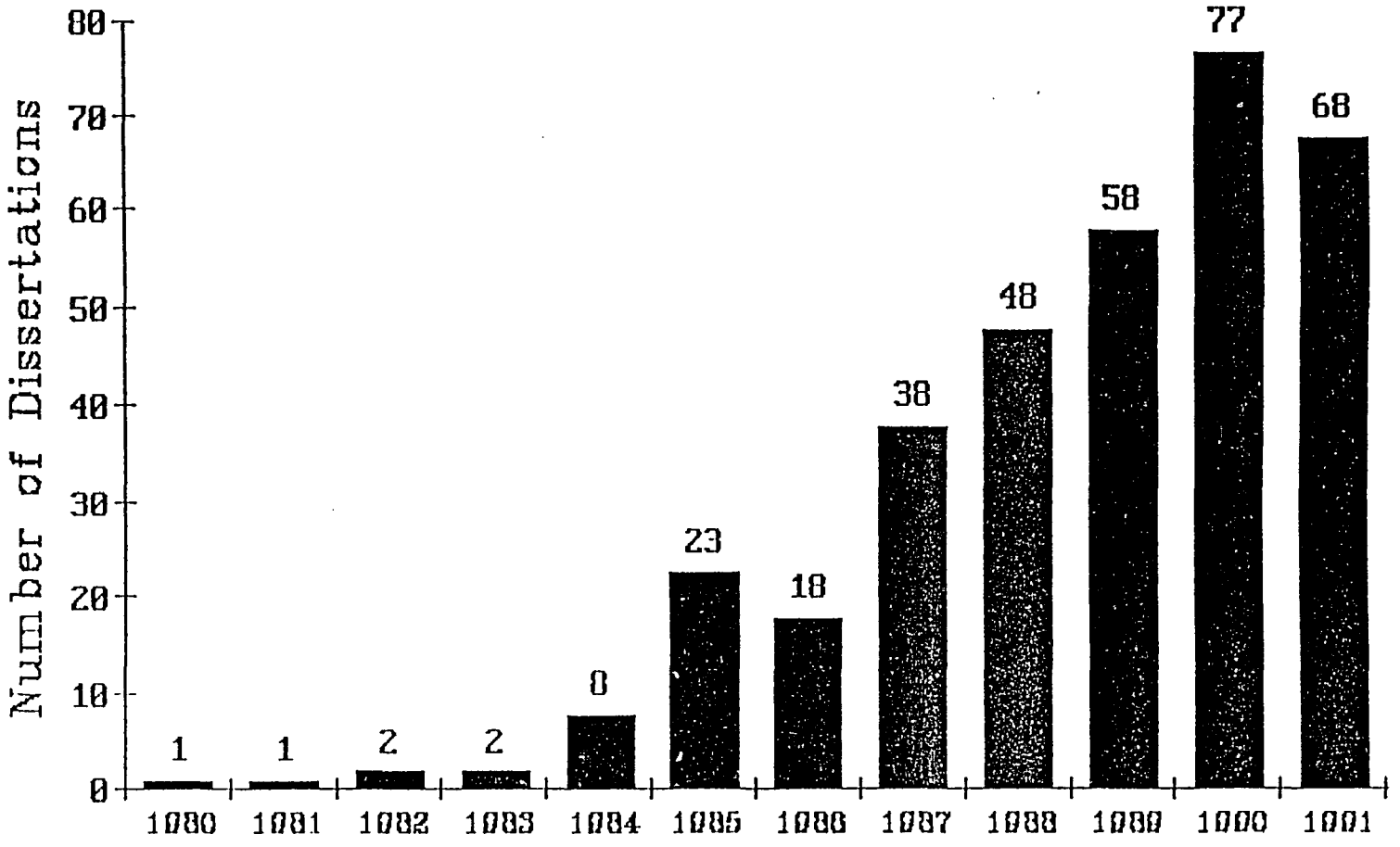

Figure 2.1 **Number of Dissertations on Fractals Published between 1980 and 1991**

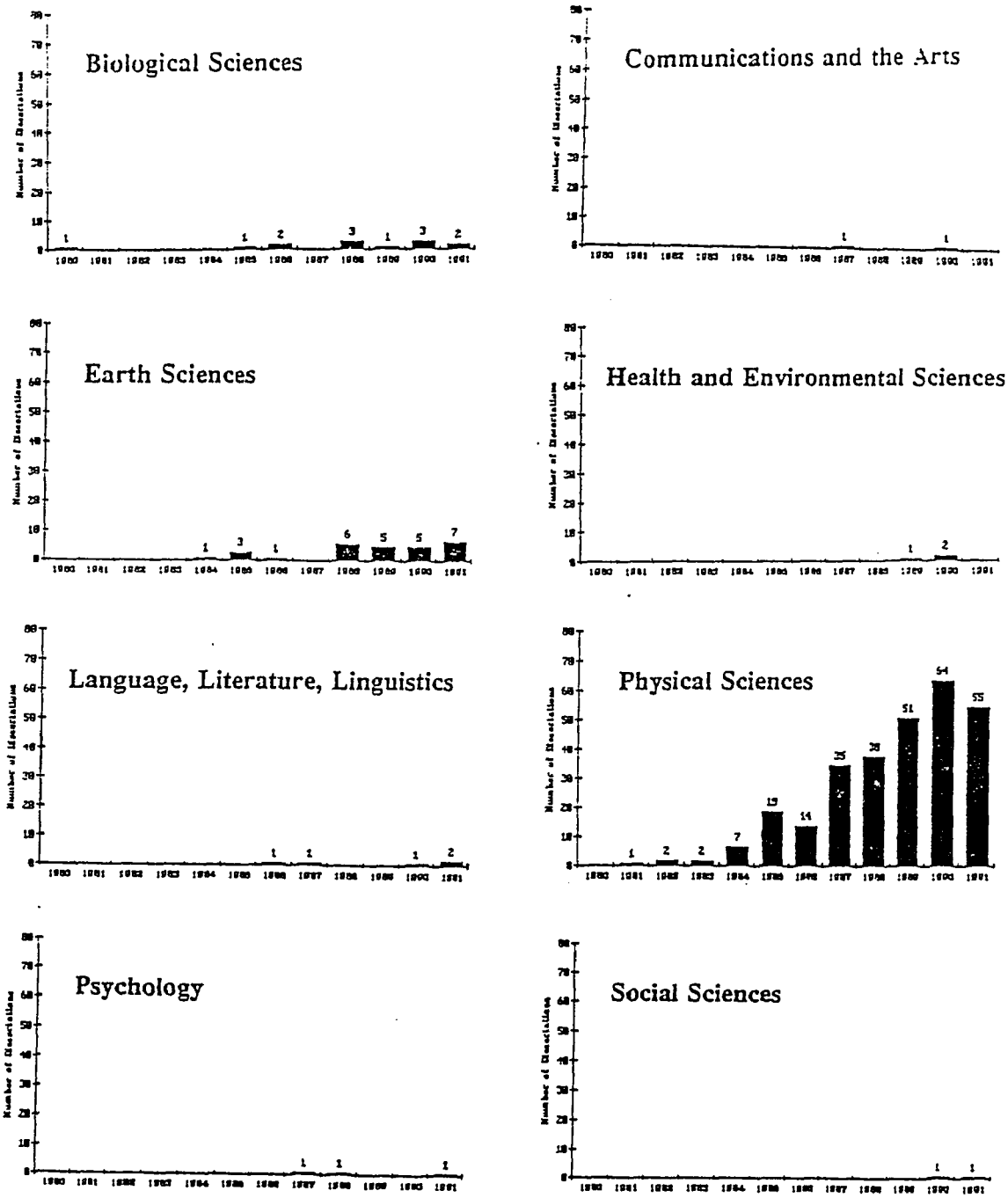

Figure 2.2 Number of Dissertations on Fractals Published in Different Disciplines

In summary, fractal geometry has become so widely used during the past fifteen years that very few, if any, scientific disciplines are still left untouched by it. The concept of fractal dimension has even been used to describe the texture of bread (Esbenshade, 1991) and instant coffee crystals (Peleg and Normand, 1985). Voss (1975) and Voss and Clarke (1978) discovered the similarity between scaling 1/f noise and music. Waschka (1990) developed algorithms involving fractal systems to compose music for his Doctor of Musical Arts dissertation. The situation seems to echo the comment made by the French humorist P. Dac,

> "*The Fractal in essence is such that the highest international authorities agree in acknowledging it to be the most startling discovery of our time, a discovery which, in a future all the nearer for being less far away, is not only pressed into the service of everything, to say the least, but also of anything, including everything which flows from it, without prejudice to anything else, etcetera, etcetera*" (see Cherbit, 1991a, p.2).

In fact, the use of the fractal concepts, models and techniques have become so widespread and important to scientific research that an American physicist, John A. Wheeler, once said, "*No one is considered scientifically literate today who does not know what a Gaussian distribution is, or the meaning and scope of the concept of entropy. It is possible to believe that no one will be considered scientifically literate tomorrow who is not equally familiar with fractals*" (see Batty, 1985, p.35).

Chapter 3 APPLICATIONS OF FRACTAL GEOMETRY IN TERRAIN MODELING: A LITERATURE REVIEW

3.1 Introduction

Coastlines, mountains, and other earth surface features were used extensively by Mandelbrot (1967b, 1975c, 1977) to develop the concepts and techniques of fractal geometry. Some of the most impressive fractal-based computer simulations are images of coastlines, mountains, lunar landscapes, and planets (see Mandelbrot, 1983; and Voss, 1988). As a result, fractal concepts have had tremendous appeal to terrain scientists since the very beginning. A year after the publication of Mandelbrot's book **"Fractals: Form, Chance, and Dimension,"** Mark (1978) compared Mandelbrot's (1975c) model of terrain surface based on a generalization of Brownian motion with the models of Seginer (1969) and Freiberger and Grenander (1977) using the "randomness" approach and found that Mandelbrot's model produced better results. In 1979, Mark published a review of Mandelbrot's book, concentrating on those parts which are particularly relevant to geo-scientists and pointed out some directions along which fractal concepts could be used. Since then, numerous studies have been carried out to test the validity of fractal geometry in describing real terrain, to develop and refine terrain simulation algorithms, to investigate the ways in which the concepts and techniques of the new geometry can be beneficially employed to provide more accurate characterization of various landforms and other linear and volumetric elements of terrain, and to improve the existing models of geomorphological processes. This chapter provides an overview of the applications of fractal geometry in terrain research. Some of the earlier studies in this area have been reviewed previously by Burrough (1984, 1985, 1989), Frederiksen et al. (1985), Goodchild and Mark (1987), Turcotte (1989, 1992), Hallet (1990), Moore et al. (1991), and Klinkenberg and Clarke (1992).

3.2 Fractal Characterization of Terrain Surfaces

During the last twelve years, fractal concepts have been widely utilized to characterize land surface topography and ocean floor bathymetry. Burrough (1981) appears to be the first to use fractal concepts to describe real terrain data. He reanalyzed the height variations of the topographic profiles of the Noiretable region of France cited by Journel and Huijbregts (1978, p.243-244) and derived a D value of 1.5 as the lag tends to zero and a D value of 1.1 at the maximum slope using the variogram method. This means that the topographic surface of the region has a fractal dimension of 2.5 in the short distance range and a fractal dimension of 2.1 in the long distance range.

Goodchild (1982) conducted the first empirical test of the fractal terrain model. The test area was Random Island, which lies just off the coast of eastern Newfoundland. Data were taken from the 1:50,000 scale topographic map. The shoreline, 250- and 500-foot contours and outlines of lakes greater than 0.05 square centimeters on the map were digitized to an accuracy of 0.25 mm. The coastline, 250- and 500-foot contours and lake outlines were treated as four different sets of lines. He used three different methods to estimate the fractal dimension of these lines: the walking dividers method, the box-counting method, and the area-perimeter method. The results are shown in Table 3.1. Although the numerical results obtained by different methods vary

Table 3.1 Estimates of D of Random Island, Newfoundland by Goodchild (1982)

METHOD	SHORELINE	250 FT. CONTOUR	500 FT. CONTOUR	LAKE OUTLINES
Divider	1.11	1.19	1.31	1.80
Box-Counting (7 cases)	1.11	1.29	1.47	1.53
Box-Counting (6 cases)	1.13	1.33	1.54	1.61
Area-Perimeter	1.14	1.17	1.19	1.30

substantially, all of them indicate that the Random Island topography exhibits the same type of behavior as the fractional Brownian process, that is, a log-log relationship

between length measures and scale, and the predicted form of loop allometry. Furthermore, they consistently suggest that the topography at the shoreline is considerably smoother than in the center of the island.

Bradbury and Reichelt (1983) and Bradbury et al. (1984) attempted to use the fractal dimension to quantify the irregularities of the coral reef topography of Myrmidon Reef. Although the algorithm for estimating the fractal dimension used in Bradbury and Reichelt (1983) was completely wrong (see Mark, 1984), thus rendering their ecological interpretations meaningless, the results in Bradbury et al. (1984) appear to be more reliable. They computed D values at seven scales and found them to fall into three distinctive scale ranges, which correspond closely to the ranges of three different levels of reef structure. The finest scale measured is 10 cm, which corresponds to the size of the individual structure of coral colonies such as their branches and convolutions. The second scale range is from 20 cm to 200 cm, which is the size range of living adult coral colonies. The third scale range, which includes 5 and 10 m scales, has the same magnitude as the spirs, grooves, buttresses and other similar geomorphological structures. Their results showed that the fractal dimension declined from a value of about 1.1 at the finest scale to a value of about 1.05, which was relatively stable over the next four scales, and then rose steeply to a value of about 1.15 at the last two scales. They speculated on the ecological significance of the coral reef complexity reflected by the fractal dimension. Since the major effect of low fractal dimension is to reduce the intimacy of contact of the living surface of the reef with the surrounding water and since this effect is most strongly expressed at the scale of coral colonies, their results seem to suggest that at the colony level corals attempt to reduce the intimacy of their contact with the medium, and that this tendency is countered by the processes within colonies and at larger scales.

Mark and Aronson (1984) carried out extensive empirical estimates of fractal dimension of topographic samples, gave an evaluation of the fractal model in the context of geomorphology, and discussed the implications of the fractal model regarding

sampling densities for digital representation of topographic data. They selected seventeen Digital Elevation Models of the 1:24,000 scale USGS topographic quadrangles from four different physiographic provinces and used the variogram method for estimating the fractal dimension. They found that of the seventeen areas examined only one (Shadow Mountain, Colorado) had a variogram totally consistent with the concept of self-similarity and with the model of a fractional Brownian surface. One of the variograms had a slope that varied continuously with scale, suggesting that the fractal model was not appropriate at all. All of the remaining fifteen areas showed that statistical self-similarity was closely approached over restricted scale ranges which were often separated by distinct breaks in the variogram. According to their analysis, over short scales (less than about 0.6 km), many of the geomorphic surfaces do indeed resemble fractional Brownian surfaces with dimensions of around 2.2 or 2.3, the dimensions generally held to produce simulated surfaces most nearly resembling natural terrain. However, at scales between 0.6 km and about 5 km, many areas are characterized by much higher dimensions, around 2.75 for six areas in Pennsylvania. At longer scales yet, it appears that the fractal model breaks down completely, and may be replaced by periodicities.

At about the same time, a group of Soviet scientists in Shirshov Institute of Oceanology, USSR Academy of Sciences (Barenblatt et al., 1984) advocated the use of fractal dimension as an index of the degree of dissection of the ocean bottom and the acoustic basement relief. They took a 2889 km long ocean bottom profile running sublatitudinally across the mid-Atlantic ridge in the vicinity of 21° 30' N and used the walking dividers method to estimate its fractal dimension. For the entire profile, they obtained a D value of 1.285. They then divided the profile into seven equal segments and computed the fractal dimension for each segment. By doing so, they found a regular decrease in fractal dimension with increasing distance from the rift. They interpreted the trend as the result of successive smoothing of the bottom relief by tectonic processes and by bottom currents and sediment accumulation.

They also carried out a similar analysis of two profiles obtained by continuous seismic profiling. One of these profiles is close to the Canary Basin, while the other adjoins the rift valley of the North Atlantic Ridge. For each of these profiles they calculated two values of D, corresponding to the bottom surface and the surface of the acoustic basement. Their results show that for both profiles the D value of the acoustic basement is significantly higher than that of the bottom surface. They have also found that the D values for the bottom surface and the acoustic basement are greater for the profile adjoining the basin. Based on these results, they concluded that the block relief of the acoustic basement formed during spreading in the rift zone tended to be smoothed out as a result of tectonic, isostatic or rheological processes and accordingly a certain compliance of the crust and lithosphere, which is contrary to what some people believe. They claimed that the fractal method of quantitative description of the degree of dissection of the surfaces discussed would enable us not only to present data on the relief of the sea bottom and the acoustic basement in concrete fashion, but also to identify new patterns involving the relationship of fractal parameters to the age of the bottom and to various physical processes in different areas of the oceans.

Nakano (1984) investigated the variation of the fractal characteristics of terrain with elevation. He selected the rias coast from Kamaishi to Shizugawa on the Pacific coast in Northeastern Japan for his study because this coastline was frequently cited as a typical example of a fractal. Contour lines of 0 m, 10 m, 30 m, and 50 m were used in his analysis using the walking dividers method. The length measurement was carried out on a compiled map which was made by connecting nineteen sheets of 1:25,000 scale topographic maps. He found that each contour line was composed of two fractal elements separated by a "cross over point" (or break point). Thus, he claimed that these contour lines were multifractals or "transient fractals" as he called them. He also reported that there was a systematic increase of fractal dimension in the short distance range from 1.15 (0 m) through 1.25 (10 m) to 1.28 (30 m and 50 m) with elevation while the D value for the long distance range remained constant at all elevations (D =

1.37). Inversely, the corresponding distances of the break points were found to decrease systematically from 1.5 km (0 m) through 0.9 km (10 m) and 0.5 km (30 m) to 0.25 km (50 m) with elevation. He interpreted that the two fractal elements were produced by a series of aggradation in rias coast such as the development of smooth seashore and waste-filled valleys. Geological studies suggest that the principal factor for the development of the rias coast in the region was the last post-glacial transgression since about 20,000 years ago. Nakano speculated that a highly irregular coast characterized by a D value of 1.37 was created when the rapid transgression occurred and then modified by aggradation through the development of waste-filled valleys or deltas charged by river systems into a smoother coast.

Brooks (1985) made the first attempt to use the fractal dimension of topography as a means of differentiating landforms developed in different lithological regions. He selected five drainage basins from the USGS 1:24,000 scale topographic maps for each of three lithological types: glacial till plain, shale, and granite. He converted the topographic data of each drainage basin into a rectangular array of elevation values by using a clear acetate quarter-inch grid overlay. The total number of elevation values within each array ranges from 216 to 564 (i.e., from 18 by 19 array to 26 by 37 array). The quarter-inch grid line spacing on 1:24,000 scale maps corresponds to 500 feet (152.4 meters) spatial resolution on the ground. The algorithm he used for estimating the fractal dimension is as follows:

$$D = \log (A / a) / \log (1 / n)$$

where

D is the fractal dimension

A is the total surface area

a is the area of one grid square

n is the reciprocal of the number of grids on a side of the DEM

Based on the results he obtained, he concluded that the landforms developed in different lithological regions could be differentiated using the fractal dimension of the topographic surface. However, a close look at his computational results indicates that the average fractal dimension of the glacial till plains (2.000076) differs very little from that of shale topography (2.00051). In addition, his D values are much lower than those obtained by other researchers. Even the highest average fractal dimension (2.03391), which was found in granite regions, is not much different from that of a featureless, non-fractal flat plane. These problems seem to raise serious doubt on the validity of his interpretation.

Fractal concepts have also been extensively used by Fox and Hayes (1985) in their efforts to develop a stochastic model for describing high spatial frequency sea-floor topography. To allow the variability of depths to be described as a function of spatial frequency, they chose the amplitude spectrum (square root of power spectrum) as the statistical measure for the sea-floor roughness. Upon the examination of many spectra, they found that a power function seemed to represent the best model for describing the relationship between the amplitude and frequency of sea-floor topography, which confirms the finding of Bell (1975, 1979) and adds additional support to the theories of fractal geometry. By confining samples to within homogeneous provinces, they have revealed an accountable variation of slope on the log-log plot of amplitude against frequency between different provinces. This contradicts the results of Bell (1975, 1979), who reported a consistent slope of -1. Fox and Hayes believe that this apparent "universal" slope is due to the absence of stationary province techniques. They used the amplitude and the slope as their criteria for delineating different roughness provinces. The boundaries of many roughness provinces coincide with obvious physiographic province boundaries. However, in many other cases, no boundary was obvious in the bathymetry. Although they did not explicitly use the fractal dimension to characterize different provinces, it can be easily derived from the values of the slope on the log-log plot, which range from -0.601 to -1.69. They related the difference in

roughness between different provinces to the contrasting geological settings and processes. In addition, they found that the spectrum for two large sedimentary provinces in the northeast Pacific Ocean and an extremely large area of the continental margin off the United States east coast was clearly separated into two distinct straight-line segments of different slopes. They interpreted this as an indication of two dominant relief-forming processes, the high frequency band representing a sedimentary regime and the low frequency band representing an underlying tectonic/volcanogenic regime. They tested the validity of using the power law relationship between amplitude and frequency to predict the roughness of a surface at scales unresolvable by surface sonar systems. The amplitude of roughness was predicted to within half an order of magnitude over five decades of spatial frequency.

Roy et al. (1987) followed Mark and Aronson's approach and modified their algorithm to avoid a sampling bias towards the long range of the variogram and to include an analysis of profile variograms. They used a USGS DEM of the Moose Bog 7.5 Quadrangle located in the White Mountains at the border of Quebec, Maine and New Hampshire as a test case and calculated the fractal dimensions of the whole quadrangle, of profiles taken across the DEM in the EW, NS directions and along the diagonals, and of three subareas representing different landscapes within the quadrangle. The surface variogram obtained from the whole DEM showed an initial straight segment up to a lag of about 2 km (64 pixels) with a constant slope (H = 0.84). D is therefore equal to 2.16. Computations from profile variograms also gave very similar average dimensions for the short range. The low D indicates the smoothness of the landscape despite a great amount of vertical relief in the area. Nevertheless, the specific D values of individual profiles showed some variability across the area. The distal part of the variogram for longer lags also has a trend (H = 0.18). The break in slope is sharp, but it occurs close to the limit of reliability of the variogram. In addition, an examination of the variograms of individual profiles indicated that the residual trend observed in the surface variogram was clearly the amalgam of highly variable behaviors at longer

distances. Thus, the surface variogram describes an apparently self-similar terrain.

They found that the fractal dimensions of the three subareas representing different landforms differed substantially. All profiles that entirely cut through the valley bottom filled with glacial sediments have a high dimension (between 1.37 and 1.44) while those on the hill side are very smooth ($D < 1.10$). Some profiles combine the attributes of both types of terrain. Thus, there is a general trend that the fractal dimensions decrease with altitude. They remarked that at this scale the lack of self-similarity was shown through a juxtaposition of terrain rather than by nesting smooth within complex structures. They suggested that the detection of self-similar patches of terrains could be used advantageously and more attention should be given to the investigation of the fractal signature of characteristic terrains. They recommended that elevation and physiographic location should be used to guide terrain sampling, data interpolation, and cartographic enhancement procedures as they are closely related to terrain complexity.

Culling and Datko (1987) subjected the fractal model to the test against empirical data from a variety of sites in southern England and from two sites in Germany investigated by Ahnert (1984). Culling's (1960, 1963, 1965) early studies convinced him that the soil-covered landscape of southern England was subjected to a general diffusion-degradation regime, which was responsible for the relatively smooth appearance of the landscape. Culling and Datko reasoned that a diffusive type degradation regime, or more generally a Davisian downwasting scenario, would tend to lower the value of Hausdorff dimension of the landscape surface. They speculated that for a soil-coved landscape in temperate regions the Hausdorff dimension would register in the range between 2.0 and 2.3. Furthermore, they pointed out that the lowering of the dimension presupposed its setting at some initial value. This initial value represents the work of the drainage system and it is upon this framework that the degradation surface is superimposed. They expected that the dimension of the surfaces produced by stream erosion would be in general of a higher value (between 2.4 and 2.6) than that for the surfaces produced by diffusive type degradation regimes. They expected to find

evidence of the two differing dimensioned structures in the soil-covered landscape.

To verify their hypothesis, they selected fifteen Ordinance Survey 1:25,000 maps or digital tapes of sites in southern England that represent a wide variety of terrains and reanalyzed the two data sets used by Ahnert (1984). In the case of printed maps, they took a traverse from opposite corners of the map sheet (NW to SE and SW to NE) and the intersections with mapped contours were then used to construct a profile. Then the estimated elevation was read off to the nearest 5 feet at 2 mm intervals representing 50 meters on the ground, which is equivalent to creating a one-dimensional elevation matrix. The variogram method was used to estimate the fractal dimension of these profiles. They also used the walking dividers method to estimate the fractal dimension of topographic contours. In general, both the walking dividers method and the variogram method have given two fractal dimensions for short and long scale ranges, although only a single dimension was given for twelve of the thirty-four profiles examined with the variogram method and for four of the seventeen maps examined with the walking dividers method. The short range dimensions are between 1.08 and 1.27 and the long range dimensions are between 1.37 and 1.76. With few exceptions, the long range dimensions estimated by the walking dividers method are significantly lower than those estimated by the variogram method. They also estimated the fractal dimension of the drainage network within each area, which ranged from 1.49 to 1.77. They considered that the drainage network represented the boundary condition, stable in the short term, to which the land surface had to fit. They also tested the distribution of increments on probability paper. In some cases they found a remarkable straight line indicating a Gaussian distribution and therefore a Brownian form to the land surface. In other cases the linearity was not quite so apparent and in still others was not apparent at all. They attempted to identify the reason for the non-linearity of each case and observed that it was only where the smoothing process of degradation has gained the upper hand that the Gaussian distribution of increments should be apparent.

Turcotte (1987) examined the global planetary spectra of topography and geoid for the earth, moon, Mars, and Venus using fractal techniques. One way to represent the variations in topography and geoid at a planetary surface is to expand the global data in terms of spherical harmonics. Harmonic expansions of topography have been given by Balmino et al. (1973) for the earth, by Bills and Ferrari (1977) for the moon, by Bills and Ferrari (1978) for Mars, and by Bills and Kobrick (1985) for Venus. Harmonic expansions of the geoid have been given by Reigber et al. (1985) for the earth, by Bills and Ferrari (1980) for the moon, by Balmino et al. (1982) for Mars, and by Mottinger et al. (1985) for Venus. Turcotte computed the power spectral densities from these harmonic expansions and plotted them against the wave number. He found that all the topographic data agreed reasonably well with the correlation

$$S(k) \propto k^{-2}$$

where S is the power spectral density and k is the wave number. This gives a fractal dimension of 1.5 for the global planetary topography. For the global planetary geoids, the spectral density and the wave number are related as follows:

$$S(k) \propto k^{-3.5}$$

which yields a fractal dimension of 0.75.

A D value of 1.5 means that topography appears to be Brownian noise, which is consistent with the results of Bell (1975, 1979). For Brown noise, the amplitude is proportional to the wavelength. Thus, if Turcotte's results were correct, the topography would be truly self-similar at all wavelengths. However, a D value of 1.5 is significantly different from the value (D = 1.2) commonly used to generate realistic-looking synthetic terrains. Turcotte interpreted that synthetic topography, though looking realistic, was only an approximate representation of the observed statistics.

He also related the fractal behavior of the geoid to the fractal behavior of topography and found that the spectral correlation for the geoid could be satisfactorily derived from the correlation for topography assuming Brown noise and no compensa-

tion. In addition, Turcotte attempted to determine the equivalent height of topography that would give the observed geoid anomalies and to provide a physical interpretation for the power spectral density for topography. With a series of approximations he showed that the power spectral density was related to the work required to create the topography.

Klinkenberg (1988) carried out another relatively extensive test of the fractal model of topography using a variety of measurement techniques (including the variogram method, the cell counting method, and the walking dividers method) and topographic data sets representing a wide range of landform types. He reanalyzed the seventeen DEMs used by Mark and Aronson (1984) and examined forty-one additional data sets, together covering nine physiographic provinces in the United States. His study showed that the fractal model generally fit those data sets from the Coastal Plain, the Great Plains, the Rocky Mountains, and the Colorado Plateau physiographic provinces well, but did not fit those data sets from the Valley and Ridge, and the Interior Low Plateau provinces, and gave quite mixed results for data sets from the Appalachian Plateau and the Basin and Range provinces. The fractal dimension was also found to vary with elevation in the Appalachian provinces, although no consistent trend was found in all data sets. The variance of D increased with increased elevation in the data sets from the Blue Ridge and the Appalachian Plateau provinces, but decreased with elevation in the twelve data sets from the Valley and Range province. He attempted to differentiate different landform types on the basis of their fractal dimensions and found that the physiographic provinces could be statistically distinguished. In addition, his study showed that the intercepts obtained from the variogram analyses could also be used to separate different landform types.

Gilbert (1989) investigated the question of whether topographic data sets were fractal by evaluating the appropriateness of fitting straight lines to the power spectra of topographic data sets in log-log space. He analyzed two digital topographic data sets: a topographic profile of a flowline from the mid-oceanic ridge to anomaly 31 between

the Moore and Rio Grande fracture zones in the western basin of the South Atlantic and a set of four topographic profiles 120 meters apart in the Sierra Nevada Batholith of the western United States extracted from the USGS Digital Elevation Models. The square root of age dependence of depth was removed from the sea-floor data and the residual depth data were used in all of the calculations. The spectra were all computed using the fast Fourier transform. In all instances the mean was removed and a Hanning taper was applied to the input data set. The sea-floor profile was divided into five segments and a smoothed spectra was produced by ensemble averaging the pieces. The continental spectra were smoothed by ensemble averaging the spectra of adjacent profiles. After computing the spectra, a line was fitted to the spectral estimates in the log-log space. The computed line was then subtracted from the original power spectra and the residuals were inspected. If a line is an adequate description of the spectra, the residuals will lie about zero and have no structure. Gilbert found that topographic spectra were poorly represented by straight lines. The sea-floor spectra consisted of a straight section between 10 and 1 km wavelengths and a section whose slope tended to flatten as wavelength increased above several 10's of kilometers. For the particular section which appeared linear, the slope was strongly dependent upon the resampling procedure. The spectra of the original Sierra Nevada data also showed striking curvature, giving an impossible fractal dimension of 0.835. Gilbert suggested that the use of fractal geometry as a quantifier of topography must be qualified by two considerations: (1) scale must be specified in the form of a band width under consideration; and (2) the particulars of the data analysis techniques must be explicitly stated.

Gilbert and Malinverno (1988) reanalyzed the topographic profile from the South Atlantic Ocean with slightly modified data processing procedure. To maximize spatial wave-bands, they calculated spectra for data from the ridge out to anomaly 31 in both the eastern basin and the western basin. The most significant change in their data processing procedure was that they prewhitened the data by first-differencing before computing the power spectra of the profiles. This modification has produced results that are

different from those presented in Gilbert (1989) for the same profile. The difference for the data produced by using moving average resampling was as high as 0.151 (15.4%). These differences further underscore the importance that data processing procedure plays in any estimation of fractal dimension.

Nevertheless, they claimed that the western and eastern basins could be discriminated on the basis of their fractal dimensions. An examination of their numerical results raises some doubt on the creditability of their claim. First of all, the D values for the data sets produced by using moving average resampling are senseless (both are less than 1). Secondly, the difference between the eastern basin and the western basin is at most 0.03 (2.5%), which is much lower than the difference caused by changing the data processing procedure.

Malinverno (1989a) evaluated the performance of two linear models for describing sea-floor topography, a fractal model and an autoregressive model. He selected three topographic profiles across the Explorer Ridge in the northeast Pacific as his test data sets. He compared the sample autocorrelation, power spectrum and variogram with the theoretical predictions of the two models. The three profiles were considered as separate realizations of the same process so that both the autocorrelations and the sample spectra of each profile have been averaged to smooth the resulting estimates. The results suggested that a linear system approach was a viable method to model and classify sea-floor topography. However, the comparison did not show substantial disagreement of the data with either the autoregressive or the fractal model. Malinverno pointed out that one obvious reason for the failure of the test was that the trace studied was quite close to a random walk, having a fractal dimension between 1.315 and 1.36. As both a fractional Brownian motion and an autoregressive integrated process converge to a random walk, they become increasingly difficult to distinguish. Nevertheless, the fractal model gave a superior fit to the autocorrelation for small lags and to the general trend of the variance of the increments.

On the other hand, the amplitudes predicted by a nonstationary fractal model for long wavelengths (of the order of 1,000 km) are unreasonably large. Malinverno speculated that when viewed through a large window, ocean floor topography was likely to have an expected value determined by isostasy and to be stationary. He suggested that nonstationary models were best applied to wavelengths of the order of 100 km or less, the range of wavelengths in which volcanism, faulting and mass-wasting create a stochastic sea-floor.

Mareschal (1989) attempted to demonstrate the fractal character of the sea-floor by constructing synthetic sea-floor topography with a fractal interpolation algorithm introduced by Barnsley (1987) and comparing these synthetic profiles with real bathymetric profiles. He constructed one profile by interpolating between the data points selected from a line across the Mathematician Ridge in the Eastern Pacific and another using the data points from a topographic profile near the Mendocino fracture zone of California. The similarity between the real and synthetic profiles was clearly shown by their Fourier amplitude spectra. On a log-log scale, both spectra showed random fluctuations superposed to a linear trend with a slope close to -1, which yields a fractal dimension of 1.5. The success of this fractal reconstruction algorithm suggests the possibility that it could be used to extrapolate, from data collected at one scale, the properties of the sea-floor at finer scales. It would also be possible to compute approximations and to determine the entire power spectrum of the sea-floor surface from bathymetric profiles.

Norton and Sorenson (1989) applied the concepts of fractal geometry to the description of geometric variations of topographic surfaces of the Sawtooth Range, Idaho, which is underlain by the Eocene Sawtooth Batholith and the surrounding Mesozoic Idaho Batholith. The topographic data they used were collected by digitizing contours from 1:24,000 and 1:250,000 scale maps. The fractal dimensions were estimated by the walking dividers method. Their study confirmed that the logarithm of contour length was actually a nonlinear function of the logarithm of ruler length for all

the data sets. The typical Mandelbrot-Richardson plot could be interpreted as three nearly linear trends. For the scale range below 400 feet, a linear trend with D = 1.05 was apparent in all data sets collected from 1:24,000 scale maps. They believe that the D value within this range is mostly determined by the map-making process and the digitizing procedure and thus lack any geological significance. For the intermediate range, there is a second linear trend in the function. This segment of the function appear to correlate closely with the variations of topography and is therefore used to compute the fractal dimension of each contour, which ranges from 1.15 to 1.26. For the long range, the number of steps falls below a statistically significant population and it is usually discarded.

Their results seem to indicate that smaller D values derive from contours where accumulation of screen or glacial erosion has smoothed the surface, whereas larger D values derive from contours along aretes and in unglaciated terrains. In each of these regions, larger D values occur locally where fractures are most frequent and/or continuous. Larger D values were also derived from regions underlain by host rocks that lie in the near-field region of the stress field caused by the pluton. Thus, the fractal dimensions derived are apparently related to the magma-hydrothermal event. Norton and Sorenson believe that they can potentially be used to derive properties of the percolation networks that were active during the hydrothermal events.

They also compared the results derived from 1:24,000 scale maps with those based on the digital data extracted from 1:250,000 scale maps. The fractal dimension of contours at the small scale is only slightly higher than the value determined from the large scale map. This agreement seems to lend additional support to the claim that the texture of contours is scale independent.

Huang and Turcotte (1989) attempted to map the land surface texture on the basis of fractal statistics. They carried out their experiment on the digitized topographic data for the State of Arizona produced by the U. S. Geological Survey (Flagstaff) on a grid

scale of about seven points per kilometer. They divided the entire state into square subregions of 32 X 32 data points (4.5 X 4.5 km) and determined the fractal dimension and roughness amplitude for each of these subregions. Maps of these quantities are then constructed for the entire state. The fractal dimensions of subregions, computed from a two-dimensional discrete Fourier transform of the original topographic data, ranged from 1.9 to 2.4, which gave an average fractal dimension of 2.09 for all of Arizona. The variation in the roughness amplitude was much more impressive. The drainage system associated with the Grand Canyon stood out as a region with high roughness in northwest Arizona. The Colorado Plateau in northeast Arizona was generally a smooth region although the boundary region where drainage has developed was quite rough. The roughness contrasts associated with the low-lying basin and range region in southwest Arizona were quite striking. Thus, the fractal analysis gives us a quantitative measure of roughness.

They also carried out a study of the one-dimensional spectral behavior of the Arizona topography. Quite strikingly, they obtained an average D value of 1.52 for a large number of tracks of Arizona. In order to substantiate their findings, they generated synthetic images for a range of fractal dimensions and calculated fractal dimensions of one-dimensional profiles of these synthetic images. For the realistic-looking topography with D = 2.1 - 2.2, they found that the corresponding one-dimensional profiles gave D = 1.6 - 1.65, which was consistent with the previously published results by other workers for one-dimensional bathymetric and topographic profiles and with their own results for the real topographic data of Arizona. Thus, they concluded that the two-dimensional spectral fractal dimension could not be obtained by adding one to the one-dimensional spectral fractal dimension. However, as Goff (1990) pointed out, their computation was based on erroneous mathematical derivation. Thus, the specific numerical values of their estimation have been systematically distorted.

Piech and Piech (1990) derived an expression of fractal scaling from the parameters of the scale space fingerprint technique and used the relationship to characterize

terrain types of different lithological regions. First, an one-dimensional array of topographic elevations is smoothed using different smoothing scales to generate a progressive sequence of scale space images. Points of inflection, or edges, of the scale space images are then plotted to give the scale space fingerprints. The relationship between the number of persisting terrain features or the feature density function and the smoothing scale is used to estimate the fractal dimension of topographic surfaces. They found that feature density functions not only differ for shale and granite landforms, but also for individual expressions of the landforms, such as arid and humid shales. They compared the results of fractal analysis based on the feature density functions with those of area scaling and length scaling methods and found strong consistency between these methods in predicting the fractal behavior for shale landforms and a lack of fractal behavior for granite landforms and in the estimated range of scaling of the shale landforms. However, they argued that the feature density evaluation of fractal behavior is superior to the other two methods in that it is more sensitive to the expression of fractal scaling and does not exhibit a dependence on measuring units in dealing with self-affine fractals.

Chase (1992) used the fractal dimension to characterize the complexity of landscapes surrounding Tucson, Arizona. He extracted ten blocks of elevation data from a digital elevation model, each of which is a 20 by 20 grid. The size of the grid cells is approximately 460 m in the N-S direction and 390 m in the E-W direction. The variogram method was used in his analysis. The scale range he chose for regression was between 460 m and 4.6 km. Chase reported that most of his data was discernibly multifractal. For length scales between 460 m and 1.5 km, the average fractal dimension is around 2.1, while for length scales between 1.5 km and 4.6 km the average D is 2.5. He suggested two alternative explanations for the multifractal nature of topographic data. It could be an inherent result of the laws governing the evolution of the landscape at present, or it might in part result from climatic and tectonic changes that have affected that evolution in the past. Using a numerical model of three

dimensional landscape evolution, he demonstrated how the variation of sediment-carrying capacity resulting from climatic changes produced a multifractal topography. He also showed how the relative importance of diffusional and erosional processes shaping the landscape could give the multifractal character to the simulated terrain surface. Nevertheless, Chase also calculated the mean fractal dimension within the entire scale range for each location and used it for comparison between different locations. It is interesting to note that all r^2 values for computing the mean fractal dimensions are extremely high (the lowest is 0.973). The mean fractal dimension varies from 2.02 to 2.40, with an average of 2.22. Another important conclusion from Chase's study is that there was no systematic relationship between the fractal dimension of topography and the estimation of relief amplitude.

Another related fractal study is the work of Woronow (1981). Although his study dealt with Martian surface features, his basic approach in inferring generating processes from morphological parameters is directly relevant to the research of earth's surface features and processes. Woronow (1981) examined the relationships between the perimeters and areas of 163 Martian ejecta blankets and found that the fractal model fit his observations well. He classified these ejecta blankets into three morphological classes: lobate, multilobate, and pedestal, and estimated the fractal dimensions of these classes. On the basis of their distinctive fractal dimensions, he conjectured that the three classes of Martian ejecta deposits were not the results of different physical sizes or evolutionary stages, but were created by distinctive physical processes.

Furthermore, several researchers also carried out investigations of the fractal properties of microtopography. The term "microtopography" refers to the configuration of the earth's surface at scales ranging from millimeters to a few meters. Using two digital surface profilers, Brown and Scholz (1985) studied the topography of several natural rock surfaces from wavelengths less than 20 microns to nearly 1 meter. The surfaces studied include fresh natural joints in both crystalline and sedimentary rocks,

a frictional wear surface formed by glaciation, and a bedding plane. The scale range they examined extends far beyond the normal range of scale studied by geomorphologists. The purpose of their study was to find a suitable way to scale the effects of surface roughness on the mechanical and hydraulic properties of joints of various sizes, which is part of rock mechanics and earthquake engineering. They examined the relationship between the power spectrum of each surface profile and spatial frequency and found that all surfaces have "red noise" power spectra over the entire frequency band studied, with the power falling off rapidly with spatial frequency. Thus, they adopted the concept of fractal dimension for describing the surface roughness. Their study reveals that the topography of these natural rock surfaces can not be described by a single fractal dimension. They divided the scale range into three frequency bands and calculated the slopes of the power spectra within each band. The fractal dimension for the high frequency band ranges from 0.82 to 1.43, for the middle frequency band from 1.19 to 1.52, and for the low frequency band from 1.18 to 1.68. This observed inhomogeneity in the scaling parameter implies that extrapolation of roughness from one band to another should be done with care.

Armstrong (1986) used the fractal concepts to study the spatial variation of transient soil properties of surface strength and microtopography. Soil surface microtopography was recorded using a profile meter. Profiles were 1 meter long, with surface height above an arbitrary datum recorded at 1 cm increments to an accuracy of 1 mm. He collected his data from two different drainage experiment sites over a succession of time intervals. The purpose of his research was to explore the possibility of using the fractal dimension to quantify the subjective assessments of surface roughness associated with differential poaching. He used the variogram methods for computing the fractal dimension. Due to the non-linearity of the log-log plots, he used the slope of the first ten lags (from 1 to 10 cm) to derive the D value for all profiles. For both sites, he obtained an average fractal dimension of 1.72. The detailed results for one of the sites, where repeated measurements were taken, indicate that the fractal dimension

is not static with time, which is to be expected in view of the continued reworking of the surface. For the profiles of another site, Armstrong calculated the fractal dimension using both the first ten lags (1 - 10 cm) and the first forty lags (1 - 40 cm). The fractal dimension calculated from the first ten points of the semi-variogram is 1.72. The fractal dimension calculated from the first forty points is 1.64. Armstrong interpreted this difference as the evidence of differing processes. Small scale variation in the range 1 - 10 cm is a response to animal treading effects, and geomorphological effects operating to create topography over the range 10 - 100 cm. However, Armstrong's study reveals no correlation between the fractal dimension and the visual roughness, while the poaching index (the standard deviation of the measurements along each profile) gives excellent agreement with the subjective assessments of surface roughness.

Power et al. (1987) extended the study of Brown and Scholz (1985) to natural fault surfaces as an attempt to quantify the roughness of fault surfaces, which is important in the mechanics of fault slip and could play a role in determining whether sliding occurs via earthquakes or fault creep. They measured the profiles of four fault surfaces in the western U. S. over the wavelength range from 10 micron to 1 meter. The most important finding of their study is that the fault surfaces are strongly anisotropic. In the direction parallel to slip all the fault surfaces are smoother than the natural joint surfaces described by Brown and Scholz (1985). Perpendicular to the slip direction fault surfaces have a roughness which is comparable to natural joint surfaces. In addition, they combined the power spectra for fault surfaces from different sources and claimed that fault surfaces were fractal over nearly eleven orders of magnitude in wavelength.

Robert (1988) examined the statistical properties of series of bed elevations measured on gravel-bed and sand-bed alluvial channels in order to identify means of quantifying bed roughness effects on streamflow. He used the semi-variogram as the basic tool for investigating roughness properties of bed profiles obtained from field work and laboratory experiments. For sand bedforms, he found that geometric properties

(bedform spacing and height) and information on the degree of regularity of bedform arrangement could be derived from the semi-variograms with superimposed exponential and periodic components. For the irregular gravel-bed profiles, Robert adopted the fractal parameters to characterize the bedform roughness. The log-log plots of all four gravel-bed profiles (each is from about 4 to 10 m long) show two distinct slopes and a maximum distance beyond which no spatial dependence is evident. The break distance ranges between 7.2 cm and 12.6 cm. The maximum distance ranges between 31 cm and 72 cm. The fractal dimension for the short distance range is from 1.52 to 1.712 and the D value for the long distance range falls between 1.779 and 1.909. A comparison of break distances with the grain sizes of gravels seem to suggest that the lower D values in the short range reflect the roughness of individual gravels and the higher D values in the longer range represent the effect of cluster bedforms on the surface roughness. Robert used the additive effects of grain and bedform roughness components to explain the greater than predicted flow resistance generally observed in gravel-bed rivers.

Using field data collected from talus slopes in Niagara Gorge and Letchworth Gorge, western New York, Andrle and Abrahams (1989) explored the possibility of adopting the self-similar fractal model to characterize and distinguish between talus slope surfaces. In their paper, they demonstrated that the conventional log-log plot of number of steps against step-lengths was an insensitive means of detecting departures from self-similarity and stressed the need for geomorphologists to employ more rigorous tests of self-similarity before adopting a single value of fractal dimension to quantify the roughness of a geomorphological feature over any range of scale. Their study also suggests that the surface roughness of talus slope is not self-similar over any range of scale and instead D varies continuously and in a systematic manner with scale of measurement. On the other hand, they claim that even where geomorphic phenomena are not self-similar, modified fractal techniques may still be used to quantify their roughness or complexity and to compare different ground surfaces as long as

the scale of measurement is held constant and the scale of roughness is consistently greater than or consistently less than the scale of measurement. They computed the fractal dimension of 40 transits on talus slope surfaces (20 pairs of intersecting profiles and transects, each of which is 10 m long). Then, they carried out a multiple regression analysis with D as the dependent variable and particle size, particle shape, gradient, and particle orientation as independent variables and found that particle size was the most important geomorphic variable controlling the fractal dimension of talus slope transits for a given scale of measurement. They also found that the fractal dimensions of profiles (which are parallel to the direction of the slope) were consistently lower than those of transects (which are normal to the direction of the slope) and explained this directional difference in surface roughness in terms of particle orientation, shape, and juxtaposition. It should be cautioned that they applied the walking dividers method to self-affine profiles, which considerably underestimates the fractal dimension of surfaces (Roy and Robert, 1990; and Andrle and Abrahams, 1990).

Elliot (1989) used the fractal dimension as a measure of microscale surface roughness to test a hypothesis that initial roughness imparted by an environment of glacial deposition would diminish progressively through time. She collected surface elevation data along fifteen profiles on the recently deglacierized moraines near Austre Okstindbreen, North Norway with a specially-designed field equipment. Each profile was 10 meters long and the altitudinal variation was recorded at 5 cm intervals and read to the nearest mm vertical resolution. She adopted the variogram method to compute the fractal dimension of these topographic profiles. However, instead of using the squared difference between values of paired samples, she used the variance with respect to the mean of differences between samples. Like many previous studies, most of the variograms produced by Elliot (1989) were clearly non-linear. She divided these variograms up to three scale ranges and computed the fractal dimension for each scale range. Values for estimated dimensions were generally higher for the lower range, lower for the middle range, and lowest for the upper range. However, this was not

always the situation: the highest value recorded was 1.98 for the 55 - 75 cm range, and the lowest value of 1.1 was also in the middle scale range (15 - 335 cm). She interpreted that the tripartiate division in some of the graphs reflected the differences in roughness between individual pebbles in the small-scale range, the interparticular surfaces in the middle-scale range and the overall outline of the profiles in the upper-scale range.

In order to establish a consistent relationship between roughness and age for the six profiles where the ages of sediments were known, she selected a single characteristic value for each profile estimated for the range 20 - 40 cm. Although the results were insufficient to define the relationship precisely, there seemed to be a general tendency that the fractal dimension increased with age, which was contrary to the interpretation based on the empirical observations in the field. This counter-intuitive result suggests that the initial hypothesis is either too simple or incorrect. She stated that factors other than time since deposition, such as particle size distribution and the nature of the parent material, seem to have affected the roughness of these surfaces at the scale examined.

3.3 Characterization of Linear and Volumetric Elements of Terrain

All the studies reviewed in the previous section dealt with the systematic variation of irregularities across terrain surfaces. In addition, there have been a large number of studies dealing with the fractal characterization of some linear and volumetric elements of terrain. Most of them are directly relevant to the treatment of terrain surfaces. The linear terrain elements which have been considered include coastlines, lake shorelines, stream networks, boundaries of drainage basins, and limestone cave passages. The volumetric elements include limestone caves and sinkholes. Any robust terrain model must incorporate these elements and account for the simultaneous and compatible development and evolution of these elements with variable degrees of irregularities along with ridges, hillslopes, and floodplains.

Coastlines were the very first type of natural fractals that Mandelbrot (1967b) described and have always attracted much attention from terrain scientists. The studies on coastlines reviewed in section 3.2 treated coastlines as part of a surface and the major focus of these studies was on the complexities of surfaces. The research work on coastlines reviewed in this section considered coastlines as irregular linear fractals and the emphasis of each study was on the irregularities of coastlines themselves. However, all studies on coastlines and lake shorelines are closely related. The separation is more a matter of convenience than of substance.

One of the earliest applications of fractal geometry in studying terrain features was that of Kent and Wong (1982). Recognizing the inadequacy of the traditional shoreline development index in describing the complexity of lake shorelines and littoral zones, they explored the possibility of using the fractal properties of the morphometric parameters of lakes as an alternative. They examined the relationships between the length of shorelines and the scale of measurement, between the shoreline length and lake area, between the number of lakes and the threshold lake size, and between the width of the littoral zone and its measured area. To study the dependence of the measured shoreline length on the measurement scale, the shorelines of eight lakes in the Muskoka and Haliburton regions of the Canadian Shield were digitized from maps at several scales (1:25,000 - 1:500,000). Their analysis indicates that the shoreline length and the measurement scale do not show a simple allometric relationship. Instead, they identified a consistent two-segment piecewise linear pattern between the total length of the shoreline and the opening size of the walking dividers for all the lakes they studied, that is, a linear model for scales below about 350 meters and a linear model for scales above about 350 meters. The fractal dimensions for scales above 350 meters cluster around a mean value of 1.44, while the fractal dimensions for scales below 350 meters cluster around a mean value of 1.14. They interpreted that the shorelines were formed by at least two different geomorphological processes. At the scales above about 350 meters, glacial action and pre-existing geological structures

were the chief factors determining the landform characteristics. At the finer scales, erosional processes became predominant.

To test the relationship between shoreline length and lake area, they used the morphometric data of twenty-one lakes, which were fitted into a single model. Their calculation gave a fractal dimension of 1.5 for the lakes in the Muskoka and Haliburton regions and a D value of 1.59 for the twenty-one lakes combined. To examine the relationship between the numbers of lakes and the threshold areas, they used a data set on lakes of six watersheds, including the Muskoka and Haliburton regions. For the watersheds covering the central portion of the Muskoka and Haliburton regions, D was estimated to be 1.51, which agrees with the result based on the relationship between shoreline length and lake area and with the estimate for scales above 350 meters using the walking dividers method. Other watersheds gave higher D values. The average fractal dimension for all six watersheds was 1.64.

To study the relationship between the width of the littoral zone and its measured area, the shoreline of Christie Lake (southern Ontario) and the boundaries of a series of littoral zones were digitized from an aerial photograph acquired at a scale of 1:7,700. They obtained a fractal dimension of 1.15, which is identical with the D value estimated by the walking dividers method for finer scales.

They suggested that the fractal indices could be used to quantify the role of the littoral zone in determining the community structure of lakes. Specifically, it may be used to separate the effects of lake size on the presence of certain fish species from those due to nearshore habitat availability. In addition, the fractal properties of lake shorelines and nearshore areas may eventually be used to predict the distribution within a lake of areas with high morpho-edaphic indices and to correct indices of productivity for the effects of shoreline irregularities.

Qiu (1988) used the Louisiana mainland coastline to test the validity and applicability of the fractal model. He divided the coastline into six segments based on the

dominant geomorphic processes and their developing stages. The western segment circumscribes the chenier plain and is dominated by the strong longshore currents in the Gulf of Mexico. The four eastern segments surround the deltaic plain of southeastern Louisiana which was formed by progressive seaward progradation of the Mississippi River deltas during the last 5,000 years. The northeastern segment corresponds to the shorelines of Lakes Pontchartrain and Borgne where tidal currents prevail. He has shown that in general coasts dominated by deltaic processes have higher fractal dimensions (ranging from 1.2755 to 1.3652) while coasts dominated by marine processes have lower fractal dimensions (ranging from 1.0040 to 1.1484). In addition, his studies seem to suggest that deltaic coasts at different developing stages are, to a certain extent, distinguishable in terms of their fractal dimensions and self-similar ranges. Fractal dimensions tend to decrease while the ranges of self-similarity tend to increase with time. He believes that these results reflect the changes in dominant geomorphic processes from deltaic to marine processes and represent progressive modifications of marine processes to the coastlines of different ages.

Nakano (1983) attempted a fractal analysis of the morphological characteristics of six rias coastlines in Japan. He used the walking dividers method for computing the fractal dimension and carried out his measurements on maps at scales of 1:25,000 and 1:200,000. He identified two linear segments on five of the six Richardson plots and three linear segments on the other plot. His calculations produced D values ranging from 1.12 to 1.27 for the short range and a fairly constant D value around 1.37 for the longer range. He examined the relationship between the fractal behavior and the geology of these areas. Although no distinctive pattern can be established, he believes that the similarities between three coastlines developed in the same tectonic unit and the difference between the coastline in the area mostly composed on Miocene igneous rocks and Tertiary sedimentary rocks and the coastlines in areas mainly composed of Pre-Tertiary sedimentary rocks seem to suggest a connection. He proposed an erosional model to account for the different fractal dimensions within different scale ranges. He

speculated that originally each rias coastline had a uniform irregularity across all scales with a D value of 1.37, which was smoothed out gradually from small to large scale by erosional processes. On the basis of this model, the position of the inflection point on the Richardson plot, that is, the scale at which the fractal dimension changes, gives us some indication on the duration or degree of land surface erosion.

Phillips (1986) adopted the fractal approach in his study to identify the most important scales of variability of shoreline erosion and to identify the controls of this spatial pattern. Recession rates along the Delaware Bay shore of Cumberland County, New Jersey were determined from two sets of 1:4,800 scale aerial photographs taken in 1940 and 1978. A number of variables believed to be important elements of shoreline processes in coastal plain estuaries were measured in the field and from maps. The variogram method was used to estimate the fractal dimension of the recession rates along the shore. The fractal dimension of erosion rates is 1.91, which means that the alongshore distribution of erosion rates is highly complex and variable and that wide variation occurs over short distances. The semivariogram of recession rate versus distance shows a range of 3,000 meters, implying that the entire range of variability can be found in any 3 km stretch of the 52 km study area shoreline. An analysis of variance on 27 variables describing the characteristics of the shoreline related to erosion susceptibility points to two factors controlling the spatial pattern of erosion. One is an alongshore pattern of differential erosion resistance related to shoreline morphology. A second factor is a complex, irregular pattern of short-range variations in exposure associated with minor points, coves, embayments, and other shoreline crenulations.

Phillips (1989) also examined the relationship between erosion and the shoreline configuration of the New Jersey shore of Delaware Bay. The 1940 and 1978 shorelines were digitized from aerial photographs and the length of each shoreline was measured by walking dividers along the digitized line using two different divider opening sizes which correspond to 50 and 100 m on the ground. The fractal dimension of each shoreline was then derived analytically as described in Chapter 5. The fractal

dimension of the 1940 shoreline is 1.20. For the 1978 shoreline, the fractal dimension is 1.46. Thus, after nearly forty years of severe erosion (average shoreline recession rate of 3.21 m/yr) the irregularity of the shoreline configuration, as measured by the fractal dimension, increased markedly. These results contradict the widely accepted model in coastal geomorphology which predicts smoothing of shoreline irregularities over time and support the instability principle of geomorphic equilibrium proposed by Scheidegger (1983), which claims that earth surface features tend to become more irregular through time as a result of the progressive loss of energy as landscapes evolve. Phillips believes that the increasing complexity of the shoreline plan form can be explained by the nature of shore erosion in the study area. Marsh sediment erosion occurs in the form of large slump blocks, which leave irregular indentations. In addition, the scarped shorelines have no geomorphic expression in the nearshore zone so that little or no wave refraction occurs in the vicinity of the water-land contact, causing the absence of rapid headland erosion and embayment infilling.

Stream networks represent another type of linear terrain element which has been intensely researched. Based on the analogous patterns displayed by Peano "plane-filling" curves and natural drainage patterns, Mandelbrot (1977, p.61) recommended that various forms of Peano curves, particularly the "plane-filling" curve constructed by R. William Gosper (see Gardner, 1976, p.125-126), were good first-order models of river networks. He wrote, "*As a matter of fact if a tree made of rivers of vanishing width is to drain an area thoroughly, it must penetrate everywhere. One who follows the rivers' combined bank performs a plane-filling motion*" (Mandelbrot, 1983, p.59). Being a natural example of Peano curves, Mandelbrot speculated that the fractal dimension for river networks ought to be 2. Recently, Culling and Datko (1987), La Barbera and Rosso (1989, 1990), Tarboton et al. (1988, 1990), and Liu (1992) attempted to confirm or to refine Mandelbrot's speculation.

Culling and Datko (1987) viewed the soil-covered landscape as the composite product of stream erosion and a general diffusion-degradation regime. They adopted a

two-segment piecewise linear fractal model and interpreted the D value for the longer distance range as representing the work of the drainage system. They considered the drainage network as a boundary condition, stable in the short term, to which the landscape surface had to fit and expected that the fractal dimension of the drainage network would be comparable to that of contour lines and profiles in the longer distance range. They calculated the fractal dimension of the drainage networks on seventeen 1:25,000 scale topographic maps of sites in southern England. The D values for their data sets range from 1.49 to 1.77, with an average D value of 1.608. They compared the D values for the drainage networks with those for contour lines and topographic profiles and found that the drainage networks were invariably of higher D values than contours and profiles. They explained the discrepancy by the degree of smoothing that took place in the delineation of the valley pattern by the contours.

La Barbera and Rosso (1989) propose that for an ordered drainage system the fractal dimension can be derived from Horton's laws of stream number and stream lengths. This results in a simple function of bifurcation and stream length ratios of the drainage system. They argue that there is not a single fractal dimension for all drainage basins, but it varies from two to unity depending upon the specific composition of a river network. The analysis of a large sample of field data showed the typical fractal dimension of river networks to lie between 1.5 and 2, with an average of 1.6 - 1.7. These results were confirmed by the estimates derived from the relationship between the observed total length of streams and basin area. They point out that the value of 2 corresponds with the modal values of Horton's order ratios for topological randomness. Thus, it describes a limiting case only, i.e., self-forming networks which have developed to maturity in the absence of geological, topographic, and sedimentological constraints. It is expected that natural networks will display fractal dimensions smaller than 2 unless the dendritic system uniformly covers the entire drainage area.

Tarboton et al. (1988) approached the problem somewhat differently. They used three empirical methods for estimating the fractal dimension of river networks: the

walking dividers method, the box counting method, and the method based on the relationship between the stream length and the number of streams or the "distribution of stream length exceedances". They selected eight river networks from New Hampshire, Connecticut and Arizona as their test cases. They have shown that river networks as a whole are practically space-filling with fractal dimension near 2 although individual rivers are extremely smooth with fractal dimension ranging from 1.05 to 1.10. Thus, their results are in complete agreement with Mandelbrot's speculated values. In order to account for the inconsistency between their results and those of La Barbera and Rosso (1989), Tarboton et al. (1990) suggested an extension to the algorithm proposed by La Barbera and Rosso (1989). They argued that the differences were due to a simplified assumption made by La Barbera and Ross (1989) that individual streams were simple linear measures. If the fractal dimension of individual streams were used as a scaling factor in La Barbera and Ross' algorithm, the results of both studies would come into complete agreement. Nevertheless, La Barbera and Rosso (1990) questioned the validity of their extension.

Liu (1992) adopted the model of loopless random aggregate trees to describe the fractal structure and properties of stream networks. He showed how the five fractal dimensions which are used to characterize loopless random aggregates, namely, topological dimension, minimum path dimension, fractal dimension of a cluster, diffusion dimension, and spectral dimension, could be similarly defined for stream networks in terms of Horton's network composition. He used his formulations to compute the fractal dimensions of twelve stream networks in the Appalachian Plateau and obtained the average values of 1.55, 1.20, 1.82, 3.02, and 1.21, respectively. He pointed out that the minimum path dimension of 1.2 supports Mandelbrot's (1977) fractal interpretation of the empirical relationship reported by Hack (1957). Using the analogy of random aggregate trees, Liu interpreted that the fractal dimension of stream networks as a whole, the topological dimension, and the minimum path dimension are static parameters which characterize geometrical and topological structures of stream networks and

the diffusion dimension and the spectral dimension are dynamic parameters which may characterize the hydrodynamic transport properties and network connectivity of stream networks, respectively. He also related the diffusion dimension to the shape parameter α and the spectral dimension to the dimensionless product G* in the instantaneous unit hydrograph, which are often used to characterize the hydrological response of stream networks.

In addition, several studies have been carried out to investigate the fractal nature of individual streams. Based on the empirical relationship between the length of the mainstream course and the area of a drainage basin derived by Hack (1957), Mandelbrot (1977, p.73) suggested that rivers were fractals with fractal dimension of about 1.2. Mandelbrot's prediction rests on one important assumption: the measured area does not change with change in map scale. To test this hypothesis and the accuracy of the predicted D value, Hjelmfelt (1988) selected maps of eight catchments in Missouri for analysis. He demonstrated that if a river channel were fractal, then its measured length would be related to the scales of source maps as follows:

$$L_2 / L_1 = (S_2 / S_1)^{1 - D}$$

where L_1 and L_2 are length measurements at different scales, S_1 and S_2 are map scales, and D is the fractal dimension. He used this relationship to estimate the fractal dimension of river channels. He found that the fractal dimension was not constant, but varied between 1.036 and 1.291 with a mean value of 1.158, which is reasonably close to the value of 1.2 hypothesized by Mandelbrot (1983). He also confirmed that the measured areas were only affected slightly by map scale, having fractal dimensions ranging between 0.9975 and 1.052 with a mean of 1.0105.

Snow (1989) performed another detailed fractal analysis of river planform for twelve single-channel stream segments in the western Ohio River drainage basin. The planforms used are mid-channel traces of streams as represented on 1:24000 scale

topographic maps, digitized at data point spacing of approximately 1 mm map distance. The analysis dealt with planform characteristics on scales ranging from 0.1 km to the total segment length, in some cases exceeding 100 km. His study showed that as the divider opening size approached the channel width or the whole length of the stream segment river paths appeared as smooth Euclidean shapes. However, at scales relevant to river meandering river traces could be most reasonably treated as fractal curves. The fractal dimensions of the twelve stream segments he studied range from 1.04 for Wabash River, Indiana to 1.38 for the Big Indian Creek near Georgetown, Indiana, giving an average D value of 1.25. Snow also used the inflection point on the Richardson plot between intermediate and large scales as a value of river course length to compute an additional measure of the irregularities of stream traces, which he termed "fractal sinuosity". It is obtained by dividing the small scale asymptote on the Richardson plot with the river course length represented by the inflection point. The values range from 1.1 to 2.6. It is interesting to note that the ranking of the streams based on "fractal sinuosity" is quite different from that based on their fractal dimensions.

Robert and Roy (1990) combined the length measurements obtained from maps of three different scales (1:20,000, 1:50,000, 1:125,000) and used the walking dividers method to estimate the fractal dimension of ten interior segments of the Eaton River in the Eastern Townships, Quebec (Canada). The fractal dimensions they obtained range from 1.035 to 1.127 with an average D value of 1.085. However, the major purpose of their study was to demonstrate that any relationship involving basin and stream length should be made for comparable map scales. They have shown that the subjective, non-systematic cartographic generalization in the representation of stream heads at different scales introduces an allometric component in the slope of the regression line between stream length and basin area and affects the intercept of the regression line. To compound the problem, this allometric component is only present at certain scales (smaller scales) but not others. The subjectiveness and lack of a systematic standard in

the process of cartographic abstraction make it extremely difficult to establish a simple relationship between the slope of the regression line of stream length against basin area and the fractal dimension of streamlines.

Another investigation on the fractal nature of streams was carried out by Nikora (1991). He calculated the fractal dimensions of forty-six morphologically homogeneous sections of eight rivers in Moldavia, both for river channels and for river valleys. He used the walking dividers method for estimating the fractal dimension of single-thread channels and the box-counting method for measuring the fractal properties of multithread rivers. The fractal dimension of river channels he obtained range between 1.0 and 1.33. The D value for most river valleys is 1.0, while eleven sections yield fractal dimension ranging between 1.10 and 1.30.

Based on his study, Nikora (1991) concluded that the estimation of fractal properties of plan patterns within separate watercourse using the relationship between the measured length of the main river channel and the area of the drainage basin, empirically derived by Hack (1957) and first used by Mandelbrot (1977), was an incorrect procedure. His conclusion was based on the relation given by Ogievsky (1951) for determining the areas of drainage basins and the assumption that the fractal nature of river plan pattern was limited by the river bed width and the width of the river valley. The formula given by Ogievsky (1951) is as follows:

$$A = s\,l$$

where

A is the area of the drainage basin

l is the distance between the headwater and river mouth along a straight line

s is a function of catchment shape, which varies from 0.3 to 0.6

The algorithm introduced by Mandelbrot (1977) implies that the fractal nature of river plan patterns extends up to the distance l, which contradicts Nikora's assumption on

the limits of statistical self-similarity. Furthermore, as mentioned previously, an important assumption for the algorithm based on the relationship between the measured length and the basin area is that the measured area does not change with change in map scale, which is inconsistent with the changing values of s in the above equation. However, the upper scale limit chosen by Nikora for studying the fractal properties of short segments of river channels may be far too small for the entire main river course within a drainage basin. In addition, Hjelmfelt's (1988) work on the effects of changing map scales on the measured areas of drainage basins indicated that the measured areas varied with map scale only slightly. Thus, additional research is needed to verify or refute the criticism of Nikora (1991).

Besides coastlines and stream networks, several studies have been carried out to examine the fractal characteristics of some terrain elements in limestone regions. Curl (1960, 1966) has previously observed that lengths of all caves in each of a number of regions are distributed hyperbolically. Recently, he (Curl, 1986) extended his studies on geometries of caves within the framework of fractal geometry. He examined the number of caves in relation to the cave size for all proper caves of Pennsylvania and derived a fractal dimension of 1.4. Using the property of self-similarity of fractals, he extrapolated the distribution of proper cave lengths from the observed range to a nominal proper modulus for estimating the total number of all proper caves in this region. He also applied these concepts to other geometrical properties of caves. On the basis of self-similarity, he postulated a linked modular element model for cave geometrical properties. He has shown that if the total length of all caves in a region is a self-similar fractal, it will have a fractal dimension between 2 and 3 and the total number of linked modular elements in a region is a self-similar fractal of the same dimension. He has also shown that the expected conditional distribution of modular element sizes in a cave, given length and modulus, is also distributed hyperbolically. Analysis of cave survey data for Little Brush Creek Cave, Utah yielded a fractal dimension of 2.79 for the distribution of sizes of linked modular elements, which is in the same range as

the Manger Sponge. He argued that the linked modular element model and his algorithm for counting modular elements between stations provided a logical definition of length of a cave. He also provided examples of estimating cave volume and the maximum number of traverses required to survey caves of different lengths.

Laverty (1987) analyzed the line skeletons of cave passages in four different regions and found that both the line skeletons projected on a plan and the actual three dimensional configurations exhibited fractal behavior with dimensions in the range between 1.074 and 1.546 over a range of measurement resolutions from 1 to 100 meters. He suggested that the combination of characteristic lengths and fractal dimensions would be of use as indicies for comparison of different cave passages both with each other and with experimental and theoretical models for passage development.

Reams (1992) utilized the area-perimeter measurements to determine whether perimeters of sinkholes were fractals. Six karst surfaces from Florida, Kentucky, Indiana and Missouri were selected for analysis. He has shown that sinkhole perimeters of large sinkholes (larger than 10,000 square meters) appear to be fractals. The fractal dimension ranges from 1.209 to 1.558. He speculated that the fractal dimension might eventually prove to have a fairly unique value for specific karst regions. He also found that when only the large sinks were considered, the perimeter-number and area-number distributions of sinkhole populations appeared to have fractal character as well.

Another linear terrain element of fundamental significance in geomorphology, which has been subjected to fractal analysis, is drainage basin perimeters. Breyer and Snow (1992) studied the perimeters of six drainage basins from southern Indiana and of an additional six from large U. S. basins and concluded that basin boundaries were fractal or near-fractal shapes. They have discovered that although the basins differ significantly in physiography, the fractal dimensions obtained fit within the narrow range 1.06 - 1.12, indicating that while basins may differ greatly in overall shape, they are very similar in terms of smaller-scale boundary irregularity.

McClelland (1985) explored the potential of using the fractal dimension as a quantitative measure of the progress of erosion along mountain fronts. He first calculated the so-called "mountain front sinuosity" (the ratio of the mountain-pediment junction to the length of the mountain front) for the Allegheny Front in eastern West Virginia (from Montgomery Run to the right fork of Linton Creek). The length of the mountain-pediment junction was determined by walking dividers along the 2,000 foot contour line on maps at three different scales (1:125,000, 1:62,500, 1:24,000). A rotating wheel map measurer was also used. It was found that the value of "mountain front sinuosity" varied with the scale of maps and the method of length measurement. These variations due to map scale and method of measurement are large enough that they may obscure the variation due to factors as progress of erosion or differential erosion due to different lithologies. To improve the comparability of results based on measurements made on maps of different regions at different scales, McClelland turned to the fractal technique. He computed the fractal dimension of the mountain-pediment junction using length measurements determined on maps of three different scales and found that the values for the fractal dimension showed less variation with scale (D = 1.123 at 1:125,000, D = 1.162 at 1:62,500, D = 1.067 at 1:24,000) and no variation with measurement method.

3.4 Development of Terrain Simulation Algorithms

The use of fractals as terrain models was first introduced by Mandelbrot (1975c) by extending his one dimensional fractional Brownian motion into two dimensions. Over the years, at least seven different algorithms have been used or suggested for approximating two dimensional fractional Brownian motion. These include (1) the independent cut method, (2) the midpoint displacement method, (3) the method of successive random additions, (4) the square-square recursive subdivision method, (5) the Fourier filtering method, (6) the modified Markov method, and (7) the method based on the two dimensional extension of the Weierstrass-Mandelbrot random fractal func-

tion. Most of these methods have been described by Voss (1988) and Saupe (1988, 1991). Jeffery (1987) and Saupe (1988, 1991) provided some pseudo code for several of these algorithms.

The idea of using fractional Brownian surfaces as models of earth's relief first occurred to Mandelbrot when he was contemplating with the figures of a scalar random walk produced by William Feller (1950) based on the results of tossing a coin (Figure 3.1). He (Mandelbrot 1963c, p.435) observed that the whole graph's shape was reminiscent of a mountain's silhouette or of a vertical section of earth's relief. Hence, he set out to search for a random surface whose vertical sections are Brownian line-to-line functions. Unfortunately, the tool box of the builder of statistical models contained no such surface. Thus, he (Mandelbrot, 1975c) adopted the Brownian plane-to-line function of a point as defined by Levy (1948) as a crude model of relief on a flat earth.

The construction of the surface starts with an earth of zero altitude or a horizontal plateau, then breaks it along a succession of rectilinear faults, and in each case displaces the two sides vertically to form a cliff. The positions of the faults and the heights of the cliffs are assumed random and mutually independent, the former being isotropic with a high average density, and the latter having zero mean and finite variance. Mandelbrot (1975c, p.3825) referred to this particular model as the "Poisson-Brown stochastic model" because the points of intersection of a set of isotropically random and mutually independent faults with any straight line form a Poisson point process and by rescaling the cliff heights to make them decrease as their number increases and letting the average number of points of intersection per unit length tends to infinity, the Poisson process tends to a Brownian motion.

The "Poisson-Brown" primary model has isotropic increments and satisfies many of the theoretical abstractions from actual observations of natural terrains. It is simple, explicit, direct, and intuitive. However, the predicted value $D = 1.5$ is not satisfactory.

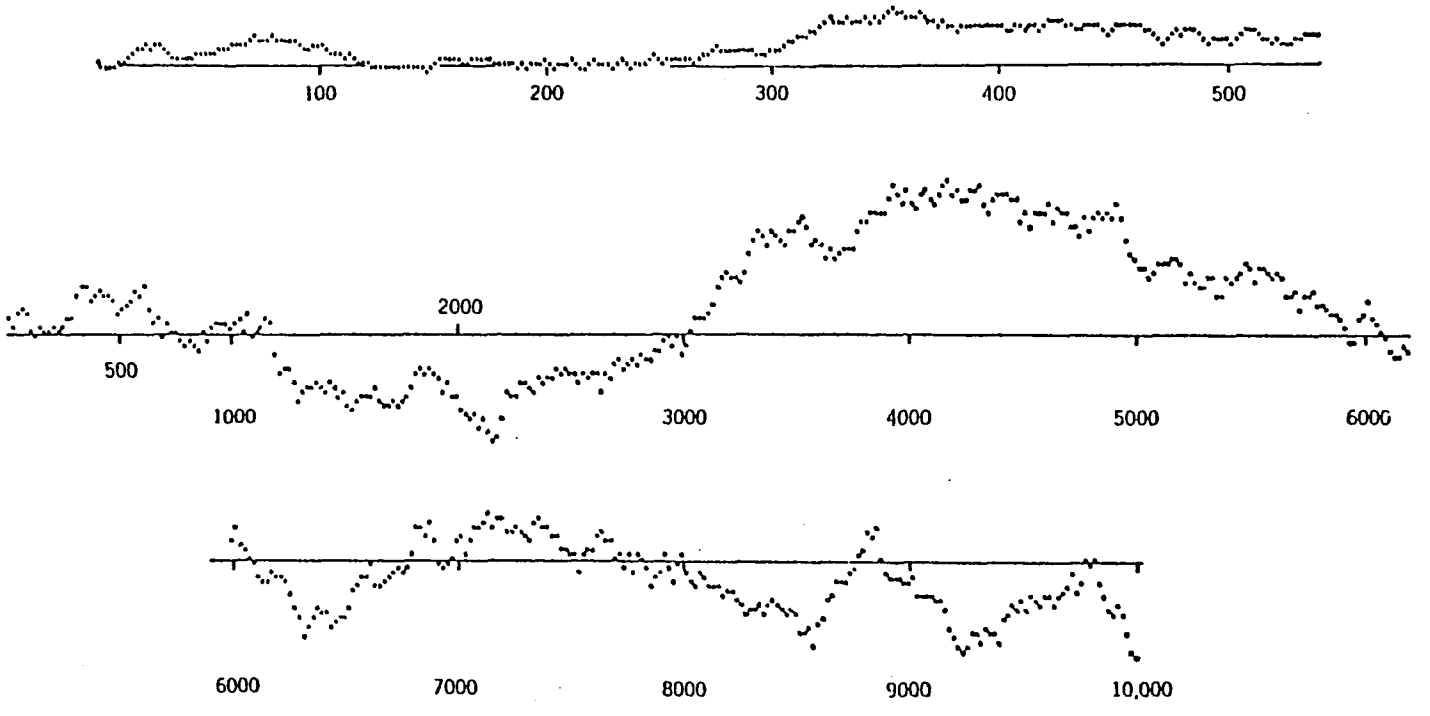

Figure 3.1 **A Sample Random Walk Approximating a Brown Line-to-Line Function. The shape of this graph is reminiscent of a mountain's silhouette and prompted Mandelbrot to use the fractional Brownian motion as a model of natural terrain. (from Feller, 1950)**

No single value can represent the relief everywhere, and most observed values are well below 1.5. This discrepancy is confirmed by the excessively irregular appearance of the simulated primary relief and coastlines. Secondly, the relative area predicted for the largest islands by the Poisson-Brown stochastic model is too small. To increase the realism of the simulated landscapes and to be able to model terrain surfaces with different degrees of irregularities, Mandelbrot replaced the Brownian function by its fractional variant. One approach for producing fractional Brownian surfaces is by resorting to cliffs with a very special kind of profile, which rise very gradually but forever on both sides of each fault. This generalization made it possible to generate surfaces with D values ranging from 2 to 3. This algorithm for calculating discrete approximations to fBm has been variously referred to as the method of "independent cuts" (Voss, 1988, p.48) or "independent jumps" (Saupe, 1988, p.80), "the random cut method" (Saupe, 1988, p.72), or "the shear displacement process" (Fournier et al., 1982a, p.375). This is the algorithm used by Goodchild (1982) and Klinkenberg (1988) for their terrain simulations.

Additional terrain simulations produced using the random cut method were included in the first English edition of Mandelbrot's book on fractals, **"Fractals: Form, Chance, and Dimension"** (Mandelbrot, 1977, p.210-215). Synthetic surfaces with different D values were made into hill-shaded images to enhance the visual effects. Mandelbrot (1977, p.216-217) also generated a fictional fractal Pangaea by implementing on the computer another random surface due to Paul Levy (1959), a fractional Brownian function from the points on the sphere (the latitude and the longitude) to scalars (the altitude). This particular model replaces the flat base surface of earth's relief used in the previous constructions by a sphere. Many of these simulations are reworked and included in Mandelbrot (1983).

In 1980, Carpenter (1980) and Fournier and Fussell (1980) presented the results of two independent research efforts on a simpler algorithm for generating fractal surfaces at the SIGGRAPH Conference in Seattle, Washington. The detailed account of

their work was later published as a joint paper (Fournier et al., 1982a).

The method used by Fournier et al. (1982a) is based on subdivisions of polygons such as triangles or quadrilaterals which are commonly used to represent real world data. This method is often referred to as the "midpoint displacement" or "recursive subdivision" method (Mandelbrot, 1988b, p.243). Each triangle is subdivided into four smaller triangles by connecting the midpoints of the sides of the triangles. The vertical positions of these midpoints are obtained by displacing them a random distance up or down. A quadrilateral can be subdivided in a slightly more complex way. First, the midpoint of each of the four sides is located. For each of the two pairs of opposed midpoints, the midpoint of the line connecting them is displaced using the same procedure. The midpoint of the line connecting these two midpoints becomes the center point of the quadrilateral subdivision and four smaller quadrilaterals are created. These subdivisions can be continued until the desired resolution is obtained, resulting in a fractal triangle whose irregular surface consists of many small triangular facets or a fractal quadrilateral whose surface is composed of many quadrilateral facets. Mandelbrot (1988b, p.251) called the midpoint displacement method using triangles as the initial lattice the "wire frame midpoint displacement" and the construction using squares as the initial lattice the "frame-tile hybrid midpoint displacement". In the "tile midpoint displacement", the surface is thought of as a collection of tiles, and one displaces points in the middle of every tile.

Mandelbrot (1982) has shown that the midpoint displacement technique does not yield true fBm for $H \neq 1/2$. This process does not have stationary increments. Points generated at different stages have different statistical properties in their neighborhoods. This defect causes the surfaces to exhibit some disturbing creases along straight lines, which are related to the underlying grid of points. The effect becomes more pronounced as H tends to 1. These artifacts, which occur at all stages, can not be eliminated by local smoothing. Mandelbrot (1988b) believes that the so-called "crease problem" is caused by the use of squares as the initial lattice and by "the nesting of

the frames". He suggested two new approaches using tiles to minimize the creases in the simulated fractal landscapes based on the midpoint displacement algorithm. A first approach avoids squares and uses the classical triangle tiles, whose frames are nested. A second approach uses tiles that are based on the hexagon, but are actually bounded by fractal curves; their frames are not nested.

Nevertheless, the midpoint displacement algorithm has many attractions. The calculations involved are simple ------ only a few additions and multiplications. More importantly, you need to perform these calculations only once for each point, so the number of calculations is linearly related to the number of points. In addition, this technique allows you to add "detail" to an existing shape. For these reasons, this algorithm became most popular after its first use by Fournier et al. (1982a). Recently, it has been included as a part of some computer graphics textbooks (see Hearn and Baker, 1986; and Harrington, 1987).

Since the work of Fournier et al. (1982a), several attempts have been made to circumvent the crease problem. Voss (1985b, 1988) introduced a modified algorithm which reduces the visual impact of creases, the method of successive random additions. In this method, you interpolate the midpoints in the same way, and then, instead of adding a displacement of a suitable variance only to the midpoints, you add it to all points at each stage of a recursive subdivision process. This modification reduces many of the visible artifacts of midpoint displacement and the generation still requires only order N operations to generate N points. The enhancement produced by the successive random additions over the original midpoint displacement method is clearly demonstrated in Figure 1.15 in Voss (1988, p.56).

With successive random additions, at each stage all points are treated equivalently. This has the additional advantage that the resolution at each successive stage can change by any factor $r < 1$. For midpoint displacement, r must be 1/2. The free choice of a value for r is an important addition for film-making. The addition of

irregularities to a surface can be accomplished continuously as the resolution is slowly increased from frame to frame.

Miller (1986) also attempted to improve the visual quality of the landscapes synthesized using the midpoint displacement techniques. In order to gain first order continuity in the interpolant, he removed the requirement of having the surface passing through the control points. He used an initial surface consisting of squares. Instead of interpolating at the midpoints of edges of squares, the new points are generated at the corners of an interior square which is half the size of an initial square. Thus, Miller's method can be referred to as the "square-square recursive subdivision method". The new elevation values are obtained with distance weighting in the proportion of 9:3:3:1, the nearer points having the greatest weights. This leads to an interpolant which in the limit is a biquadratic surface. With this method the control points deflect the surface but do not normally lie on it. When randomization is incorporated into the generation of height values, a wide variety of terrains ranging from rolling hills to rough mountains can be synthesized by changing the H parameter and by exaggerating the elevations of control points. Sample images produced using this algorithm show no creasing artifacts as seen in landscapes generated by the midpoint displacement methods.

The fifth algorithm for approximating the fractional Brownian motion is the fast Fourier transform filtering method (Voss, 1988, p.49). This method is also known as the "spectral synthesis method" (Saupe, 1988, p.90). Voss used this method to generate most of the color plates of realistic-looking fractal terrains included in Mandelbrot (1983). The specific procedures of the fast Fourier transform filtering method involve the generation of Gaussian white noise, in which all frequencies are equally represented, and then filtering it using fast Fourier transform techniques in order to force the different frequencies to fall off as required by the value of the parameter H for the particular fractional Gaussian noise desired. The mathematics of the algorithm was elaborated in Voss (1985a, 1985b, 1988) and Saupe (1988, 1991).

The images generated using the fast Fourier transform filtering method do not resemble many of the valleys on the earth's surface which are significantly eroded. Voss approximated a flat bottomed basin by taking the height variations and scaling them by a power law. The effect of a power greater than 1 is to flatten the lower elevations near the water emphasizing the peaks. Scaling with a power less than one has the opposite effect of flattening the peaks while increasing the steepness near the water. However, it should be pointed out that the use of such nonlinear processing is entirely based on the visual appearance of simulated images without any consideration of its physical significance.

Another approach for calculating discrete approximations to fBm involves a modified Markov process which uses the weighted sum of previous values plus a random component (Mandelbrot and Wallis, 1969, and Mandelbrot, 1971). This method is based on an algorithm to compute an approximation to discrete fractional Gaussian noise, which is the increment of fBm. The algorithm computes what Mandelbrot called the "fast fractional Gaussian noise" as a sum of a low frequency term and a high frequency term. The high frequency term is a Markov-Gauss process. The low frequency term is a weighted sum of M Markov-Gauss processes, M being a number proportional to log (N).

Yfantis et al. (1988) extended the modified Markov process introduced by Mandelbrot (1971) and Mandelbrot and Wallis (1969) for generating surfaces passing through a given network of points on a three-dimensional space. These surfaces can also be produced using kriging, bicubical splines, and an algorithm based on the assumption that the network of points constitutes a multivariate normal. However, unlike these methods, the fractal-based method does not depend on the assumption of normality. In addition, the newly generated points using the fractal-based algorithm preserve the mean of the random process and preserve the autocorrelations with neighboring points from which these new points were generated. All nonfractal techniques for surface generation introduce a degree of smoothness in the estimation process,

whereas the fractal methods introduce a roughness, and yet they preserve the long-range structural characteristics of the surface. The algorithm described by Yfantis et al. (1988) differs from other fractal algorithms in that the surface generation is controlled by a given network of points.

The surface construction begins by connecting the given network of points to form quadrilaterals which provide a first approximation to the surface. For each quadrilateral, a new elevation value is calculated for the midpoint of each edge using the modified Markov process. Subsequently, the algorithm is used to find midpoints of the two line segments joining opposite midpoints of the original edges. The average of these two midpoints constitutes a new midpoint at the center of the quadrilateral, and the five new vertices along with the four original corner points help to define four new quadrilateral patches. The process continues in each one of the patches until the length of the maximum edge is less than a prespecified resolution. So far, no implementation of this algorithm has been carried out.

The last possible algorithm for generating fractal terrain surfaces is based on the generalization of the Weierstrass-Mandelbrot random fractal function. The Weierstrass-Mandelbrot random fractal function is a periodic function. Extensions to E > 1 are possible with periodic functions in all E coordinates. Voss (1988) pointed out that both the midpoint displacement process and the successive random additions are related to Mandelbrot's generalization of the Weierstrass non-differentiable function. Both midpoint displacement and successive random additions correspond to a triangle periodic function in place of sin (x). In addition, midpoint displacement sets all ϕ (a random phase) = constant.

There is one thing in common to all of these fractal-based terrain simulation algorithms. They were developed by mathematicians and computer scientists who were more interested in the simplicity of mathematical functions and the visual appearance of simulated images and less concerned with the constraints exerted by natural

geomorphological processes. As a result, when these algorithms were tested against natural surfaces, many discrepancies emerge. Mandelbrot (1988b) described three defects of the simulated landscapes. The most basic defect of past fractal forgeries of landscape is that every one of them fails to include river networks. A second defect is specific to the midpoint displacement method. It is related to the so-called "creasing problem". A third defect present in most forgeries is that the valleys and the mountains are symmetric because of the symmetry of the Gaussian distribution. Some of these defects were pointed out by Mark (1979) when he first introduced Mandelbrot's book on fractals to geo-scientists.

These deficiencies prompted some geo-scientists to improve the preliminary models proposed by mathematicians. The most notable example is the scale-based model of topographic relief developed by Clarke (1988). Clarke's model was based on the belief that scale itself must form the basis for a model of terrain. Geomorphological studies clearly indicate that different geomorphological processes dominate within different scale ranges. At small scales, topography consists of slopes with fairly predictable characteristics, determined largely by gravity and tectonic processes. At intermediate scales, both structural and geomorphological processes determine the geometrical characteristics of landforms. At large scales, down to the level where distances are in meters and tens of meters, individual boulders, mass wasting, vegetation characteristics, human intervention, landslides and a myriad of other local processes tend to dominate. These processes result in small features with a larger stochastic component. Mark (1979, p.203) commented that "*few if any geomorphologists would accept the idea of self-similarity of terrain: different geomorphic processes tend to show their effects at specific scales, and for most coastline or contour segments, a trained geomorphologist could assign an approximate scale based on such features.*" Clarke (1988) believes that two types of variations exist within topography. On one hand, large features in the landscape are scale-dependent and show significant scale and size relationships. On the other hand, the residual characteristics of terrain when

the scale-dependent structure is extracted can be modeled effectively as scale-independent features. This implies that the much-discussed fractal model of topography is actually a special case for landscapes where structure is missing.

The scale-based model views the elevation value at any particular point as the sum of four distinctive components and uses trend surface analysis, Fourier techniques, fractal method based on power spectrum, and a local erosion operator in the simulation process. The model can be calibrated using highly generalized, real terrain data and then inverted to simulate land surfaces with specific characteristics. It begins by computing and subtracting a linear trend surface from the terrain equivalent to the extraction of a scale component with an extremely large wavelength. Then, small scale features are modeled using sets of trigonometric series, in particular the sums of pairs of sine and cosine waves with different wavelengths and amplitudes. These two steps are designed to capture the essential geometric elements of large "topographic structure". The residual stochastic "textural features" are modeled as a fractional Brownian fractal. The final phase of the model involves a local operator to find pits and fill them by averaging their elevations with the next lowest neighboring grid cell. The local operator accounts for the effects of local processes, in particular mass wasting.

Clarke calibrated his model using digital representations of actual terrain and then inverted the model to simulate topographic surfaces. His initial test has shown that the scale-based model can produce quite realistic terrain with some desirable cartographic traits. His later study (Clarke, 1992) suggested that for the structural element of topography the more components were used in the inverse Fourier transform, the more realistic the image appeared and when the fractal texture reached more than five percent of the total relief the image began to look too rough and artificial.

Yokoya et al. (1989) also attempted to improve terrain simulations by using fractal parameters extracted from real terrain data to produce digital elevation models of higher spatial resolution. The purpose of their study was to produce digital elevation

models of various spatial resolutions needed in sensor simulations for an earth resource satellite from the existing coarse resolution terrain data. The modelling process consisted of two steps. First, fractal parameters were extracted from real digital terrain data. The fractal parameters they examined included the fractal dimension, the distribution function, the scale limits, and a measure of linearity of fractal plots. And then ,these parameters were incorporated into their algorithm for stochastic interpolation to extend the statistical characteristics of terrain shape to higher spatial resolutions than the original data set. The sample data set they used was produced by sampling the elevations at an equal interval of 250 meters. The interpolation algorithm they adopted was a recursive midpoint displacement scheme using four neighbors. Based on the fractal analysis of real terrain data, they concluded that real terrain surfaces have fractal features in a rather wide range of scales and therefore the surfaces can be approximately described as fractals using fractional Brownian functions. On the other hand, their study also revealed that fractal parameters are not constant over all areas of the real terrain surface but vary smoothly from place to place. Thus, they used locally computed fractal parameters to interpolate the original surface, giving the name "adaptive dynamic interpolation" to their interpolation method. They compared the result of adaptive dynamic interpolation with a simple enlargement of the contour map generated from the original digital terrain data, a contour map produced by using linear interpolation of the original terrain data, and a contour map manually drawn from a topographic map. Their experiments indicate that the terrain surface can be well interpolated by using the extracted fractal parameters, which preserves the intrinsic characteristics of a real terrain shape in the smaller scales, and the fractal-based interpolation produces much better representation of the real terrain surface than simple linear interpolation.

3.5 Improving Existing Geomorphological Models

So far, relatively little attention has been given to linking the fractal geometrical form to the underlying geomorphological processes and to integrating fractal research with some classical geomorphological models. Nevertheless, there have been several studies that point our way into these directions.

Upon examining a series of synthetic terrain simulations he generated using a fractal-based algorithm, Goodchild (1982) noted the resemblance of these synthetic terrain surfaces to natural landscapes lacking in deterministic geologic controls or the influence of geomorphological processes, such as the lunar surface, dead-ice topography, or landscapes dominated by recent tectonic activity. Recently, he (Goodchild, 1988) investigated the usefulness of fBm simulations of surfaces as the basis for statistical analyses of lake-rich landscapes. One tradition in geomorphological studies is to view the present landforms as the result of processes operating on some pre-existing form. Obviously, a complete understanding of the landform characteristics requires models both of the process and of the prior form. Goodchild suggested that fractal simulations could be regarded as appropriate null hypotheses for terrain, because the simulations lack any evidence of modification by geomorphic processes. They therefore represent a point of reference or norm against which to compare results of statistical analyses of real landscapes. The use of fBm surfaces as starting points in process simulation is particularly attractive because these surfaces are irregular surfaces and probably more typical of the initial landforms present in the real world than regular surfaces such as an uplifted block (Davis, 1899) or tilted planes (Sprunt, 1972; and Hugus and Mark, 1985).

Being convinced that erosional landforms are generally scale invariant and fractal, Newman and Turcotte (1990) proposed a non-linear dynamic model for the evolution of erosional landforms that will produce self-similar topography. Their model is based on the belief that the largest storms produce the greatest erosion. Great storms create

new gullies on all scales and thereby renew the erosional features that have been gradually removed by smaller storms. Recognizing the inadequacy of all linear models in describing actual erosional topography, they introduced a modified Fourier series based on wave numbers, which forms the basis for a renormalization approach. Their non-linear erosion model involves the cascading decay of each modified Fourier series coefficient. They have shown that their model gives an evolving fractal distribution of morphology even if the initial distribution is not fractal. They argued that the fractal nature of erosional landforms indicated a fractal distribution of erosion, which in turn suggested a fractal distribution of storms and floods.

Very recently, Clarke (1992) extended his scale-based model by introducing two additional erosion operators: a fluvial erosion operator and a parallel retreat erosion operator. By so doing, he transformed his original model for terrain simulation into a dynamic model of landform evolution. The addition of these two local operators was clearly an attempt to incorporate the elements of two of the most popular landform evolution models, namely, the downwasting model of William Morris Davis (1899) and the parallel retreat model of Walther Penck (1924), into fractal terrain simulation. The fluvial erosion operator works on an eight-cell neighborhood and simulates the movement of water locally, moving material from the highest point to the lowest within the neighborhood. It simulates the effect of smoothing of surface roughness by overland and stream erosion. The operator combines the fluvial effects of cutting and deposition of material into a single pass and allows headward erosion and downcutting of stream channels until it reaches the overall grid minimum, a sort of "base level" for the erosion. The parallel retreat erosion operator is designed to simulate terrain in extra-terrestrial and desert environments. In this case, erosion takes place only in areas of high gradients, and material is allowed to disperse widely over the less steep areas.

Clarke examined the differences between these two erosion models in the rate of erosion and their effects on the standard deviation of elevation which has traditionally been used as a measure of surface roughness. In the case of the parallel retreat

operator, successive passes resulted in less material being removed, with a resulting increase then stabilization of the elevation standard deviation. On the contrary, the stream erosion continued to remove material during each pass and resulted in smoother and smoother slopes after an initial increase in roughness.

The concept of fractal dimension has also been used by Chase (1992) to develop a three dimensional model of fluvial landscape evolution based on cellular automata. The model works by accumulating the effects of randomly seeded storms or floods (precipitons) that cause diffusive smoothing then move downslope on digital topographic grids, that erode portions of elevation differences, that transport a slope-limited amount of eroded material, and that deposit alluvium when their sediment-carrying capacity is exceeded. Chase believes that these processes sculpt the land surface into fractal landscapes which in return provide feedback to affect the operation of on-going processes or to initiate new surface processes. The fractal geometry arises from the balance between roughening at all scales by erosive processes and smoothing at small scales by diffusive processes augmented with smoothing at large scales by depositional processes. Chase used the mean fractal dimension to assess quantitatively the effects of the various processes on the complexity of the model landscapes.

Using his model, Chase studied the effects of terrain slope, the areal size, the erodibility of the surface materials, and the amount of rainfall on the efficiency of diffusive smoothing, and the influence of slope and discharge, particularly the maximum effective storm size (proxied by sediment-carrying capacity), on the ability to erode and the transport capacity of the precipiton. The erodibility of model materials, the ratio of diffusive action to erosive action, and the sediment-carrying capacity are all to some extent proxies for climatic variables. Chase also examined the problem of how tectonic activity (block uplift) would affect the model fractal dimension. His experiment showed surprisingly that during the uplift the fractal dimension reached some sort of steady state, then actually rose slightly when the uplift stopped. Chase believes that the reason for the negative correlation between tectonic activity and the

fractal dimension is because tectonically active areas do not allow adequate time for much landscape dissection by lower-order streams. Thus, the degree of landscape complexity appears much more responsive to climatic influences than to tectonic control. Chase's findings based on numerical modelling were substantiated by Lifton and Chase (1992) by analyzing the landform characteristics of the San Gabriel Mountains, California.

Mayer (1992) and Snow (1992) attempted to improve our understanding of geomorphic processes by adopting fractals to model the temporal distribution of geomorphic events. Mayer (1992) fitted the daily precipitation sequences from eight desert climate stations in southern California and Nevada to a Cantor dust model. He pointed out that "*it is clear that a precipitation sequence will not exhibit self-similarity at all precipitation amounts (magnitudes) because at long time intervals, the occurrence of an event appears to be dominated by a Poisson process.*" Thus, he examined the sequences of precipitation events of similar magnitudes. His study shows that desert storm sequences exhibit fractal characteristics at time intervals less than 100 days and non-fractal characteristics at time intervals greater than 100 days. He calculated the fractal dimension of the precipitation sequence recorded at each station using the data points for time intervals less than 30 days. The fractal dimension varies from 0.372 for the Bishop (California) climate record to 0.260 for the Eagle Mountain (California) record. These values are much different from the fractal dimension for Oxford, Ohio (D = 0.939), where the climate is humid continental. However, by comparing the results of real climatic records with those of a Poisson generated sequence of events, Mayer has found that the precipitation sequences retain the characteristics of a random component as well. He argues that the clustering of precipitation events plays an important role in determining the final outcome of geomorphic processes. The fractal dimension provides a useful measure of event clustering and allows more precise characterization of a climatic type, which is a crucial element in every model of geomorphic processes.

Snow (1992) adopted the Cantor dust model to describe the temporal discontinuity in geomorphic processes that is responsible for the dependence of measured process rates on the time intervals measurement reported in literature. Points along the length of the dust represent geomorphic process events arrayed through time. Gaps in the dust are time intervals of process inactivity. Specifically, he used the Cantor dust to model of the temporal discontinuity of uplift and denudation rates. Snow found that uplift events were slightly more clustered in time than were denudation events. The fractal dimensions estimated for processes of uplift and denudation are 0.75 and 0.81 respectively. He has also shown that the results obtained from application of the Cantor dust model are unaffected by the variability in the magnitude of geomorphic events.

3.6 Some Remaining Fundamental Questions

The use of terrain elements in developing fractal models and the seemingly realistic terrain simulations demonstrated the direct relevance of fractal concepts to terrain research. Most previous investigations on the fractal nature of terrain features seem to provide confirmation to the claim that **"fractals are everywhere"** (Barnsley, 1988). In a recent review, Hallet (1990) included the scale invariance of drainage networks and topography as one of three most fundamental spatial patterns identified in geomorphology. The other two patterns are periodic structures and polygonal patterns.

Without doubt, fractal geometry has given real meaning to many traditionally elusive concepts used in geomorphology such as the length of irregular geographic lines and the complexity of highly contorted surfaces. Fractal techniques have also provided practical solutions to some of the historically intractable problems such as comparing length measurements made at different scales and extrapolating the measured terrain properties to unmeasurable spatial domains (Fox and Hayes, 1985; Mareschal, 1989; and Yokoya et al., 1989). The large number of fractal-based terrain studies clearly testifies that fractal geometry has provided a novel approach to terrain model-

ling and added new vitality to this fascinating field.

Particularly, some studies have shown that fractal parameters are potentially useful geomorphometric variables. Recently, Klinkenberg (1992) carried out an in-depth exploration of the relationship between fractal parameters based on the variogram method (the fractal dimension, the log-log ordinate intercept, and the break distance) and twenty-four traditional morphometric parameters. His study shows that the correlations between the fractal dimension and the traditional parameters are all very weak, suggesting that the fractal parameters are capturing some unique aspects of surface morphological characteristics. Several authors have demonstrated that fractal parameters can be used to characterize different types of landforms, to delineate geomorphic regions, and to quantify the effects of various geomorphological factors on the complexity of terrain elements (Fox and Hayes, 1985; Roy et al., 1987; Klinkenberg, 1988; Elliot, 1989; and Huang and Turcotte, 1989). The use of fractal concepts and techniques in the measurement, quantification and analysis of terrain form will undoubtedly lead to a deeper understanding of geomorphological processes that have shaped and are continuing to shape the landscapes of our planet.

On the other hand, there are still many unanswered questions. To a large degree, our understanding of the fractal nature of terrain features is still quite rudimentary. Much remains to be learned. First of all, the answer to the question of how well the fractal model fits the real terrain data is at best incomplete. All we know is that the fractal model describes certain types of terrain better than others and when the fractal model is applicable it is only valid within a limited scale range. However, specifically, what types of terrain are well modeled by fractal parameters are yet to be determined. Likewise, all previous studies used either digital elevation models of relatively small areas or of very coarse spatial resolution. Thus, the actual maximum or average scale range of statistical self-similarity within each type of terrain has never been explored. Furthermore, many studies have come to the conclusion that terrain features are multifractals (Kent and Wong, 1982; Bradbury et al., 1984; Mark and Aronson, 1984;

Nakano, 1984; Culling and Datko, 1987; Klinkenberg, 1988; and Chase, 1992). An overview of all previous fractal studies of terrain surfaces also leads to the same conclusion. Although each study was only concerned with features within a rather limited scale range, together we have pretty much covered the entire scale range that concerns geomorphologists. Armstrong (1986) studied soil surface roughness at scales ranging from 1 cm to 1 meter and obtained relatively high D values (around 1.72). Elliot (1989) reported that the fractal dimension of the glacial moraines she studied changed from about 2.7 in the short scale range (5 - 20 cm) to about 2.4 in the middle and far ranges (20 - 100 cm). Burrough (1981) found a similar decrease in D value (from 1.5 for the short range to 1.1 for longer range) within the scale range between a few centimeters and ten meters. Mark and Aronson (1984) reported that the fractal dimension of the DEMs they selected increased from around 2.3 for the short scale range (from 30 m to about 600 m) to around 2.75 for the longer scale range (between 600 m and 5,000 m). Turcotte (1987) obtained a fractal dimension of 2.5 from the power spectrum of topography of the entire earth. Nevertheless, we are still far from reaching a general agreement. Some authors have found perfect fit between the fractal model and the real terrain data within the scale ranges they examined (Turcotte, 1987). Others have reported the presence of two linear segments on the log-log plots (Culling and Datko, 1987). Still other researchers have fitted three linear fractals within the scale ranges they investigated (Mark and Aronson, 1984). Many of these terrain features may indeed be natural examples of multifractals. However, the disturbing problem is that different researchers or the use of different methods sometimes gave quite contrasting results for the same data sets. Careful examination of the specific procedures used by some early researchers also indicates that the fitting of the regression line to the log-log plot was quite often a matter of subjective judgement, which could be the sole determining factor of the final outcome of their calculations.

Secondly, there seems to be little agreement among terrain scientists as to the average fractal dimension of natural topography. Scientists working in computer

graphics including Mandelbrot, speculated that the typical fractal dimension of natural terrain should be around 2.2 because this is the dimension that produced most realistic-looking terrain simulations (Mandelbrot, 1983; and Voss, 1988). Many geophysicists have obtained an average fractal dimension of about 2.5 for the earth's surface (Bell, 1975, 1979; Turcotte, 1987; and Mareschal, 1989). All other studies have given D values ranging between 2.0 and 2.98 (for example, Mark and Aronson, 1984; and Elliot, 1989). The reasons for these conflicting claims need to be uncovered. Obviously, a good estimate of the average fractal dimension of terrain surfaces requires the study of a large number of samples representing diversified types of terrain. Most previous estimates were based on rather limited terrain samples.

Thirdly, if it turns out that the fractal model is only applicable to certain types of terrain within limited scale ranges, then what else is needed to develop a robust terrain model which would be applicable to all types of terrain? In fact, there are good reasons to suspect that the fractal model is not a panacea for terrain description and modelling. After all, we spent many decades to study phenomena with normal distribution before we paid much attention to features showing hyperbolic distribution. In the field of geostatistics, there are spherical, logarithmic, and exponential models of regionalized variables besides the linear model that forms the basis of fractal models (Journel and Huijbregts, 1978). Thus, as many authors have already pointed out, the fractal model may be valid only for some special cases, though they seem to be more common than we used to believe them to be, or captures only a certain component of the real world (Goodchild, 1982; and Clarke, 1988). As a result, other classical or new models and techniques need to be combined with the fractal-based methods. In addition, studies of the fractal characteristics of different terrain elements such as coastlines, topographic surfaces, stream networks, planform of major river channels, and drainage basin boundaries have been largely separated from one another. Different elements need to be integrated into a coherent numerical terrain model.

Fourthly, several researchers have recommended that fractal parameters can be used as the basis for delineating physiographic regions (Klinkenberg, 1988). Chase's (1992) study has shown that fractal parameters are more responsive to climatic variables and surface processes than to tectonic control. The use of fractal parameters represents a fundamental departure from the traditional approach which emphasizes structural control and endogenetic processes, and would lead us into a new direction which could improve our understanding of long neglected but equally important surface processes. The fractal approach subdivides the land surface into contrasting provinces on the basis of some easily measurable and quantifiable terrain properties, which will facilitate the automation of the mapping process. But, so far, the feasibility of using fractal parameters for such purpose has only been tested using very limited data sets. Further study is needed to substantiate the finding of early investigations. We also need to determine what fractal parameters should be used for mapping various landform regions.

Finally, as briefly mentioned above, fractal terrain studies have been, up to now, largely restricted to the testing of the validity of the fractal model in describing the real terrain data, the characterization of various landforms, and the generation of realistic-looking terrain simulations. There have been very few studies designed to uncover the underlying geomorphological processes that have created the landscapes of various degrees of irregularities. Linking the various geometric characteristics to the corresponding processes is a critical step for us in order to achieve a higher level of understanding of natural systems and to add predictive power to our models. Also, the question of how the fractal model is related to some of the classical geomorphological models or how the fractal approach can be integrated with other approaches of terrain research is virtually untouched.

In summary, fractal geometry has offered us an enlightening new approach to terrain modelling and has given us some additional tools to handle the complexity of natural systems which had defied accurate numerical description for centuries. It has

provided us useful solutions to some of our long unsolved problems in terrain research. Previous studies indicate that fractal geometry captures some of the unique aspects of natural terrain. Fractal parameters have been shown to be potentially useful geomorphometric variables. Nevertheless, many fundamental questions are remaining to be answered before its full potential can be exploited. Most importantly, different algorithms for estimating the fractal dimension need to be evaluated. We need to separate method-produced variations from terrain-related variations before we can attach any real meaning to the derived estimates of fractal dimension. Without rigorous numerical procedures or a clear understanding of the magnitude of the method-induced error, inconsistency will persist and meaningless interpretations will continue to cause greater confusion. Terrain models based on the subjective and inaccurate estimates of parameters, no matter how esoteric they may seem and how many variables they involve, are merely useless artificial constructs. In addition, much more extensive empirical study is needed to reveal the wide range of uses and all practical limitations of fractal geometry in terrain modelling. The present project was designed to address some of these basic but crucial problems.

Chapter 4 FUNDAMENTALS OF FRACTAL GEOMETRY

4.1 Introduction

The content of fractal geometry is well presented by Mandelbrot in his book **"The Fractal Geometry of Nature"** (Mandelbrot, 1983), which was written for the purpose of popularizing the subject. In his own words, "*this work ... is neither a text-book nor treatise in mathematics. ... it serves as both a casebook and a manifesto*" (see Mandelbrot, 1983, p.2). Other systematic treatments of the subject include Feder (1988), Kaye (1989), Stewart (1989), Takayasu (1990), Lauwerier (1991), Schroeder (1991), and Stewart and Golubitsky (1992). More rigorous mathematical presentations are given by Falconer (1985, 1990), Barnsley (1988), Devaney (1989, 1990), Edgar (1990), and Le Mehaute (1991). The most comprehensive presentation of fractal geometry is provided by Peitgen et al. (1992a, 1992b). Peitgen et al. (1992a) is the first part of a two-part series which is specially designed for teaching fractal geometry and chaos theory to students. The first part of the series, **"Introduction to Fractals and Chaos,"** is complemented by **"strategic activities,"** which come in several volumes and provide hands-on experience to students. The first volume of strategic activities was published in 1991 (Peitgen et al., 1991). Peitgen et al. (1992b) is intended for a much larger audience and is not written as a standard textbook. It combines most segments of the two-part series with many extensions and two appendices dealing with image compression and multifractal measures respectively. This chapter summarizes only the basic concepts of fractal geometry which are most relevant to the present study.

4.2 The Definition of Fractals

The term "fractal" was derived by Mandelbrot in 1975 from the Latin adjective "fractus". The corresponding Latin verb "frangere" means "to break" to create irregular fragments. This coinage was responding to the need for a term to denote a mathemati-

cal set or a concrete object whose form is extremely irregular and/or fragmented at all scales. Although fractal research has become so prominent in almost every scientific discipline, the term "fractal" has never been properly defined, which sometimes becomes a source of serious criticism (Krantz, 1989). Mandelbrot (1983, p.361) believes that "*one would do better without a definition.*" Thus, in the French edition of his book (Mandelbrot, 1975b), **"Les Objets Fractals: Forme, Hasard et Dimension,"** he deliberately avoided providing a definition. Nevertheless, in the first English edition of his book (Mandelbrot, 1977, p.15), he advanced a tentative definition, acknowledging its arbitrariness. According to Mandelbrot (1983, p.15), "*A fractal is by definition a set for which the Hausdorff-Besicovitch dimension strictly exceeds the topological dimension.*"

This definition was found to be unsatisfactory in that it excludes a number of sets that clearly ought to be regarded as fractals (Mandelbrot, 1983, p.361). Thus, Mandelbrot (1986a, p.8) retracted this tentative definition and proposed instead the following: "*A fractal is a shape made of parts similar to the whole in some way*" (see Feder, 1988, p.11). Falconer (1990, p.xx) suggests that the definition of "fractals" should be regarded in the same way as the biologist regards the definition of "life". There is no hard and fast definition, but just a list of properties characteristic of a living thing, such as the ability to reproduce or to move or to exist to some extent independently of the environment. Most living things have most of the characteristics on the list, though there are living objects that are exceptions to each of them. In the same way, it seems best to regard a fractal as a set that has certain specified properties rather than to look for a precise definition which almost certainly excludes some interesting cases. The list of properties suggested by Falconer (1990, p.xx) includes: (1) it has a fine structure, i.e., detail on arbitrarily small scales; (2) it is too irregular to be described in traditional geometrical language, both locally and globally; (3) often it has some form of self-similarity, perhaps approximate or statistical; (4) usually, the 'fractal dimension' of the set (defined in some way) is greater than its topological dimension; and (5) in most

cases of interest it is defined in a very simple way, perhaps recursively.

4.3 Self-Similarity and Self-Affinity

One of the most important properties of fractals is scaling. Mandelbrot (1983, p.18) defined scaling to mean invariance under certain transformations of scale. Specifically, fractals possess a geometric invariance property called contraction and/or dilation invariance (Mandelbrot, 1987). Contraction refers to the transformation of a geometric shape that decreases its size of every point, that is, contracts the distance between two points by a factor having an upper bound $r^{-1} < 1$. Dilation refers to the transformation of a geometric shape that increases its size at every point, that is, dilates distances by a factor having a lower bound $r^{-1} > 1$.

There are two basic forms of scaling: self-similarity and self-affinity. When each piece of a shape is geometrically similar to the whole, that is, when an object is composed of N copies of itself (with possible translations and rotations) and each copy is scaled down by the same ratio in all E Cartesian coordinates from the whole, both the shape and the cascading process that generates it are said to be self-similar (Mandelbrot, 1983, p.34). Self-similarity is manifested in two different ways: it can be exact or statistical. The concept of exact self-similarity can be illustrated with one of the early mathematical monsters: the von Koch snowflake curve (Figure 4.1). If one were to take a portion of the perimeter of the von Koch snowflake of the n-th order and look at it under a microscope, the magnified portion would look exactly the same as the original large part of the boundary.

Quite obviously, objects in nature rarely exhibit such exact self-similarity. Nevertheless, they do often possess a related property, statistical self-similarity. Statistical self-similarity means that upon magnification a small portion of an object looks very much like, but never exactly like, the configurations at other scales. The simplest example of statistically self-similar fractals is a coastline. As with the von Koch curve, the closer one looks at a coastline, the more detail one sees. Unlike the von Koch

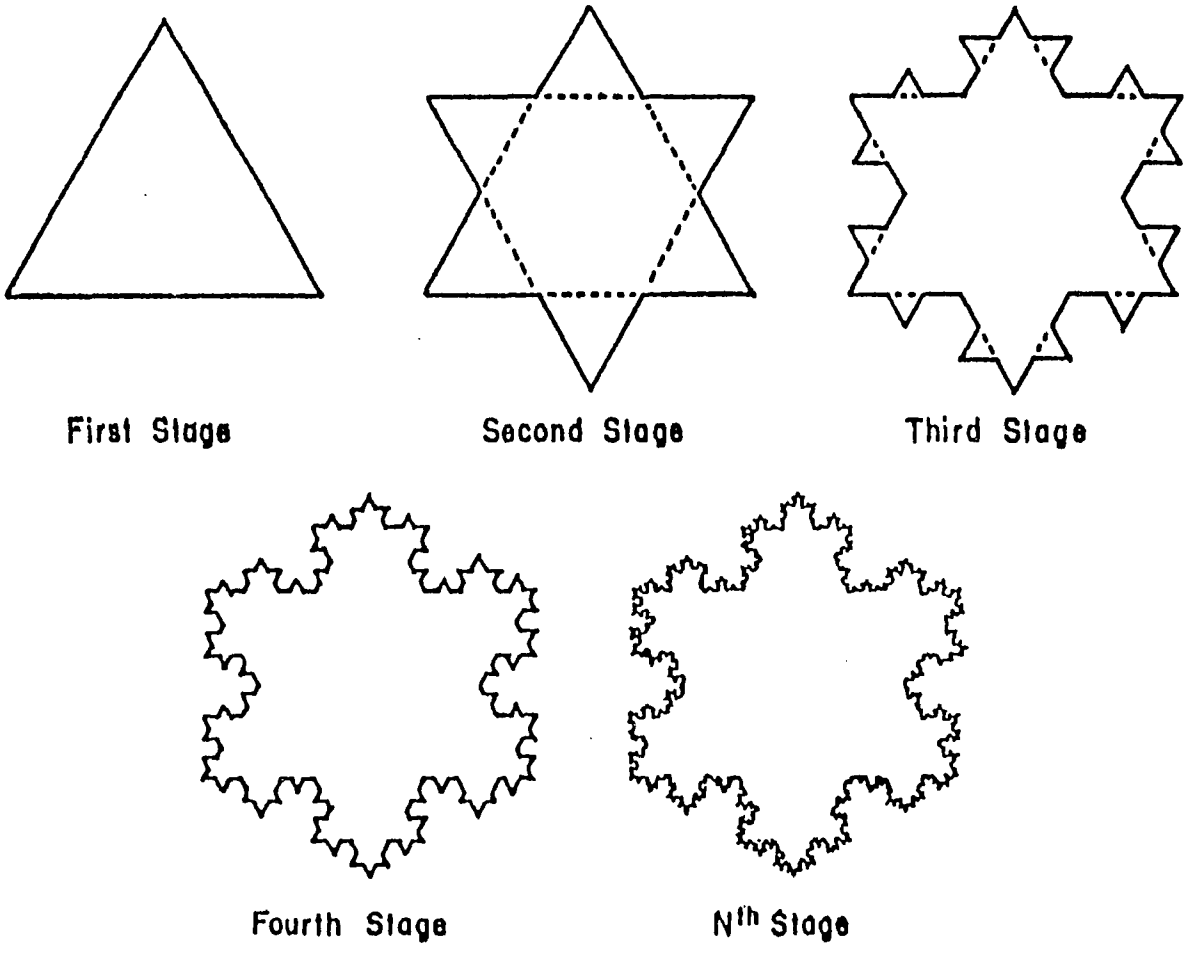

Figure 4.1 The Nth Order Koch's Triadic Island or the Koch Snowflake Curve. The Koch snowflake curve is one of the classical fractal shapes. It is self-similar so that each part is a reduced version of the same configuration. The Koch snowflake curve was suggested by Mandelbrot as a model of coastlines. (from Mandelbrot, 1983)

curve, a small scale view of the coastline is insufficient to predict the exact details of a magnified view.

Other fractals show a different kind of scaling behavior, namely, they are self-affine. Self-affine fractals are anisotropic. They look the same only if the length scales along different directions are changed by different factors (Voss, 1985a, 1985b, 1988; and Mandelbrot, 1986). A good example of self-affine fractals is the traces of a fractional Brownian motion, which will be discussed below, or topographic profiles of natural terrain.

It should be pointed out that some fractal dusts, curves, and surfaces are only scaling in an asymptotic or otherwise limited sense (Mandelbrot, 1983, p.147-165). Fractals that are either fully invariant under similitudes or at least nearly self-similar represent the fractal counterparts of straight lines in Euclidean geometry. For this reason, these fractals are sometimes called "linear fractals" (Mandelbrot, 1987). There are also more complicated and "enormously richer" nonlinear fractals (see Mandelbrot, 1983, p.166-199). So far, three kinds of nonlinear fractals have been identified since Mandelbrot began working on them in 1976: self-inverse fractals (which have had a significant impact on an area of mathematics called Kleinian groups), self-squared fractals, and a not well understood miscellaneous category that contains many of the geometrical shapes called, in non-linear dynamics, strange attractors.

4.4 Fractal Dimension

The ancient notions of dimension play a central role in fractal geometry. In the Euclidean or Newtonian universe, dimension is defined as the number of distinct coordinates needed to specify the position of a point in space. A point has zero dimension; a line, whether straight or curved, has one dimension. Any point on the line can be represented by a single parameter, for example its distance along the line from a fixed point. Similarly, points on a plane or any normal curved surface can be represented by two values, for example (x, y) coordinates in a Cartesian plane, or latitude and

longitude on the surface of a globe, which makes such surfaces two-dimensional. The Newtonian description of the space we live in is three-dimensional. Any point in our universe can be located by three values, for example the Cartesian coordinates (x, y, z). However, this definition of dimension is not satisfactory for a proper understanding of irregularity or fragmentation in nature. A rigorous analysis reveals that the loose notion of dimension turns out to have many mathematical facets that not only are conceptually distinct but may lead to different numerical values (Mandelbrot, 1983, p.14). Within this framework, Euclidean geometry is limited to sets for which all the useful dimensions coincide, that is, dimensionally concordant sets. On the other hand, fractal geometry is devoted to the study of dimensionally discordant sets.

For our purpose, we can distinguish at least two very important types of dimension: the topological dimension (D_T) and the fractional dimension (D). It can be shown that the topological dimension coincides with the intuitive dimension we have learned in Euclidean geometry. The notion of a fractional dimension was established by Felix Hausdorff in 1919 in order to put a "size" to highly irregular non-rectifiable sets and in particular to Cantor sets. It is for this reason that the fractional dimension is sometimes called the "Hausdorff dimension". Later, Besicovitch (1929) introduced the idea of a dimension number, which is not the same as the Hausdorff dimension in its most general form but for those sets of interest to geomorphologists, they are equivalent. Thus, the fractional dimension has also been known as the "Hausdorff-Besicovitch dimension".

Whenever we work in the Euclidean span R^E, both D_T and D are at least 0 and at most E. But the resemblance ends here. The topological dimension is always an integer, but the Hausdorff-Besicovitch dimension need not be an integer. It is for this reason that the Hausdorff-Besicovitch dimension is often called the fractional dimension. In addition, the two dimensions need not coincide. The Hausdorff-Besicovitch dimensions of all sets studied in fractal geometry are greater than their topological

dimensions.

In order to emphasize the fact that a fractal may also have an integer D and to avoid the confusion of Hausdorff-Besicovitch dimension with the dimension of the Hausdorff topological space, Mandelbrot (1983, p.15-17) proposes to call D the fractal dimension. On the other hand, most people continue using fractional dimension, Hausdorff dimension, Hausdorff-Besicovitch dimension, and fractal dimension interchangeably. Nevertheless, it should be realized that Mandelbrot's fractal dimension was quite loosely defined. His definitions were proposed for the purpose of facilitating the analysis of empirical data. Many of his definitions have not yet been proven to coincide with the Hausdorff-Besicovitch dimension despite that they possess many properties of a dimension. He recommended that fractal dimension should be used as a generic term "*when there is no need of being more precise ------ or one is not sure ------ about the definition*" and "*Hausdorff-Besicovitch dimension should be used only when Hausdorff's definition has actually been followed*" (Mandelbrot, 1987, p.588). According to Mandelbrot (1987, p.579), in cases of self-avoiding fractal curves or surfaces, fractal dimension is a real number that measures the degree of their irregularity. More generally, fractal dimension refers to any one of several real numbers that characterize a fractal and enter as exponents in analytic relations concerning these shapes.

The Hausdorff dimension of a fractal dust ranges between 0 and 1. A good example is Cantor's ternary set, which has a fractal dimension of 0.6309. For a fractal curve, D may range between 1 and 2. A D value of 2 implies that the curve is so 'plane-filling' that it effectively takes up the whole of a two-dimensional space. Two classical examples are the Brownian line graph, which has a fractal dimension of 1.5, and the Koch curve, which has a fractal dimension of 1.2618. For fractal surfaces, the D value ranges between 2 and 3. A value of 2 indicates that the surface is completely smooth. As the value increases, the surface becomes increasingly crumpled until eventually it becomes so irregular that it virtually occupies the entire three dimensional Euclidean space.

4.5 The Fractional Brownian Motion

The fractional Brownian motion (fBm) of Mandelbrot and Van Ness (1968) has been considered as the most useful mathematical model for the random fractals found in nature. Almost all computer simulations of natural fractals, including fractal mountains, fractal continents, lunar landscape, and imaginary planets, are based on an extension of fBm to higher dimensions (Voss, 1985a, 1985b). It is also the standard by which various generating algorithms may be compared. In addition, fractional Brownian motion is a good starting point for understanding anomalous diffusion and random walks on fractals (Voss, 1988).

The fractional Brownian motion was first introduced in hydrology to help generalize autoregressive processes based on Gaussian normal distribution to situations where both short-range and long-range (or persistence) effects occurred (Mandelbrot and Van Ness, 1968). It is an extension of the central concept of Brownian motion that has played an important role in physics, chemistry, and mathematics.

The term Brownian motion was originally used to describe the irregular movement of pollen suspended in water, observed by the Scottish botanist Robert Brown in 1828. This random process was later found to have wide-ranging applications. The first quantitative work on Brownian motion is due to Bachelier (1900), who was interested in stock price fluctuations. Einstein (1905) derived the transition density for Brownian motion from the molecular-kinetic theory of heat. Jean Baptiste Perrin (1906, 1909, 1923) carried out extensive experiments to observe the path of a particle in Brownian motion under the microscope and compared it with continuous nondifferentiable curves. Perrin's 1909 paper chanced to catch the attention of Norbert Wiener (see Wiener, 1956, p.38-39) and inspired him to develop a rigorous probabilistic model of Brownian motion (Wiener, 1923, 1924). However, the most profound work in the early period is that of Paul Levy (1939, 1948). He introduced the construction by interpolation, studied in detail the passage times and other related functionals,

described the so-called fine structure of the typical sample path, and discovered the notion and properties of the local time. To honor the work of these early researchers, the Brownian motion random process is sometimes known as the Bachelier-Wiener-Levy process.

Brownian motion B (t, ε), where ε designates the set of all the values of a random function, is a measurable function, that for almost all ε it is a continuous function of t and for which almost no sample function is of bounded variation. This makes its line graph non-rectifiable. Brownian motion is said to be a statistically self-similar process in the sense that if the time intervals are divided by a positive, but arbitrary ratio r and B (t, ε) is rescaled in the ratio r^H, where H = 0.5, the rescaled function has a probability distribution that is identical to that of the original function. In other words, examination of the Brownian line function at larger scale reveals an identical Brownian function at that scale.

One of the most important characteristics of a standard Brownian motion is that it possesses the so-called martingale property, that is, at any time it is as likely to increase as to decrease. More precisely, the value at time n supplies the mean value to the distribution at time n + 1. In contrast, many natural time series such as long run hydrologic data fail to show the martingale property and the square root scaling relationship of a Gaussian-Markov process, thereby implying some form of long term dependence. This observation motivated Mandelbrot and Van Ness (1968) to extend the notion of Brownian motion and define fractional Brownian motion as a Weyl fractional integral, which in effect weights past values. The scaling parameter is no longer 0.5 but may take values between 0 and 1 ($0 < H < 1$). This upsets the martigale property of the standard Brownian motion and for values $H > 0.5$ the graph is progressively smoothed as the sign of the increment is likely to persist and for $H < 0.5$, to become increasingly more erratic as the sign of the increment is antipersistent and therefore more likely to be reversed on any occasion. By allowing H to vary between

0 and 1, Mandelbrot has shown that a whole family of statistically self-similar variations could be produced that cover the range of spatial intricacy from smooth differentiable curves to plane-filling noise.

A fractional Brownian motion, $V_H (t)$, is a single valued function of one variable, t (usually time). Its increments $V_H (t_2) - V_H (t_1)$ have a Gaussian distribution with variance:

$$< | V_H (t_2) - V_H (t_1) |^2 > \propto | t_2 - t_1 |^{2H}$$

where the brackets < and > denote ensemble averages over many samples of $V_H (t)$ and the parameter H has a value $0 < H < 1$. Such a function is both stationary and isotropic. Its mean square increments depend only on the time difference $t_2 - t_1$ and all t's are statistically equivalent. The special value H = 1/2 gives the familiar Brownian motion with

$$\Delta V^2 \propto \Delta t.$$

As with the usual Brownian motion, although $V_H (t)$ is continuous, it is nowhere differentiable. Nevertheless, many constructs have been developed to give meaning to the "derivative of fractional Brownian motion" as fractional Gaussian noises. The derivative of normal Brownian motion, for which H = 1/2, corresponds to the uncorrelated white Gaussian noise and the Brownian motion is said to have independent increments.

As with coastlines, $V_H (t)$ shows a statistical scaling behavior. If the time scale t is changed by the factor r (t becomes rt), then the increments ΔV_H change by a factor r^H. Formally,

$$< \Delta V_H (rt)^2 > \propto r^{2H} < \Delta V_H (t)^2 >.$$

Unlike statistically self-similar coastlines, however, a V_H (t) trace requires different scaling factors in the two coordinates (r for t but r^H for V_H) reflecting the special status of the t coordinate. Each t can correspond to only one value of V_H but any specific V_H may occur at multiple t's. Thus, the traces of fractional Brownian motion are self-affine.

The zeroset of fBm is the intersection of the trace of V_H (t) with the t axis: the set of all points such that V_H (t) = 0. The zeroset is a disconnected set of points with topological dimension zero and a fractal dimension D = 1 - H, that is less than 1 but greater than 0. Although the trace of V_H (t) is self-affine, its zeroset is self-similar.

The strong resemblance of the traces of fBm to a mountain's silhouette or of a vertical section of the earth's relief motivated Mandelbrot (1975c, see Figure 3.1) to generalize the traces of fBm to higher dimensions for modelling the irregular surface of the earth and the morphology of the moon. In the surface model, the single variable t is replaced by coordinates x and y in the plane to give V_H (x,y) as the surface altitude at position (x,y). The fractal dimension of the surface is D = 3 - H. The intersection of a vertical plane with the surface V_H (x,y) is a self-affine fBm trace characterized by H and has a fractal dimension one less than the surface itself. The zeroset of V_H (x,y), its intersection with a horizontal plane, has a fractal dimension D_0 = 2 - H. This intersection, which produces a family of (possibly disconnected) curves, forms the coastlines of the V_H (x,y) landscape. Since the two coordinates x and y are, however, equivalent, the coastlines of the self-affine V_H (x,y) are self-similar.

4.6 Multifractals

The first mention of multifractals was in 1968, in Mandelbrot's paper on mature turbulence (see Mandelbrot, 1986d, p.11). But, the work had started about 1962 (see Mandelbrot, 1989b, p.6). And then, he published extensively on the topic in the 1970s

(Mandelbrot, 1972, 1974, 1975a, 1975b, 1976). He provided a sketchy survey on multifractals in his book **"Fractal Geometry of Nature"** under the title of "nonlacunar fractals" (Mandelbrot, 1983, p.375-376). However, this unfortunate term has not been used anywhere else, and has soon been replaced by the coinage "multifractal" due to Frisch and Parisi (1985).

A multifractal is not a set, rather a "measure". The generalization from fractal sets to multifractal measures involves the passage from geometric objects characterized primarily by one number, to geometric objects characterized primarily by a function. This function can be a probability distribution that has been renormalized and plotted suitably. In a different single phrase, the generalization from fractal sets to multifractal measures involves the passage from a finite number of fractal dimensions to an infinite number of "dimensions". Moreover, these "dimensions" can be negative. In-depth discussions on multifractals are given by Feder (1988) Mandelbrot (1989a, 1989b), and Evertsz and Mandelbrot (1992).

Chapter 5 AN EVALUATION OF METHODS FOR ESTIMATING THE FRACTAL DIMENSION OF TOPOGRAPHIC SURFACES

5.1 Introduction

The most important concept of fractal geometry that is used to characterize topographic surfaces numerically is the fractal dimension or Hausdorff-Besicovitch dimension. However, "*the Hausdorff-Besicovitch dimension is a very non-intuitive notion. ... this dimension can be no use in empirical work, and is unduly complicated in theoretical work, except for self-similar fractals*" (Mandelbrot, 1985, p.258). Specifically, "*the essential feature of the Hausdorff dimension is that it calls for successive passages to limits, which makes it quite useless in science, because it is impossible to measure it*" (Mandelbrot, 1991, p.6). Therefore, Mandelbrot introduced several alternative definitions of fractal dimension and provided theoretical justification for the development of many empirical methods for estimating the fractal dimension. Burrough (1984) listed six algorithms most commonly used in the geosciences. Rigaut (1991) described nine different methods used in biometry, most of which are also widely used for estimating the fractal dimension of terrain features. Table 5.1 lists the algorithms most commonly used for estimating the fractal dimension of terrain features. Other methods or variations have been proposed by Houck (1983), Eastman (1985), Clarke (1986), Hough (1990), Matsushita and Ouchi (1989), Malinverno (1990), Ouchi (1990), Piech and Piech (1990), Clarke and Schweizer (1991), and Ouchi and Matsushita (1992). However, these empirically-based techniques lack the rigor generally found in analytical solutions and the implementation of these methods often involves many subjective decisions in selecting computational parameters. Thus, it is not uncommon that different researchers has produced quite contrasting results for the same data sets. On the other hand, relatively little work has been done so far to evaluate systematically the reliability of each method when applied to topographic surfaces and the comparability of results based on different algorithms. The notable exceptions are Goodchild

Table 5.1 MOST COMMONLY USED ALGORITHMS FOR ESTIMATING THE FRACTAL DIMENSION OF TERRAIN FEATURES

NAME OF METHOD	ALGORITHM	ESTIMATION OF D	REFERENCES
Walking Dividers Method (Richardson's Law)	$L(\lambda) = k\,\lambda^{1-D}$ λ is step size $L(\lambda)$ is estimated total length D is fractal dimension k is a constant	Plot log L against log λ; D = 1 - b b is slope of the regression line	Mandelbrot (1967) Goodchild (1980) Shelberg et al. (1982)
Variogram Method	$2\gamma(d) = k\,d^{(4-2D)}$ $2\gamma(d)$ is incremental variance d is sampling interval D is fractal dimension k is a constant	Plot log $\gamma(d)$ against log d; D = 2 - H for profiles D = 3 - H for surfaces H = b / 2 b is the slope of the regression line	Mark and Aronson (1984) Roy et al. (1987)
Box-Counting Method	$N = k\,l^{-D}$ N is the average # of adjacencies l is the cell size D is fractal dimension k is a constant	Plot log N against log l; D = - b b is the slope of the regression line	Goodchild (1982) Shelberg et al. (1983)
Power Spectrum Method	$P(\omega) = \omega^{-(5-2D)}$ ω is frequency $P(\omega)$ is the power D is fractal dimension	Plot log $P(\omega)$ against log (ω); D = (5 - b) / 2 for profiles D = (8 - b) / 2 for surfaces b is the slope of the regression line	Turcotte (1987) Goff (1990)
Area-Perimeter Method	$A = k\,P^{2/D}$ A is estimated area P is estimated perimeter D is fractal dimension k is a constant	Plot log A against log P; D = 2 / b	Kent and Wong (1982)
Size-Frequency Method (Korcak's Law)	$N(A > a) = k\,a^{-(D/2)}$ $N(A > a)$ is the number of islands above size a D is fractal dimension k is a constant	Plot log $N(A > a)$ against log a; D = - 2 b b is the slope of the regression line	Kent and Wong (1982)
Stream Number-Stream Length Method	$D = \log R_b / \log R_L$ for $R_b > R_L$ R_b is the bifurcation ratio R_L is the stream length ratio D is fractal dimension		La Barbera and Rosso (1989)

(1982), Culling and Datko, (1987), Roy et al. (1987), and Klinkenberg and Goodchild (1992).

Goodchild (1982) used the walking dividers method, the box-counting method and the area-perimeter relationship for estimating the fractal dimensions of the coastline, 250- and 500-foot contours, and lake outlines of Random Island, Newfoundland. He found that the box-counting method produced consistently higher estimates of D. The difference between the box-counting method and the area-perimeter method for the 500-foot contour was as large as 0.35. Comparatively, the results based on the area-perimeter relationship were in reasonable agreement with those by the walking dividers method although the difference in D for the lake shorelines obtained by these methods was as large as 0.5.

Culling and Datko (1987) estimated the fractal dimensions of 17 topographic data sets from southern England using the variogram method and the walking dividers method. Their computations did not yield any consistent pattern. For eight data sets, the variogram method gave relatively higher D values, while the walking dividers method produced higher D values for the remaining topographic quadrangles. In addition, for nine of their data sets, one method gave two D values while the other method produced a single D value.

Roy et al. (1987) compared the results obtained by the variogram method, the walking dividers method and the box-counting method using a single DEM of an area located in the White Mountains at the border of Quebec, Maine and New Hampshire. They found close agreement between the result by the variogram method (2.16) and that by the walking dividers method (2.17). On the other hand, the box-counting method gave a somewhat lower D value (2.09).

Klinkenberg and Goodchild (1992) compared the results by the walking dividers method, the box-counting method and the variogram method for fifty-five digital elevation models from seven different United States physiographic provinces. They con-

cluded that the variogram method was a robust method and produced consistent results while the fractal dimensions produced by the contour or elevation-dependent methods (the walking dividers method and the box-counting method) were not representative of the dimensions of topographic surfaces. However, their conclusion needs to be treated with caution. One major reason for being cautious is related to the way they chose the scale ranges for determining the slope of the best-fitting curve. The standards they used were "the first and last points which appeared to envelope a reasonably linear cluster," the scatter of points was not too great or too curved, and the r squared value was above 0.90. Such standards are quite arbitrary choices. Different choices of scale ranges will give quite variable results.

In addition, Benzer (1989) carried out a comparative study of fractal estimates using the walking dividers method and the variogram method. He used these methods to compute the fractal dimensions of seventeen data sets (eight coastlines, three joint and fault profiles and their corresponding "joint roughness coefficient" profiles, a portion of the von Koch snowflake, a straight line, and a Brownian noise). He concluded that the walking dividers method produced fractal dimensions commensurate with one's visual perception of roughness of a profile, but the variogram method only produced the "desired" fractal dimension for some special cases (a straight line, the Brownian noise, and the white noise). However, an examination of his source data and log-log plots reveals that his study was seriously flawed with the ways these methods were used. First, the joint and fault profiles and their corresponding "joint roughness coefficient" profiles are self-affine fractals. As will be discussed later in this chapter, the application of the walking dividers method developed on the basis of self-similar fractals considerably underestimates the irregularities of these profiles. Secondly, he used the variogram method to calculate the fractal dimension of contour lines (coastlines) rather than the topographic profiles from which the variogram algorithm was originally derived. Although Mandelbrot pointed out that the contour lines and profiles should give similar fractal dimensions, it is highly suspicious whether the relationship

between the variance or semivariance of elevation changes and the separation distance originally derived from self-affine fractals is also applicable to self-similar contour lines. In fact, when he applied the variogram method to vertical profiles (the Brownian noise, a straight line tilted at 45 degrees, the Busted Butte joint profile, and the JRC (Joint Roughness Coefficient 10-12) profile), the results seem quite reasonable. Especially noteworthy is that according to his calculations the fractal dimension for the Brownian noise by the variogram method was 1.5 as expected while the walking dividers method produced a D value of 1.0. Thirdly, it appears that some of the unreasonable D values are the results of improper choice of scale range for regression line-fitting. Some variograms clearly show periodic features, but they were ignored in the regression line-fitting process. Fourthly, some regression line-fitting was based on inadequate distance classes. In one particular case, only three distance classes were used in regression. Finally, the number of data samples within each distance class, especially for longer distance classes, was extremely limited. All these problems raise serious doubt on the reliability of his conclusions.

Thus, previous studies have failed to produce consistent results. More importantly, these algorithms were only tested on very limited data sets. How each of these methods would respond to the variations of landform characteristics of contrasting physiographic regions remains unknown. Furthermore, some methods have been used indiscriminatingly to problems that are clearly out of their limits of applicability (Brown, 1987b; and Roy and Robert, 1990). For example, the walking dividers method, originally developed using self-similar fractals, has been widely applied to self-affine fractals (Aviles et al., 1987; and Andrle and Abrahams, 1989). Occasionally, computations of fractal dimension were based on erroneous mathematical formulation (Bradbury and Reichelt, 1983; and Huang and Turcotte, 1989; also see Bradbury et al., 1984; Mark, 1984; Goff, 1990; and Huang and Turcotte, 1990). All these problems present major difficulties for choosing the most suitable technique for a particular application and raise serious suspicion on the interpretation of some earlier studies.

Only if we know precisely the way each method works, the sensitivity of the final result to the selection of computational parameters, and the limits of its applicability, can we begin to appreciate the true meaning of fractal dimension in relation to the complexity of terrain features.

This chapter provides a comprehensive review and assessment on the uses and limitations of three most commonly used techniques for computing the fractal dimension: the walking dividers method, the box-counting method, and the variogram method. Factors affecting the numerical value of fractal dimension will be identified for each of these methods. Results obtained by different methods will be compared with one another, with theoretically predicted values, and with earlier studies. The reliability of each method and the comparability of results from different methods will be discussed.

5.2 The Variogram Method

The variogram was originally developed for analysis of spatially dependent "regionized variables" (Matheron, 1963). A variogram is a plot of incremental variance between two locations along the ordinate against the distance separating the two locations along the abscissa. It has been the cornerstone of mining geostatistics (Journel and Huijbregts, 1978). Recently, it has been extensively used to model the variations of soil properties and geomorphic variables (Campbell, 1978; Burgess and Webster, 1980; and Oliver and Webster, 1986).

The variogram method for estimating the fractal dimension of topographic profiles or surfaces is based on one of the important properties of the fractional Brownian motion which was proposed by Mandelbrot (1975c) as a model of the irregular surface of the earth. It has been shown that for a random time series the variance of its increments $V_H (t_2) - V_H (t_1)$ has the following relation to the time difference (see Voss, 1986, p.2):

$$< | V_H (t_2) - V_H (t_1) |^2 > = k | t_2 - t_1 |^{2H}$$

where the brackets < and > denote averages over many samples of V_H (t) and the parameter H has a value between 0 and 1 ($0 < H < 1$). Taking logarithms on both sides, we get

$$\log < | V_H (t_2) - V_H (t_1) |^2 \geq \log k + 2H \log | t_2 - t_1 |.$$

It can be seen that if we produce a log-log plot of variance against time difference, the slope of the plot will be equal to 2H and the intercept will be equal to log (k). The fractal dimension of a fractional Brownian line function is given by D = 2 - H (Orey, 1970).

When the relationship is generalized to model the irregular surface of the earth, the single variable t is replaced by spatial coordinates x and y in the plane to give V_H (x,y) as the surface elevation at position x,y. In this case, the elevation variations along any straight line path at a constant interval in the xy plane is a fractional Brownian motion. If the mean of the squared differences in elevation is computed for different distances, D can be estimated from the slope of a log-log plot of variance against distance by D = 3 - H (Voss, 1988).

In addition to fractal dimension, other fractal parameters associated with the variogram method have also been used for characterizing terrain features. These include the "break distance", the "gamma value", and the r^2 value of the regression line. The "break distance" refers to the maximum distance to which a least squares line could be fitted. The gamma value represents the expected squared distance in elevation for points a unit distance apart, which is 30 meters in the case of the USGS DEMs.

The variogram method was first used by Burrough (1981, 1983a) for empirically estimating the fractal dimensions of soil properties and other environmental variables. It was then used by Mark and Aronson (1984), Culling and Datko (1987), Roy et al.

(1987), Klinkenberg (1988), and Chase (1992) to estimate the fractal dimension of land surface topography. Armstrong (1986) and Elliot (1989) used the variogram method to characterize the irregularities of microtopography measured over small distances. Robert (1988) used it to investigate the fractal properties of series of bed elevations measured on gravel-bed and sand-bed alluvial channels, to determine scales of bed roughness associated with grain sizes and small-scale bedforms, and to estimate the fractal dimension corresponding to each scale. It has also been used by Armstrong (1986) and Culling (1986a) to estimate the fractal dimension of soil properties such as pH and soil surface strength.

The specific procedure for computing the fractal dimension of topographic surfaces in this study is as follows:

(1) The largest square array of data points is selected from each regular USGS Digital Elevation Model (DEM). The use of a square array facilitates the comparison of results obtained for different directions because it eliminates the effects of variable lengths of profiles on the numerical value of fractal dimension. Klinkenberg (1988) also used square arrays of elevations for his fractal analysis of topographic data. His sampling areas were of a constant size of 256 by 256 pixels and much smaller than the size of arrays selected in the present study. Mark and Aronson (1984) restricted their sampling to the largest circle that could be drawn within a map area. Their choice of sampling area ensures equal representation of all directions. However, with the exceptions of E-W, N-S, NW-SE, and NE-SW directions, all other directions would involve interpolated values and the resulting variogram would not reflect the variability of the raw data.

(2) The extracted DEM files are then converted into ERDAS image files. Gray tone images and hill-shaded images are created and displayed to visually evaluate the overall quality of the particular data set. This step is necessary because many of the DEMs released earlier by the USGS contain serious errors. When major errors are

found, the data set is excluded in the fractal analysis.

(3) The squared height differences are calculated for all possible distances within the selected array, which range from one pixel (30 m) to the maximum length of the array. Previous researchers have used random sampling for selecting pairs of data points (Mark and Aronson, 1984; Roy et al., 1987; and Klinkenberg, 1988). However, the present study intends to minimize the effects of extraneous factors on the estimated D value and uses all data pairs to avoid the possible error from inadequate random sampling. The variance for each distance represents an average of all data pairs in the E-W, N-S, NE-SW and NW-SE directions. The largest number of elevation pairs for the shortest distance class (30m) included in computing the average incremental variance is 606,062. Fractal dimensions were also estimated for each of the DEMs using only the elevation pairs in the E-W and N-S directions for the purpose of comparison. To detect the presence of anisotropies, the variance for each of the four directions is also calculated separately. One problem associated with using all data pairs is that the mean variances for different distances are derived from variable number of data pairs. This may not be a problem when all the data pairs in the four directions are averaged together or when we compute the mean variance of data pairs in the E-W or N-S directions because even the largest distance class still contains at least three hundred elevation pairs. However, for profile variograms in the NE-SW and NW-SE directions, the number of elevation pairs used for computing the mean variance decreases rapidly as the distance becomes large. For the largest distance class, there is only a single elevation pair. Thus, caution is needed when interpreting the results for these directions.

(4). A plot is produced using log (variance) as the ordinate and log (distance) as the abscissa and visually inspected to identify the general relationship between these variables and to detect the presence of periodicity. If periodic variations are present, the raw variance table is examined to determine the critical distance of periodic features. The critical distance is a very useful fractal parameter for characterizing land

surfaces because natural terrain roughness is only self-similar over limited ranges and different types of topographic surfaces have different scale ranges over which the statistical properties remain statistically self-similar.

(5). Linear regression is carried out to find the best-fitting line for the distance classes before the periodicity sets in and the slope of the best-fitting line is determined. The slope of the regression line is then used to compute the fractal dimension as described above. Previous researchers have fitted multiple linear segments to the log-log plot, suggesting that topographic features are multifractals (Mark and Aronson, 1984; Culling and Datko, 1987; and Klinkenberg, 1988). Attention has been paid to identify break points on the log-log plot through visual inspection. However, an examination of the plots produced in this study reveals no such distinct breaks although it is clear that topography is not strictly self-similar across all scales (Figure 5.1). Thus, It appears that the selection of break points is a quite subjective procedure. Attempt was then made to choose a specific threshold r-squared value and to determine the break points recursively (Figure 5.2). This proved to be a quite time-consuming process. It was not uncommon that a variogram could be approximated into more than ten different linear segments. For the sample plot shown in Figure 5.2, five linear segments were separated using a r-squared value of 0.99. Furthermore, what r-squared value to use still remains an arbitrary decision. As an alternative, the beginning point of periodicity was used as the upper scale limit for regression analysis. Although there is no theoretical justification for choosing the threshold of periodicity, its use does provide a more objective and unique choice.

5.3 The Box-Counting Method

The box-counting or cell-counting method is based on the fact that the length measurement of contour lines increases with scale. The length of each contour line is approximated by overlaying a grid and counting the number of cells it intersects (Figure 5.3). By changing the size of grid cells, we can evaluate the effects of changing

E —— W Direction

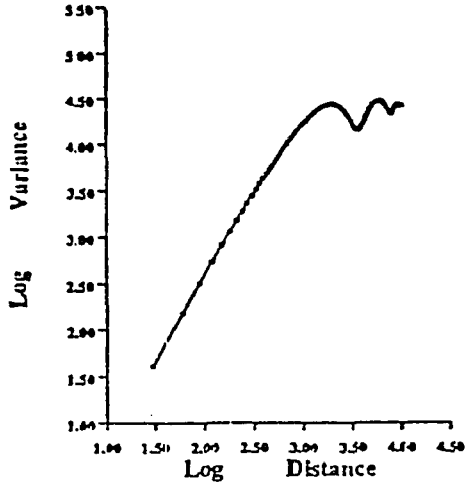

N —— S Direction

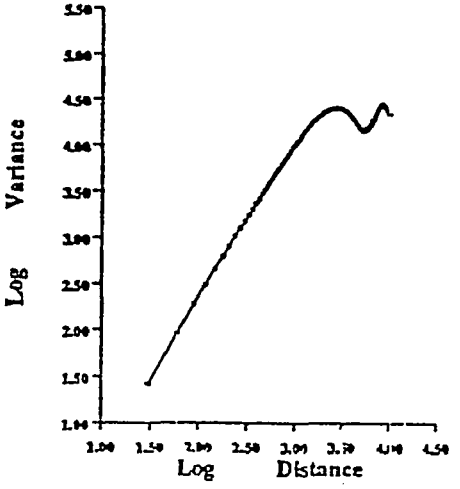

NW —— SE Direction

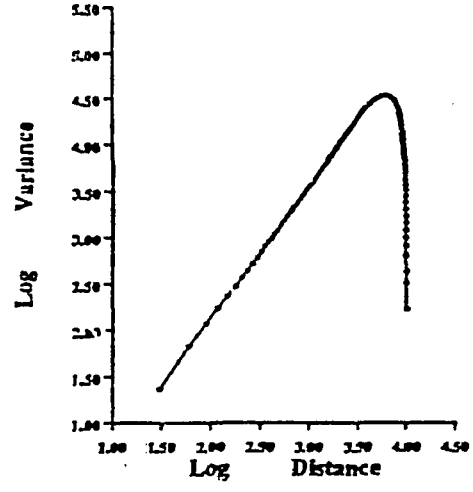

NE —— SW Direction

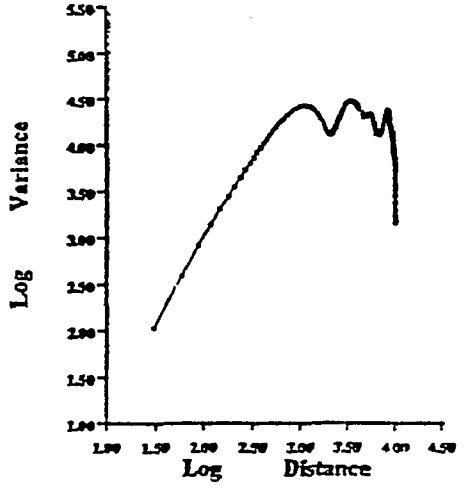

Aughwick, Pennsylvania

(Map Scale = 1 : 24,000; Used Map Size: 340 X 340 Pixels; Resolution: 30 meters)

Figure 5.1 Sample Variograms of Topographic Data. This figure clearly shows that in this particular area topography is only self-similar within quite limited scale range and that the relationship between the incremental variance and distance varies with sampling direction.

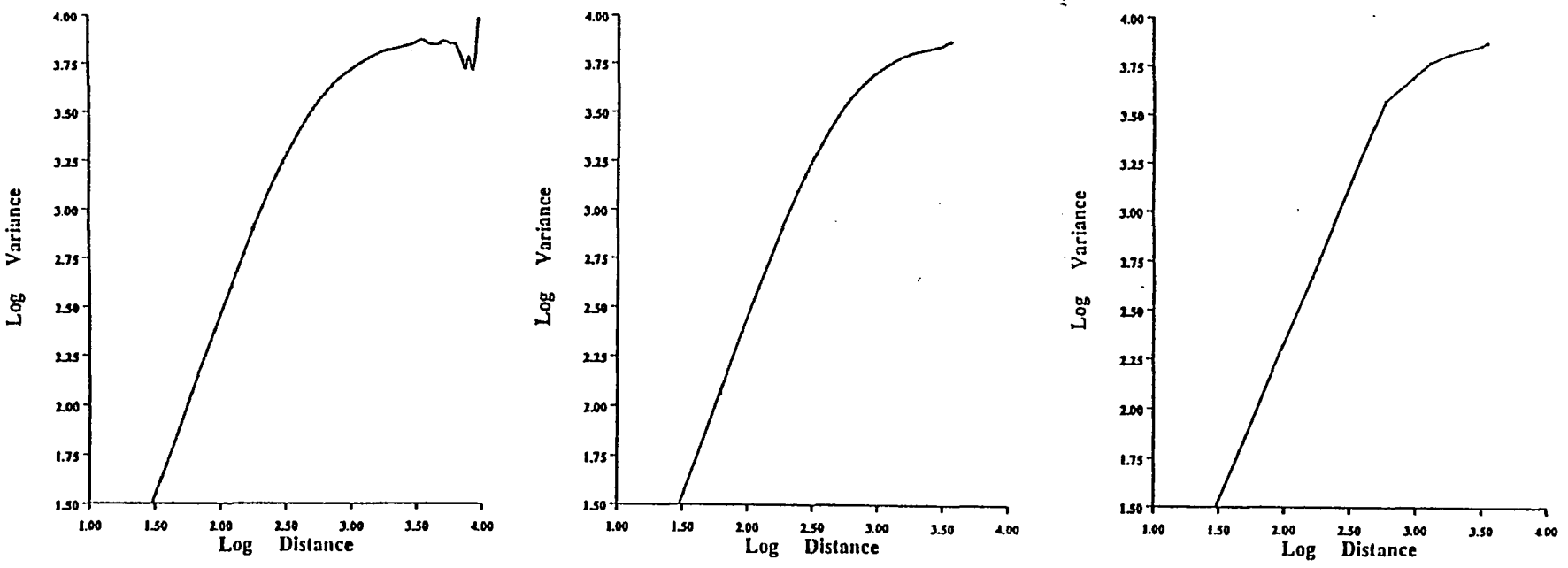

Figure 5.2 Subjective Assignment of Break Points. This procedure follows three steps: (a) plot the original variogram, (b) separate the non-periodic component, and (c) select "break points" through recursive curve-fitting using a r-squared value of 0.99. However, as discussed in the text, such procedure is quite subjective. The beginning point of periodicity is used in this study as the upper scale limit for regression. Though suffering somewhat from non-linearity, it provides an objective and unique choice. The results are always repeatable.

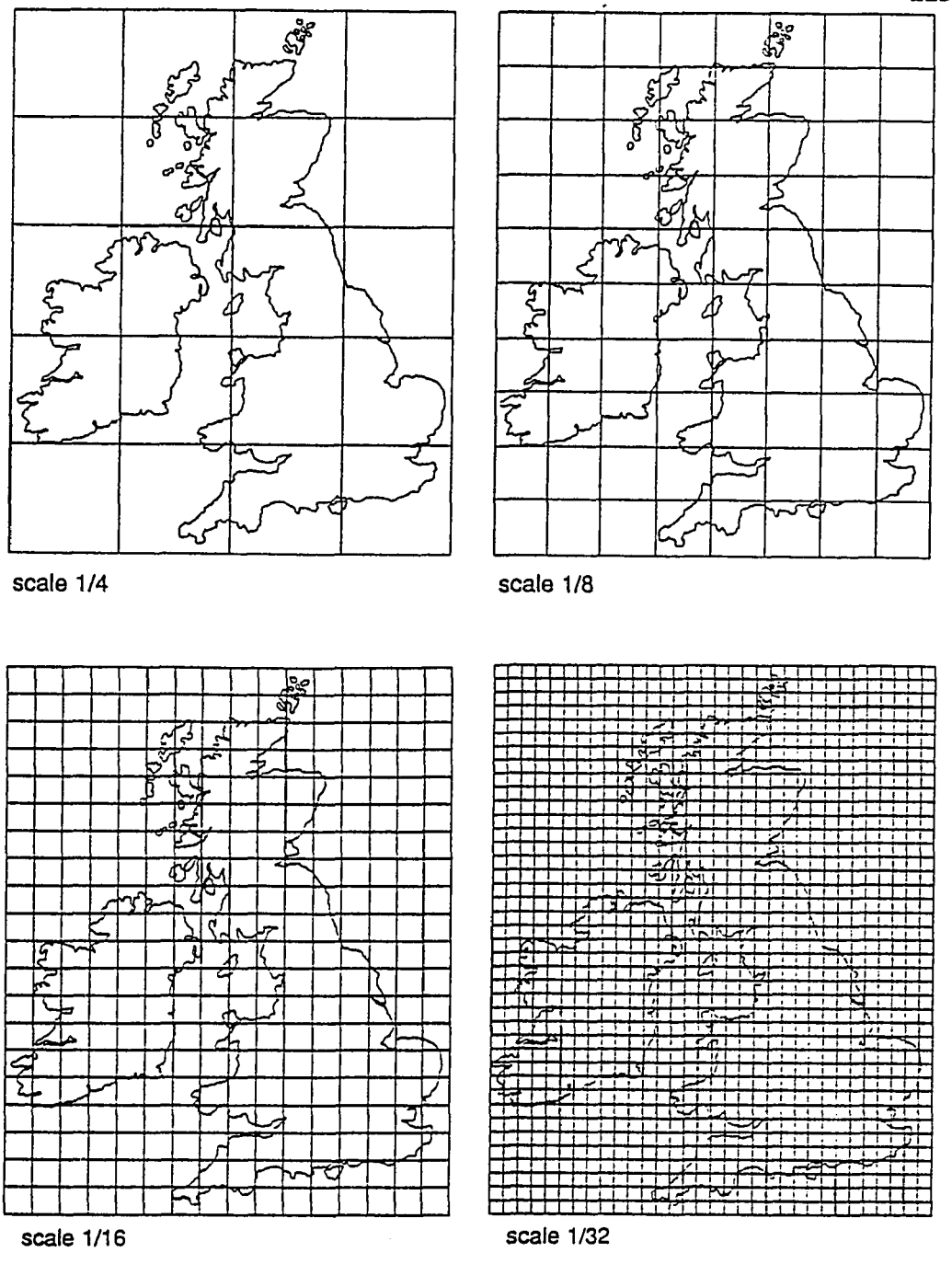

Figure 5.3 **Implementation of the Box-Counting Method for Estimating the Fractal Dimension of Terrain Features. Overlaying a grid on the coastline and count the grid cells intersected by the coastline to derive an estimate of its length. The smaller the grid cells one uses, the longer the coastline becomes. (after Peitgen et al., 1991)**

scale, or a systematic scheme of line generalization, on the length of contour lines. As cell size becomes smaller, finer details are reflected, giving a larger length estimate.

The box-counting method has long been used in the determination of the area of surface features (Gierhart, 1954). Hakanson (1978, 1981) was probably the first to use this method to determine the length of closed geomorphic lines such as shorelines of lakes and islands and topographic contour lines and open geomorphic lines such as coastlines. He called this method the "checkered transparent paper method", or the "CTP method". Hakanson defined the length of a line by overlaying a grid and counting the intersections between a grid and the geomorphic line of interest. However, as Goodchild (1980) pointed out, while in general we would expect two intersections for each intersected grid cell, in principle any even number of intersections is possible. As a result, the scale of the map, which determines the size of the grid, is not strictly related to a sampling interval. Goodchild (1980) suggested that it would be more appropriate, in terms of an analysis of fractal dimensionality, to count the number of cells intersected, rather than the number of intersections.

Goodchild (1980) tested the box-counting method on several strictly self-similar surfaces generated using a fractal simulation algorithm. He selected a contour on each surface at a height equal to the mean of the minimum and maximum heights. Cells were aggregated into larger aggregates of 5X5, 7X7, 9X9, and up to 19X19, and classified as black or white depending on whether the central cell lay above or below the contour respectively. To estimate the number of boundary cells, and thus the length of the contour line, as a function of aggregate size, a count was made of the number of black aggregates containing at least one white cell, which means that the cell was cut by the contour. The log of the number of boundary cells was then regressed against the log of the aggregate size. The fractal dimension is calculated by using the slope of the log-log curve similar to the walking dividers method, which will be described below. Goodchild found close agreement between the estimated D values and the fractal dimensions used to generate the self-similar surfaces.

In order to use the box-counting method to estimate the fractal dimension of real terrain data, Shelberg et al. (1983) extended Goodchild's work to take into consideration the variation of irregularities of natural surfaces at different elevations. Using three different algorithms, Goodchild (1982) computed the fractal dimensions of the coastline, 250 and 500 foot contours and lake outlines of Random Island, Newfoundland. His calculations revealed a systematic increase of fractal dimension with elevation, suggesting that the topography at the shoreline is considerably smoother than in the center of the island. On the other hand, Roy et al. (1987) found that the fractal dimension of the particular terrain surface they studied decreased with altitude. Culling and Datko (1987) revealed nonsystematic variation of fractal dimension in one of their data sets. To acquire an overall representation of surface irregularities in a particular region, Shelberg et al. modified the procedure to allow the computation of a composite fractal dimension for the surface by averaging the D values of any selected number of contour lines.

The algorithm of Shelberg et al. begins with the user specifying whether the fractal dimension will be determined by rows or columns. This option is provided so that a trend in the surface may be captured. The contour interval is then entered, which determines the number of contour lines that will be used in the analysis. The next step is to choose the maximum cell size, which is comparable to the opening width of the walking dividers. For each contour line, cells are aggregated into larger aggregates, up to the maximum cell size, and classified as above (black) or below (white) the contour line. To determine the length of the contour line as a function of aggregate size, a count is made of the number of boundary cells, black aggregates containing at least one white cell. The number of cells and the grid cell size are then used in deriving the fractal dimension as described above.

In order to interpret the results by the box-counting method meaningfully, it is important that we examine the effects of computational parameters on the estimated D values. The results of such an analysis is shown in Table 5.2. It is obvious that the

Table 5.2 EFFECTS OF COMPUTATIONAL PARAMETERS OF THE BOX-COUNTING METHOD ON THE NUMERICAL VALUE OF FRACTAL DIMENSION

CELL SIZE	FRACTAL DIMENSION	MINIMUM R^2 VALUE	FRACTAL DIMENSION	CONTOUR INTERVAL	FRACTAL DIMENSION
10	2.122677	0.0	2.165781	10 m	2.256209
20	2.158159	0.1	2.198698	20 m	2.256816
30	2.204458	0.2	2.268342	30 m	2.247748
40	2.249275	0.3	2.279559	40 m	2.256310
50	2.256209	0.4	2.277130	50 m	2.251831
60	2.263235	0.5	2.274752	60 m	2.257682
70	2.260707	0.6	2.260047	70 m	2.264620
80	2.248659	0.7	2.228063	80 m	2.242570
90	2.245598	0.8	2.213343	90 m	2.248537
100	2.254402	0.9	2.207882	100 m	2.251885

proper choice of the maximum cell size, the contour interval, and the minimum r^2 value plays a decisive role in the final outcome. The variation of D value due to these computational parameters can be as large or larger than the differences between different landform regions. For this particular data set (Shadow Mountain, Colorado), the number of contour lines included in the analysis seems having little effect on the D value. However, tests on other DEMs show that the contour interval does produce significant variations in the D value.

5.4 The Walking Dividers Method

The walking dividers method is also known as "the ruler method" (Aviles et al., 1987, p.337), "the compass method" (Brown, 1987b, p.1096), "the random walk technique" (Kaye, 1989, p.17), "the structured walk method" (Longley and Batty, 1989a, p.171), "the yardstick method" (Ouchi, 1990, p.69), the Richardson technique" (Roy and Robert, 1990, p.284), "the length-of-path method" (Newman and Turcotte, 1990, p.434), or "the divider method" (Andrle and Abrahams, 1989, p.198). This method has evolved from early attempts to measure the length of geographic lines (Steinhaus, 1954; Perkal, 1958a, 1958b; and Maling, 1968, p.151). Nevertheless, the walking dividers method for estimating fractal dimension as used today is directly based on the research of Lewis Fry Richardson, who died in 1953 and whose work was published posthumously in 1961.

In his studies on the causes of wars, Richardson (1961) considered the effects of geographical contiguity. He divided the entire world into "homoplatic" regions of approximately equal population and compared the incidence of wars between groups possessing a common boundary and those not possessing it. His search in encyclopedias revealed notable differences in the lengths of the common land frontiers claimed by different countries. Thus, he made a special investigation on the effect of intricacy of land frontiers or coastlines on the length estimates of geographic boundaries. He measured the lengths of coastlines and land frontiers by walking a pair of

dividers and found that as the opening size of the dividers becomes smaller the total length of the measured line becomes longer. He plotted the logarithms of total lengths against the logarithms of divider's widths and discovered a linear relationship between these two variables (Figure 5.4). From the plot, he derived the following empirical formula relating the total length of a line to the opening size of the dividers:

$$\Sigma \varepsilon \propto \varepsilon^{-\alpha}.$$

On the basis of this empirical finding, he speculated that "*it is doubtful whether the total polygonal length of a seacoast tends to any limit as the side of the polygon tends to zero*" (Richardson, 1961, p.170). He pointed out that α is a positive constant which is characteristic of each geographic line and reflects one's immediate visual perception of the irregularity of a line.

In the above empirical relationship, Mandelbrot (1967b) saw a similar mathematical structure to Zipf's law of word frequency in linguistics and Pareto's law of income distribution in economics he encountered previously. He viewed the seacoast shapes as examples of highly convolved curves that have the property of "statistical self-similarity". He commented that "*to speak of a length for such figures is usually meaningless*" and suggested that "*quantities other than length are thus needed to discriminate between various degrees of complication for a geographic curve.*" He proposed that "*when a curve is self-similar, it is characterized by an exponent of similarity, D, which possesses many properties of a dimension, though it is usually a fraction greater than the dimension 1 commonly attributed to curves.*" He transformed Richardson's empirical finding into the following form:

$$L(\varepsilon) = F \varepsilon^{1-D}$$

where

L is the total length of a curve,

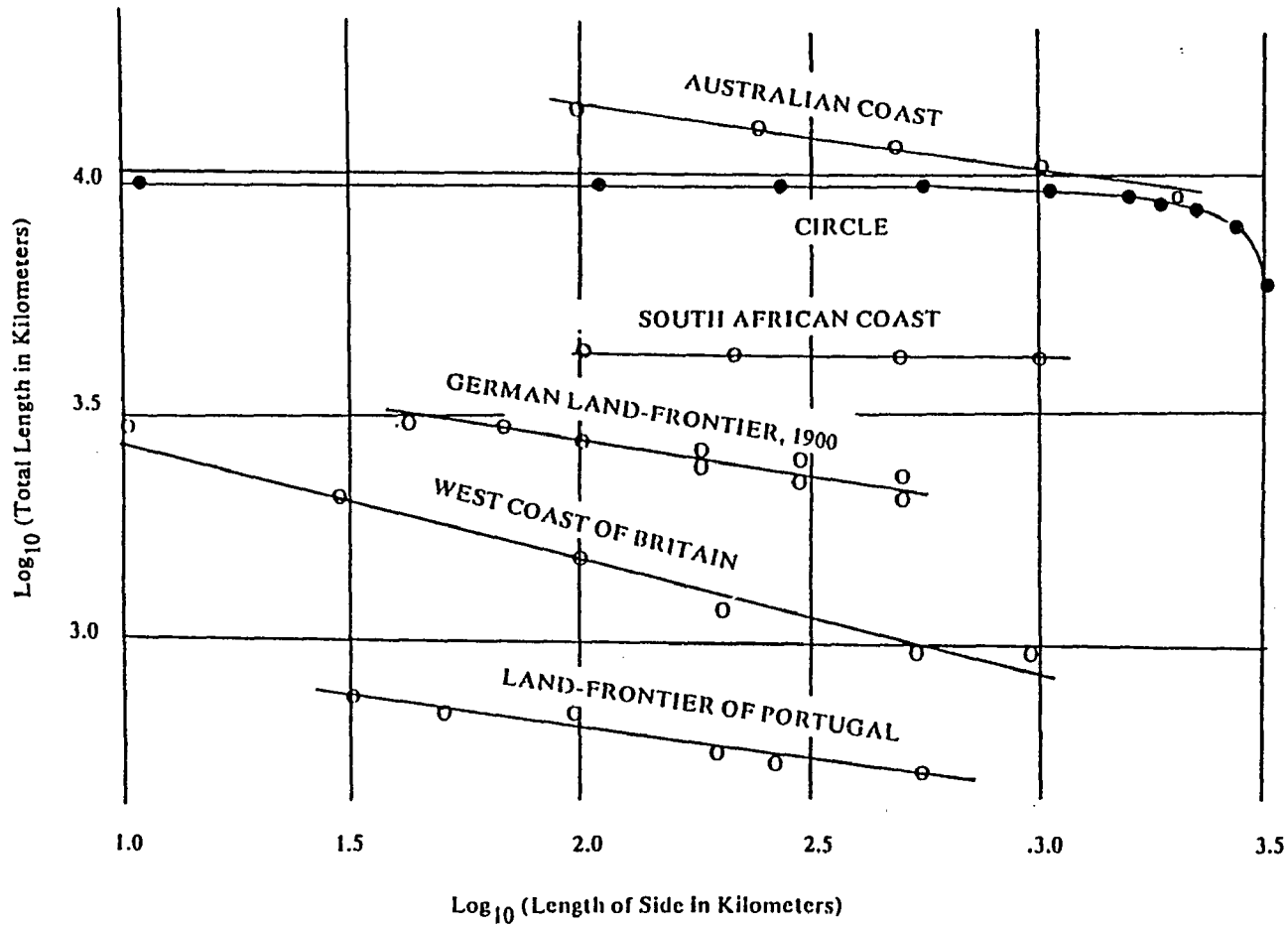

Figure 5.4 **The Empirical Relationship between the Opening Size of the Walking Divider and the Estimated Length of Geographic Lines Discovered by Richardson (1961)**

ε is the opening width of the divider,

F is a positive constant, and

D is equal to $1 - (- \alpha)$.

Taking logarithms on both sides of the equation yields

$$\log (L (\varepsilon)) = \log F + (1 - D) \log (\varepsilon).$$

The above formula points a way by which the fractal dimension can be evaluated empirically. We can measure the length using a series of step sizes and produce a log-log plot of the total length against the step size. Then, a least-squares linear regression analysis is used to estimate the slope of the log-log curve. If we use α to represent the slope of the log-log curve, we have

$$(1 - D) = - \alpha.$$

After rearrangement, we obtain the following equation:

$$D = 1 + \alpha.$$

Just as varied as its name, there are many variations in the implementation of the walking dividers method. Longley and Batty (1989a) compared the results of three different implementations. Klinkenberg and Goodchild (1992) described five variations of the walking dividers method. Altogether, there are at least eight different variants. Three options arise from the ways the last, partial step length is handled. Longley and Batty (1989a) described an "equipaced polygon method" and a "hybrid walk method". Some researchers used the total length of a line against the step length during regression. Others regressed the total number of steps against the step length. Most people carried out length measurement on a single map or maps of the same scale using multiple step sizes. Some authors used a single step size to estimate the total length of a certain line on maps of different scales. In a few cases, only two step sizes were used and the fractal dimension was determined analytically.

The implementation of the traditional walking dividers method is quite simple. The same procedure has been applied to both contour lines and topographic profiles (Figure 5.5). First, measurements are made by the progressive stepping of uniform intervals of known length along the line and counting the total number of steps. When the swinging divider intersects the measured line in more than one point, the intersection to be chosen is the one which comes next in order forward along the line. After the dividers are walked along the curve with one step size, the dividers are set to another opening size, which is usually a geometrical adding of the first step length. The geometric progression eliminates biasing when using linear regression to find the line of best fit and determine the slope of a log-log plot. After each time the dividers are walked along the curve, the number of steps and the corresponding step length are saved. These are then used in the linear regression. Finally, the fractal dimension of the curve is determined by using the above equation. To provide an indication of the degree of fit of data points to the regression line, r^2 is commonly computed.

The walking dividers method is probably the most commonly used method for estimating the fractal dimension. However, it should be realized that the results obtained by the walking dividers method are affected by many extraneous factors. First of all, when using the walking dividers method, the step length is usually fixed in advance and a strategy must be adopted to handle the remainder of the curve between the end of the last whole ruler and the curve's end point. The proper handling of the remainder is important, particularly for long ruler lengths because otherwise a change in the measured length of the curve could be indicating the unmeasured remainder rather than changes in complexity resolved along the curve. Generally, there are three different ways of handling the remainder. The first way is taking only those divider opening sizes that give a remainder less than a specified value or tolerance (Aviles et al., 1987; and Norton and Sorenson, 1989). In the second approach, the straight line distance between the ruler and the end of the curve is added to the total length (Richardson, 1961; and Shelberg et al., 1982). The third approach is to round up the

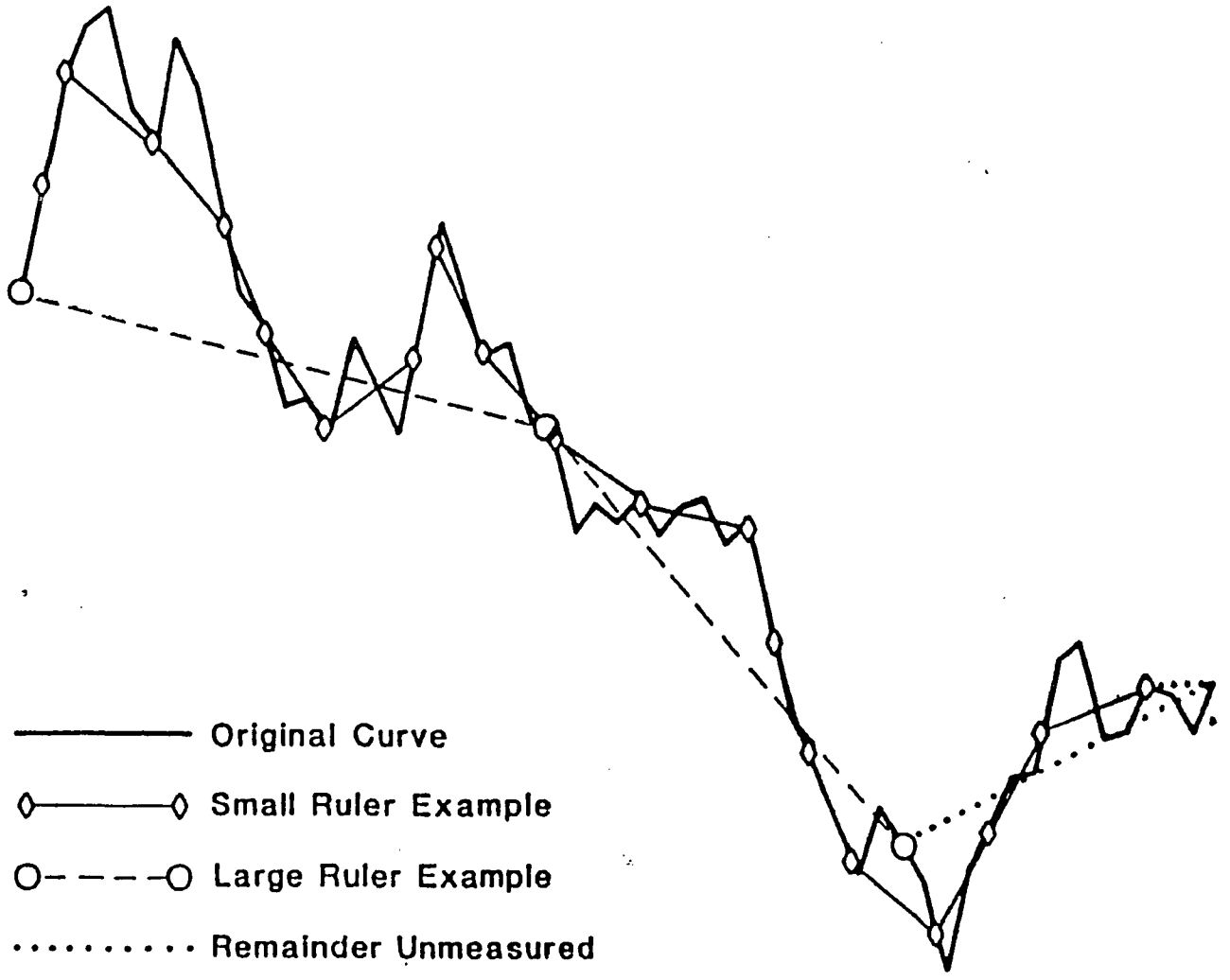

Figure 5.5 **Implementation of the Traditional Walking Dividers Method for Estimating the Fractal Dimension of Topographic Features (from Aviles et al., 1987)**

remainder left between the ruler and the end of the curve. Aviles et al. (1987) conducted an assessment on the variation in fractal dimension caused by the way by which the remainder was handled using Koch curves with known fractal dimensions. They found that the tolerance approach had the least oscillations in the Richardson curves; the second approach showed significantly larger oscillations in the Richardson curves, particularly for the longer rulers; and the rounding up method had the largest oscillations in the Richardson curves for all ruler lengths examined. Although all three methods reproduced the known values for the Koch curves, the tolerance method displayed the most stability and gave the best fit to the original curve. On the other hand, Andrle (1992) argued that the first approach was the worst choice among the three alternatives, the rounding method would provide a closer approximation, and adding the last, partial step as a fraction of the step length was the most favorable approach of all.

It is worth noting that regardless of which option is adopted, the error resulting from the last, partial step can not be eliminated entirely and its effect on the estimation of D will persist. As the step size increases, error in estimating D increases. Richardson (1961) used the step lengths which reach the end point of the line in a whole number of steps to eliminate the error caused by the last, partial step. However, this procedure severely reduces the number of step lengths available for regression and fitting more suitable step lengths can be extremely time-consuming. Andrle (1992) suggested to limit the maximum size of step length used in the analysis to minimize the error related to the handling of the remainder.

In the present study, the remainder is added to the total length as a fraction of the dividers opening size. This approach is adopted because it is the method used in most previous studies and adopting the same procedure facilitates comparison of results from this study with those of other researchers.

Secondly, Shelberg et al. (1982) pointed out the importance of selecting the appropriate initial step length. They suggested that because a digitized cartographic line is not an infinitely subdivided fractal curve, the selection of the initial step length must be based on some attribute of the digital curve. An extremely small opening size would extend the fractal character of the curve beyond its primitive subelements, biasing the measurement of fractal dimension toward a smoother line. In their study, the lower limit of the step length was determined by calculating the distance between each two consecutive digitized points on the curve and taking half the average distance. However, their own study reveals that an initial step length selected in this way normally falls below the primitive subelements of curves. Thus, they suggested that the initial step length should be determined by observing the behavior of scatterplots, r-square values, and the number of step lengths. Longley and Batty (1989a) suggested the use of the mean length of the chords between digitized points representing the curve as the initial step length.

An initial step length which is too short can be easily detected by either examining the amount of curvature present in the scatterplot or the low r^2 value. In Figure 5.6, the first six points are intentionally selected to fall below the resolution of the Digital Elevation Models, causing the curvature in the log-log plot.

Another important factor affecting the numerical value of fractal dimension is the number of step sizes used to approximate the total length of the curve. Shelberg et al. (1982) used 5 different step lengths in their analysis. Longley and Batty (1989a) suggested a minimum of 8 step lengths. The effects of the number of step sizes on the D value is illustrated in Figure 5.6. The last six points used step lengths greater than the straight line distance between the starting and ending points of the measured curve. In each case, the estimated total length of the curve is only a fraction of the used step length. Thus, all these step lengths yield basically the same total length. If not careful, we may obtain a much lower D value or misinterpret the log-log plot as an indication

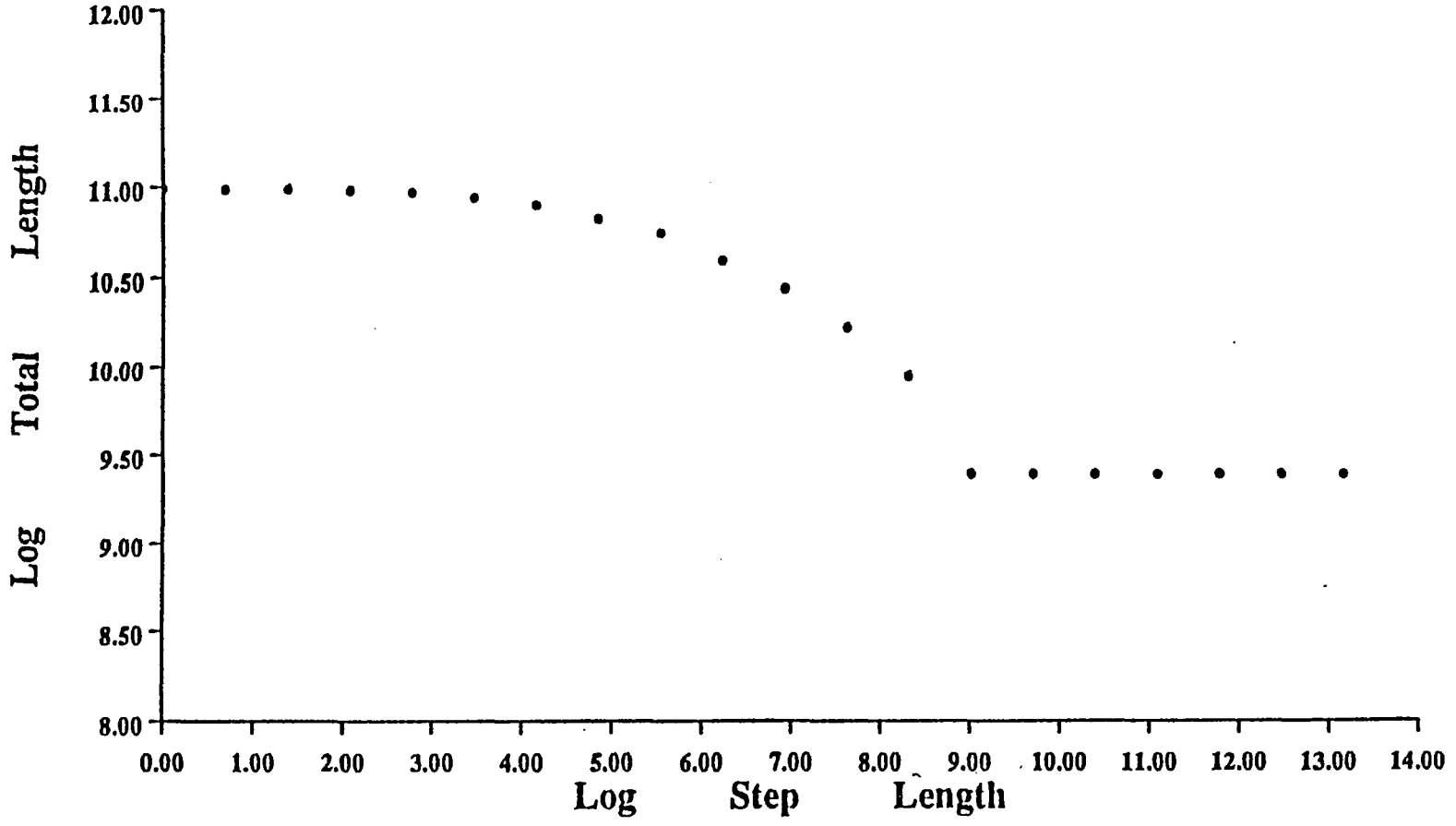

Figure 5.6 **Effects of the Initial Step Length and the Number of Step Sizes on the Estimation of Fractal Dimension**

of multifractals.

When using the walking dividers method to determine the fractal dimension of surfaces, the selection of contours that we submit to fractal analysis may also be critical. In a strictly self-similar terrain, this would not be of concern since all contours display similar complexity. However, natural terrains may exhibit systematic or non-systematic variations in complexity (Goodchild, 1982; and Roy et al., 1987). Goodchild (1982) and Roy et al. (1987) attributed the systematic variations of D values with elevation to different geomorphological processes operating at a large scale. However, when deriving a composite measure of surface roughness for a particular area from individual contour lines and comparing it with those of other areas, these variations need to be taken into consideration. Shelberg et al. (1983) suggested that a set of contours should be used in the analysis. Similarly, the surface irregularities may vary from profile to profile. Clarke and Schweizer (1991) developed a method to compute the fractal dimension by averaging the D values of all profiles in two orthogonal directions.

In addition, Richardson (1961) discovered that the total polygonal length usually depends on the point that is taken as the starting point. Aviles et al. (1987) also reported disagreement between the backward and forward calculation of the total length for the short dividers opening sizes. To minimize this problem, Kaye and Clark (1985) have taken coarse scale measurements from a small number of different starting points, and then averaged them to get a more stable final value. A similar procedure was also used by Kent and Wong (1982). Longley and Batty (1989a) have taken this approach to the limit by using the average of the lengths recorded by starting measurement from every successive point on the digitized curve. However, this approach is only applicable to closed curves. Besides, it is probably too time-consuming for most applications. Andrle (1992) carried out a special study of the effect of the starting point on D and found that for the four geographic lines he studied the standard deviation of estimates of D reached a stable low value before the number of starting points

reached 50.

Finally, it is very important to realize that the walking dividers method, originally developed using self-similar fractals, will give the correct fractal dimension only under certain conditions when applied to self-affine fractals such as the coordinate plots of the fractional Brownian motion or vertical cuts of terrain relief (Mandelbrot, 1985; Brown, 1987b; and Wong, 1987). Most commonly, the walking dividers method will greatly underestimate the fractal dimension of self-affine fractals such as topographic profiles (Roy and Robert, 1990). On the other hand, Brown (1987) demonstrated that the proper fractal dimension of self-affine fractals could be derived using the dividers method by exaggerating the vertical scale. However, the present study shows that changing the vertical scale does not always lead to the desirable results. Figure 5.7 shows the variations of D with changing vertical scales for two topographic profiles randomly selected from two different DEMs. It can be seen that the D value of both profiles stablizes when the vertical scaling factor reaches a certain threshold. However, the scaling factor at which the D value stablizes is quite different for each profile. The D value of one profile stablizes when the vertical elevation is exaggerated by about 30 times while the D value of the other profile becomes stablized at an exaggeration of approximately 130 times. Finding the most suitable scaling factor can be a very time-consuming recursive procedure. In addition, the initial step length and the number of step sizes need to be adjusted when the vertical exaggeration reaches a certain limit. It is not uncommon that the D value does not stablize before the initial step length and the number of step sizes need to be adjusted. However, when these parameters are changed, it becomes impossible to evaluate the effects of changing vertical exaggeration on the D value since varying the initial step length and the number of step sizes also introduce large changes in the fractal dimension. For one particular profile extracted from the Coharie NW Quadrangle (North Carolina), vertical exaggerations up to 2400 times, involving three adjustments of initial step length and the total number of step sizes, still show no sign of stablization of the D value.

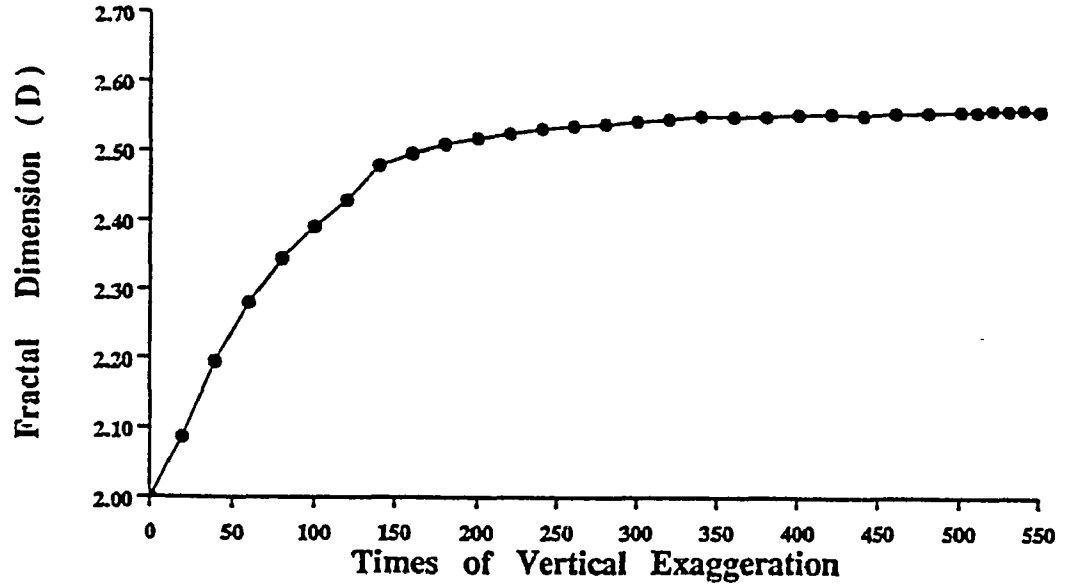

(a)

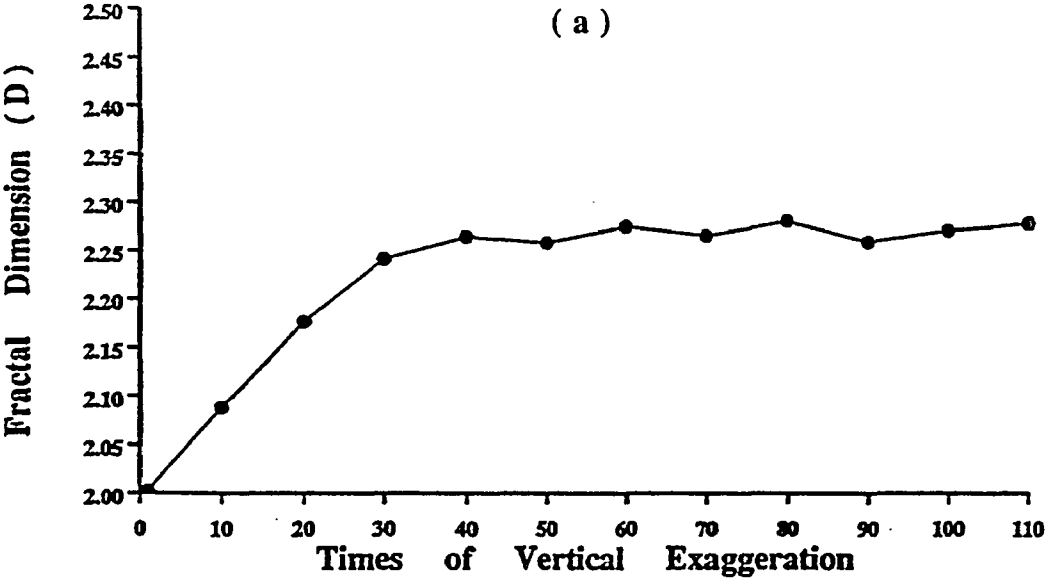

(b)

Figure 5.7 Variation of D with Changing Vertical Exaggeration

5.5 A Comparison of Results by Different Methods

The three methods described above are tested using close to two hundred Digital Elevation Models acquired from the U. S. Geological Survey. The variogram method and the box-counting method are used for estimating the fractal dimension of all DEMs. The results are given in Table 5.3. The fractal dimensions by the variogram method shown here are the composite fractal dimensions for the E-W and N-S directions, that is, the squared difference in elevation for each distance class represents the average of all elevation pairs of that class in both directions. The fractal dimensions by the box-counting method are calculated both using rows and using columns to reveal the effects of the presence of a general trend. The contour intervals used are either 10 meters or 2 meters depending on the relief of each area. This procedure ensures that there are a minimum of ten contour lines included in deriving the average fractal dimension for each DEM in order to reflect the variability of terrain characteristics. The maximum cell size used is 100 and the minimum r^2 value for a particular contour line to be included in deriving the average fractal dimension is 0.64. As can be seen, the differences between the fractal dimensions estimated by the variogram method and by the box-counting method are quite small. If we compute the difference between the variogram method and the box-counting method by comparing the two closer values, we find surprisingly good agreement between the two methods, considering the fact that many computational parameters play a role in determining the final outcome of the fractal computation. The vast majority of DEMs have differences smaller than 0.1. This seems to suggest that these results are relatively reliable and both of these methods work equally well on topographic data. However, comparatively, the use of the variogram method involves fewer subjective decisions on the selection of computational parameters. In fact, the only decision that needs to be made when using the variogram method is the selection of the scale range for regression analysis. By adopting the beginning point of periodicity as the upper limit of scaling, the choice will become unique for each individual data set. In addition, the variogram method

Table 5.3 A COMPARISON OF THE ESTIMATED FRACTAL DIMENSIONS BY THE VARIOGRAM METHOD AND THE BOX-COUNTING METHOD

NAME OF TOPO QUAD	VARIOGRAM	BOX-COUNTING			SMALLER DIFFERENCE
		USING ROWS	USING COLUMNS	DIFFERENCE	
Barbara, MS	2.54 (0.99)	2.65 (0.91)	2.66 (0.93)	0.01	0.11
Barlow, KY-IL	2.49 (0.99)	2.55 (0.87)	2.30 (0.91)	0.25	0.06
Coharie NW, NC	2.79 (0.88)	2.91 (0.92)	2.92 (0.89)	0.01	0.12
Coharie SE, NC	2.80 (0.91)	2.86 (0.94)	2.92 (0.92)	0.06	0.06
Coharie SW, NC	2.80 (0.84)	2.91 (0.91)	2.91 (0.91)	0.00	0.11
Dobbersville, NC	2.77 (0.87)	2.86 (0.89)	2.89 (0.93)	0.03	0.09
Faison, NC	2.78 (0.91)	2.92 (0.90)	2.90 (0.91)	0.02	0.14
Grantham, NC	2.38 (1.00)	2.42 (0.81)	2.25 (0.81)	0.17	0.04
Horn Lake SW, MS	2.59 (0.99)	2.72 (0.89)	2.55 (0.95)	0.17	0.04
Newton Grove North, NC	2.61 (0.98)	2.63 (0.90)	2.70 (0.88)	0.07	0.02
Calahain, NC	2.61 (0.99)	2.65 (0.93)	2.62 (0.92)	0.03	0.01
Central, NC	2.48 (0.97)	2.67 (0.83)	2.54 (0.91)	0.13	0.06
Church Road, VA	2.68 (0.99)	2.77 (0.93)	2.72 (0.93)	0.05	0.04
Cleveland, NC	2.61 (0.98)	2.73 (0.91)	2.73 (0.94)	0.00	0.12
Cool Springs, NC	2.71 (0.95)	2.68 (0.91)	2.72 (0.93)	0.04	0.01
Harmony, NC	2.66 (0.97)	2.75 (0.92)	2.75 (0.89)	0.00	0.09
Shepherds, NC	2.66 (0.98)	2.66 (0.89)	2.78 (0.92)	0.12	0.00
Statesville East, NC	2.68 (0.95)	2.71 (0.86)	2.80 (0.93)	0.09	0.03
Statesville West, NC	2.70 (0.94)	2.79 (0.89)	2.78 (0.93)	0.01	0.08
Troutman, NC	2.73 (0.96)	2.68 (0.94)	2.74 (0.94)	0.06	0.01
Prentiss, NC	2.35 (0.99)	2.50 (0.81)	2.39 (0.86)	0.11	0.04
Shining Rock, NC	2.37 (0.99)	2.49 (0.86)	2.43 (0.83)	0.06	0.06
Mt. Le Conte, TN-NC	2.29 (1.00)	2.27 (0.84)	2.35 (0.80)	0.08	0.02
Smokemont, NC	2.53 (0.95)	2.46 (0.87)	2.49 (0.84)	0.03	0.04
Aughwick, PA	2.27 (0.98)	2.54 (0.84)	2.61 (0.83)	0.07	0.27
Baker, WV	2.42 (0.97)	2.35 (0.86)	2.47 (0.83)	0.12	0.05
Blain, PA	2.54 (0.90)	2.48 (0.79)	2.44 (0.81)	0.04	0.06
Blair Mills, PA	2.35 (0.97)	2.57 (0.85)	2.57 (0.84)	0.00	0.22
Burem, TN	2.66 (0.89)	2.64 (0.90)	2.66 (0.86)	0.02	0.00
Camelot, TN	2.49 (0.92)	2.61 (0.86)	2.59 (0.88)	0.02	0.10
Duffield, VA	2.48 (0.96)	2.53 (0.87)	2.55 (0.88)	0.02	0.05
Kyles Ford, VA	2.56 (0.89)	2.65 (0.85)	2.61 (0.84)	0.04	0.05
Looneys Gap, TN	2.38 (0.96)	2.70 (0.84)	2.67 (0.86)	0.03	0.29
McCoysville, PA	2.46 (0.97)	2.59 (0.82)	2.43 (0.83)	0.16	0.03
Plum Grove, VA	2.53 (0.89)	2.78 (0.84)	2.61 (0.87)	0.17	0.08
Rio, West VA	2.41 (0.97)	2.42 (0.86)	2.48 (0.85)	0.06	0.01
Stickleyville, VA	2.56 (0.89)	2.61 (0.78)	2.43 (0.90)	0.18	0.05
Stony Point, TN	2.56 (0.86)	2.63 (0.81)	2.60 (0.81)	0.03	0.04
Wardensville, WV	2.46 (0.95)	2.39 (0.80)	2.46 (0.79)	0.07	0.00
Yellow Springs, WV	2.43 (0.96)	2.48 (0.85)	2.53 (0.83)	0.05	0.05
Arena, NY	2.51 (0.91)	2.40 (0.74)	2.47 (0.84)	0.07	0.04
Broad Bottom, KY	2.48 (0.90)	2.80 (0.87)	2.80 (0.89)	0.00	0.32
Cameron Dent Run Proj, PA	2.58 (0.87)	2.68 (0.84)	2.59 (0.81)	0.09	0.01
Downsville, NY	2.49 (0.90)	2.42 (0.77)	2.53 (0.79)	0.11	0.04
Emporium, PA	2.53 (0.89)	2.61 (0.89)	2.61 (0.86)	0.00	0.08
Fayetteville, WV	2.61 (0.89)	2.60 (0.83)	2.56 (0.81)	0.04	0.01
First Fork, PA	2.55 (0.91)	2.61 (0.85)	2.53 (0.85)	0.08	0.02
Fish Eddy, NY	2.49 (0.92)	2.46 (0.82)	2.60 (0.82)	0.14	0.03
Fleischmanns, NY	2.28 (0.97)	2.40 (0.74)	2.48 (0.74)	0.08	0.12
Hancock, PA-NY	2.56 (0.85)	2.50 (0.84)	2.56 (0.77)	0.06	0.00
Harold, KY	2.64 (0.81)	2.78 (0.89)	2.74 (0.89)	0.04	0.10
Horton, NY	2.40 (0.92)	2.46 (0.76)	2.53 (0.84)	0.07	0.06
Hunter, NY	2.42 (0.96)	2.44 (0.75)	2.42 (0.82)	0.02	0.00
Keating Summit, PA	2.66 (0.85)	2.41 (0.81)	2.72 (0.85)	0.32	0.06
Lancer, KY	2.52 (0.87)	2.74 (0.90)	2.76 (0.90)	0.02	0.22
Lee Fire Tower, PA	2.62 (0.89)	2.70 (0.84)	2.59 (0.85)	0.11	0.03
Lewbeach, NY	2.56 (0.87)	2.40 (0.78)	2.48 (0.76)	0.08	0.08
Lexington, NY	2.33 (0.97)	2.51 (0.70)	2.51 (0.85)	0.00	0.18
Livingston Manor, NY	2.54 (0.91)	2.39 (0.79)	2.53 (0.79)	0.14	0.01
Long Eddy, PA	2.57 (0.84)	2.51 (0.79)	2.62 (0.76)	0.11	0.05
Margaretville, NY	2.47 (0.89)	2.44 (0.77)	2.47 (0.73)	0.03	0.00
Marshlands, PA	2.61 (0.90)	2.58 (0.88)	2.62 (0.85)	0.04	0.01
Martin, KY	2.67 (0.76)	2.79 (0.88)	2.80 (0.89)	0.01	0.12
Mc Dowell, KY	2.68 (0.75)	2.82 (0.85)	2.73 (0.89)	0.09	0.05

Table 5.3 continued.

NAME OF TOPO QUAD	VARIOGRAM	BOX-COUNTING			SMALLER DIFFERENCE
		USING ROWS	USING COLUMNS	DIFFERENCE	
Pikeville, KY	2.60 (0.82)	2.77 (0.87)	2.76 (0.87)	0.01	0.16
Prestonburg, KY	2.62 (0.80)	2.80 (0.88)	2.81 (0.90)	0.01	0.18
Roscoe, NY	2.46 (0.90)	2.47 (0.78)	2.54 (0.77)	0.07	0.01
Seager, NY	2.41 (0.94)	2.43 (0.78)	2.39 (0.78)	0.04	0.02
Thomas, KY	2.59 (0.83)	2.83 (0.87)	2.81 (0.90)	0.02	0.22
Wayland, KY	2.52 (0.86)	2.75 (0.87)	2.72 (0.88)	0.03	0.20
West Kill, NY	2.35 (0.96)	2.47 (0.79)	2.33 (0.75)	0.14	0.02
Wharton, PA	2.53 (0.89)	2.59 (0.88)	2.69 (0.84)	0.10	0.06
Whitwell, TN	2.36 (0.96)	2.36 (0.82)	2.35 (0.77)	0.01	0.00
Chatham, NJ	2.49 (0.94)	2.60 (0.82)	2.58 (0.84)	0.02	0.09
Hancock, MA-NY	2.34 (0.97)	2.46 (0.82)	2.35 (0.77)	0.11	0.01
Lyndonville SE, VT	2.42 (0.97)	2.37 (0.83)	2.40 (0.85)	0.03	0.02
Pound Ridge, CT	2.60 (0.94)	2.63 (0.89)	2.59 (0.86)	0.04	0.01
Roselle, NJ	2.48 (0.98)	2.45 (0.85)	2.43 (0.86)	0.02	0.03
Mammoth Cave, KY	2.64 (0.86)	2.65 (0.85)	2.77 (0.86)	0.12	0.01
Park City, KY	2.62 (0.91)	2.55 (0.90)	2.65 (0.88)	0.10	0.03
Rhoda, KY	2.62 (0.86)	2.68 (0.87)	2.69 (0.88)	0.01	0.06
Smiths Grove, KY	2.67 (0.87)	2.54 (0.84)	2.59 (0.88)	0.05	0.08
Williams, IN	2.63 (0.89)	2.70 (0.91)	2.69 (0.89)	0.01	0.06
Bartlett Blue Mound, KS-MO	2.58 (0.97)	2.60 (0.92)	2.60 (0.90)	0.00	0.02
Chetopa Blue Mound, KS-MO	2.72 (0.96)	2.86 (0.89)	2.65 (0.94)	0.21	0.07
Harvey, IA	2.56 (0.97)	2.51 (0.88)	2.49 (0.92)	0.02	0.05
Labette, KS-MO	2.60 (0.99)	2.74 (0.92)	2.64 (0.86)	0.10	0.04
Leighton, IA	2.56 (0.94)	2.61 (0.85)	2.54 (0.88)	0.07	0.02
Missouri Valley NW, NE	2.62 (0.98)	2.61 (0.93)	2.62 (0.92)	0.01	0.00
Oswego Blue Mount, KS-MO	2.64 (0.97)	2.65 (0.86)	2.50 (0.89)	0.15	0.01
Paxton NW (Perdueville), IL	2.42 (0.99)	2.49 (0.86)	2.56 (0.89)	0.07	0.07
Paxton SE (Gifford), IL	2.44 (1.00)	2.43 (0.90)	2.44 (0.89)	0.01	0.00
Paxton SW (Rantoul), IL	2.49 (0.99)	2.47 (0.90)	2.51 (0.90)	0.04	0.02
Pella, IA	2.59 (0.96)	2.50 (0.87)	2.57 (0.86)	0.07	0.02
Peoria, IA	2.53 (0.98)	2.57 (0.90)	2.57 (0.88)	0.00	0.04
Bar C Bar Ranch, NM	2.37 (1.00)	2.50 (0.91)	2.24 (0.82)	0.26	0.13
Derrick Draw, NM	2.41 (0.99)	2.61 (0.86)	2.29 (0.81)	0.32	0.12
Dexter East, NM	2.46 (0.98)	2.42 (0.90)	2.25 (0.79)	0.17	0.04
Double Mill Draw NE, TX	2.44 (0.99)	2.49 (0.88)	2.50 (0.82)	0.01	0.05
Double Mill Draw NW, TX	2.50 (0.99)	2.46 (0.90)	2.48 (0.84)	0.02	0.02
Double Mill Draw SE, TX	2.42 (0.99)	2.50 (0.87)	2.46 (0.88)	0.04	0.04
Forks Ranch, MT	2.56 (0.96)	2.50 (0.90)	2.56 (0.90)	0.06	0.00
Fort Hood, TX	2.63 (0.92)	2.47 (0.87)	2.60 (0.90)	0.13	0.03
Holmes Ranch, MT	2.50 (0.99)	2.44 (0.88)	2.56 (0.90)	0.12	0.06
Hot Springs, SD	2.48 (0.97)	2.51 (0.88)	2.45 (0.84)	0.06	0.03
Indio Hill, TX	2.52 (0.97)	2.48 (0.86)	2.41 (0.83)	0.07	0.04
North Fort Hood, TX	2.49 (0.99)	2.41 (0.86)	2.49 (0.88)	0.08	0.00
North Loup Hord, NE	2.63 (0.97)	2.49 (0.90)	2.65 (0.89)	0.16	0.02
Pine Butte School, MT	2.50 (0.99)	2.64 (0.84)	2.56 (0.91)	0.08	0.06
Post Oak Mountain, TX	2.54 (0.96)	2.45 (0.86)	2.58 (0.85)	0.13	0.04
Shell Mountains, TX	2.53 (0.98)	2.48 (0.85)	2.50 (0.87)	0.02	0.03
Bowen Mountain, CO	2.34 (0.97)	2.44 (0.73)	2.31 (0.73)	0.13	0.03
Granby, CO	2.48 (0.97)	2.37 (0.84)	2.37 (0.85)	0.00	0.11
Grand Lake, CO	2.36 (0.99)	2.45 (0.76)	2.42 (0.77)	0.03	0.06
Isolation Peak, CO	2.39 (0.95)	2.46 (0.77)	2.43 (0.74)	0.03	0.04
Mc Henrys Peak, CO	2.44 (0.96)	2.38 (0.76)	2.35 (0.77)	0.03	0.06
Monarch Lake, CO	2.51 (0.93)	2.41 (0.74)	2.47 (0.71)	0.06	0.04
Shadow Mountain, CO	2.32 (0.99)	2.42 (0.74)	2.24 (0.83)	0.18	0.08
Strawberry Lake, CO	2.44 (0.98)	2.44 (0.84)	2.39 (0.81)	0.05	0.00
Trail Mountain, CO	2.39 (0.97)	2.22 (0.84)	2.51 (0.76)	0.29	0.11
Big Horn, WY	2.39 (0.99)	2.32 (0.88)	2.58 (0.83)	0.26	0.07
Flaming Gorge, UT	2.45 (0.98)	2.42 (0.84)	2.36 (0.85)	0.06	0.03
Pat O'Hara Mountain, WY	2.28 (0.99)	2.45 (0.75)	2.28 (0.87)	0.17	0.00
Atlanta West, ID	2.45 (0.94)	2.34 (0.82)	2.47 (0.83)	0.13	0.02
Bata Mountain, MT	2.39 (0.99)	2.35 (0.84)	2.40 (0.82)	0.05	0.01
Belmont Point, MT	2.37 (0.99)	2.29 (0.84)	2.41 (0.82)	0.12	0.04
Belmore Sloughs, MT	2.50 (0.88)	2.39 (0.75)	2.38 (0.80)	0.01	0.11
Cedar Lake, MT	2.45 (0.94)	2.54 (0.76)	2.23 (0.76)	0.31	0.09
Chief Mountain, MT	2.24 (1.00)	2.27 (0.82)	2.26 (0.76)	0.01	0.02
Condon, MT	2.23 (1.00)	2.45 (0.77)	2.43 (0.73)	0.02	0.20

Table 5.3 continued.

NAME OF TOPO QUAD	VARIOGRAM	BOX-COUNTING			SMALLER DIFFERENCE
		USING ROWS	USING COLUMNS	DIFFERENCE	
Crimson Peak, MT	2.29 (0.97)	2.59 (0.72)	2.41 (0.79)	0.18	0.12
Elevation Mountain, MT	2.52 (0.91)	2.46 (0.80)	2.52 (0.81)	0.06	0.00
Gold Creek Peak, MT	2.57 (0.84)	2.44 (0.78)	2.43 (0.81)	0.01	0.13
Gray Wolf Lake, MT	2.54 (0.88)	2.44 (0.79)	2.35 (0.76)	0.09	0.10
Hemlock Lake, MT	2.34 (0.99)	2.43 (0.79)	2.23 (0.78)	0.20	0.09
Holland Peak, MT	2.46 (0.93)	2.44 (0.73)	2.36 (0.72)	0.18	0.02
Lake Inez, CO	2.36 (0.99)	2.48 (0.80)	2.14 (0.79)	0.34	0.12
Lake Marshall, MT	2.40 (0.98)	2.33 (0.81)	2.38 (0.76)	0.05	0.02
Morrell Lake, MT	2.51 (0.94)	2.56 (0.76)	2.51 (0.75)	0.05	0.00
Morrell Mountain, MT	2.58 (0.89)	2.46 (0.78)	2.54 (0.75)	0.08	0.04
Peck Lake, MT	2.23 (1.00)	2.53 (0.80)	2.15 (0.80)	0.38	0.08
Porcupine Creek, MT	2.43 (0.98)	2.53 (0.80)	2.31 (0.78)	0.22	0.10
Priest Lake NE, ID	2.30 (0.98)	2.40 (0.72)	2.10 (0.86)	0.30	0.10
Salmon Lake, MT	2.37 (0.96)	2.41 (0.81)	2.40 (0.84)	0.01	0.03
Seeley Lake East, MT	2.39 (0.98)	2.32 (0.80)	2.32 (0.85)	0.00	0.07
Seeley Lake West, MT	2.38 (0.99)	2.43 (0.80)	2.23 (0.81)	0.20	0.05
Upper Jocko Lake, MT	2.47 (0.96)	2.41 (0.81)	2.47 (0.83)	0.06	0.00
Wapiti Lake, MT	2.51 (0.93)	2.42 (0.73)	2.39 (0.78)	0.03	0.09
Woodworth, MT	2.35 (0.98)	2.28 (0.78)	2.31 (0.90)	0.03	0.04
Yew Creek, MT	2.24 (0.99)	2.23 (0.87)	2.23 (0.81)	0.00	0.01
Wilcox, WA	2.55 (0.95)	2.70 (0.86)	2.53 (0.92)	0.17	0.02
Yakima East, WA	2.24 (0.99)	2.17 (0.73)	2.31 (0.97)	0.14	0.07
Anvil Points, CO	2.45 (0.98)	2.41 (0.76)	2.55 (0.79)	0.14	0.04
Greasewood Canyon, CO	2.66 (0.88)	2.57 (0.84)	2.52 (0.88)	0.05	0.09
Moccasin Mesa, CO	2.56 (0.88)	2.52 (0.83)	2.79 (0.81)	0.27	0.04
Moqui Canyon, CO	2.52 (0.91)	2.45 (0.85)	2.56 (0.84)	0.11	0.04
Wetherill Mesa, CO	2.60 (0.87)	2.44 (0.87)	2.79 (0.86)	0.35	0.16
Zion National Park NE, UT	2.58 (0.93)	2.66 (0.86)	2.58 (0.85)	0.08	0.00
Adel, OR	2.40 (0.95)	2.21 (0.77)	2.15 (0.81)	0.06	0.19
Buffalo Springs NW, NV	2.23 (1.00)	2.55 (0.81)	2.27 (0.84)	0.28	0.04
Buffalo Springs SW, NV	2.27 (0.99)	2.33 (0.78)	2.18 (0.79)	0.15	0.06
Cain Mountain NE, NV	2.28 (1.00)	2.28 (0.85)	2.19 (0.73)	0.09	0.00
Cain Mountain NW, NV	2.42 (0.96)	2.29 (0.82)	2.19 (0.78)	0.10	0.13
Cain Mountain SE, NV	2.22 (1.00)	2.24 (0.78)	2.28 (0.72)	0.04	0.02
Cain Mountain SW, NV	2.24 (1.00)	2.12 (0.77)	2.35 (0.80)	0.23	0.11
Calderwood Resevoir, OR	2.41 (0.99)	2.26 (0.80)	2.41 (0.77)	0.15	0.00
Coleman Lake, OR	2.38 (0.96)	2.27 (0.83)	2.45 (0.73)	0.18	0.07
Collins Rim, OR	2.21 (1.00)	2.25 (0.80)	2.25 (0.80)	0.00	0.04
Cortez NE, NV	2.32 (1.00)	2.30 (0.87)	2.33 (0.78)	0.03	0.02
Cortez NW, NV	2.41 (0.99)	2.34 (0.75)	2.40 (0.85)	0.06	0.01
Cortez SE, NV	2.35 (0.97)	2.38 (0.83)	2.24 (0.79)	0.14	0.03
Cortez SW, NV	2.33 (1.00)	2.39 (0.88)	2.29 (0.84)	0.10	0.04
Crump Lake, OR	2.43 (0.97)	2.39 (0.77)	2.24 (0.70)	0.15	0.04
Drake Peak, OR	2.41 (0.97)	2.36 (0.77)	2.22 (0.79)	0.14	0.05
Fencemaker NE, NV	2.28 (0.99)	2.34 (0.85)	2.20 (0.76)	0.14	0.06
Fencemaker SE, NV	2.23 (0.99)	2.33 (0.81)	2.07 (0.77)	0.26	0.10
Glamis SE, CA	2.43 (0.98)	2.56 (0.88)	2.55 (0.88)	0.01	0.12
Kyle Hot Springs NE, NV	2.29 (1.00)	2.41 (0.81)	2.19 (0.84)	0.22	0.10
Kyle Hot Springs SE, NV	2.28 (1.00)	2.27 (0.77)	2.32 (0.80)	0.05	0.01
May Lake, OR	2.37 (0.99)	2.24 (0.88)	2.28 (0.80)	0.04	0.09
Mt. Moses NW, NV	2.26 (1.00)	2.38 (0.79)	2.21 (0.83)	0.17	0.05
Mt. Moses SW, NV	2.27 (0.99)	2.26 (0.86)	2.31 (0.81)	0.05	0.01
Mt. Tobin NE, NV	2.20 (1.00)	2.36 (0.82)	2.06 (0.73)	0.30	0.14
Mt. Tobin NW, NV	2.23 (1.00)	2.30 (0.83)	2.19 (0.81)	0.11	0.04
Mt. Tobin SW, NV	2.31 (0.99)	2.39 (0.79)	2.15 (0.85)	0.24	0.08
Priday Resevoir, OR	2.42 (0.96)	2.19 (0.80)	2.19 (0.80)	0.00	0.22
Sage Hen Butte, OR	2.58 (0.89)	2.51 (0.81)	2.42 (0.76)	0.09	0.07
Mt. Langley, CA	2.23 (1.00)	2.35 (0.76)	2.19 (0.85)	0.16	0.04
Mount Tom SW, CA	2.52 (0.91)	2.37 (0.77)	2.34 (0.72)	0.03	0.15
Yosemite NW, CA	2.42 (0.95)	2.25 (0.81)	2.36 (0.81)	0.11	0.06
Pacifico Mountain, CA	2.46 (0.98)	2.39 (0.88)	2.45 (0.84)	0.06	0.01

provides a convenient means of studying the anisotropy of terrain. On the other hand, the numerical value of fractal dimension obtained by the box-counting method is affected by the maximum cell size, the contour interval and thus the number of contour lines included in analysis, and the minimum $\bar{r}^2$ value for selecting the contours to compute the composite fractal dimension of a particular DEM. In particular, a decision has to be made on the minimum r^2 value in order to produce some meaningful results. Yet, the choice of a particular value is largely a quite arbitrary decision. Nevertheless, the box-counting method has the advantage of allowing us to quantify the variation of complexities of terrain at different elevations.

The walking dividers method is only tested using a small selection of DEMs due to the numerous problems described previously. Table 5.4 compares the results obtained by the walking dividers method with those by the variogram method and the box-counting method. It is obvious that the walking dividers method, when applied to the original topographic profiles, greatly underestimates the complexity of topographic surfaces. Considering the possibility of method-induced variations due to the arbitrary choice of a number of measurement and computational parameters, the fractal dimension derived by the walking dividers method implies an almost perfect featureless two-dimensional plane, which is evidently contrary to what we see in reality.

In conclusion, among the three methods tested, the variogram method seems to be the most suitable method for estimating the fractal dimension of topographic profiles or surfaces. This reinforces the conclusion of many earlier studies. Klinkenberg and Goodchild (1992) reported that the variogram method produced robust and consistent results in their study while the contour or elevation-dependent methods (the walking dividers method and the box-counting method) produced dimensions that are not representative of the dimensions of the surfaces. Chase (1992) found the variogram method more intuitive than other ways of estimating the fractal dimension, such as the power spectrum method. Culling (1986a) preferred the variogram method to the walk-

Table 5.4 A COMPARISON OF THE RESULTS BY THE WALKING DIVIDERS METHOD WITH THE ESTIMATED D VALUES BY THE VARIOGRAM METHOD AND THE BOX-COUNTING METHOD

Method of Computation		Name of the Selected DEM	
	Vertical Scaling	Shadow Mountain, Colorado	Marshlands, Pennsylvania
Walking Divider Method	1X	D = 2.0044	D = 2.0036
	10X	D = 2.0964	D = 2.1314
	20X	D = 2.2486	D = 2.1418
	30X	D = 2.1596	D = 2.2486
	40X	D = 2.1646	D = 2.2585
	50X	D = 2.1644	D = 2.2641
	60X	D = 2.1648	D = 2.2601
	70X	D = 2.1597	D = 2.2573
	80X	D = 2.1577	D = 2.2524
	90X	D = 2.1591	D = 2.2522
	100X	D = 2.1561	D = 2.2461
Variogram Method		D = 2.3157	D = 2.6116
Box-Counting Method		D = 2.2832	D = 2.6952

ing dividers method in his study of spatial variability of soil pH. The box-counting method also gives satisfactory results when careful consideration is given to the selection of the maximum cell size, contour interval and the minimum r-squared value. The walking dividers method appears to be the least reliable and the most time-consuming method for estimating the fractal dimension of self-affine topographic profiles.

Chapter 6 AN EMPIRICAL TEST OF STATISTICAL SELF-SIMILARITY OF TOPOGRAPHY

6.1 Introduction

Although self-similarity is one of the most fundamental concepts in fractal geometry and it possesses mathematical elegance and simplicity, its validity when applied to topographic data has not been adequately tested. Previous studies have produced quite conflicting results. On the one hand, Mandelbrot (1977, 1983), Sayles and Thomas (1978a), Turcotte (1992), and many others are convinced that self-similarity is a fundamental structure of nature, including land surface topography. For example, Sayles and Thomas (1978a) have compiled topographic data from a variety of sources which span eight decades of spatial scale and fitted them into a single self-similar linear model. On the other hand, serious skepticism has been expressed on the applicability of self-similarity to topographic data. Soon after Mandelbrot (1967b) published his work on the length of coastlines, Scheidegger (1970, p.9) commented that it seemed physically absurd to postulate the validity of Richardson's law, and therewith of self-similarity down to the size of pebbles on the coasts and to the molecular interstices of these pebbles. He (Scheidegger, 1991, p.8) pointed out that to apply Richardson's law to all size ranges of length measurement would lead to "ultraviolet" and "infrared" catastrophes (divergences at very small and very large values of length measurement). Similar criticism has also been given by Bibby (1972, p.214). In addition, some recent studies have revealed that terrain features are only self-similar over limited scale ranges (Armstrong, 1986; and Roy et al., 1987). Other studies seem to indicate that topographic features are examples of multifractals, that is, topographic data display distinct horizontal scale domains within which D remains substantially constant but have sharp breaks at certain sampling intervals (Goodchild, 1980; Nakano, 1983; Bradbury et al., 1984; Mark and Aronson, 1984; Fox and Hayes, 1985; Culling and Datko, 1987; Klinkenberg, 1988; and Chase, 1992).

One major reason for these conflicting conclusions and for the lack of confidence in some of these earlier interpretations is that they were based on extremely limited empirical testing using one or a few data sets. One of the objectives of the present research is to test the validity of the fractal model as applied to topography using a much larger sample size representing a wide variety of topographic features. Specifically, one hundred and ninety one Digital Elevation Models (DEMs) selected from sixteen different physiographic provinces were used in the present study. This chapter presents the results from such an extensive empirical testing. First, we will look at how well the fractal model fits the real terrain data in general and what type of landforms is most accurately characterized by fractal parameters. The results on the scale ranges within which topographic data remain self-similar will be presented. Then, the question of whether topographic data are translationally invariant as assumed in the fractal model will be examined and the relationship between fractal parameters and the directions of data sampling will be described. A discussion on the variation of fractal parameters with terrain elevations will follow. Finally, the result of this study with regard to the average fractal dimension of topographic data will be presented.

6.2 The Scale Range of Self-Similarity of Topography

Theoretically, strict self-similarity implies symmetry applicable to the whole continuum between the infinitely small and the infinitely large. However, it seems quite obvious intuitively that topographic characteristics can not be self-similar across all scales. In fact, identification of characteristic horizontal and vertical scales in landscape has been an area of considerable research within geomorphometry (Mark, 1980). For example, Hunt (1974, p.59-61) suggested that landforms may be considered on four very different scales. The largest, represented by the continents and the oceans, have horizontal dimensions measurable in thousands of miles and a vertical relief of more than 10 miles. The next smaller scale of landforms is that represented by the physiographic provinces which are scores or hundreds of miles wide. The next smaller scale

of landforms reflects differences within the physiographic provinces. The smallest scale of landforms is measurable in centimeters. Geological studies have revealed that landforms at different scales are created by different processes. The two larger scales of landforms are governed primarily by geological structures. The differentiation of continents and oceans is a result of plate subduction and continental fragmentation and involves the circulation of convection currents in the asthenosphere. The variations of physiographic provinces are caused by continental collision and intra-plate tectonic activities. On the other hand, the two smaller scales of landforms are governed partly by their structure but primarily by the processes of erosion and sedimentation. Similarly, Gerrard (1988) combined the various subdivisions used by Fenneman (1916) and those of Linton (1951) and divided the earth's surface into seven hierarchical orders of relief. These include continents, divisions, provinces, sections, tracts, stows and sites. Different factors and processes were suggested as the determinants of surface features at different scales. It seems reasonable to expect that these processes should have left different clues In landforms. Thus, the fractal model appears to be in fundamental conflict with conventional geomorphic wisdom. Mandelbrot (1983, p.38) acknowledges that "*in Nature every cascade must stop or change character. ... the notion that they are self-similar can only apply between certain limits.*" Then, the question becomes: "within what scale range is topographic data self-similar?"

Richard F. Voss (1985b, p.809) speculated that "*The largest variations may be limited by the size of the planet or the force of gravity (the materials may not be strong enough to support arbitrarily high mountains). The smallest scales may be limited by the smoothing of erosion, the basic grain size of the rock and sand or, at the very least, by the atomic nature of the particles.*" However, the real world appears to be much more limited than what Voss or Mandelbrot envisioned. Appendix I shows the results of the present study using the variogram method. In this study, individual DEMs were used for calculating the fractal dimension. The largest array size used is 390 X 390 pixels and the smallest array size is 290 X 290 pixels. Thus, the scale

range considered is from 30 meters to a maximum of 11,700 meters. Within this scale range, the current study shows that none of the DEMs has a variance monotonously increasing with distance in all directions. However, as mentioned in Chapter 5, this could be a result of inadequate data points for long distance classes in the NE-SW and NW-SE directions. Five of the DEMs are self-similar up to the maximum length of these quadrangles in both the E-W and N-S directions and also when data points in these two or all four directions are combined (Table 6.1). In addition, 54 DEMs show self-similarity up to the maximum length of the map at least in one direction. All other DEMs are self-similar only within limited scale ranges (i.e., less than the maximum length of the square array used in the analysis) in all directions or when different directions are combined.

These results confirm the earlier finding of Mark and Aronson (1984) that the scale ranges of self-similarity of most topographic data sets are below the physical dimension of the standard USGS 7.5-minute topographic quadrangles. Of the seventeen Digital Elevation Models they examined only one was found to be truly self-similar up to the maximum length of a 7.5-minute quadrangle map.

In terms of physiographic provinces, one surprising result is that all DEMs from the Basin and Range Province have a much wider scale range of self-similarity than the DEMs from other provinces despite the fact that in this province highly contrasting ranges and basins form a seemingly inhomogeneous mosaic. Moreover, these DEMs generally show higher positive correlation. Their fractal dimensions are closest to the D values commonly used to create realistic synthetic terrain.

Efforts were made to determine whether the scale range of self-similarity of topographic data is related to one of the conventional geomorphometric parameters, that is, terrain relief. The term "relief" has been defined differently by various authors (Mark, 1975). For the purpose of this study, it refers to the difference between the highest and lowest elevations occurring within the square array that is used for computing fractal

Table 6.1 DEMS SHOWING POWER LAW RELATIONSHIP IN AT LEAST ONE DIRECTION BETWEEN VARIANCE AND DISTANCE UP TO THE MAXIMUM DISTANCE WITHIN THE QUADRANGLE

NAME OF TOPO QUAD	DIRECTION	SCALE RANGE	FRACTAL DIMENSION	R-SQUARED
Adel, OR	N-S	328 pixels	2.378247	0.976457
	EW+NS	328 pixels	2.398252	0.948792
	combined	328 pixels	2.450906	0.929796
Anvil Points, CO	N-S	343 pixels	2.426712	0.979988
	EW+NS	343 pixels	2.447350	0.978557
	combined	343 pixels	2.478822	0.978751
Bar C Bar Ranch, NM	N-S	384 pixels	2.403732	0.988496
Barlow, KY	EW+NS	360 pixels	2.485946	0.986328
Bata Mountain, MT	E-W	303 pixels	2.379085	0.994049
	N-S	303 pixels	2.420389	0.976528
	EW+NS	303 pixels	2.393474	0.994423
	NW-SE	303 pixels	2.268502	0.986238
	combined	303 pixels	2.415374	0.992951
Belmore Sloughs, MT	E-W	299 pixels	2.476494	0.924314
Big Horn, WY	N-S	318 pixels	2.263950	0.994374
	combined	318 pixels	2.435285	0.994908
Buffalo Springs SW, NV	EW+NS	351 pixels	2.265412	0.991783
	combined	351 pixels	2.318101	0.990787
Cain Mountain NE, NV	N-S	351 pixels	2.220647	0.990061
Cain Mountain SE, NV	N-S	351 pixels	2.194825	0.997712
	EW+NS	351 pixels	2.223878	0.996846
	combined	351 pixels	2.275967	0.992596
Cain Mountain SW, NV	N-S	351 pixels	2.197554	0.996928
	EW+NS	351 pixels	2.235960	0.999068
Coleman Lake, OR	N-S	330 pixels	2.260045	0.994757
Condon, MT	E-W	298 pixels	2.159518	0.993429
	EW+NS	298 pixels	2.233106	0.996066
	combined	298 pixels	2.279109	0.987880
Cortez NW, NV	E-W	352 pixels	2.460687	0.970856
	EW+NS	352 pixels	2.406388	0.989056
	combined	352 pixels	2.444881	0.987990
Crump Lake, OR	EW+NS	328 pixels	2.427924	0.966335
Derrick Draw, NM	E-W	384 pixels	2.312122	0.994303
	EW+NS	384 pixels	2.412471	0.991164
	combined	384 pixels	2.426480	0.995881
Dexter East, NM	N-S	384 pixels	2.432863	0.987273
	EW+NS	295 pixels	2.457119	0.978196
Double Mill Draw NE, TX	N-S	389 pixels	2.355714	0.991689
	EW+NS	389 pixels	2.436438	0.987305
Double Mill Draw NW, TX	E-W	388 pixels	2.493771	0.983995
Double Mill Draw SE, TX	E-W	390 pixels	2.333472	0.988474

Table 6.1 continued

NAME OF TOPO QUAD	DIRECTION	SCALE RANGE	FRACTAL DIMENSION	R-SQUARED
Elevation Mountain, MT	N-S	304 pixels	2.638988	0.645529
	NW-SE	304 pixels	2.442897	0.988064
Fencemaker SE, NV	N-S	350 pixels	2.312106	0.993420
Grantham, NC	E-W	366 pixels	2.351237	0.993364
Gray Wolf Lake, MT	E-W	298 pixels	2.400612	0.974588
	EW+NS	298 pixels	2.543317	0.878909
Harmony, NC	EW+NS	374 pixels	2.658544	0.972411
Holmes Ranch, MT	E-W	318 pixels	2.427298	0.986715
Kyle Hot Springs NE, NV	NE-SW	348 pixels	2.268128	0.977863
Lake Inez, CO	E-W	300 pixels	2.281142	0.994344
	EW+NS	300 pixels	2.360167	0.991776
Lake Marshall, MT	NE-SW	300 pixels	2.329054	0.977114
	combined	300 pixels	2.482852	0.965480
Lyndonville SE, VT	E-W	315 pixels	2.460079	0.973417
	combined	315 pixels	2.545858	0.934624
McCoysville, PA	E-W	340 pixels	2.450552	0.985266
	N-S	340 pixels	2.469097	0.952524
	EW+NS	340 pixels	2.460292	0.971027
	combined	340 pixels	2.492268	0.969877
Moccasin Mesa, CO	N-S	357 pixels	2.409541	0.978519
Mount Tom, CA	EW+NS	360 pixels	2.517499	0.912289
Mt. Langley, CA	E-W	367 pixels	2.157425	0.999016
	N-S	367 pixels	2.325882	0.986757
	EW+NS	367 pixels	2.227448	0.997900
	combined	367 pixels	2.265470	0.998261
Mt. Moses SW, NV	EW+NS	352 pixels	2.269456	0.994785
	combined	352 pixels	2.335543	0.990674
Mt. Tobin NE, NV	E-W	349 pixels	2.161576	0.998067
	EW+NS	349 pixels	2.199202	0.997960
	NE-SW	349 pixels	2.205324	0.976702
Mt. Tobin NW, NV	E-W	349 pixels	2.204680	0.996327
	N-S	349 pixels	2.292395	0.996826
	EW+NS	349 pixels	2.232633	0.996896
	NW-SE	349 pixels	2.107672	0.995272
	combined	349 pixels	2.252051	0.998413
Mt. Tobin SW, NV	E-W	349 pixels	2.240253	0.995194
	EW+NS	349 pixels	2.306573	0.991705
	combined	349 pixels	2.351586	0.976097
Pat O'Hara Mountain, WY	E-W	320 pixels	2.204837	0.995943
	EW+NS	320 pixels	2.277310	0.993931
	combined	320 pixels	2.310963	0.997502
Prentiss, NC	NE-SW	368 pixels	2.320515	0.989847
Priday Resevoir, OR	EW+NS	328 pixels	2.419498	0.956092
	combined	328 pixels	2.419498	0.956092
Priest Lake NE, ID	EW+NS	305 pixels	2.300423	0.983041
Roselle, NJ	EW+NS	348 pixels	2.481237	0.976005
	combined	348 pixels	2.527788	0.963573

Table 6.1 continued

NAME OF TOPO QUAD	DIRECTION	SCALE RANGE	FRACTAL DIMENSION	R-SQUARED
Seeley Lake East, MT	N-S	301 pixels	2.347997	0.990105
	EW+NS	301 pixels	2.385777	0.976334
	NE-SW	301 pixels	2.283076	0.963035
	combined	301 pixels	2.415589	0.975939
Seeley Lake West, MT	N-S	301 pixels	2.453697	0.983720
	EW+NS	301 pixels	2.375319	0.991379
	NW-SE	301 pixels	2.262943	0.939569
	combined	301 pixels	2.413147	0.986905
Shadow Mountain, CO	E-W	350 pixels	2.285123	0.998581
	EW+NS	350 pixels	2.315689	0.994729
Smokemont, NC	EW+NS	367 pixels	2.534819	0.951119
Strawberry Lake, CO	E-W	350 pixels	2.398526	0.984252
	N-S	350 pixels	2.509639	0.963170
	EW+NS	350 pixels	2.444696	0.978034
	NW-SE	350 pixels	2.444696	0.978034
	combined	350 pixels	2.462722	0.983947
Trail Mountain, CO	N-S	349 pixels	2.276435	0.985405
	EW+NS	349 pixels	2.385363	0.968731
	NW-SE	349 pixels	2.277532	0.967953
	combined	349 pixels	2.404131	0.977740
Upper Jocko Lake, MT	N-S	300 pixels	2.544011	0.900830
Wapiti Lake, MT	N-S	300 pixels	2.598491	0.837660
	EW+NS	300 pixels	2.511966	0.933827
Wetherill Mesa, CO	N-S	358 pixels	2.432781	0.966820
	combined	358 pixels	2.584850	0.937745
Yakima East, WA	N-S	304 pixels	2.237195	0.994854
	EW+NS	304 pixels	2.239105	0.994907
	combined	304 pixels	2.271701	0.997118
Yew Creek, MT	N-S	294 pixels	2.244193	0.997951

parameters. Figure 6.1 shows the relationship between these two parameters. It is somewhat surprising to find that the scale range of self-similarity of topographic data seems to show no correlation with the terrain relief.

Special attention has also been paid to test the validity of the multifractal model. Mark and Aronson (1984) suggested that the domains could be interpreted in terms of the different geomorphological processes and geological constraints operating at different scales. Their finding and interpretation, if confirmed, could have enormous impact on geomorphological studies. It could provide a new and useful way of identifying characteristic scales of landscapes. In addition, it seems reasonable to speculate that the scales at which dimension changes represent scales at which the relative importance of different processes, of structural effects, and of time scales also change. Unfortunately, this study has shown that no break points can be identified with confidence on any of the variograms. Thus, the separation of scale ranges appears to be a rather subjective decision. It was then attempted to define an r-squared criterion for a somewhat more objective division of scale ranges. However, it is not uncommon that this procedure produces more than ten different scale ranges. In addition, the recursive procedure is extremely time-consuming and the selection of the r-squared value remains an arbitrary choice.

It should be pointed out that whether topographic data will show different levels of complexity below about 100 meters or beyond the maximum physical dimension of a single DEM still remains to be tested. The data required for investigating the fractal nature of landforms at these scales are not readily available. It is conceivable that land surfaces may have quite different morphologic characteristics at these scales because different processes are known to be at work in shaping the very large or very small scale land surface features. What we have learned in this study is that at the outcrop scale the majority of topographic data sets show linear self-similarity within limited short scale ranges but invariably display periodicity beyond certain distances.

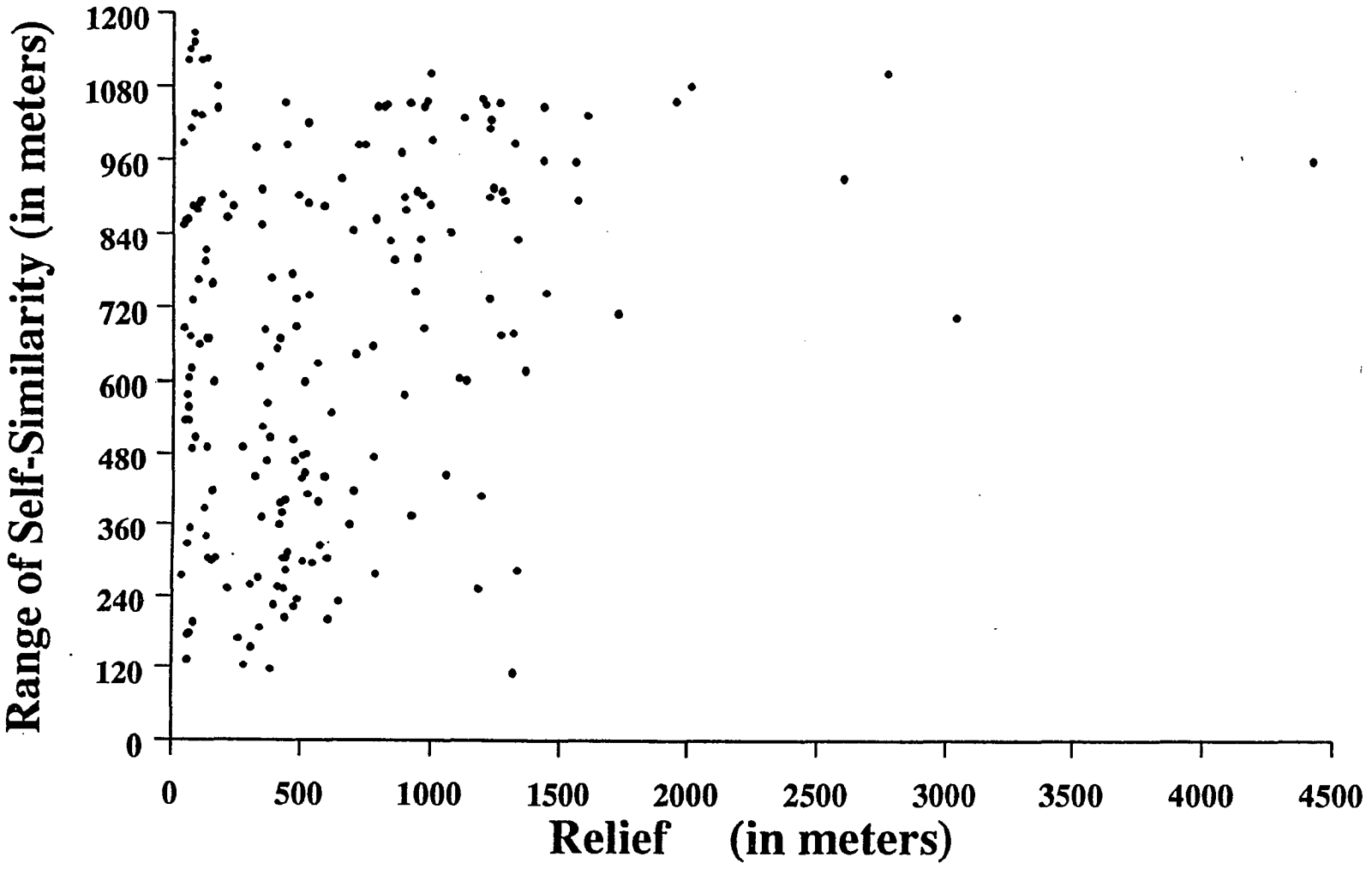

Figure 6.1 The Relationship between Terrain Relief and the Range of Self-Similarity

6.3 The Limits of Spatial Homogeneity of Topography

A corollary of self-similarity is spatial homogeneity, which means that the geometric complexities of topographic surfaces remain invariant under locational displacement. Clearly, land surface features do not possess such homogeneity in a strict sense. The entire field of landform regionalization is based on the observation that the geometric characteristics of land surface features vary from region to region and there are certain identifiable similarities within each region. Furthermore, spatial heterogeneity persists within each physiographic province in the form of juxtaposition of terrain elements of contrasting character such as basins and ranges or ridges and valleys. Thus, while introducing the concept of spatial homogeneity, Mandelbrot (1983, p.18) noted that when we study fractals the invariance under displacement must be modified and/or restricted in its scope. The best fractals are those that exhibit the maximum of invariance. The purpose of the present research is to assess the degree of variability within each physiographic province. Such knowledge is important when we attempt to attach significance to fractal parameters characterizing various landforms and to evaluate the reliability of some of the earlier fractal studies.

The spatial variability of landforms is examined in two ways. First, fractal parameters were calculated for blocks of contiguous DEMs within several physiographic provinces (Table 6.2). The differences in fractal dimension and the scale range of self-similarity provide some indication on the level of deviation of terrain data from strict spatial homogeneity. The smaller the differences, the more homogeneous terrain features are. Each block of DEMs was intentionally selected from a visually homogeneous area as shown on Landsat imagery. The choice was so made because the study was originally designed to be a first step in testing the possibility of numerically characterizing different physiographic provinces. The use of seemingly homogeneous blocks of DEMs was intended to minimize the variability within each physiographic province and to maximize the difference between different provinces. As can be seen, under these idealized situations, the fractal dimensions of most DEMs within each

Table 6.2 VARIATIONS OF FRACTAL DIMENSION WITHIN EACH PHYSIOGRAPHIC PROVINCE

(a) Block of DEMs from the Basin and Range Province (I)

Kyle Hot Springs NE, NV 249 pixels 2.286389 0.996554	Mount Tobin NW, NV 349 pixels 2.232633 0.996896	Mount Tobin NE, NV 349 pixels 2.199202 0.997960	Buffalo Springs NW, NV 329 pixels 2.229702 0.998333
Kyle Hot Springs SE, NV 337 pixels 2.283931 0.997378	Mount Tobin SW, NV 349 pixels 2.306573 0.991705		Buffalo Springs SW, NV 351 pixels 2.265412 0.991783
Fencemaker NE, NV 158 pixels 2.278471 0.993349	Cain Mtn. NW, NV 282 pixels 2.417817 0.958248	Cain Mtn. NE, NV 267 pixels 2.276207 0.997842	Mount Moses NW, NV 265 pixels 2.264200 0.996671
Fencemaker SE, NV 225 pixels 2.232705 0.993591	Cain Mtn. SW, NV 351 pixels 2.235960 0.999068	Cain Mtn. SE, NV 351 pixels 2.223878 0.996846	Mount Moses SW, NV 352 pixels 2.269456 0.994785

(b) Block of DEMs from the Basin and Range Province (II)

Drake Peak, OR 324 pixels 2.409228 0.971645	Priday Reservoir, OR 328 pixels 2.419498 0.956092	Crump Lake, OR 328 pixels 2.427924 0.966335
Sage Hen Butte, OR 223 pixels 2.580000 0.885662	Adel, OR 328 pixels 2.398252 0.948792	Calderwood Reservoir, OR 285 pixels 2.411135 0.985441
Collins Rim, OR 310 pixels 2.207549 0.998905	May Lake, OR 297 pixels 2.365200 0.994168	Coleman Lake, OR 230 pixels 2.375453 0.975920

Table 6.2 continued

(c) Block of DEMS from the Northern Rocky Mountains Province

Wapiti Lake, MT 300 pixels 2.511966 0.933827	Belmore Sloughs, MT 202 pixels 2.495999 0.886392	Gray Wolf Lake, MT 298 pixels 2.543317 0.878909
Gold Creek Peak, MT 276 pixels 2.567558 0.836703	Upper Jocko Lake, MT 277 pixels 2.467464 0.963289	Lake Marshall, MT 193 pixels 2.396570 0.978762
Belmont Point, MT 288 pixels 2.366713 0.992019	Seeley Lake W, MT 301 pixels 2.375319 0.991379	Lake Inez, MT 300 pixels 2.360167 0.991776
Salmon Lake, MT 99 pixels 2.368590 0.960757	Seeley Lake E, MT 301 pixels 2.385777 0.976334	Morrell Lake, MT 245 pixels 2.507283 0.940965
Woodworth, MT 160 pixels 2.348775 0.980858	Morrell Mtn., MT 281 pixels 2.579307 0.886962	Crimson Peak, MT 84 pixels 2.290468 0.968688

(d) Block of DEMs from the Southern Rocky Mountains Province

Bowen Mtn., CO 148 pixels 2.342403 0.971972	Grand Lake, CO 303 pixels 2.358322 0.985438	Mc Henrys Peak, CO 248 pixels 2.436514 0.962398
Trail Mtn., CO 349 pixels 2.385363 0.968731	Shadow Mtn., CO 350 pixels 2.315689 0.994729	Isolation Peak, CO 94 pixels 2.391567 0.946678
Granby, CO 210 pixels 2.484130 0.969440	Strawberry Lake, CO 350 pixels 2.444696 0.978034	Mornarch Lake, CO 319 pixels 2.511075 0.934985

Table 6.2 continued

(e) Block of DEMs from the Appalachian Plateaus Province

Prestonsburg, KY 56 pixels 2.615581 0.802663	Lancer, KY 41 pixels 2.520328 0.869317	Thomas, KY 51 pixels 2.588797 0.827928
Martin, KY 86 pixels 2.673188 0.757502	Harold, KY 90 pixels 2.643500 0.809792	Broad Bottom, KY 37 pixels 2.478128 0.902758
Wayland, KY 62 pixels 2.520259 0.857755	Mc Dowell, KY 104 pixels 2.675941 0.745490	Pikeville, KY 68 pixels 2.595703 0.821165

(f) Block of DEMs from the Valley and Ridge Province

	Stickleyville, VA 183 pixels 2.559569 0.892811	Duffield, VA 108 pixels 2.482490 0.957582
Kyles Ford, VA 101 pixels 2.557185 0.894322	Looneys Gap, TN 39 pixels 2.384990 0.960470	Plum Grove, VA 75 pixels 2.528612 0.889745
Pressmens Home, TN 94 pixels 2.487415 0.917303	Burem, TN 164 pixels 2.662728 0.888641	Stony Point, TN 124 pixels 2.564928 0.862999

(g) Block of DEMs from the Piedmont Province

Central, NC 327 pixels 2.476842 0.972201	Harmony, NC 374 pixels 2.658544 0.972411	Calahaln, NC 164 pixels 2.611465 0.987150
Statesville W, NC 129 pixels 2.701320 0.943193	Statesville E, NC 169 pixels 2.677521 0.952403	Cool Springs, NC 255 pixels 2.713145 0.950208
Troutman, NC 345 pixels 2.734364 0.959725	Shepherds, NC 297 pixels 2.659848 0.975796	Cleveland, NC 65 pixels 2.608724 0.975361

block indeed appear to be quite uniform. Nevertheless, there are still some exceptions. Within each block, there are DEMs that give either unusually high or unusually low D value. The largest difference in D was calculated for each block of DEMs. These differences are close to or greater than 0.2, which are no less than the differences between different physiographic provinces. These deviations are generally caused by localized features. The presence of large lakes within a DEM lowers the average fractal dimension of the entire quadrangle as is the case in the Shadow Mountain, CO Quadrangle. The dominance of a rough mountain terrain within a particular quadrangle will give a much higher D value than its surrounding DEMs, such as the Morrell Mountain, MT and the Troutman, NC Quadrangles.

The variability of geometric characteristics is also shown by the differences in fractal dimension calculated for different parts of each DEM. All DEMs have a larger number of lines in the E-W direction than the number of samples or columns in the N-S direction. When calculating the fractal dimension of each DEM, we can use either the largest square array of elevations in the northern part of the DEM or in the southern part. Most lines of elevations are included in each of these choices. Generally, about two thirds of the northern square array overlap the southern square array. Nevertheless, when different square arrays of a DEM are used, the numerical value of D also varies substantially. Table 6.3 shows the results for 94 arbitrarily selected DEMs. Among them, 33 quadrangles show differences greater than 0.05 and 9 greater than 0.1. The largest difference is found in the Broad Bottom, KY Quadrangle, which is as high as 0.24.

6.4 Variation of Fractal Parameters with Sampling Directions

Another aspect of deviation of terrain surfaces from idealized self-similar fractals is their anisotropies. This becomes quite obvious when we examine the geomorphometry of the North American continent. At the continental scale, strong lineaments are created by the folded mountains and intervening valleys as well as associated frac-

Table 6.3 VARIATION OF FRACTAL DIMENSION WITHIN A SINGLE DEM

NAME OF TOPO QUAD	LOCATION	SCALE RANGE	FRACTAL DIMENSION	R-SQUARED	DIFFERENCE
Atlanta West, ID	South	241 pixels	2.470119	0.972348	0.022336
	North	136 pixels	2.447783	0.941332	
Baker, WV	South	112 pixels	2.459397	0.949983	0.039350
	North	133 pixels	2.420047	0.966408	
Bar C Bar Ranch, NM	South	384 pixels	2.456370	0.982998	0.081482
	North	220 pixels	2.374888	0.996979	
Bartlett Blue Mound, KS-MO	South	141 pixels	2.564039	0.970945	0.019987
	North	186 pixels	2.584026	0.972101	
Bata Mountain, MT	South	303 pixels	2.333764	0.997971	0.059710
	North	303 pixels	2.393474	0.994423	
Broad Bottom, KY	South	132 pixels	2.718005	0.757377	0.239877
	North	37 pixels	2.478128	0.902758	
Burem, TN	South	178 pixels	2.676086	0.869723	0.013358
	North	164 pixels	2.662728	0.888641	
Cain Mountain NE, NV	South	351 pixels	2.282740	0.992213	0.006533
	North	267 pixels	2.276207	0.997842	
Cain Mountain NW, NV	South	261 pixels	2.332944	0.987204	0.084873
	North	282 pixels	2.417817	0.958248	
Cain Mountain SE, NV	South	351 pixels	2.264250	0.976848	0.040372
	North	351 pixels	2.223878	0.996846	
Cain Mountain SW, NV	South	351 pixels	2.239003	0.992330	0.003043
	North	351 pixels	2.235960	0.999068	
Calahain, NC	South	161 pixels	2.612077	0.986719	0.000612
	North	164 pixels	2.611465	0.987150	
Camelot (Pressmens Home), TN	South	95 pixels	2.501793	0.918460	0.014378
	North	94 pixels	2.487415	0.917303	
Cameron Dent Run Proj, PA	South	127 pixels	2.527667	0.905254	0.049061
	North	134 pixels	2.576728	0.866735	
Central, NC	South	334 pixels	2.532587	0.972830	0.078511
	North	201 pixels	2.454076	0.943020	
Chetopa Blue Mound, KS-MO	South	61 pixels	2.695408	0.945067	0.022466
	North	91 pixels	2.717874	0.953860	
Cleveland, NC	South	66 pixels	2.629409	0.974776	0.020685
	North	65 pixels	2.608724	0.975361	
Coharie NW, NC	South	73 pixels	2.795851	0.896760	0.003716
	North	58 pixels	2.792135	0.883461	
Coharie SE, NC	South	103 pixels	2.806300	0.908490	0.003015
	North	109 pixels	2.803285	0.913712	
Coharie SW, NC	South	57 pixels	2.800291	0.858260	0.002629
	North	59 pixels	2.802920	0.844778	
Cool Springs, NC	South	317 pixels	2.716296	0.967191	0.003151
	North	255 pixels	2.713145	0.950208	
Cortez NE, NV	South	309 pixels	2.425150	0.955727	0.103291
	North	319 pixels	2.321859	0.996417	
Cortez NW, NV	South	352 pixels	2.332944	0.987204	0.073444
	North	352 pixels	2.406388	0.989056	
Cortez SE, NV	South	348 pixels	2.308619	0.991236	0.040360
	North	310 pixels	2.348979	0.967406	
Cortez SW, NV	South	210 pixels	2.321843	0.994619	0.012689
	North	235 pixels	2.334532	0.996358	
Crimson Peak, MT	South	69 pixels	2.282862	0.959976	0.007606
	North	84 pixels	2.290468	0.968688	
Derrick Draw, NM	South	384 pixels	2.381393	0.998208	0.031078
	North	384 pixels	2.412471	0.991164	
Dexter East, NM	South	308 pixels	2.528225	0.936598	0.071106
	North	295 pixels	2.457119	0.978196	
Dobbersville, NC	South	43 pixels	2.756532	0.895551	0.011964
	North	44 pixels	2.768496	0.874013	
Duffield, VA	South	89 pixels	2.537934	0.934814	0.055444
	North	108 pixels	2.482490	0.957582	
Emporium, PA	South	211 pixels	2.647147	0.868513	0.116954
	North	85 pixels	2.530193	0.886261	
Faison, NC	South	59 pixels	2.776994	0.896338	0.011462
	North	59 pixels	2.778064	0.907800	
First Fork, PA	South	89 pixels	2.474315	0.911737	0.074875
	North	156 pixels	2.549190	0.912193	

Table 6.3 continued

NAME OF TOPO QUAD	LOCATION	SCALE RANGE	FRACTAL DIMENSION	R-SQUARED	DIFFERENCE
Forks Ranch, MT	South	262 pixels	2.609441	0.943990	0.045112
	North	200 pixels	2.564329	0.959795	
Fort Hood, TX	South	326 pixels	2.567134	0.974842	0.059957
	North	375 pixels	2.627091	0.917706	
Gold Creek Peak, MT	South	267 pixels	2.387727	0.981657	0.179831
	North	276 pixels	2.567558	0.836703	
Grantham, NC	South	161 pixels	2.428871	0.994907	0.052856
	North	179 pixels	2.376015	0.995140	
Gray Wolf Lake, MT	South	218 pixels	2.490975	0.930114	0.052342
	North	298 pixels	2.543317	0.878909	
Greasewood Canyon, CO	South	279 pixels	2.629523	0.923782	0.031456
	North	256 pixels	2.660979	0.876463	
Harold, KY	South	86 pixels	2.635977	0.810507	0.007523
	North	90 pixels	2.643500	0.809792	
Holmes Ranch, MT	South	295 pixels	2.544876	0.976262	0.042833
	North	295 pixels	2.502043	0.986372	
Horn Lake SW, MS	South	193 pixels	2.550430	0.988692	0.041263
	North	228 pixels	2.591693	0.990391	
Kyles Ford, VA	South	107 pixels	2.726352	0.938932	0.169167
	North	101 pixels	2.557185	0.894322	
Labette, KS-MO	South	180 pixels	2.568755	0.993818	0.033248
	North	179 pixels	2.602003	0.990267	
Lake Inez, CO	South	285 pixels	2.366193	0.980977	0.006026
	North	300 pixels	2.360167	0.991776	
Lancer, KY	South	45 pixels	2.540314	0.853979	0.019986
	North	41 pixels	2.520328	0.869317	
Looneys Gap, TN	South	82 pixels	2.565851	0.854509	0.180861
	North	39 pixels	2.384990	0.960470	
Mammoth Cave, KY	South	106 pixels	2.651725	0.837568	0.015157
	North	101 pixels	2.636568	0.860841	
Martin, KY	South	60 pixels	2.579488	0.828680	0.093700
	North	86 pixels	2.673188	0.757502	
Mc Dowell, KY	South	112 pixels	2.669517	0.778549	0.006424
	North	104 pixels	2.675941	0.745490	
Missouri Valley NW, NE	South	326 pixels	2.568747	0.989343	0.054837
	North	298 pixels	2.623584	0.981651	
Moccasin Mesa, CO	South	75 pixels	2.511538	0.903117	0.046284
	North	77 pixels	2.557822	0.876723	
Moqui Canyon, CO	South	136 pixels	2.522678	0.929917	0.001228
	North	137 pixels	2.523906	0.911337	
Morrell Lake, MT	South	170 pixels	2.381638	0.965374	0.125645
	North	245 pixels	2.507283	0.940965	
Morrell Mountain, MT	South	263 pixels	2.447069	0.977441	0.132238
	North	281 pixels	2.579307	0.886962	
Mt. Moses NW, NV	South	256 pixels	2.300160	0.993038	0.035960
	North	265 pixels	2.264200	0.996671	
Mt. Moses SW, NV	South	352 pixels	2.320552	0.988994	0.051096
	North	352 pixels	2.269456	0.994785	
Mt. Langley, CA	South	367 pixels	2.233062	0.997964	0.005614
	North	367 pixels	2.227448	0.997900	
Newton Grove North, NC	South	232 pixels	2.689676	0.941359	0.078746
	North	288 pixels	2.610931	0.980741	
North Fort Hood, TX	South	245 pixels	2.543782	0.970423	0.052607
	North	271 pixels	2.491175	0.985592	
North Loup Hord, NE	South	246 pixels	2.674262	0.953728	0.050372
	North	344 pixels	2.623890	0.971360	
Oswego Blue Mount, KS-MO	South	171 pixels	2.564316	0.982322	0.078171
	North	287 pixels	2.642487	0.973889	
Park City, KY	South	311 pixels	2.505208	0.991052	0.116802
	North	139 pixels	2.622010	0.905287	
Paxton NW (Perdueville), IL	South	200 pixels	2.415769	0.995695	0.006271
	North	285 pixels	2.422040	0.993423	
Paxton SW (Rantoul), IL	South	347 pixels	2.528979	0.979463	0.039853
	North	329 pixels	2.489126	0.991750	
Pikeville, KY	South	66 pixels	2.558715	0.848041	0.036988
	North	68 pixels	2.595703	0.821165	
Plum Grove, VA	South	67 pixels	2.520380	0.919815	0.008232
	North	75 pixels	2.528612	0.889745	

Table 6.3 continued

NAME OF TOPO QUAD	LOCATION	SCALE RANGE	FRACTAL DIMENSION	R-SQUARED	DIFFERENCE
Post Oak Mountain, TX	South	247 pixels	2.520203	0.979986	0.017327
	North	223 pixels	2.537530	0.963132	
Prestonburg, KY	South	58 pixels	2.622883	0.800713	0.007302
	North	56 pixels	2.615581	0.802663	
Priest Lake NE, ID	South	305 pixels	2.285518	0.988636	0.014905
	North	305 pixels	2.300423	0.983041	
Rhoda, KY	South	99 pixels	2.619116	0.862766	0.000320
	North	99 pixels	2.619436	0.862919	
Rio, WV	South	156 pixels	2.413753	0.969678	0.04611
	North	159 pixels	2.409142	0.971121	
Seeley Lake East, MT	South	301 pixels	2.343185	0.991823	0.042592
	North	301 pixels	2.385777	0.976334	
Seeley Lake West, MT	South	225 pixels	2.367094	0.994664	0.008225
	North	301 pixels	2.375319	0.991379	
Shell Mountains, TX	South	253 pixels	2.526163	0.976945	0.026827
	North	229 pixels	2.552990	0.956257	
Shepherds, NC	South	150 pixels	2.688583	0.952004	0.028735
	North	297 pixels	2.659848	0.975796	
Smiths Grove, KY	South	133 pixels	2.581765	0.963739	0.085725
	North	223 pixels	2.667490	0.868445	
Smokemont, NC	South	202 pixels	2.485400	0.943256	0.049419
	North	367 pixels	2.534819	0.951119	
Statesville East, NC	South	145 pixels	2.657327	0.967512	0.020194
	North	169 pixels	2.677521	0.952403	
Statesville West, NC	South	111 pixels	2.664087	0.969516	0.037233
	North	129 pixels	2.701320	0.943193	
Stickleyville, VA	South	90 pixels	2.479757	0.922614	0.079812
	North	183 pixels	2.559569	0.892811	
Stony Point, TN	South	99 pixels	2.507510	0.877543	0.057418
	North	124 pixels	2.564928	0.862999	
Thomas, KY	South	61 pixels	2.614422	0.808667	0.025625
	North	51 pixels	2.588797	0.827928	
Troutman, NC	South	279 pixels	2.717549	0.962305	0.016815
	North	345 pixels	2.734364	0.959725	
Wapiti Lake, MT	South	291 pixels	2.511571	0.915711	0.000395
	North	300 pixels	2.511966	0.933827	
Wardensville, WV	South	248 pixels	2.461065	0.930556	0.003637
	North	295 pixels	2.464702	0.951448	
Wayland, KY	South	96 pixels	2.612526	0.790376	0.092267
	North	62 pixels	2.520259	0.857755	
Wetherill Mesa, CO	South	99 pixels	2.582802	0.863659	0.013924
	North	101 pixels	2.596726	0.867554	
Wharton, PA	South	101 pixels	2.536069	0.888124	0.004566
	North	101 pixels	2.531503	0.892191	
Wilcox, WA	South	309 pixels	2.631888	0.937350	0.086815
	North	84 pixels	2.545073	0.948142	
Williams, IN	South	104 pixels	2.624776	0.884859	0.005980
	North	113 pixels	2.630756	0.894183	
Yellow Springs, WV	South	225 pixels	2.515883	0.933057	0.084445
	North	132 pixels	2.431438	0.962614	
Yosemite NW, CA	South	279 pixels	2.371306	0.986177	0.046579
	North	237 pixels	2.417885	0.952131	
Zion National Park NE, UT	South	116 pixels	2.535640	0.941510	0.041512
	North	125 pixels	2.577152	0.929414	

ture zones in the Appalachians, the Rockies, and the Cascades, and by the uplifted fault blocks and adjoining sedimentary basins in the Great Basin region. Such lineaments are clearly visible on hill-shaded images created from Digital Elevation Models. At the outcrop and microscopic scales, preferred orientation of flaky and platy minerals is a distinctive structural element of all regionally metamorphosed terrains.

The variation of fractal parameters with sampling directions was first shown by Roy et al. (1987). Following their procedures, fractal dimensions were also calculated in this study for each DEM using samples taken in each of the four directions (E-W, N-S, NW-SE, and NE-SW directions). Table 6.4 shows the differences in fractal dimension between E-W and N-S directions. It can be seen that the differences are quite significant for most of the DEMs used in this study. Specifically, 118 of the DEMs (61.8 percent) show differences greater than 0.05; 68 DEMs greater than 0.1; 13 of them greater than 0.2; and 5 DEMs greater than 0.3. The largest difference is found in the Peck Lake, MT Quadrangle, which is as large as 0.37.

It should be noted that many of the DEMs do not show the largest differences between the E-W and N-S directions. Instead, the highest variability occurs between the NE-SW and SE-NW directions. For example, most of the DEMs from the Valley and Ridge Province (Blain, PA; Blair Mills, PA; Kyles Ford, VA; Looneys Gap, TN; McCoysville, PA; and Plum Grove, VA) show much higher variability between the NE-SW and SE-NW directions than what is indicated in Table 6.4 (see Appendix I).

6.5 The Relationship between Fractal Parameters and Terrain Elevation

The fractal parameters have also been found to vary with terrain elevation (Goodchild, 1982; Roy et al., 1987; and Klinkenberg, 1988). In an empirical test of the fractal model using the Random Island, Newfoundland as the test area, Goodchild (1982) computed the fractal dimensions of four contour lines by three different methods (the divider method, the box-counting method, and the area-perimeter method). Results from all three methods revealed a consistent trend in the D values, that is, D increases

Table 6.4 DIFFERENCE IN FRACTAL DIMENSION BETWEEN E-W AND N-S DIRECTIONS

NAME OF TOPO QUAD	DIFFERENCE IN D	NAME OF TOPO QUAD	DIFFERENCE IN D
Adel, OR	0.089838	Anvil Points, CO	0.016428
Arena, NY	0.211907	Atlanta West, ID	0.064093
Aughwick, PA	0.014511	Baker, WV	0.105353
Barbara, MS	0.013813	Bar C Bar Ranch, NM	0.097729
Barlow, KY	0.148430	Bartlett Blue Mound, KS-MO	0.012889
Bata Mountain, MT	0.041304	Belmont Point, MT	0.126501
Belmore Sloughs, MT	0.207385	Big Horn, WY	0.317724
Blain, PA	0.033424	Blair Mills, PA	0.006336
Bowen Mountain, CO	0.057541	Broad Bottom, KY	0.044171
Buffalo Springs NW, NV	0.334902	Buffalo Springs SW, NV	0.151930
Burem, TN	0.139839	Cain Mountain NE, NV	0.046944
Cain Mountain NW, NV	0.066394	Cain Mountain SE, NV	0.014373
Cain Mountain SW, NV	0.087104	Calahain, NC	0.007566
Calderwood Resevoir, OR	0.023939	Camelot, TN	0.131780
Cameron Dent Run Proj, PA	0.022474	Cedar Lake, MT	0.016123
Central, NC	0.141233	Chatham, NJ	0.054846
Chetopa Blue Mound, KS-MO	0.069149	Chief Mountain, MT	0.030987
Church Road, VA	0.046712	Cleveland, NC	0.124342
Coharie NW, NC	0.071639	Coharie SE, NC	0.003581
Coharie SW, NC	0.077713	Coleman Lake, OR	0.132905
Collins Rim, OR	0.052343	Condon, MT	0.292650
Cool Springs, NC	0.042230	Cortez NE, NV	0.090419
Cortez NW, NV	0.095920	Cortez SE, NV	0.018032
Cortez SW, NV	0.028815	Crimson Peak, MT	0.040778
Crump Lake, OR	0.048812	Derrick Draw, NM	0.310244
Dexter East, NM	0.000553	Dobbersville, NC	0.003020
Double Mill Draw NE, TX	0.143144	Double Mill Draw NW, TX	0.017562
Double Mill Draw SE, TX	0.205857	Downsville, NY	0.077281
Drake Peak, OR	0.067946	Duffield, VA	0.070691
Elevation Mountain, MT	0.178812	Emporium, PA	0.099763
Faison, NC	0.018301	Fayetteville, WV	0.121814
Fencemaker NE, NV	0.158948	Fencemaker SE, NV	0.112116
First Fork, PA	0.012005	Fishs Eddy, NY	0.230360
Flaming Gorge, UT	0.014355	Fleischmanns, NY	0.050148
Forks Ranch, MT	0.024513	Fort Hood, TX	0.064982
Glamis SE, CA	0.021779	Gold Creek Peak, MT	0.102598
Granby, CO	0.051102	Grand Lake, CO	0.150745
Grantham, NC	0.023868	Gray Wolf Lake, MT	0.004708
Greasewood Canyon, CO	0.159392	Hancock, MA	0.197994
Hancock, PA-NY	0.163094	Harmony, NC	0.017708
Harold, KY	0.125415	Harvey, IA	0.044390
Hemlock Lake, MT	0.179534	Holland Peak, MT	0.031400
Holmes Ranch, MT	0.092087	Horn Lake SW, MS	0.124856
Horton, NY	0.040576	Hot Springs, SD	0.064328
Hunter, NY	0.048506	Indio Hill, TX	0.039511
Isolation Peak, CO	0.056592	Keating Summit, PA	0.077060
Kyle Hot Springs NE, NV	0.279872	Kyle Hot Springs SE, NV	0.183228
Kyles Ford, VA	0.073536	Labette, KS-MO	0.085969
Lake Inez, CO	0.133497	Lake Marshall, MT	0.027019
Lancer, KY	0.038130	Lee Fire Tower, PA	0.006284
Leighton, IA	0.044513	Lewbeach, NY	0.093150

Table 6.4 continued

NAME OF TOPO QUAD	DIFFERENCE IN D	NAME OF TOPO QUAD	DIFFERENCE IN D
Lexington, NY	0.309492	Livingston Manor, NY	0.103942
Long Eddy, PA	0.068770	Looneys Gap, TN	0.089338
Lyndonville SE, VT	0.100351	Mammoth Cave, KY	0.057971
Margaretville, NY	0.145311	Marshlands, PA	0.025103
Martin, KY	0.039887	May Lake, OR	0.122113
McCoysville, PA	0.018545	Mc Dowell, KY	0.098381
Mc Henrys Peak, CO	0.098406	Missouri Valley NW, NE	0.063016
Moccasin Mesa, CO	0.030226	Monarch Lake, CO	0.045150
Moqui Canyon, CO	0.016060	Morrell Lake, MT	0.012186
Morrell Mountain, MT	0.193221	Mount Tom, CA	0.092562
Mt. Langley, CA	0.168457	Mt. Le Conte, TN	0.149100
Mt. Moses NW, NV	0.174020	Mt. Moses SW, NV	0.097167
Mt. Tobin NE, NV	0.162305	Mt. Tobin NW, NV	0.087715
Mt. Tobin SW, NV	0.165898	Newton Grove North, NC	0.121873
North Fort Hood, TX	0.072057	North Loup Hord, NE	0.172733
Oswego Blue Mount, KS-MO	0.030441	Pacifico Mountain, CA	0.088641
Park City, KY	0.070242	Pat O'Hara Mountain, WY	0.119014
Paxton NW (Perdueville), IL	0.003866	Paxton SE (Gifford), IL	0.065486
Paxton SW (Rantoul), IL	0.006356	Peck Lake, MT	0.365044
Pella, IA	0.008657	Peoria, IA	0.007570
Pikeville, KY	0.128315	Pine Butte School, MT	0.180058
Plum Grove, VA	0.060091	Porcupine Creek, MT	0.200508
Post Oak Mountain, TX	0.101097	Pound Ridge, CT	0.077838
Prentiss, NC	0.102169	Prestonburg, KY	0.002584
Priday Resevoir, OR	0.201745	Priest Lake NE, ID	0.104955
Rhoda, KY	0.158160	Rio, WV	0.020633
Roscoe, NY	0.051814	Roselle, NJ	0.031372
Sage Hen Butte, OR	0.114132	Salmon Lake, MT	0.178447
Seager, NY	0.127713	Seeley Lake East, MT	0.032776
Seeley Lake West, MT	0.157089	Shadow Mountain, CO	0.040356
Shell Mountains, TX	0.011533	Shepherds, NC	0.012450
Shining Rock, NC	0.086766	Smiths Grove, KY	0.075612
Smokemont, NC	0.033333	Statesville East, NC	0.073405
Statesville West, NC	0.047609	Stickleyville, VA	0.010109
Stony Point, TN	0.124742	Strawberry Lake, CO	0.111113
Thomas, KY	0.166408	Trail Mountain, CO	0.123404
Troutman, NC	0.008283	Upper Jocko Lake, MT	0.136336
Wapiti Lake, MT	0.155345	Wardensville, WV	0.054957
Wayland, KY	0.046486	West Kill, NY	0.143996
Wetherill Mesa, CO	0.064055	Wharton, PA	0.047379
Whitwell, TN	0.097438	Wilcox, WA	0.064847
Williams, IN	0.036472	Woodworth, MT	0.048609
Yakima East, WA	0.001668	Yellow Springs, WV	0.021081
Yew Creek, MT	0.030667	Yosemite NW, CA	0.106995
Zion National Park NE, UT	0.042162		

with terrain elevation. Goodchild interpreted the lower D value at the shoreline as a result of smoothing by coastal processes. On the other hand, Roy et al. (1987) described a case where fractal dimension decreases with altitude. They interpreted that this was partly related to the distribution of erratic glacial deposits at the lower elevations and partly due to the gradual disappearance of the crenulations associated with fluvial erosion towards the summits. Klinkenberg's (1988) study has found examples of both systematic trends. In addition, he discovered a U-shaped pattern between the fractal dimension and terrain elevation in 6 of the datasets he used, that is, the fractal dimension decreases from a very high value associated with the lowest contours, to a low value associated with the middle contours, and then increases to the highest contours. Efforts were made in this study to determine whether these systematic variations represent a general pattern in the natural landscapes or just isolated phenomena related to local geological conditions.

The results presented in this section are obtained by the box-counting method because only this method allows the examination of the relationship between fractal parameters and terrain elevation. It was found that very few DEMs displayed systematic variation of fractal dimension with elevation. In fact, only four of the thirty-two DEMs that have average r-squared values greater than 0.9 under "USING COLUMNS" in Table 5.1 show such regular variations. The results of these four DEMs are shown in Figure 6.2 and Table 6.5. Among these four DEMs, only the Thomas, KY Quadrangle shows a general increasing trend of D values with increasing elevation. In the other three cases, the fractal dimensions of contour lines generally decrease with increasing elevation. Two of these DEMs show the U-shaped pattern described by Klinkenberg (1988). This confirms the result of Klinkenberg (1988) that "*although the fractal dimension generally declines with elevation, but it does not necessarily do so.*" However, contrary to Klinkenberg's (1988) finding that the majority of DEMs (58 percent) have D values decreasing with elevation, this study reveals that although most of the DEMs show the same level of variations in the D value they

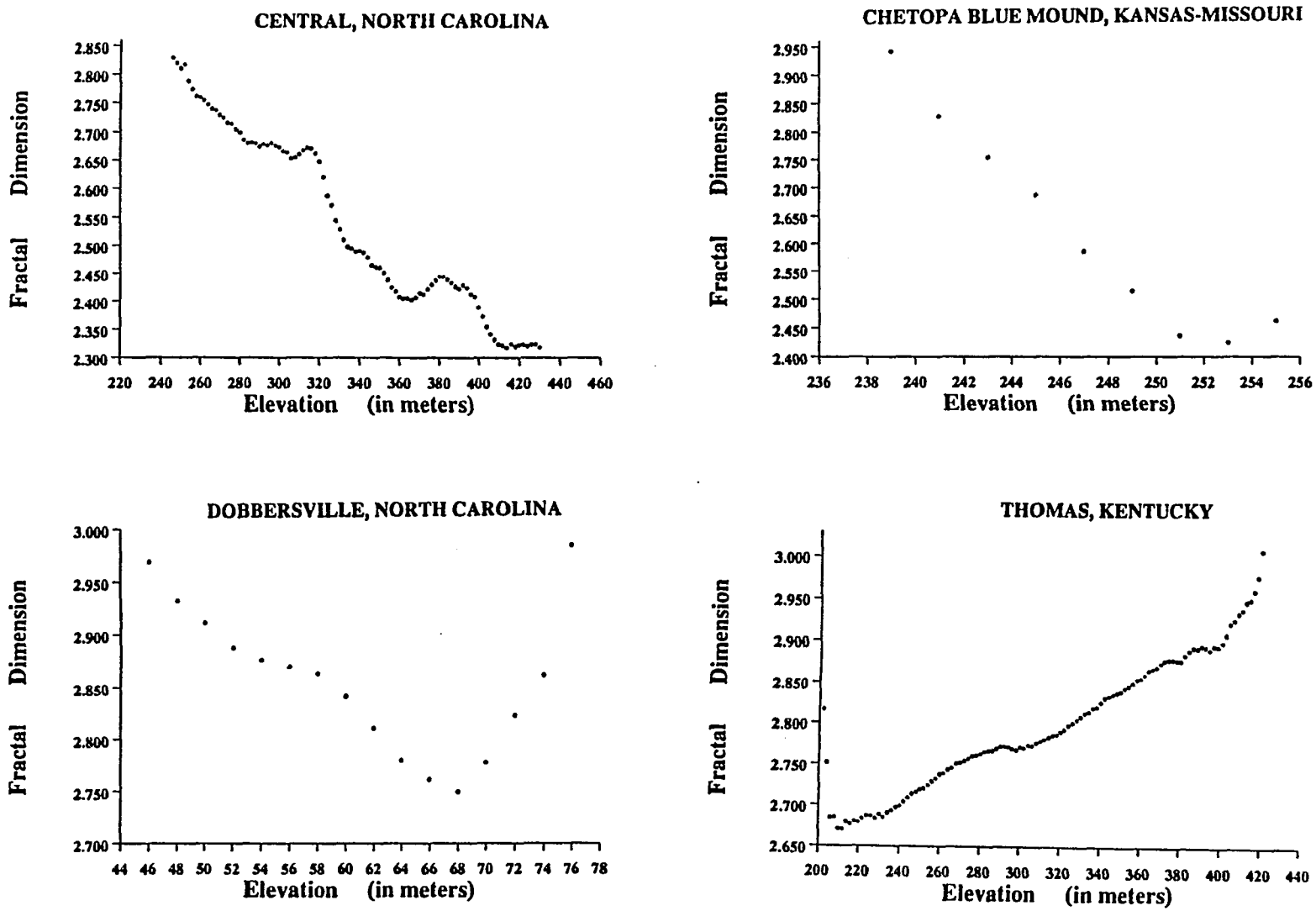

Figure 6.2 Systematic Variation of Fractal Dimensions with Terrain Elevation

Table 6.5 SYSTEMATIC VARIATIONS OF FRACTAL DIMENSION WITH TERRAIN ELEVATION

(a) CENTRAL, NORTH CAROLINA

ELEVATION	D	R-SQUARED
246 m	2.82972	0.72247
248 m	2.82068	0.80589
250 m	2.81128	0.82273
252 m	2.81758	0.82979
254 m	2.78899	0.85738
256 m	2.77387	0.86993
258 m	2.76199	0.89749
260 m	2.75995	0.91738
262 m	2.75548	0.92145
264 m	2.74774	0.92776
266 m	2.74066	0.92193
268 m	2.73798	0.92571
270 m	2.73062	0.91842
272 m	2.72526	0.91617
274 m	2.71717	0.92135
276 m	2.71504	0.92503
278 m	2.70606	0.92897
280 m	2.69951	0.93011
282 m	2.68746	0.93031
284 m	2.68153	0.93107
286 m	2.68329	0.92957
288 m	2.68094	0.93525
290 m	2.67567	0.93983
292 m	2.67975	0.94574
294 m	2.67699	0.94655
296 m	2.68138	0.94881
298 m	2.67733	0.95226
300 m	2.67454	0.95143
302 m	2.66730	0.95194
304 m	2.66455	0.95384
306 m	2.65390	0.95410
308 m	2.65582	0.95360
310 m	2.66158	0.95551
312 m	2.66845	0.96071
314 m	2.67339	0.96493
316 m	2.67189	0.96871
318 m	2.66369	0.96909
320 m	2.64851	0.97190
322 m	2.62141	0.97396
324 m	2.58838	0.97606
326 m	2.57246	0.97701
328 m	2.54527	0.97728
330 m	2.53008	0.97671
332 m	2.51148	0.97628
334 m	2.49859	0.97415
336 m	2.49494	0.96967
338 m	2.48946	0.96538
340 m	2.49037	0.96564
342 m	2.48827	0.96843
344 m	2.47932	0.97273

(b) THOMAS, KENTUCKY

ELEVATION	D	R-SQUARED
202 m	2.81663	0.87336
204 m	2.75181	0.86829
206 m	2.68475	0.87436
208 m	2.68527	0.89025
210 m	2.67062	0.89958
212 m	2.67042	0.91649
214 m	2.68006	0.91726
216 m	2.67695	0.92569
218 m	2.68026	0.93584
220 m	2.67941	0.93630
222 m	2.68357	0.93986
224 m	2.68680	0.94243
226 m	2.68686	0.94609
228 m	2.68406	0.94799
230 m	2.68886	0.94993
232 m	2.68546	0.94960
234 m	2.69075	0.94797
236 m	2.69391	0.94815
238 m	2.69768	0.94749
240 m	2.69945	0.94749
242 m	2.70427	0.94614
244 m	2.70935	0.94515
246 m	2.71423	0.94479
248 m	2.71671	0.94476
250 m	2.72000	0.94463
252 m	2.72138	0.94427
254 m	2.72498	0.94205
256 m	2.72953	0.94286
258 m	2.73296	0.94069
260 m	2.73794	0.93869
262 m	2.73968	0.93656
264 m	2.74365	0.93441
266 m	2.74626	0.93378
268 m	2.75129	0.93224
270 m	2.75267	0.93123
272 m	2.75471	0.93159
274 m	2.75705	0.93061
276 m	2.76043	0.92995
278 m	2.76158	0.93000
280 m	2.76330	0.92945
282 m	2.76573	0.92764
284 m	2.76722	0.92583
286 m	2.76754	0.92580
288 m	2.76959	0.92435
290 m	2.77243	0.92384
292 m	2.77262	0.92373
294 m	2.77206	0.92363
296 m	2.76992	0.92259
298 m	2.76848	0.92275
300 m	2.77211	0.92204

Table 6.5 continued

(a) CENTRAL, NORTH CAROLINA

ELEVATION	D	R-SQUARED
346 m	2.46580	0.97294
348 m	2.46239	0.97833
350 m	2.46030	0.97925
352 m	2.45158	0.98004
354 m	2.43867	0.97832
356 m	2.42498	0.97571
358 m	2.41869	0.97253
360 m	2.40799	0.97195
362 m	2.40539	0.96857
364 m	2.40599	0.96594
366 m	2.40301	0.96137
368 m	2.40766	0.95358
370 m	2.41524	0.95402
372 m	2.41300	0.94993
374 m	2.42142	0.94570
376 m	2.42971	0.94845
378 m	2.43773	0.94953
380 m	2.44422	0.95061
382 m	2.44419	0.94664
384 m	2.43932	0.94565
386 m	2.43328	0.94167
388 m	2.42675	0.94157
390 m	2.42268	0.94391
392 m	2.42913	0.94894
394 m	2.42459	0.94800
396 m	2.41330	0.94433
398 m	2.40798	0.93654
400 m	2.38941	0.92190
402 m	2.37361	0.89621
404 m	2.35527	0.87897
406 m	2.34223	0.85411
408 m	2.33326	0.83253
410 m	2.32481	0.80836
412 m	2.32308	0.79624
414 m	2.31857	0.77328
416 m	2.32481	0.76642
418 m	2.32046	0.74276
420 m	2.32328	0.72999
422 m	2.32380	0.72077
424 m	2.32157	0.69069
426 m	2.32416	0.68340
428 m	2.32426	0.67021
430 m	2.31903	0.64888

(b) THOMAS, KENTUCKY

ELEVATION	D	R-SQUARED
302 m	2.77083	0.92180
304 m	2.77448	0.92149
306 m	2.77382	0.92159
308 m	2.77745	0.92063
310 m	2.77888	0.91960
312 m	2.78115	0.91787
314 m	2.78365	0.91781
316 m	2.78621	0.91691
318 m	2.78683	0.91632
320 m	2.79049	0.91568
322 m	2.79346	0.91506
324 m	2.79849	0.91453
326 m	2.80172	0.91372
328 m	2.80501	0.91339
330 m	2.80929	0.91260
332 m	2.81340	0.91163
334 m	2.81497	0.91268
336 m	2.81943	0.91282
338 m	2.82097	0.91287
340 m	2.82633	0.91247
342 m	2.83205	0.91306
344 m	2.83410	0.91400
346 m	2.83630	0.91485
348 m	2.83874	0.91593
350 m	2.84022	0.91661
352 m	2.84424	0.91662
354 m	2.84677	0.91709
356 m	2.85015	0.91602
358 m	2.85479	0.91582
360 m	2.85662	0.91631
362 m	2.86090	0.91743
364 m	2.86655	0.91761
366 m	2.86852	0.91793
368 m	2.87064	0.91788
370 m	2.87497	0.91794
372 m	2.87854	0.91832
374 m	2.88001	0.91945
376 m	2.87995	0.92074
378 m	2.87925	0.91906
380 m	2.87831	0.91874
382 m	2.88529	0.91838
384 m	2.89012	0.91696
386 m	2.89419	0.91232
388 m	2.89337	0.91254
390 m	2.89642	0.90836
392 m	2.89493	0.90184
394 m	2.89194	0.89578
396 m	2.89637	0.88951
398 m	2.89579	0.88166
400 m	2.90042	0.87408
402 m	2.90958	0.86080
404 m	2.92283	0.84144
406 m	2.92706	0.82671
408 m	2.93517	0.81493
410 m	2.93922	0.79827
412 m	2.94917	0.78542

Table 6.5 continued

(c) DOBBERSVILLE, NORTH CAROLINA

ELEVATION	D	R-SQUARED
46 m	2.96960	0.92900
48 m	2.93285	0.95090
50 m	2.91211	0.96636
52 m	2.88829	0.97445
54 m	2.87653	0.98205
56 m	2.87038	0.98584
58 m	2.86417	0.98508
60 m	2.84207	0.98199
62 m	2.81165	0.97958
64 m	2.78072	0.97684
66 m	2.76231	0.97385
68 m	2.75025	0.96216
70 m	2.77826	0.94975
72 m	2.82434	0.92514
74 m	2.86332	0.88806
76 m	2.98681	0.80466

(d) CHETOPA BLUE MOUND, KS-MO

ELEVATION	D	R-SQUARED
239 m	2.94258	0.92882
241 m	2.82818	0.95650
243 m	2.75405	0.95795
245 m	2.68720	0.96026
247 m	2.58615	0.97059
249 m	2.51443	0.96476
251 m	2.43742	0.96582
253 m	2.42505	0.96598
255 m	2.46251	0.95010

obviously lack any systematic pattern as identified by Goodchild (1982) and Roy et al. (1987). Two examples of nonsystematic variation of fractal dimensions are shown in Figure 6.3 and Table 6.6. It appears that systematic variation of D values with elevation, and thus terrain surface irregularities, represent localized, exceptional cases rather than the rule.

It was also interesting to note that the magnitude of variation in fractal dimension with elevation was surprisingly high. For example, the difference between the lowest and the highest D values for the Chetopa Blue Mound, KS-MO Quadrangle is as large as 0.52. Whether such variation is related to terrain characteristics or at least partially related to the procedural errors such as inadequate sampling at higher elevations remains to be investigated.

6.6 The Average Fractal Dimension of Topography

It was also attempted in this study to make a general assessment on the range of variability in the complexity of terrain features. Mandelbrot (1983) concluded that fractal dimensions in the range D = 2.1-2.2 produced the most realistic synthetic topography. On the other hand, Turcotte (1987), Huang and Turcotte (1989), and Newman and Turcotte (1990) have obtained a D value of 2.5 for the real topographic data based on one-dimensional spectral decompositions of topographic profiles. Thus, topography appears to be Brownian noise. Similar results have been obtained by other researchers for both topography and bathymetry (Balmino et al., 1973; Bell, 1975, 1979; and Mareschal, 1989). In developing their statistical model of surface topography, Sayles and Thomas (1978a) also assumed that topographic data behave similarly to a random walk.

The results from this study do not conform to either of these models. A much wider range of variability is displayed in the real topographic data, as Burrough (1981) discovered for soil properties and other environmental variables. The lowest fractal dimension obtained is 2.22 (Mt. Tobin NE, Nevada) and the highest fractal dimension

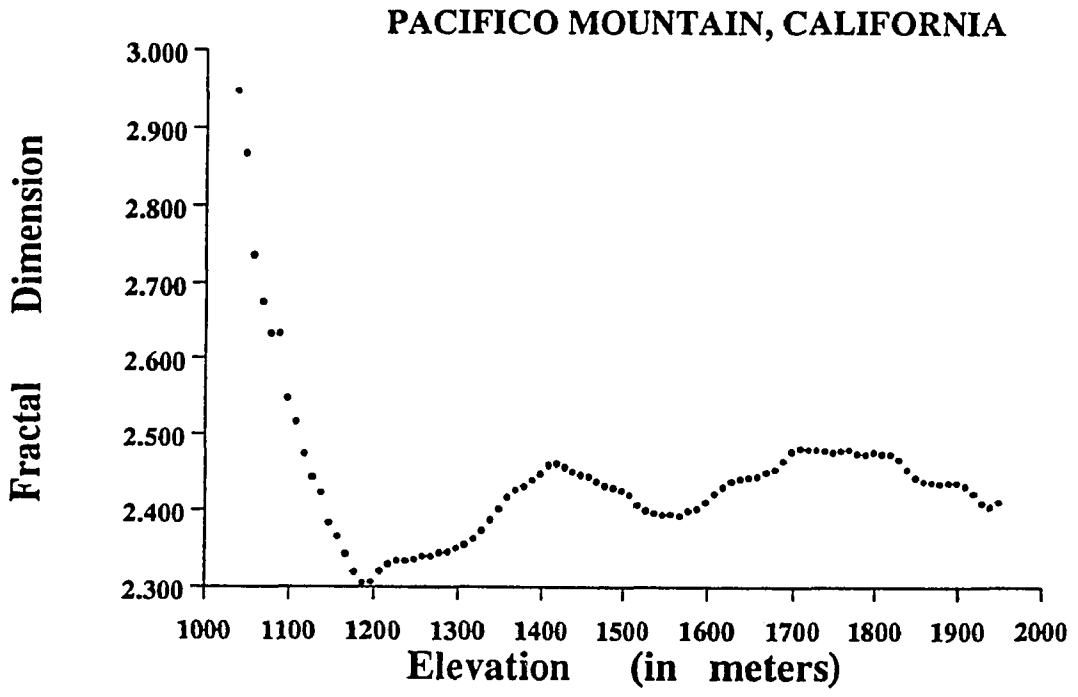

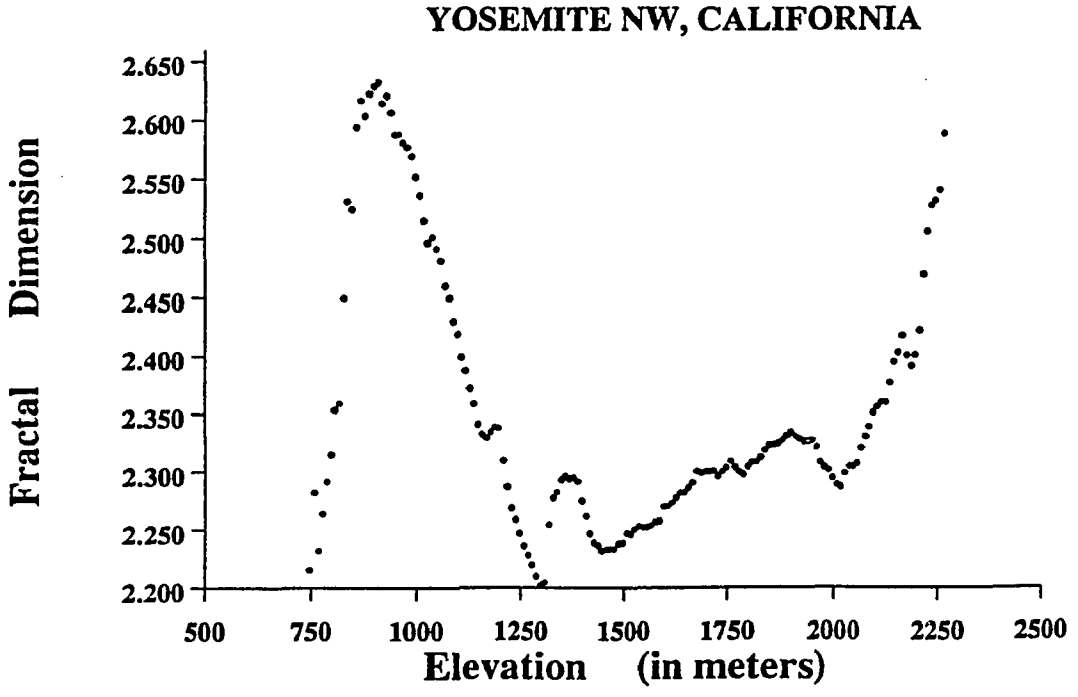

Figure 6.3 Nonsystematic Variation of Fractal Dimensions with Terrain Elevation

Table 6.6 NON-SYSTEMATIC VARIATIONS OF FRACTAL DIMENSION WITH TERRAIN ELEVATION

(a) PACIFICO MOUNTAIN, CA

ELEVATION	D	R-SQUARED
1037 m	2.94804	0.68530
1047 m	2.86823	0.71761
1057 m	2.73647	0.74488
1067 m	2.67555	0.75599
1077 m	2.63352	0.77286
1087 m	2.63348	0.77260
1097 m	2.54836	0.79177
1107 m	2.51677	0.79675
1117 m	2.47415	0.82154
1127 m	2.44380	0.81852
1137 m	2.42339	0.82567
1147 m	2.38296	0.82647
1157 m	2.36532	0.85200
1167 m	2.34248	0.87074
1177 m	2.31913	0.88158
1187 m	2.30563	0.89183
1197 m	2.30659	0.89617
1207 m	2.32017	0.89555
1217 m	2.32902	0.89849
1227 m	2.33363	0.90318
1237 m	2.33345	0.90956
1247 m	2.33542	0.91964
1257 m	2.33929	0.92847
1267 m	2.33929	0.93883
1277 m	2.34429	0.95155
1287 m	2.34561	0.95342
1297 m	2.34991	0.94119
1307 m	2.35446	0.93591
1317 m	2.36182	0.91690
1327 m	2.37349	0.90541
1337 m	2.38766	0.89842
1347 m	2.40233	0.89923
1357 m	2.41815	0.89604
1367 m	2.42715	0.89324
1377 m	2.43211	0.88959
1387 m	2.44017	0.88830
1397 m	2.44884	0.88546
1407 m	2.46004	0.89029
1417 m	2.46240	0.89355
1427 m	2.45748	0.88959
1437 m	2.45149	0.88598
1447 m	2.44763	0.88784
1457 m	2.44500	0.88673
1467 m	2.43852	0.88524
1477 m	2.43287	0.88207
1487 m	2.42984	0.88489
1497 m	2.42623	0.88249
1507 m	2.42065	0.88455
1517 m	2.40683	0.88961
1527 m	2.40055	0.88176
1537 m	2.39680	0.87809
1547 m	2.39406	0.87167
1557 m	2.39492	0.86680
1567 m	2.39298	0.86237
1577 m	2.39983	0.85992

(b) YOSEMITE NW, CA

ELEVATION	D	R-SQUARED
747 m	2.21571	0.73381
757 m	2.28182	0.77445
767 m	2.23186	0.75838
777 m	2.26338	0.78576
787 m	2.29142	0.83631
797 m	2.31486	0.79916
807 m	2.35373	0.82585
817 m	2.35906	0.79434
827 m	2.44974	0.81731
837 m	2.53120	0.80282
847 m	2.52514	0.77494
857 m	2.59442	0.77702
867 m	2.61688	0.74485
877 m	2.60410	0.72725
887 m	2.62293	0.71752
897 m	2.62884	0.72737
907 m	2.63235	0.70992
917 m	2.61464	0.72800
927 m	2.62068	0.72218
937 m	2.60686	0.71337
947 m	2.58766	0.71314
957 m	2.58814	0.68830
967 m	2.58127	0.67334
977 m	2.57704	0.65453
987 m	2.56958	0.64306
997 m	2.55217	0.64915
1007 m	2.53665	0.66979
1017 m	2.51537	0.67990
1027 m	2.49650	0.70019
1037 m	2.50160	0.75397
1047 m	2.49130	0.74448
1057 m	2.48136	0.74899
1067 m	2.46018	0.74846
1077 m	2.44995	0.74041
1087 m	2.43058	0.72597
1097 m	2.41904	0.71385
1107 m	2.39972	0.69942
1117 m	2.38783	0.68874
1127 m	2.37233	0.67749
1137 m	2.35912	0.67031
1147 m	2.34151	0.65907
1157 m	2.33312	0.65059
1167 m	2.32968	0.64892
1177 m	2.33494	0.66371
1187 m	2.33897	0.66137
1197 m	2.33810	0.68240
1207 m	2.30984	0.65235
1217 m	2.28716	0.62843
1227 m	2.26870	0.61794
1237 m	2.25861	0.63508
1247 m	2.24706	0.65131
1257 m	2.23580	0.65939
1267 m	2.22794	0.66437
1277 m	2.21998	0.68513
1287 m	2.20987	0.69976

Table 6.6 continued

(a) PACIFICO MOUNTAIN, CA

ELEVATION	D	R-SQUARED
1587 m	2.40289	0.85508
1597 m	2.41150	0.84854
1607 m	2.42226	0.84677
1617 m	2.43154	0.83969
1627 m	2.43861	0.84051
1637 m	2.44200	0.83255
1647 m	2.44420	0.82323
1657 m	2.44537	0.81753
1667 m	2.45050	0.81611
1677 m	2.45441	0.81236
1687 m	2.46443	0.82162
1697 m	2.47813	0.82697
1707 m	2.48140	0.82608
1717 m	2.48038	0.83129
1727 m	2.47998	0.83398
1737 m	2.47869	0.83558
1747 m	2.47690	0.82893
1757 m	2.47874	0.82239
1767 m	2.47993	0.81769
1777 m	2.47528	0.81155
1787 m	2.47392	0.80204
1797 m	2.47667	0.79331
1807 m	2.47437	0.78450
1817 m	2.47387	0.77670
1827 m	2.46627	0.77631
1837 m	2.45431	0.76622
1847 m	2.44397	0.76414
1857 m	2.43846	0.76207
1867 m	2.43758	0.77004
1877 m	2.43530	0.77246
1887 m	2.43679	0.77831
1897 m	2.43686	0.77848
1907 m	2.43306	0.77224
1917 m	2.42286	0.75239
1927 m	2.40968	0.72224
1937 m	2.40499	0.69587
1947 m	2.41123	0.67671

(b) YOSEMITE NW, CA

ELEVATION	D	R-SQUARED
1297 m	2.20182	0.71996
1307 m	2.20457	0.75601
1317 m	2.25447	0.77011
1327 m	2.27732	0.76546
1337 m	2.28222	0.77460
1347 m	2.29270	0.79456
1357 m	2.29636	0.80373
1367 m	2.29364	0.82983
1377 m	2.29514	0.85812
1387 m	2.29159	0.87418
1397 m	2.27472	0.87061
1407 m	2.26145	0.87068
1417 m	2.24659	0.85450
1427 m	2.23911	0.84422
1437 m	2.23639	0.84942
1447 m	2.23144	0.83950
1457 m	2.23267	0.81286
1467 m	2.23317	0.79541
1477 m	2.23319	0.78703
1487 m	2.23810	0.79314
1497 m	2.23892	0.78874
1507 m	2.24701	0.80473
1517 m	2.24650	0.79839
1527 m	2.25048	0.79955
1537 m	2.25295	0.79952
1547 m	2.25189	0.79737
1557 m	2.25179	0.83235
1567 m	2.25350	0.85078
1577 m	2.25659	0.86701
1587 m	2.25756	0.87622
1597 m	2.26940	0.87678
1607 m	2.26987	0.87750
1617 m	2.27254	0.88482
1627 m	2.27749	0.87687
1637 m	2.28159	0.87896
1647 m	2.28198	0.88232
1657 m	2.28644	0.89340
1667 m	2.29033	0.89683
1677 m	2.30030	0.91137
1687 m	2.29881	0.91316
1697 m	2.29979	0.91346
1707 m	2.29976	0.91647
1717 m	2.30049	0.91418
1727 m	2.29610	0.91658
1737 m	2.29969	0.92180
1747 m	2.30338	0.92561
1757 m	2.30851	0.93015
1767 m	2.30374	0.92920
1777 m	2.29985	0.92610
1787 m	2.29774	0.92549
1797 m	2.30430	0.93274
1807 m	2.30784	0.92439
1817 m	2.30870	0.92812
1827 m	2.31269	0.92868
1837 m	2.31877	0.93601
1847 m	2.32313	0.94089
1857 m	2.32325	0.94289
1867 m	2.32455	0.94402

Table 6.6 continued

(b) YOSEMITE NW, CA

ELEVATION	D	R-SQUARED
1877 m	2.32735	0.94571
1887 m	2.33084	0.94252
1897 m	2.33399	0.94325
1907 m	2.33069	0.93749
1917 m	2.32800	0.93432
1927 m	2.32606	0.93429
1937 m	2.32646	0.93046
1947 m	2.32692	0.93380
1957 m	2.32111	0.93564
1967 m	2.30772	0.92944
1977 m	2.30378	0.93069
1987 m	2.30111	0.93426
1997 m	2.29415	0.93780
2007 m	2.28849	0.93983
2017 m	2.28650	0.93029
2027 m	2.29838	0.93560
2037 m	2.30437	0.93345
2047 m	2.30407	0.93728
2057 m	2.30698	0.93197
2067 m	2.32027	0.93283
2077 m	2.33007	0.92763
2087 m	2.33845	0.92657
2097 m	2.35099	0.91027
2107 m	2.35564	0.90087
2117 m	2.35990	0.89068
2127 m	2.35982	0.87198
2137 m	2.37640	0.86878
2147 m	2.39484	0.85358
2157 m	2.40309	0.82037
2167 m	2.41769	0.80409
2177 m	2.40041	0.77355
2187 m	2.39116	0.75030
2197 m	2.40101	0.73732
2207 m	2.42233	0.71706
2217 m	2.46976	0.71158
2227 m	2.50618	0.70030
2237 m	2.52814	0.69713
2247 m	2.53235	0.67897
2257 m	2.54099	0.64468
2267 m	2.58888	0.64018

is 2.83 (Coharie SW, North Carolina). However, when the fractal dimensions of all 191 DEMs (the fractal dimensions estimated when elevation pairs in all four directions are combined) are averaged, we arrive at a mean D value of 2.50, which is the fractal dimension of standard Brownian noise. The distribution of fractal dimensions of all DEMs is shown in Figure 6.4. Thus, a D = 2.1-2.2 only represents the lower end of the results obtained in this study and a D value of 2.5 merely represents the mean condition of land surface topography, which confirms the claim of Sayles and Thomas (1978b). Only some exceptional topographic features appear to be true Brownian noise. It is quite possible that the average D value of 2.5 produced by Huang and Turcotte (1989) and others is a result of artificial agglomeration of diversified land surface features.

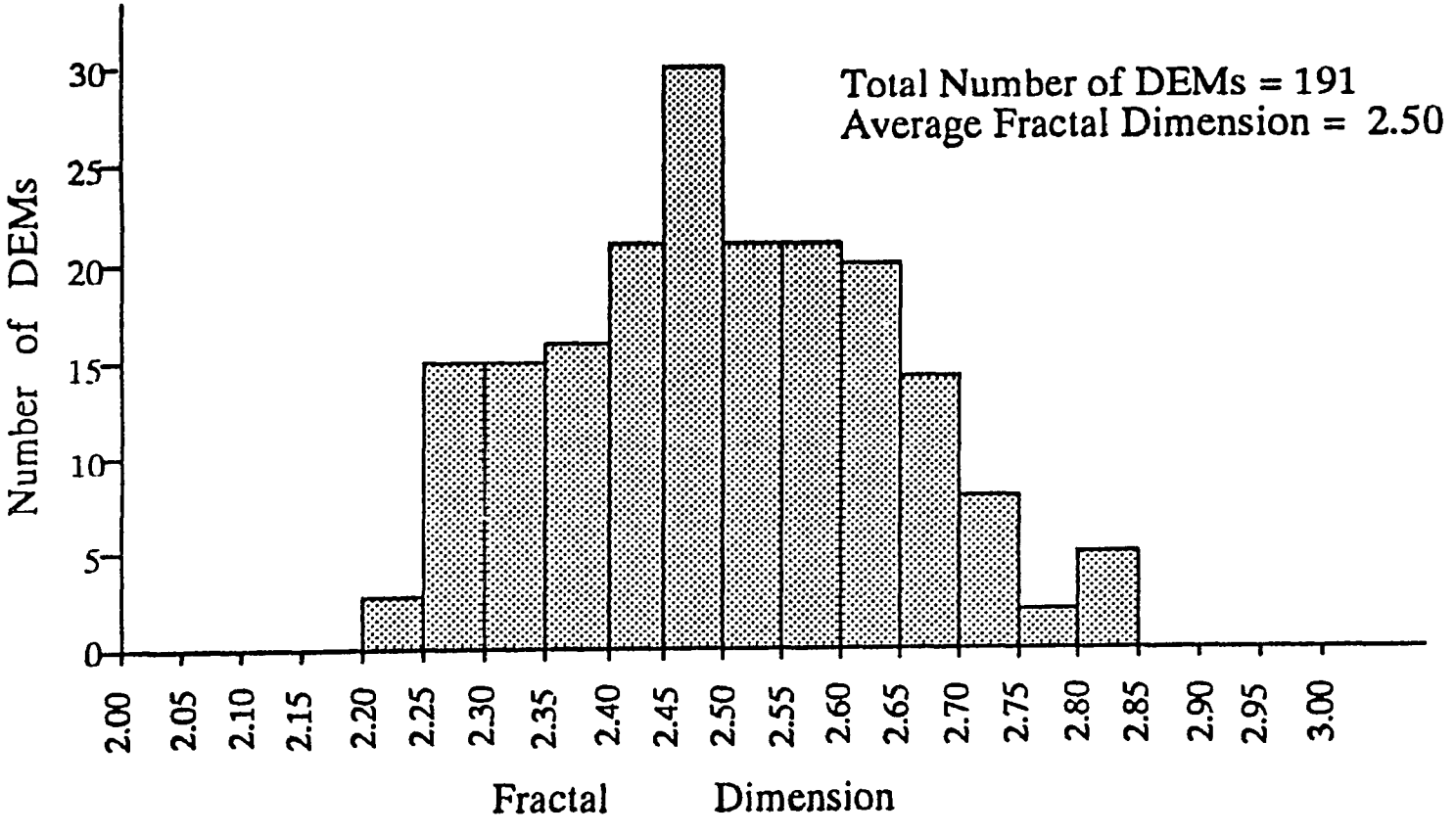

Figure 6.4 The Distribution of Fractal Dimensions of Topographic Data

Chapter 7 TOWARDS MORE INNOVATIVE USE OF FRACTAL GEOMETRY IN GEOMORPHOLOGY

7.1 Introduction

As reviewed in Chapter 3, most of the fractal studies by terrain scientists have so far focused on the characterization of terrain surface morphology. The major purposes of terrain characterization are discrimination and identification of diversified landforms and construction of process models incorporating meaningful and quantitative morphological parameters. This chapter put the fractal studies of terrain features in a geomorphological context and helps highlight the direct relevance of fractal concepts to some of the traditional geomorphological problems. Specifically, it presents the results of an attempt to use fractal parameters to discriminate various landform regions and to quantify the the effects of geomorphological factors on the characteristics of terrain surfaces. It is well known that the most important factors affecting the characteristics of landforms include rock types, geological structure, climate, and stage of landform evolution (Pitty, 1971; Hunt, 1974; and Chorley et al., 1984). The relationships between these factors and fractal parameters are examined or discussed below.

7.2 Discrimination of Physiographic Regions

A physiographic region is defined by Thornbury (1965, p.8) as "*an area or division of the land in which the topographic elements of altitude, relief, and type of land forms are characteristic throughout and as such is set apart or contrasted with other areas or units with different sets of characteristic topographic elements.*" The division of the land surface into physiographic regions has been a subject of scientific investigation for almost a century (Thornbury, 1965). It is quite possible that not long after scientists began to observe land surface features and speculate about their origin, they also noted regional variations in the character of landscapes. In North America, many attempts have been made during the last one hundred years to divide the United States

or the whole continent into geomorphic regions (Powell, 1895; Bowman, 1911; Joerg, 1914; Fenneman, 1914, 1916, 1928; Hammond, 1954, 1964; and Hunt, 1967, 1974). A number of books have been written to document the physiography of different regions (Bowman, 1911; Fenneman, 1931, 1938; Loomis, 1937; Atwood, 1940; Thornbury, 1965; Hunt, 1967, 1974; and Graf, 1987).

Recognition of geomorphic regions involves a consideration of the fundamental bases or criteria for establishment of such units. Unfortunately, there has been no consensus among geomorphologists as to what constitutes the proper bases for distinguishing geomorphic units. Nevertheless, most of the earlier landform classifications were strongly influenced by the work of William Morris Davis. It was widely accepted that the dominant factors in determining the characteristics of landforms were geological structure, erosional and depositional processes, and the stage of landform evolution. The word 'structure' was commonly used in a very comprehensive sense, covering all the work of constructive agencies. In addition, it was made to include the nature of the surface materials and even the initial form before the work of erosive agencies began. The major agents of erosion and deposition include stream flow, sheet flow, glacial ice, wind, and waves. Each of these processes produces its own characteristic forms. For example, valleys eroded by streams tend to have V-shaped cross sections; valleys deepened by glaciers have U-shaped cross sections. Similarly, streams create alluvial fans, oxbow lakes, and natural levees, glacial ice builds drumlins, eskers, ground moraines, lateral and terminal moraines, and wind builds various types of sand dunes. The third factor, stage, indicates that in the destruction of a land form by any one of the above-named processes, the form passes through a regular cycle of changes as the work progresses. Each stage has its own characteristics, differing according to the process at work and the structure involved. Thus, a type of topography was commonly designated by stating the types of surface materials, the initial geological structure, the surface process at work, and the stage reached in the cycle of landform evolution.

Among these factors, geological structure was considered by many as by far the most crucial factor in shaping the observed landscapes (Fenneman, 1928; and Hunt, 1967, 1974). For example, Hunt (1974, p.3) stated that "*The face of our land is the net result of a complex of processes and changes that occurred in the past and continue to occur today, but the basic differences between various parts of the land surface are structural.*" Strong emphasis was also put on the geomorphic histories of different regions. As a result, the boundaries of most physiographic provinces delineated by the early researchers corresponded more or less exactly to geologic lines such as the edge of certain strata, the limits of glacial drift sheets, and the surface traces of fracture zones.

There are at least two serious drawbacks with these traditional landform classifications. First, although they are useful in relating land surface features to endogenetic geological processes, they are less suitable for studying surface geomorphological processes which are equally important in creating the landscapes of our planet. It is true that geological structure and geomorphic history play more important roles in determining the very large scale topographic expressions. However, the characteristics of landforms at the mesoscopic and microscopic scales appear to be more closely related to erosional and sedimentary processes operating at the surface of the earth. As the utilization of the land intensifies, an accurate description of detailed surface features and a clear understanding of the processes responsible for creating these features are needed. Secondly, when no clearly identifiable geological lines exist, the placement of the boundaries between many regions was often a quite arbitrary decision. Some of the boundaries were placed to follow natural lines such as rivers, which have no intrinsic geomorphologic meaning. Others are "*merely straight lines, which, within limits of a number of miles, might as well be drawn at one place as another*" (Fenneman, 1928, p.269).

To facilitate the understanding of surface processes and to make the procedure of landform regionalization more objective, some researchers suggested that

physiographic regions should be divided on the basis of certain quantifiable characteristics of landforms. The most notable example of this new trend is the land form mapping of the United States carried out by Hammond (1954, 1964). Other studies along the same line include Wood and Snell (1960), Eyles (1971), Scott and Austin (1971), Drewry (1975), Evans (1980), and Zevenbergen and Thorne (1987). On the other hand, these morphologically oriented studies were troubled by another common problem, that is, what terrain variables should be used for discriminating various types of landform regions. The choice of different parameters has often given quite varied results. Studies have shown that many of the parameters used by these researchers are ineffective in discriminating the differences between adjacent physiographic regions. For example, Klinkenberg (1988) carried out a discriminant analysis to determine the adequacy of the traditional physiographic classifications using four morphometric parameters: the mean elevation, the standard deviation, the kurtosis of the elevations, and the coefficient of dissection. He discovered that some intra-provincial variations were just as great as or even greater than inter-provincial variations. More importantly, many traditional parameters are not adequately defined (Mark, 1975). It is not uncommon that a particular parameter means quite different things to different people. Similarly, various names are often used to describe the same feature. The perpetuation of this situation has continued for so many decades such that there exists extreme confusion as to the meaning of numerous geomorphological terms. In addition, digital terrain data did not become widely available until about the late 1970s. Without the digital terrain data, quantification of pervasive terrain properties such as slope, aspect, convexity, and percentage of area occupied by surfaces of certain character becomes extremely difficult if not impossible. The derivation of some meaningful terrain parameters could only be based on limited manual sampling. Thus, many data sets used by these researchers, although quantitative in nature, were merely rough estimates. Some values were simply assigned on the basis of visual estimation from topographic maps.

On the other hand, some recent fractal studies have suggested that fractal parameters seem to provide a viable alternative. In a systematic investigation on the use of amplitude spectrum to model the high-frequency variability of the sea-floor, Fox and Hayes (1985) found it possible to divide the sea-floor into relatively homogeneous regions on the basis of the slope of power spectra, which is functionally related to the fractal dimension. Berkson and Matthews (1983) also discovered a significant variation of regression coefficients for power spectra generated from different ocean bottom types. Berry and Hannay (1978) reanalyzed the topographic data collected by Sayles and Thomas (1978a) and found that the slope of the power spectral density varies from 1.07 to 3.03, which yields fractal dimensions between 1 and 2 for profiles or between 2 and 3 for surfaces. Most recently, Klinkenberg (1988) carried out a preliminary study to evaluate the possibility of using fractal criteria to delineate physiographic provinces. He conducted a one-way analysis of variance and found that the DEMs from different physiographic provinces were distinguishable solely on the basis of their fractal dimensions. However, the distribution of Klinkenberg's data sets is highly clustered and the sample size is relatively small (a total of fifty-eight DEMs). The present research was designed to extend Klinkenberg's study and to provide another independent verification of these earlier findings.

In order to substantiate these findings, blocks of DEMs were selected from 16 different physiographic provinces of Fenneman (1946) (see Appendix I). However, the number of DEMs from several provinces (Columbia Plateaus, Cascade-Sierra Mountains, and Pacific Border Provinces) is extremely small. Furthermore, some DEMs were selected intentionally for studying the characteristics of some localized features such as landforms developed in areas covered by loess, limestone, sand dune, and granite. The samples from these regions may not provide a fair representation of the regional characteristics. Thus, they were excluded in computing the average fractal dimension of each physiographic province and in the comparative study of fractal parameters characterizing various types of landforms.

First, the separability of broadly similar landforms is tested. Figure 7.1 shows the distribution of DEMs from physiographic regions of mountains, plains, and plateaus in a two-dimensional space formed by two important fractal parameters, that is, the fractal dimension and the scale range of self-similarity. A first look at this figure does not seem to reveal any obvious pattern. However, a closer examination indicates that most DEMs from the mountain regions can be separated from those of plains or plateaus. This becomes clearer when the results for the plains and plateaus are plotted separately. Figure 7.2 shows the distribution of DEMs of mountain regions and plateaus. It can be seen from this diagram that the vast majority of DEMs from regions of plateaus have much higher fractal dimensions than the DEMs of mountainous areas. Figure 7.3 shows the distribution of DEMs of mountain areas and plains. Figure 7.3a includes all DEMs from the regions of plains. On this diagram, the separation of mountains from plains appears to be more difficult. A careful examination of the fractal dimensions of DEMs from the provinces of plains suggests that the overlapping of fractal parameters between mountains and plains is mostly caused by the DEMs of the Great Plains Province. Figure 7.3b excludes the DEMs from the Great Plains Province. With a few exceptions, most DEMs from the Coastal Plain and Central Lowland Provinces can be separated from those of mountainous regions by their higher fractal dimensions. It is believed that the overlapping of fractal parameters between the mountains and the plains is a reflection of the transitional nature of the Great Plains Province. Figure 7.4 is a plot of the fractal parameters of DEMs of different plains. It can be seen that there is a gradual transition from the Coastal Plain to the Central Lowland and finally to the Great Plains. Such a transition is also evident from a visual examination of the actual landscapes of these regions. It is for this reason that on the traditional maps of physiographic regions the boundary "*between the Central Lowlands and the Great Plains is arbitrary along much of its length*" (Shimer, 1972, p.4).

Nevertheless, there are a few DEMs in each type of terrain that appear significantly different from the adjacent DEMs in the same province but are

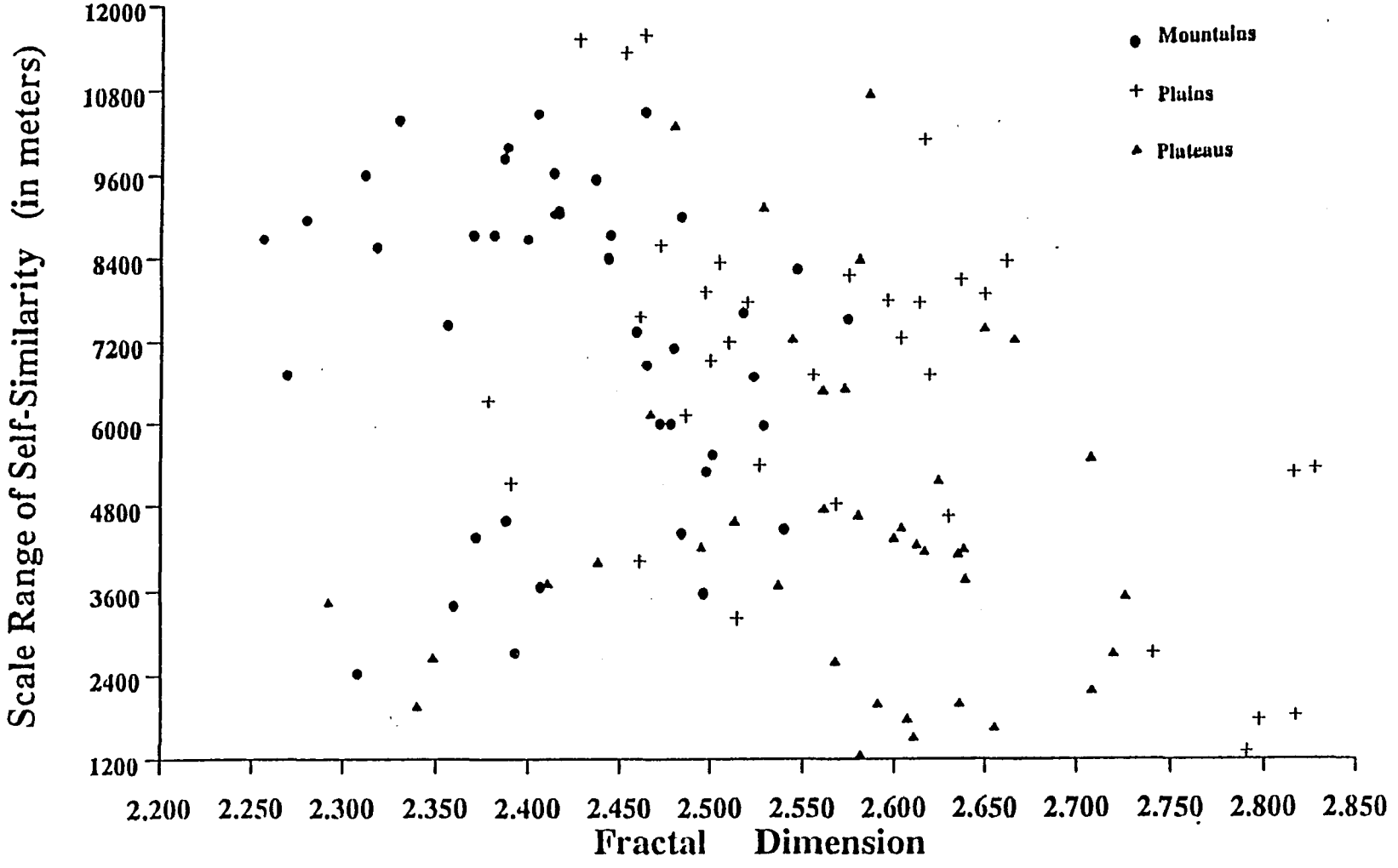

Figure 7.1 **Separability of Mountains, Plains and Plateaus**

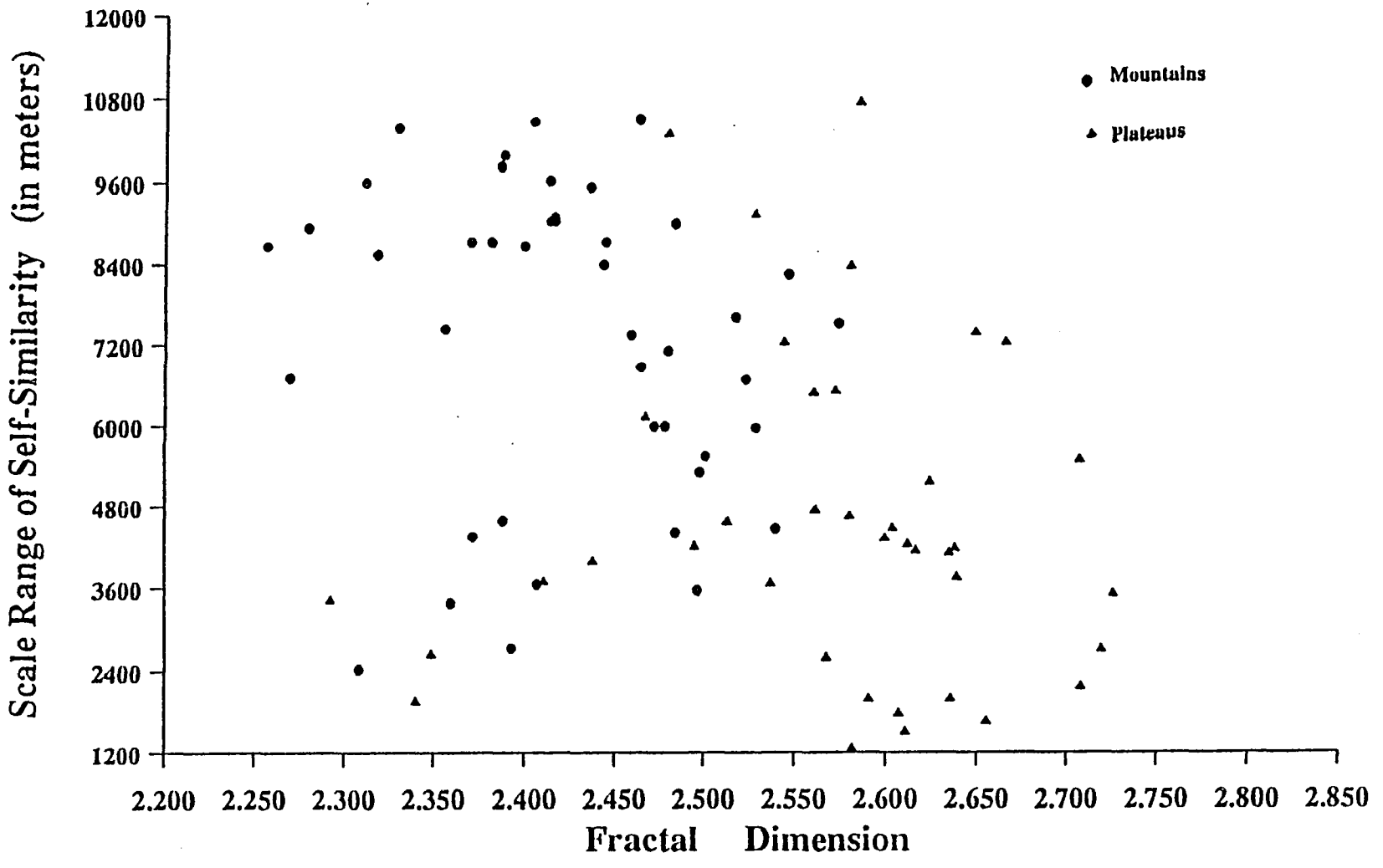

Figure 7.2 **Separability of DEMs of Mountains from Those of Plateaus**

(a)

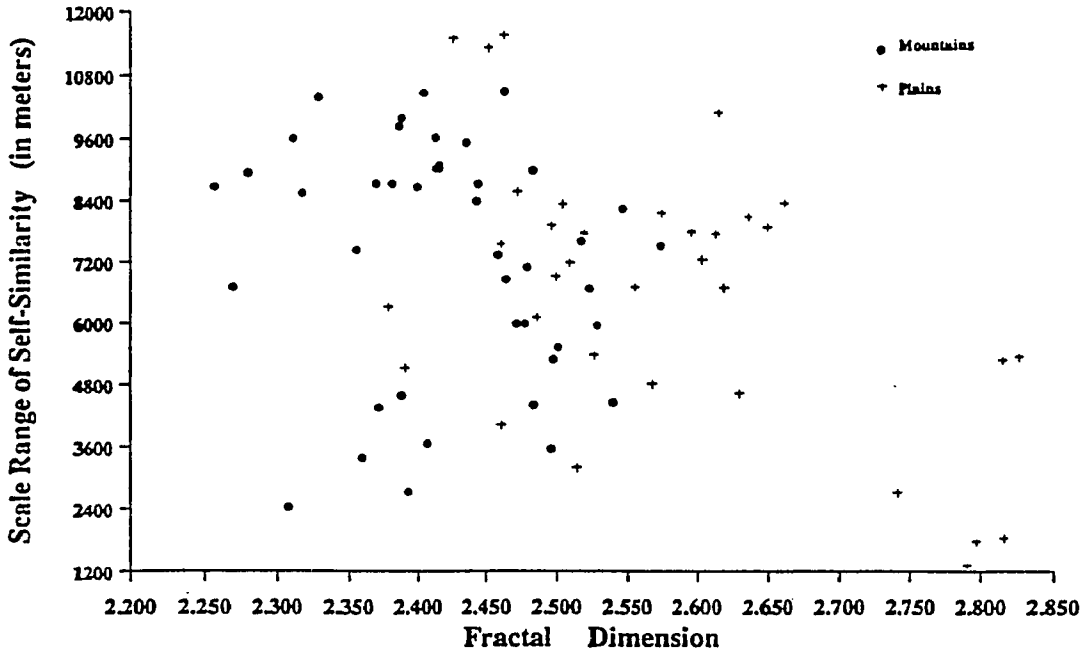

(b)

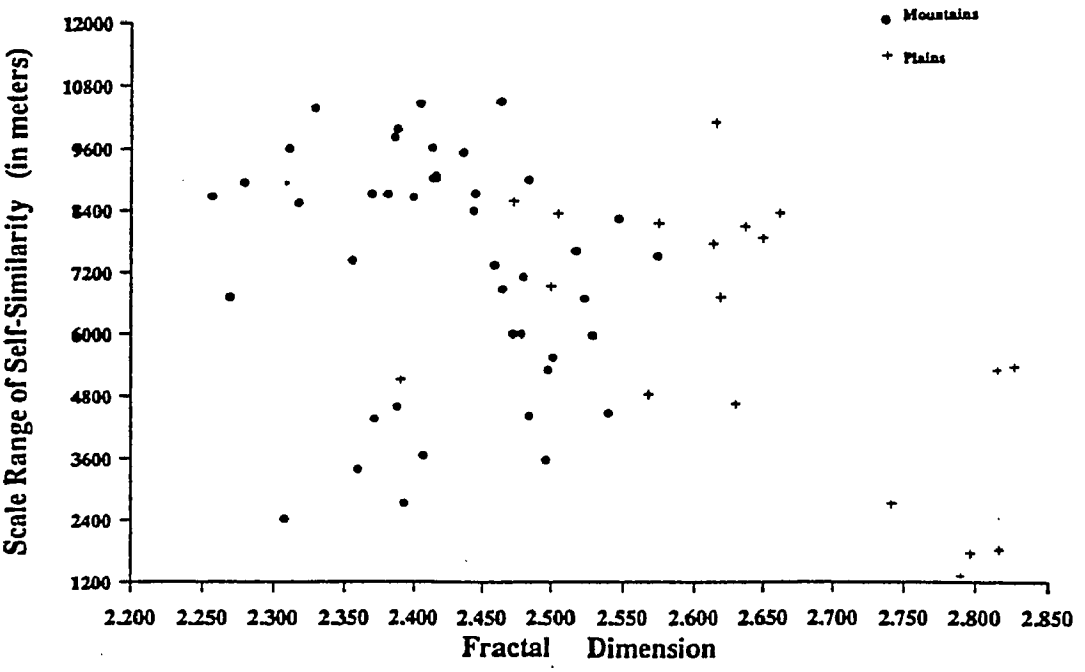

Figure 7.3 **Separation of DEMs of Mountains from DEMs of Plains. (a) includes DEMs of the Great Plains, and (b) excludes DEMs of the Great Plains.**

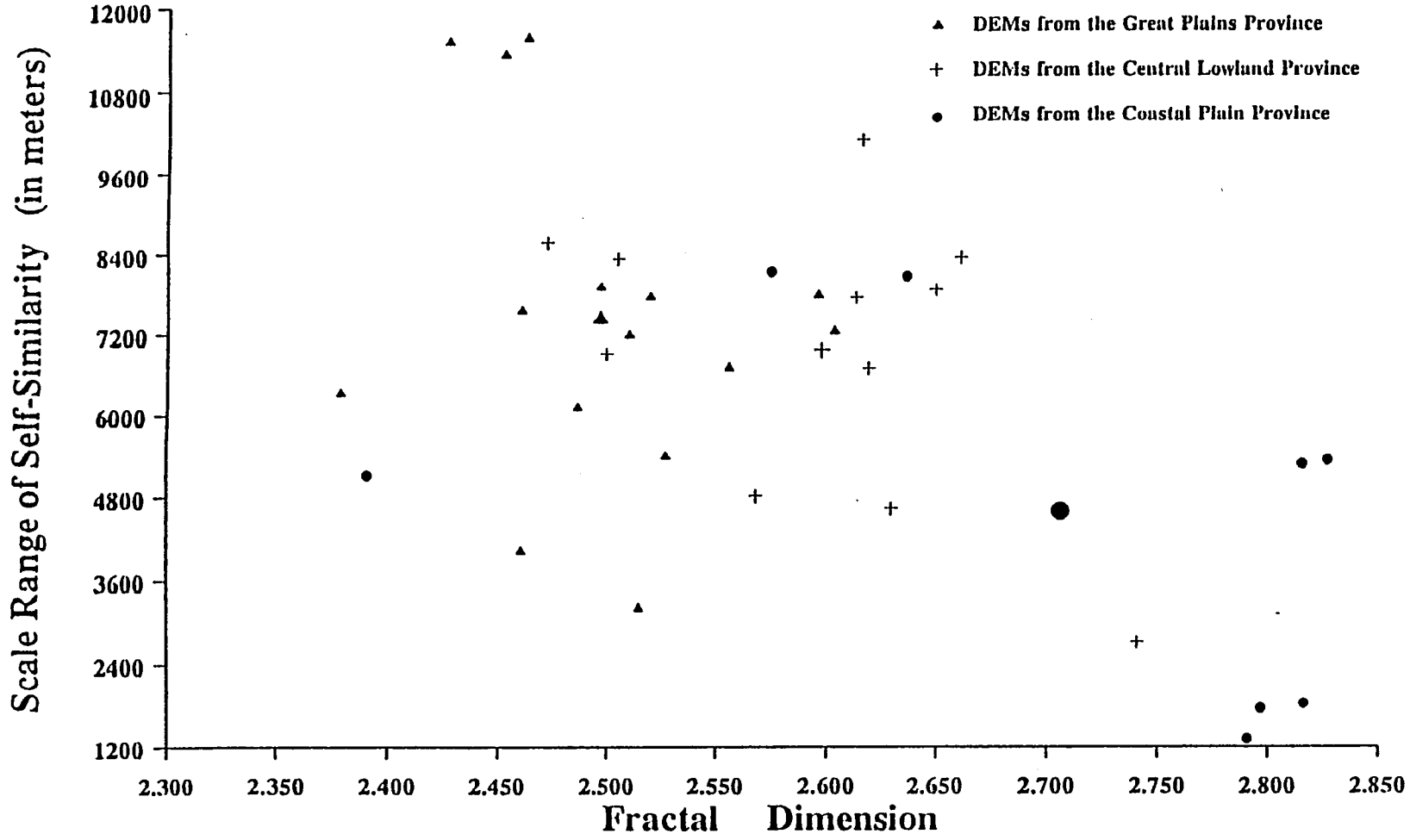

Figure 7.4 The Gradual Transition from the Coastal Plain to the Central Lowland and to the Great Plains

indistinguishable from those of other physiographic provinces. These exceptional cases are the major contributors to the wide range of variability of fractal parameters within each province (see Table 7.1). As pointed out in the previous chapter, these unusually high or low fractal dimensions for a particular type of terrain are caused by the juxtaposition of inhomogeneous patches of terrain surfaces and represent the deviation of real terrain from the idealized fractal model. As shown by the examples presented here, this kind of DEM are relatively few in number. They may be considered as "outliers".

Outliers are not unique to the fractal approach. In the traditional landform classifications, "*the problem of outliers is a common one, sometimes on a small scale, sometimes on a large scale*" (Thornbury, 1965, p.11). Thornbury (1965, p.11) pointed out that "*the general principle that followed is that outliers belong to the geomorphic unit of which they are geographically a part rather than to the area to which they are more closely akin geologically and geomorphically.*" On the other hand, the fractal parameters of landforms are based on the ensemble averages of numerous observations and statistical in nature. The presence of outliers revealed in this study merely reflects the inhomogeneity of terrain at a particular scale, that is, when DEMs of 1:24,000 scale topographic maps are used as individual units for computing the fractal dimensions of land surfaces. It is possible that when adjacent topographic quadrangles are mosaicked to create larger data sets, the number of outliers may be largely reduced or eliminated. Similar results may also be obtained by a smoothing operation of maps of fractal parameters.

Figure 7.5 shows the distribution of different physiographic provinces as represented by their average fractal parameters. The averaging process suppresses the effects of outliers. On this diagram, the mountain provinces can be separated from other provinces easily. The Basin and Range Province can be distinguished from other provinces by its lowest fractal dimension. On the other hand, the provinces of plateaus and plains are intermixed. This is due to the fact that geomorphologically plains are

Table 7.1 DISCRIMINATIONABILITY OF PHYSIOGRAPHIC PROVINCES

Physiographic Province	# of DEMs Used	Fractal Dimension
(1) Coastal Plain Province	10 (-2)	2.705919
(2) Piedmont Province	10	2.666693
(3) Blue Ridge Province	4	2.403024
(4) Valley and Ridge Province	16	2.524640
(5) Appalachian Plateaus Province	33	2.566595
(6) New England Province	5	2.517931
(7) Interior Low Plateaus Province	5	2.676545
(8) Central Lowland Province	12 (-1)	2.597473
(9) Great Plains Province	16 (-1)	2.496496
(10) Southern Rocky Mountains Province	9	2.450198
(11) Middle Rocky Mountains Province	3	2.407882
(12) Northern Rocky Mountains Province	27	2.433701
(13) Columbia Plateaus Province	2 (-1)	2.271701
(14) Colorado Plateaus Province	6	2.506629
(15) Basin and Range Province	29 (-1)	2.364369
(16) Cascade-Sierra Mountains Province	3	2.305707
(17) Pacific Border Province	1	2.443909

* The numbers in the parentheses are the numbers of DEMs excluded for computing the average fractal dimension.

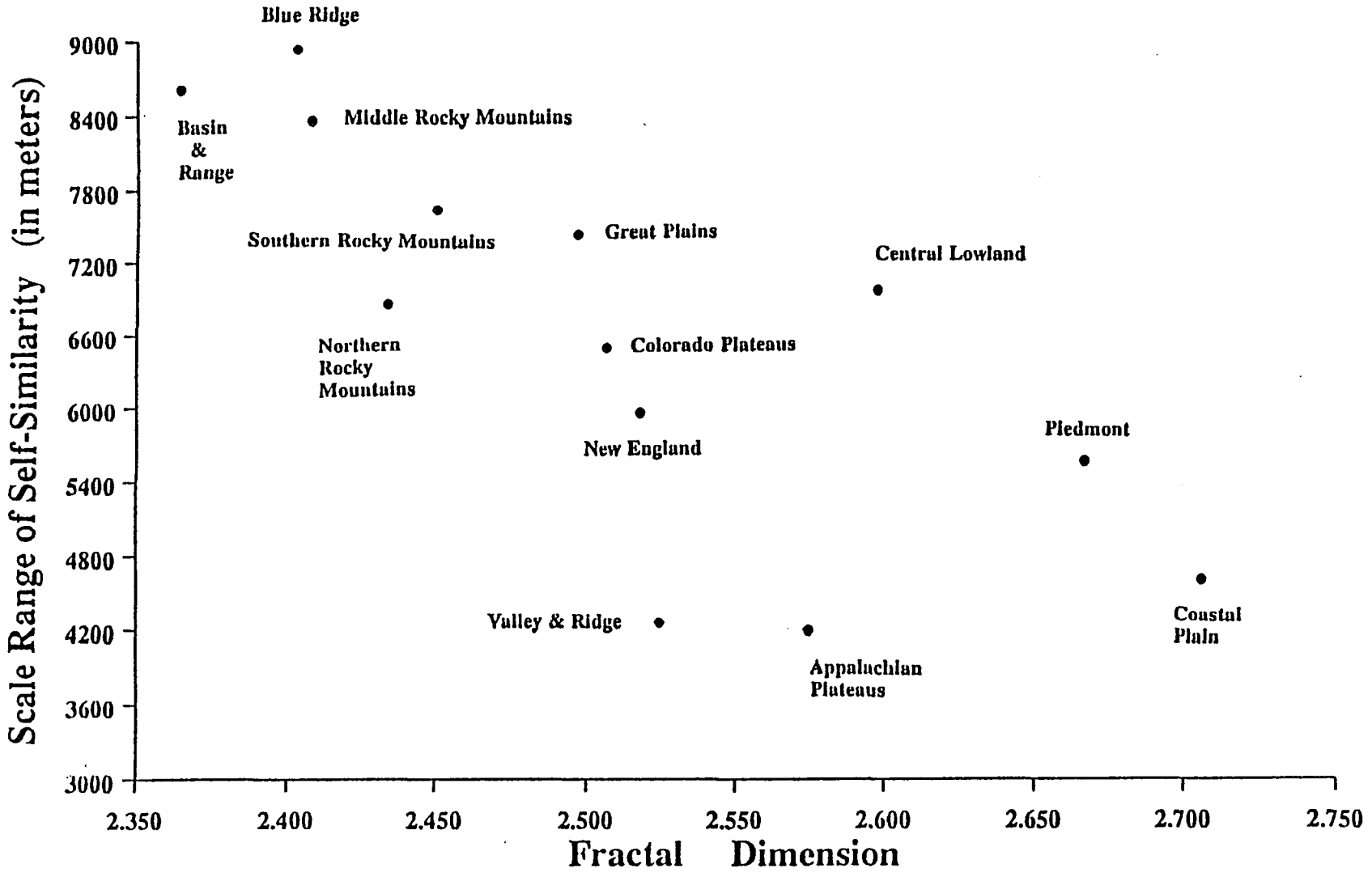

Figure 7.5 **Fractal Characterization of Physiographic Provinces**

not fundamentally different from plateaus. Both are characterized by their comparatively flat or level ground. The major difference between them is elevation. A plateau is an elevated tract of land, which has higher gravitational potential and is likely to experience more intensified surface erosion. Thus, plateaus may be dissected by deep valleys. However, the level of dissection varies from region to region and there is no clear-cut boundary value between plateaus and plains. As pointed out by Fenneman (1916), "*A plateau may also be a plain, or the uneroded part of it may be a plain.*"

Nevertheless, when plateaus and plains are considered together, two interesting points emerge. First, there appears to be a continuous transition from the Coastal Plain to the Piedmont Province, to the Central Lowland, to the Appalachian Plateaus, and finally to the Great Plains. This gradual transition seems to be consistent with the ground observations. Secondly, certain similarities exist between the Colorado Plateaus, the Great Plains, and the New England Province although these provinces are widely separated geographically. However, further research is needed to determine whether such similarities are an indication of similar geological history or geomorphological processes.

Next, the separability of landforms at the province level by using fractal parameters is examined. The results from this study show that each physiographic province does not have a unique "signature" dimension (Table 7.1). On the other hand, adjacent physiographic provinces do differ significantly. Figure 7.6 shows the distribution of DEMs from the five adjacent provinces along the east coast of the U. S. The large size symbols indicate the average fractal dimensions of different physiographic provinces. The small-sized symbols show the fractal dimensions of individual DEMs. Most of the DEMs in each province, with the exception of those from the Appalachian Plateaus, have their distinctive fractal parameters. DEMs from the Coastal Plain Province have higher fractal dimensions than those from the Piedmont Province. The separation of the Blue Ridge Province from the Piedmont Province is made extremely easy by its lowest fractal dimensions. The difference in fractal dimension between the Blue Ridge

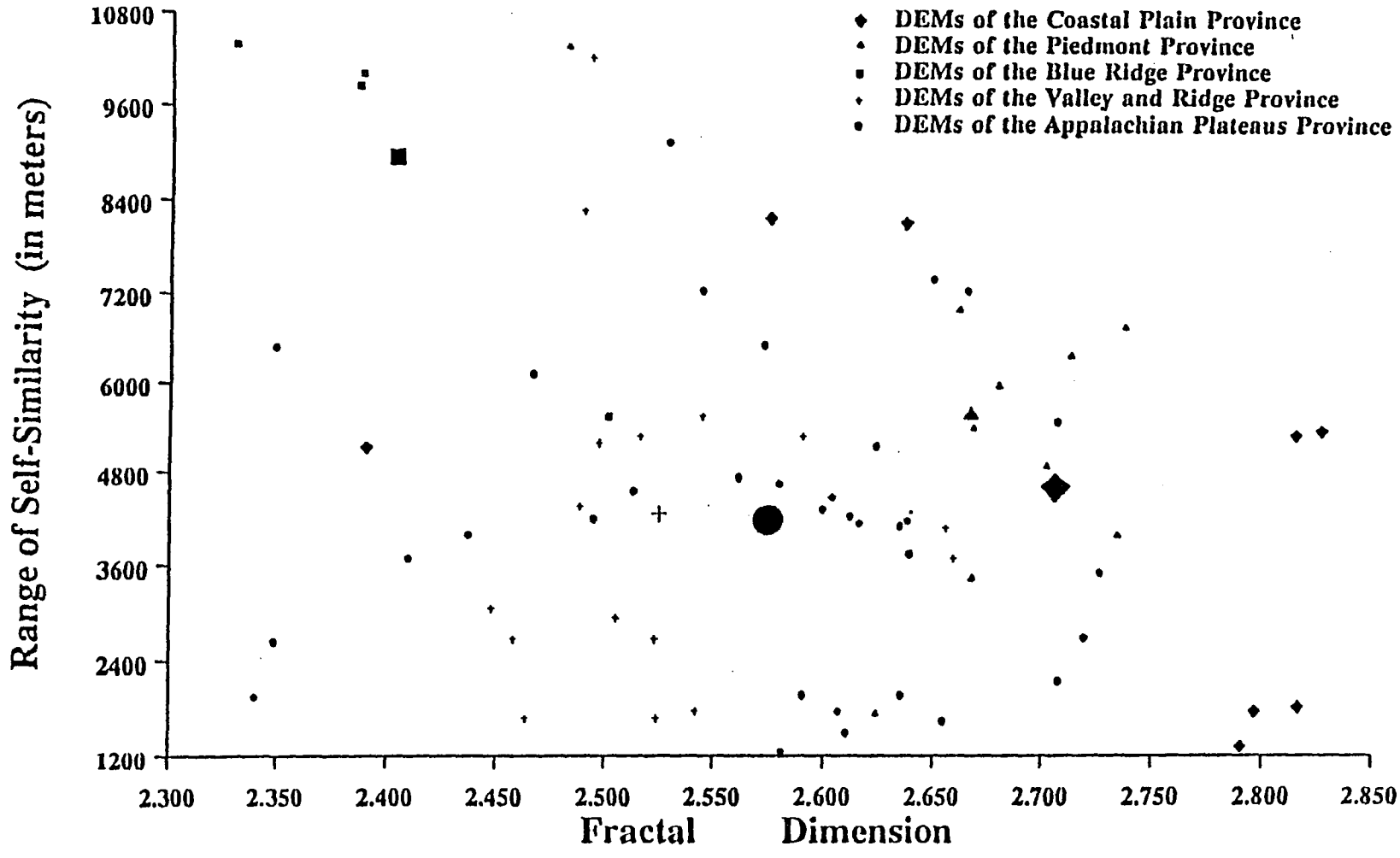

Figure 7.6 **Discrimination of Southeastern Physiographic Provinces**

Province and the Valley and Ridge Province is somewhat smaller but still distinctive. Most of the DEMs in the Appalachian Plateaus have relatively higher fractal dimensions than those from the Valley and Ridge Province.

However, it should be pointed out that it is very unlikely that all physiographic provinces are separable on the basis of fractal parameters. It is expected that the separation of physiographic provinces is only possible when adjacent provinces display highly contrasting morphological characteristics as seen in the eastern part of the U. S. After all, fractal parameters represent a completely new set of discriminating criteria. It would be no less than a miracle that Fenneman (1914) could have delineated the physiographic provinces on an entirely different set of criteria almost eighty years ago, which could be duplicated using the fractal approach. The use of Fenneman's provinces, on the one hand, provides a framework of reference when the complete coverage of DEMs is not available. Furthermore, it gives us some idea on how well the traditional landform classification reflects the similarity of geometric form within each province as well as the difference between different regions. Eventually, the partition of terrain surface into contrasting regions will be implemented without any reference to the traditional subdivisions. It is only through such unbiased application of the new approach that unknown patterns may be revealed and a whole new territory of scientific inquiry may emerge into the horizon.

7.3 Effects of Rock Types on the Characteristics of Topography

Whether one considers that rocks are the most important elements in the formation of the physical landscape or not, their great importance cannot be denied (Sparks, 1971; and Gerrard, 1988). Pitty (1971, p.91) wrote, "*viewed from all angles, landforms almost invariably reflect in some degree the differing resistances to erosion of the underlying rocks.*" A number of previous studies have demonstrated a relationship between rock type and average altitude (Flint, 1963; Chorley et al., 1984; and Costa and Cleaves, 1984). Resistant rocks such as sandstone and quartzite commonly form

high ridges while weak rocks such as shale occupy the intervening valleys. In searching for clues of mineralization, we have discovered that raised narrow rock walls often indicate the presence of igneous dikes or zones of silicification. The effect of lithology on landform characteristics is probably best demonstrated by the occurrence of certain types of landforms exclusively within certain types of rocks. Karst topography is generally developed in areas of limestone. Badlands are usually found in places where horizontal or gently tilted strata is dominated by argillaceous rocks. Many specialized books have been written on the relationship between rocks and landform characteristics (Yatsu, 1966; Sparks, 1971; Twidale, 1982; Trudgill, 1985; and Gerrard, 1988). Ehlen (1981) attempted the identification of rock types by analyzing landform assemblages from aerial photographs.

Rocks affect the characteristics of the land surface in two ways. First, the processes of weathering and erosion are governed in their attack on rocks by the mineral and chemical composition of the rocks, by the ways in which the individual particles forming the rocks are bonded together, and by such minor structural features of rocks as joints, bedding planes, cleavage and schistosity (Sparks, 1971). Second, rocks affect the landforms through their depositional arrangements. A succession of rocks of equal resistance to denudation will result in a uniformity of relief but alternations of resistant and non-resistant beds will form a varied relief.

This section presents the results of an assessment of the differences in fractal parameters of landforms developed in areas of contrasting rock materials. To assess the influence of rock types on the characteristics of landforms, DEMs were selected from areas where loess, granite, limestone, and sand dune are exposed to the surface. The selected DEMs represent the simplest cases. Each area is covered by a single type of rock material. The particular lithological types are considered here because landforms developed on these rocks appear most chaotic and each is visually characteristic.

Loess consists of wind-deposited silt and dust (< 0.05 mm in diameter). It blankets the middle western plains of this country and forms the rich soil of that area. The loess dates from the glacial periods, and originated as dust blown eastward out of the great river valleys, which were left as bare mud flats after the floods of glacial melt waters subsided. Visually, landforms developed in areas of loess are characterized by their fine texture and by the lack of any ordered stream system.

Well-known karst topography is mostly developed in limestone regions. Karst topography is characterized by the frequent occurrence of gorges and natural bridges, meander caves, half-blind valleys, blind valleys, solution dolines, disorganized surface drainage, and tower karst (Sweeting, 1972; and Jennings, 1985, p.88-134). In addition, many types of characteristic minor surface solution forms have been identified on the surfaces of limestone rocks. These include rain pits, solution ripples, solution flutes, solution bevels, solution funnels, rain solution funnels, grikes, karst wells, solution spikes, clints, solution pans, solution notches, and swamp slots (Sweeting, 1972; and Jennings, 1985, p.73-82). Obviously, these characteristic surface forms are not represented by the DEMs. However, it is well known that maps of limestone regions do furnish important clues related to the mesoscopic features, which are reflective of the nature of surface materials.

Because granite is both homogeneous and resistant, erosion produces irregular topography without orderly patterns. At the outcrop scale, major forms characteristic of granitic exposures are boulders, inselbergs, all-slopes topography and plains (Twidale, 1982).

Sand dunes occur in a large variety of forms. The basic dune types include sheet, stringer, dome, barchan, barchanoid, transverse, blowout, parabolic, linear or longitudinal, reversing, and star dunes (McKee, 1979, p.10). In addition, a number of combinations of the basic types can occur. For example, compound dunes are composed of two or more dunes of the same type, and complex dunes are composed of two or more

different types of dunes. Visual examination of sand dunes in deserts and beaches on aircraft and satellite imagery and on the ground suggests that the forms of some sand dunes are just scaled versions of one another. This led Burrough (1984, p.40) to speculate that certain types of sand dunes might be good examples of natural fractals.

Table 7.2 lists the DEMs selected for studying the effects of the types of rock materials on the characteristics of landforms and their derived fractal parameters. Although the sample sizes are relatively small, the results suggest that landforms developed in regions where these rocks dominate can be differentiated solely on the basis of their fractal dimensions (Figure 7.7). Meanwhile, landforms in granite and sand dune regions show high positive correlation while karst and badlands topography shows high negative correlation. These results provide a quantitative confirmation of our visual impression. Karst topography and landforms developed in loess are well known for their extremely rough appearance and high irregularity. On the other hand, granite landforms and sand dunes often appear to display certain levels of order and smoothness.

7.4 Effects of Geological Structure on the Characteristics of Topography

Tectonic processes and the resultant geological structure undoubtedly play a decisive role in shaping the landscapes of certain regions (Twidale, 1971; and Tricart, 1974). Mountain-building processes associated with the convergent plate boundaries contribute to the increase of rate of surface erosion and affect the efficiency of different geomorphological processes. Tectonic shields such as the Canadian Shield, where ancient basement rocks are exposed, are usually flat. Horizontal or gently tilted rock beds are often associated with physiographic plains or plateaus. Of course, the most splendid examples of structural control of landforms are the Basin and Range Province formed by normal faulting and the Ridge and Valley Province in the Appalachian mountains created by folding.

Table 7.2 **FRACTAL DIMENSIONS OF LANDFORMS DEVELOPED IN REGIONS OF DIFFERENT ROCK MATERIALS**

Quadrangle Name	Rock Types	Fractal Dimension	Average Dimension
Barlow, Kentucky	Loess	2.517043	
Horn Lake SW, Mississippi	Loess	2.590327	
Missouri Valley NW, Iowa	Loess	2.618164	2.571279
North Loup, Nebraska	Loess	2.561730	
Wilcox, Washington	Loess	2.569132	
Glamis SE, California	Sand Dune	2.444263	2.444263
Mammoth Cave, Kentucky	Limestone	2.657728	
Park City, Kentucky	Limestone	2.673001	
Rhoda, Kentucky	Limestone	2.681976	2.676545
Smiths Grove, Kentucky	Limestone	2.685213	
Williams, Indiana	Limestone	2.684806	
Atlanta West, Idaho	Granite	2.419224	
Mt. Langley, Carlifornia	Granite	2.265470	2.322591
Priest Lake NE, Idaho	Granite	2.313819	
Yosemite NW, California	Granite	2.291849	

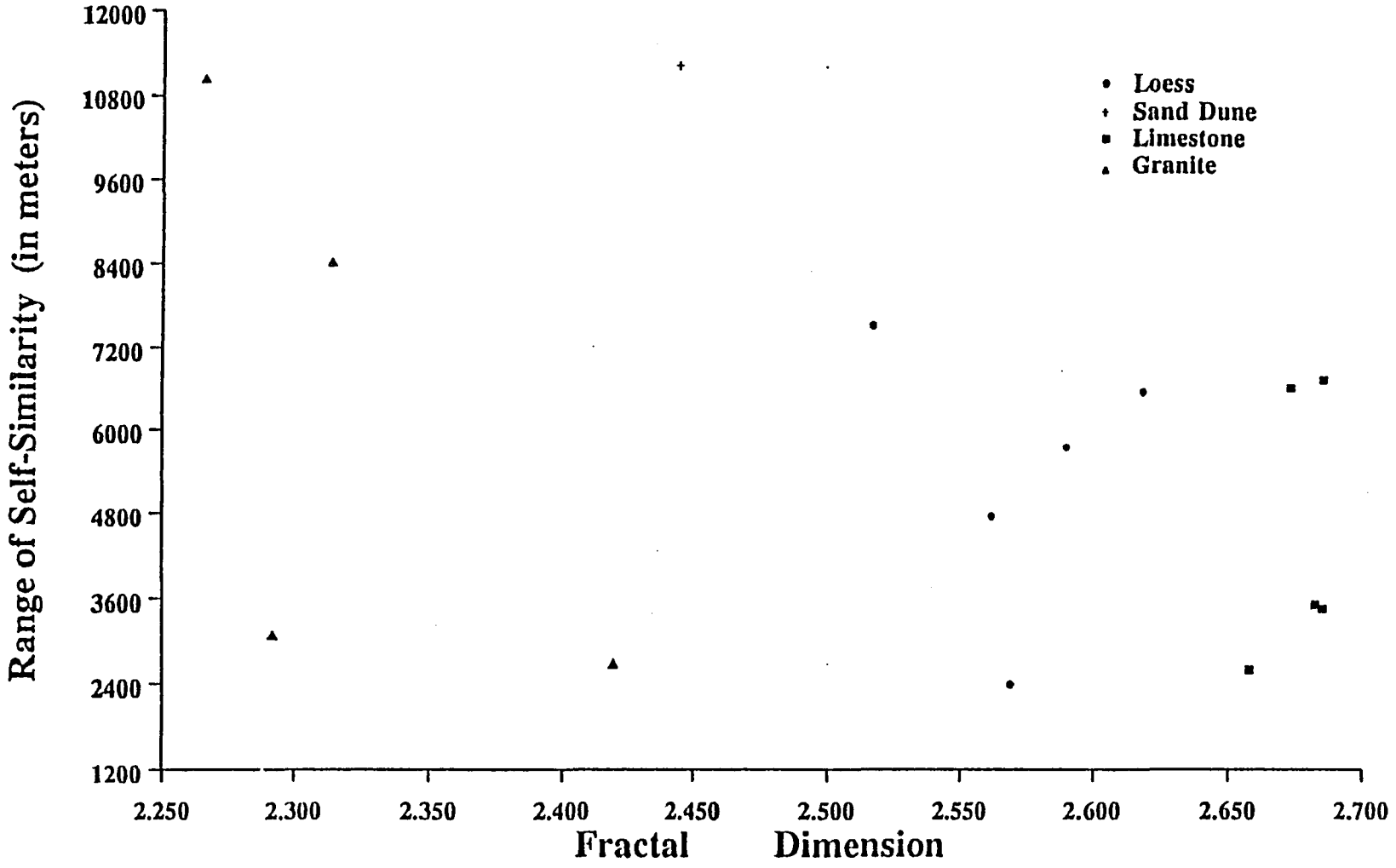

Figure 7.7 Separability of Landforms Developed in Regions of Different Rock Materials

Previously, Clarke (1988) observed that the fractal model seemed to provide a better fit to areas where structural disturbance is minimal. This study has revealed another interesting relationship between the fractal model and geological structure. Figure 7.5 indicates that the fractal dimension of topography seems to be inversely related to the prominence of geological structure. On a broad scale, the Blue Ridge, Basin and Range, and Rocky Mountains Provinces are largely remnants of highly deformed orogenic belts and the most important structural elements in these provinces are close folds and associated thrusts. The DEMs from these provinces have relatively lower fractal dimensions. The rocks in the Appalachian Plateaus, Central Lowland, Colorado Plateaus, New England, and Great Plains Provinces are usually moderately deformed. The DEMs from these provinces have somewhat higher fractal dimensions. The fractal dimensions of DEMs from the Valley and Ridge Province are of the same magnitude although this province has a distinctive pattern of alternating anticlines and synclines. The relatively higher fractal dimensions are probably related to the particular type of folds exposed in this region. The narrow anticlines are separated by the wide-opening flat synclines. The Coastal Plain and Piedmont provinces contain gently tilted or nearly horizontal rock strata. The landforms of these regions tend to have the highest fractal dimension.

The inverse relationship between the numerical value of fractal dimension and the prominence of geological structure is also well displayed at a regional scale between adjacent physiographic provinces with distinctive structural styles. This is best shown in the southeastern provinces of the U. S. The Coastal Plain Province is an elevated sea bottom consisting of relatively recent sedimentary deposits. It has low topographic relief and shows little structural deformation. On the other hand, the rocks in the Piedmont Province are mostly metamorphic with complex structures. Nevertheless, they are generally truncated by the plateau surface. The landforms therefore only locally reflect the rock structures. The Blue Ridge Province in the middle has the highest peaks in the Appalachian Highlands. The rocks in this province include Precambrian

granite and gneiss and other metamorphosed sedimentary and volcanic rocks. To the northwest, the Valley and Ridge Province consists of Paleozoic sedimentary rocks and is world famous for its fold mountains. And finally, the Appalachian Plateaus Province is an elevated tract of nearly horizontal or gently folded strata. Topographically, it is not as deeply dissected as the Valley and Ridge Province. This symmetrical pattern of landforms is clearly shown by the fractal dimensions of these provinces. The Coastal Plain Province has the highest fractal dimension. The D value gradually decreases towards the northwest, reaches the minimum in the highly deformed Blue Ridge Province, and then increases again.

7.5 Effects of the Evolutionary Stage of Landforms on the Characteristics of Topography

For about a hundred years after James Hutton published his **"Theory of the Earth"** in 1795, the subject of geomorphology was largely restricted to non-systematic description of relief forms. Towards the end of last century, William Morris Davis (1899) introduced the historical approach into the study of landforms. His approach helped structure much of the thinking and fact-finding of the nineteenth century into a coherent body of knowledge and provided a systematic framework for organizing geomorphological studies.

The historical approach is embodied in Davis' famous model of the "cycle of erosion", which refers to "*the complete, progressive, and systematic sequence of natural changes or stages in a landscape from the start of its erosion on a newly uplifted or exposed surface through its dissection into mountains and valleys until it has been reduced in the final stage to a low, featureless plain or to a base level (such as sea level) that limits the activity of the agents involved*" (Bates and Jackson, 1987, p.165). Davis proposed his idea in a cursory way in 1889. The fully documented and formulated theory was published in 1899 (Davis, 1899).

Specifically, Davis divided the evolution of landforms into three consecutive stages: the youth, the stage of maturity, and the old age. In the youthful stage, streams cut down the surface rapidly and erode deep valleys which are V-shaped in cross-section. Areas of low relief persist as isolated upland patches. When the landform matures, the whole land mass is dissected into an all-slope topography. Ridges are sharp-crested. A well-integrated drainage system is established. The main streams meander and flood plains begin to appear. The terrain relief has reached its maximum. At the stage of old age, the rivers continue to erode their beds but erosional processes cause the divides to be lowered more rapidly than the river beds. The relief gradually decreases and flood plains widen. The terrain surface changes from one of all-slopes through broadly rounded divides and wide flood plains to a low, flat peneplain.

Although there have been intensive debates among geomorphologists on the reality of the peneplain and the validity of the cyclic pattern of landform evolution and strong criticism on the assumption of an idealized flat surface as an initial state, the general erosional reduction of rapidly elevated structural features has occurred repeatedly in geological time. For example, the Canadian Shield experienced four major mountain-building orogenies between 1,000 and 2,500 million years ago and has been reduced to a low, flat peneplain during the last 1,000 million years. The Appalachian mountains that once stood more than 10 kilometers above sea level now display quite moderate relief. The "evolutionary stages of landforms" is used in this discussion within this quite general framework. "Stages" are time intervals in a progressive sequence of events, each of which corresponds to a particular state of landform development.

For quantifying the effects of the evolutionary stage of landforms, two series of DEMs were selected. These topographic quadrangles were among the one hundred topographic maps assembled by William B. Upton, Jr. (1955) to illustrate a wide variety of well portrayed physiographic features. To isolate the effects of evolutionary stage on landform characteristics, DEMs were selected from areas of uniform

lithology. One series represents an evolutionary sequence of landforms in plateaus and the other series includes DEMs of till plains at different stages. These DEMs are listed in Table 7.3. The fractal dimensions of these two series seem to show a rather consistent pattern. When the landform is at the youth stage, the fractal dimension is relative low. Mature topography tends to have higher dimensions. When landforms reach the old age, their fractal dimension decreases. This general trend conforms well to the traditional model of stream erosion. The original land surface is relatively smooth. Dissection of the terrain by incision, extension and rejuvenation of the drainage network introduces irregularities and creates a land surface of high roughness. After the mature stage, degradational processes gradually become dominant. They tend to smooth the surfaces of the interfluves and fill in irregular ravines. Ideally, in a tectonically stable region, they will eventually create a flat, featureless terrain, which has a fractal dimension of 2. This systematic pattern has also been demonstrated by Culling (1986b).

7.6 The Effects of Climate on the Characteristics of the Land Surface

The effect of climate on landforms is realized largely through its influence on chemical and biological processes. In either arid or cold regions, precipitation provides an inadequate water supply for the weathering and transportation of rocks. In humid climatic regions, where moisture is abundant and temperature remains high, the rates of weathering and erosion increases and chemical processes tend to dominate. Furthermore, climate determines the types and abundance of vegetation in different regions, which also contribute directly or indirectly to the variations of soils and landforms.

Qualitatively, there seems to be a clear connection between climate and landforms, which has led many geomorphologists to define morphoclimatic zones or regions (Budel, 1948, 1977; Troll, 1958; Tanner, 1961; Birot, 1960; Stoddart, 1969; Wilson, 1969; Tricart and Cailleux, 1972; and Chorley et al., 1984). For example, in humid regions shale formations are reduced to low, gently rounded land surfaces; in

Table 7.3 FRACTAL DIMENSIONS OF LANDFORMS AT DIFFERENT EVOLUTIONARY STAGES

Quadrangle Name	Evolutionary Stage	Fractal Dimension	Average Dimension
Double Mill Draw NE, Texas	Young Plateau	2.462423	
Double Mill Draw Nw, Texas	Young Plateau	2.509666	2.487609
Double Mill Draw SE, Texas	Young Plateau	2.451954	
Indio Hill, Texas	Young Plateau	2.526394	
Fort Hood, Texas	Mature Plateau	2.603376	
North Fort Hood, Texas	Mature Plateau	2.496723	2.562856
Post Oak Mountain, Texas	Mature Plateau	2.555372	
Shell Mountains, Texas	Mature Plateau	2.595952	
Forks Ranch, Montana	Old Plateau	2.514480	
Holmes Ranch, Montana	Old Plateau	2.485863	2.506641
Pine Butte School, Montana	Old Plateau	2.519580	
Paxton NW, Illinois	Young Till Plain	2.471906	
Paxton SE, Illinois	Young Till Plain	2.499419	2.491970
Paxton SW, Illinois	Young Till Plain	2.504585	
Harvey, Iowa	Mature Till Plain	2.618893	
Leighton, Iowa	Mature Till Plain	2.649490	2.612910
Pella, Iowa	Mature Till Plain	2.615499	
Peoria, Iowa	Mature Till Plain	2.567757	
Bar C Bar Ranch, New Mexico	Old Plain	2.378287	
Derrick Draw, New Mexico	Old Plain	2.426480	2.421735
Dexter East, New Mexico	Old Plain	2.460439	

arid or semiarid regions they form distinctive badlands. Poorly consolidated sandstone formations in arid environments erode to castellate landforms, whereas in humid environments they are reduced to nondescript, low, rounded mounds. In humid plateaus the valley sides generally are smoothly sloped and mantled with loose debris, but in semiarid plateaus valley sides are usually angular, with cliffs and ledges of bare rock. Still another example of differences in landforms developed on similar structures but in different climates is illustrated by the differences between hogbacks in arid and humid regions. Hogbacks, formed by the eroded upturned edges of resistant formations, commonly produce rough, serrate ridges in arid and semiarid environments. In humid regions similar structures erode to form long, smooth-topped and smooth-sided ridges. In arid and semiarid regions, closely spaced but small washed and gullies are deeply cut into the flanks of the hogbacks, whereas only the main streams disrupt the hogbacks in humid regions (See Hunt, 1974, p.64-66).

The distinctiveness of climatic regions and its possible implications for landform study were first considered by Albrecht Penck in 1883, and he attempted to classify correlations between climatic areas and surface relief in 1910. In the same year, E. de Martonne introduced the term "climatic geomorphology". The awareness of the distinctive impression of different climates on landform led William Morris Davis (1905) to the formulation of an arid cycle of erosion. Today, climatic geomorphology has become a strong tradition in landform analysis (Budel, 1948, 1982; Tricart and Cailleux, 1972; and Derbyshire, 1973, 1976).

The quantification of the effect of climate on landforms is no easy task. First, climate is not a single definable factor, but consists of two variables (temperature and precipitation) which are partially independent but largely inter-related in most complicated patterns. Secondly, the morphological characteristics of terrain surfaces are the composite product of a variety of exogenetic and endogenetic processes. In most cases, it is extremely difficult, if not impossible, to separate the effects of different factors. As a result, the question that to what degree climate determines landforms in different

environments still remains obscure. Pitty (1971, p.60) commented that "*some earlier claims for morphoclimatic subdivisions in geomorphology were over-optimistic, disintegrated on the irregularities of local conditions and configurations, and became confused because of convergences in both forms and processes.*" He pointed out that "*the formulation of more precise statements on morphoclimatic geomorphology, which are not inferences from climatic data, awaits the measurement of forms.*"

Most of the DEMs used in this study were not specifically selected for examining the effects of climate on landform characteristics. However, samples of some broadly similar landforms are distributed in different climatic regions. Thus, attention was directed to a comparison of results for each group of DEMs representing plains, plateaus and mountain systems. However, it is somewhat disappointing to find that the effects of climate on landform characteristics are not clearly reflected in fractal parameters. For example, the average fractal dimension of the Colorado Plateaus (semiarid environment) is virtually identical to that of the Appalachian Plateaus (humid environment). The average D value for the five DEMs of the Colorado Plateaus is 2.56 and the average D value for the Appalachian Plateaus ranges from 2.46 in Delaware County of New York to 2.55 in north central Pennsylvania to 2.59 in eastern Kentucky. Part of the reason for the insensitivity of fractal parameters is probably related to the relatively coarse spatial resolution of the DEMs used in the study. The effects of climate on landforms are realized through its control on the nature of the surface processes operating in a particular environment. The imprints of various surface processes are usually revealed at much larger scales, ranging from meters to millimeters rather than tens to hundreds of meters.

Even if data of adequate resolution becomes available, interpretation of climatic effects from fractal parameters is still complicated by the difficulty of separating the climatic effects from those of other variables such as the change of structure, lithological variation and the stage of landform evolution. For example, the average fractal dimension of DEMs from the Coastal Plain Province (2.68) is much different from that

of the Great Plains Province (2.49). However, it is virtually impossible to tell how much of this difference in D is related to the change of climate or to the variation of structural features.

Two of the DEMs specially chosen for testing the possibility of using fractal parameters to quantify the climatic effects on landform are those of Mount Tom Quadrangle of California (D = 2.36) and Chief Mountain Quadrangle of Montana (D = 2.7). These two quadrangles were also included in the set of topographic maps specially chosen for illustrating certain physiographic features. Specifically, these two maps provide excellent examples of landforms created by Alpine glaciation. However, the fractal dimensions of these DEMs are not much different from the fractal dimensions of other quadrangles in the same physiographic province or other areas which were unaffected by glaciation (see Appendix I). Again, the lack of significant difference is probably a result of inadequate spatial resolution of the data. It is also interesting to note that although glaciation produces visually quite rough surfaces, the D values of both of these DEMs are surprisingly low.

Chapter 8 CONCLUSIONS

Until not too long ago, geomorphological studies had been invariably conducted within one of two distinctive organizing frameworks. Beginning with the "cycle of erosion" of William Morris Davis, most geomorphologists concentrated almost exclusively on the deciphering of temporal patterns of landform evolution for more than half of a century and this tradition still continues today. Since the 1950s, the quantitative revolution in the geosciences has greatly broadened the scope of geomorphology and directed our attention to the revelation of spatial regularities of land form and geomorphological processes. Today, fractal geometry has introduced another new way of thinking, which focuses on the study of regular patterns across scales, both temporal and spatial.

Although terrain features were used extensively in the development of fractal geometry and terrain scientists have made widespread use of fractal concepts and techniques in their research during the last ten years, many fundamental questions remain unanswered concerning the degree of symmetry of terrain features across scales and their implications on the generating processes of such symmetry. The present study was designed to address some of these important questions. The analysis of the results of this study has led to the following conclusions:

(1) Although fractal geometry has been extremely fruitful in the studies of chaotic dynamic systems and turbulence, its use in characterizing and modelling land surface topography and ocean floor bathymetry has produced some quite mixed results. On the one hand, none of the one hundred ninety-one DEMs analyzed in the present study is truly self-similar. Specifically, they are only self-similar either within limited scale ranges or in certain direction(s). On the other hand, six of the DEMs are self-similar up to the maximum length of the quadrangle map in both the E-W and N-S directions and also when all data pairs in the E-W, N-S, NW-SE, and NE-SW directions are combined together. In addition, forty-eight DEMs show self-similarity up to the maximum length of the map at least in one direction.

(2) Mandelbrot (1983) stated that fractal dimensions around 2.2 produced the most realistic synthetic topography. On the other hand, studies by some geophysicists (Balmino et al., 1973; Bell, 1975, 1979; Turcotte, 1987; and Mareschal, 1989) suggested that both topography and bathymetry could be well modelled by a fractional Brownian motion with a D value of about 2.5. However, the results of this study display much greater variability in the complexity of terrain features, concurring with Mark and Aronson (1984) and a number of other early studies. The lowest fractal dimension obtained in this study is 2.22 for the Mt. Tobin NE Quadrangle of Nevada and the highest fractal dimension is 2.83 for the Coharie SW Quadrangle of North Carolina. When the fractal dimensions of all DEMs are averaged, a mean D value of 2.50 is obtained. Thus, a D = 2.2 only represents the lower end of the results obtained in this study and a D value of 2.5 merely represents the mean condition of terrain surface morphology.

(3) Some earlier studies (Fox and Hayes, 1985; and Klinkenberg, 1988) have indicated that it is possible to use fractal parameters as discriminators for separating different physiographic regions. The results from the present study seem to lend additional support to their finding. It was found that most DEMs from the mountain regions can be easily separated from those of plains or plateaus. At the province level, although each physiographic province does not possess a unique "signature", the fractal parameters for adjacent provinces do differ significantly. Some exceptions were found. However, these exceptions were expected considering that the separation of different provinces on Fenneman's map was largely based on non-morphological criteria and the placement of many boundaries was admitted to be quite arbitrary. In addition, topography clearly does not display the strict self-similarity and homogeneity as required by the mathematical model. At the scale represented by the 1:24,000 USGS topographic maps which were used in this study, the juxtaposition of inhomogeneous patches of terrain surfaces are expected to be reflected in the fractal parameters of certain DEMs.

(4) The present study also shows that the fractal parameters can be used to quantify the effects of different geomorphological factors on the geometrical characteristics of land surfaces. The fractal dimensions of landforms developed in granite, limestone, loess, and sand dune were found to differ significantly from each other. The numerical value of the fractal dimension also appears to be closely related to the stage of landform evolution. At the young stage, land surfaces are relatively smooth and thus have low fractal dimensions. As landforms reach the mature stage, surfaces become increasingly rough, giving higher fractal dimensions. When a certain region is reduced to a featureless terrain as a result of prolonged stream erosion, the fractal dimension will approach 2. Furthermore, the fractal dimensions of the Appalachian provinces seem to reveal an inverse relationship to the level of structural disturbances in these regions.

(5) Among the three methods tested (the variogram method, the box-counting method and the walking dividers method), the variogram method is the most suitable method for estimating the fractal dimension of topographic profiles or surfaces. The box-counting method also produces satisfactory results when careful consideration is given to the selection of the maximum cell size, contour interval and the minimum r-squared value. The walking dividers method, originally developed for use with self-similar fractals, is the least reliable and the most time-consuming method when used for estimating the fractal dimension of self-affine topographic profiles.

It should be emphasized that some of the conclusions reached in this study are preliminary and need to be substantiated by further research. Particularly, the potential of fractal parameters in delineating physiographic provinces and revealing spatial patterns of surface processes is still largely unknown. The number of DEMs used in this study, although quite large comparing to the earlier studies and adequate for answering the other questions addressed here, is far from sufficient to yield a definite answer to this particular question. Examination of DEMs of a much broader and contiguous region is required, which was not possible for this study due to the limited availability of DEMs.

It should also be noted that despite the phenomenal proliferation of fractal-based terrain studies, our understanding of the true value of fractal geometry to terrain research is still quite rudimentary. Many fundamental issues remain virtually untouched. Most importantly, we need to go beyond the stage of geometrical description and conduct inference from landform to the underlying geomorphological processes. The quantitative study of the effects of geomorphological variables on the morphological characteristics of terrain surface as described in Chapter 7 is only a first step towards this direction. It is expected that such interpretation inevitably becomes incalculably more difficult and controversial because the processes may be manifold, multifaceted, complex, and rapidly changing. However, only through such thought-provoking interpretation can we truly reach a higher level of understanding of complex geomorphic systems. In identifying directions for future fractal research, Kadanoff (1986, p.7) commented, "*Further progress in this field depends upon establishing a more substantial theoretical base in which geometrical form is deduced from the mechanisms that produce it. Without such a theoretical underpinning much of the work on fractals seems somewhat superficial and even slightly pointless. It is easy, too easy, to perform computer simulations upon all kinds of models and to compare the results with each other and with real-world outcomes. But without organizing principles, the field tends to decay into a zoology of interesting specimens and facile classifications.*" His comments certainly apply to the fractal study of terrain features.

Appendix I FRACTAL PARAMETERS ESTIMATED BY THE VARIOGRAM METHOD

PHYSIOGRAPHIC PROVINCE	NAME OF TOPO QUAD	DIRECTION	SCALE RANGE	FRACTAL DIMENSION	R-SQUARED
Coastal Plain	Barbara, MS	E-W	268 pixels	2.544725	0.984498
		N-S	317 pixels	2.530912	0.983248
		EW+NS	293 pixels	2.544663	0.986688
		NW-SE	56 pixels	2.707525	0.961716
		NE-SW	192 pixels	2.486401	0.981697
		Combined	272 pixels	2.574447	0.989171
	Barlow, KY	E-W	333 pixels	2.438161	0.980885
		N-S	234 pixels	2.586591	0.967009
		EW+NS	360 pixels	2.485946	0.986328
		NW-SE	252 pixels	2.419487	0.982615
		NE-SW	143 pixels	2.632633	0.955590
		Combined	251 pixels	2.517043	0.990103
	Coharie NW, NC	E-W	28 pixels	2.733168	0.896185
		N-S	71 pixels	2.804807	0.885311
		EW+NS	58 pixels	2.792135	0.883461
		NW-SE	30 pixels	2.788509	0.907581
		NE-SW	44 pixels	2.811104	0.910087
		Combined	61 pixels	2.816281	0.890953
	Coharie SE, NC	E-W	108 pixels	2.790332	0.926676
		N-S	69 pixels	2.786751	0.903530
		EW+NS	109 pixels	2.803285	0.913712
		NW-SE	57 pixels	2.791440	0.950603
		NE-SW	80 pixels	2.805545	0.941520
		Combined	177 pixels	2.815371	0.954209
	Coharie SW, NC	E-W	28 pixels	2.724180	0.888626
		N-S	59 pixels	2.801893	0.866644
		EW+NS	59 pixels	2.802920	0.844778
		NW-SE	45 pixels	2.815959	0.891073
		NE-SW	37 pixels	2.811218	0.872365
		Combined	179 pixels	2.826847	0.937357
	Dobbersville, NC	E-W	37 pixels	2.757820	0.862930
		N-S	44 pixels	2.760840	0.897188
		EW+NS	44 pixels	2.768496	0.874013
		NW-SE	44 pixels	2.808526	0.889566
		NE-SW	45 pixels	2.805499	0.897956
		combined	44 pixels	2.790687	0.885851
	Faison, NC	E-W	60 pixels	2.776561	0.900046
		N-S	44 pixels	2.758260	0.926398
		EW+NS	59 pixels	2.778064	0.907800
		NW-SE	43 pixels	2.801036	0.916207
		NE-SW	57 pixels	2.794084	0.944425
		combined	59 pixels	2.796968	0.915942
	Grantham, NC	E-W	366 pixels	2.351237	0.993364
		N-S	172 pixels	2.375105	0.993834
		EW+NS	179 pixels	2.376015	0.995140
		NW-SE	151 pixels	2.372061	0.992673
		NE-SW	190 pixels	2.380771	0.994641
		combined	171 pixels	2.390399	0.994037
	Horn Lake SW, MS	E-W	193 pixels	2.545034	0.990244
		N-S	250 pixels	2.669890	0.983960
		EW+NS	193 pixels	2.550430	0.988692
		NW-SE	147 pixels	2.551420	0.996357

Appendix I continued

PHYSIOGRAPHIC PROVINCE	NAME OF TOPO QUAD	DIRECTION	SCALE RANGE	FRACTAL DIMENSION	R-SQUARED
Coastal Plain		NE-SW	229 pixels	2.557723	0.974126
		combined	192 pixels	2.590327	0.993864
	Newton Grove North, NC	E-W	141 pixels	2.669965	0.918034
		N-S	288 pixels	2.548092	0.982460
		EW+NS	288 pixels	2.610931	0.980741
		NW-SE	192 pixels	2.623940	0.983492
		NE-SW	160 pixels	2.639996	0.979967
		combined	270 pixels	2.636354	0.984520
Piedmont	Calahaln, NC	E-W	147 pixels	2.604290	0.984428
		N-S	193 pixels	2.611856	0.990739
		EW+NS	164 pixels	2.611465	0.987150
		NW-SE	184 pixels	2.687293	0.972144
		NE-SW	79 pixels	2.599940	0.973362
		combined	180 pixels	2.667932	0.971759
	Central, NC	E-W	256 pixels	2.568257	0.985380
		N-S	325 pixels	2.427024	0.956363
		EW+NS	327 pixels	2.476842	0.972201
		NW-SE	368 pixels	2.308797	0.954777
		NE-SW	104 pixels	2.681907	0.890188
		combined	345 pixels	2.481489	0.976769
	Church Road, VA	E-W	159 pixels	2.696661	0.974077
		N-S	267 pixels	2.649949	0.988272
		EW+NS	163 pixels	2.676606	0.988344
		NW-SE	80 pixels	2.649054	0.980887
		NE-SW	171 pixels	2.714625	0.987545
		combined	163 pixels	2.701751	0.983259
	Cleveland, NC	E-W	197 pixels	2.688391	0.972517
		N-S	54 pixels	2.564049	0.987900
		EW+NS	65 pixels	2.608724	0.975361
		NW-SE	42 pixels	2.578401	0.977839
		NE-SW	121 pixels	2.674110	0.993780
		combined	58 pixels	2.624096	0.974766
	Cool Springs, NC	E-W	350 pixels	2.658882	0.967512
		N-S	111 pixels	2.616652	0.983615
		EW+NS	255 pixels	2.713145	0.950208
		NW-SE	119 pixels	2.661006	0.977731
		NE-SW	210 pixels	2.680001	0.987537
		combined	212 pixels	2.712638	0.957160
	Harmony, NC	E-W	61 pixels	2.606672	0.958060
		N-S	319 pixels	2.588964	0.984971
		EW+NS	374 pixels	2.658544	0.972411
		NW-SE	200 pixels	2.654228	0.934837
		NE-SW	99 pixels	2.679154	0.955161
		combined	199 pixels	2.679467	0.970904
	Shepherds, NC	E-W	52 pixels	2.613641	0.952671
		N-S	289 pixels	2.601191	0.989657
		EW+NS	297 pixels	2.659848	0.975796
		NW-SE	43 pixels	2.617631	0.963022
		NE-SW	269 pixels	2.553927	0.967361
		combined	233 pixels	2.661150	0.975233
	Statesville East, NC	E-W	243 pixels	2.682268	0.983276
		N-S	109 pixels	2.608863	0.969816
		EW+NS	169 pixels	2.677521	0.952403
		NW-SE	77 pixels	2.636823	0.982391

Appendix I continued

PHYSIOGRAPHIC PROVINCE	NAME OF TOPO QUAD	DIRECTION	SCALE RANGE	FRACTAL DIMENSION	R-SQUARED
Piedmont		NE-SW	77 pixels	2.644031	0.971108
		combined	115 pixels	2.667694	0.959599
	Statesville West, NC	E-W	333 pixels	2.661187	0.982183
		N-S	55 pixels	2.613578	0.961461
		EW+NS	129 pixels	2.701320	0.943193
		NW-SE	59 pixels	2.693874	0.955186
		NE-SW	46 pixels	2.632080	0.973056
		combined	133 pixels	2.733970	0.925321
	Troutman, NC	E-W	72 pixels	2.659759	0.941564
		N-S	241 pixels	2.668042	0.989203
		EW+NS	345 pixels	2.734364	0.959725
		NW-SE	61 pixels	2.713139	0.918871
		NE-SW	178 pixels	2.685169	0.980731
		combined	225 pixels	2.736739	0.959021
Blue Ridge	Prentiss, NC	E-W	327 pixels	2.313992	0.993374
		N-S	337 pixels	2.416161	0.992822
		EW+NS	331 pixels	2.354272	0.994100
		NW-SE	117 pixels	2.534249	0.950057
		NE-SW	368 pixels	2.320515	0.989847
		combined	328 pixels	2.385873	0.995199
	Shining Rock, NC	E-W	349 pixels	2.332439	0.993254
		N-S	292 pixels	2.419205	0.992498
		EW+NS	342 pixels	2.370201	0.994506
		NW-SE	328 pixels	2.280155	0.996367
		NE-SW	158 pixels	2.562620	0.956770
		combined	333 pixels	2.387528	0.996230
	Mt. Le Conte, TN	E-W	155 pixels	2.345248	0.988718
		N-S	344 pixels	2.196148	0.996580
		EW+NS	344 pixels	2.287077	0.997911
		NW-SE	192 pixels	2.282963	0.996114
		NE-SW	256 pixels	2.271121	0.993193
		combined	346 pixels	2.329189	0.993438
	Smokemont, NC	E-W	184 pixels	2.498460	0.929680
		N-S	312 pixels	2.465127	0.977731
		EW+NS	367 pixels	2.534819	0.951119
		NW-SE	265 pixels	2.579513	0.913752
		NE-SW	156 pixels	2.457420	0.971382
		combined	185 pixels	2.500842	0.949446
Valley & Ridge	Aughwick, PA	E-W	64 pixels	2.253597	0.981809
		N-S	91 pixels	2.268108	0.982798
		EW+NS	74 pixels	2.266378	0.980206
		NW-SE	37 pixels	2.256029	0.981910
		NE-SW	199 pixels	2.298243	0.995875
		combined	102 pixels	2.448028	0.911221
	Baker, WV	E-W	118 pixels	2.415406	0.967228
		N-S	275 pixels	2.520759	0.926482
		EW+NS	133 pixels	2.420047	0.966408
		NW-SE	65 pixels	2.405742	0.970217
		NE-SW	118 pixels	2.430497	0.991084
		combined	185 pixels	2.544311	0.917553
	Blain, PA	E-W	190 pixels	2.492431	0.895877
		N-S	257 pixels	2.525855	0.914931
		EW+NS	258 pixels	2.540220	0.896181
		NW-SE	42 pixels	2.326609	0.963807

Appendix I continued

PHYSIOGRAPHIC PROVINCE	NAME OF TOPO QUAD	DIRECTION	SCALE RANGE	FRACTAL DIMENSION	R-SQUARED
Valley & Ridge		NE-SW	340 pixels	2.241555	0.956786
		combined	176 pixels	2.515503	0.927609
	Blair Mills, PA	E-W	79 pixels	2.350655	0.967917
		N-S	78 pixels	2.344319	0.972432
		EW+NS	78 pixels	2.346054	0.970684
		NW-SE	42 pixels	2.360567	0.964822
		NE-SW	130 pixels	2.594780	0.899817
		combined	89 pixels	2.457982	0.936931
	Burem, TN	E-W	55 pixels	2.491400	0.952081
		N-S	150 pixels	2.631239	0.932865
		EW+NS	164 pixels	2.662728	0.888641
		NW-SE	60 pixels	2.614071	0.902937
		NE-SW	115 pixels	2.650090	0.950790
		combined	123 pixels	2.659285	0.904905
	Camelot, TN	E-W	91 pixels	2.453144	0.947878
		N-S	140 pixels	2.584924	0.851365
		EW+NS	94 pixels	2.487415	0.917303
		NW-SE	32 pixels	2.381232	0.956804
		NE-SW	170 pixels	2.501735	0.981292
		combined	89 pixels	2.522867	0.923261
	Duffield, VA	E-W	96 pixels	2.457200	0.970258
		N-S	137 pixels	2.527891	0.934212
		EW+NS	108 pixels	2.482490	0.957582
		NW-SE	80 pixels	2.494059	0.951385
		NE-SW	139 pixels	2.552059	0.972461
		combined	98 pixels	2.504954	0.956658
	Kyles Ford, VA	E-W	88 pixels	2.489137	0.945426
		N-S	46 pixels	2.415601	0.945070
		EW+NS	101 pixels	2.557185	0.894322
		NW-SE	31 pixels	2.428481	0.941507
		NE-SW	72 pixels	2.566362	0.927568
		combined	136 pixels	2.655738	0.846796
	Looneys Gap, TN	E-W	61 pixels	2.435776	0.961100
		N-S	32 pixels	2.346438	0.967970
		EW+NS	39 pixels	2.384990	0.960470
		NW-SE	21 pixels	2.355221	0.967870
		NE-SW	70 pixels	2.504535	0.974852
		combined	59 pixels	2.541892	0.900055
	McCoysville, PA	E-W	340 pixels	2.450552	0.985266
		N-S	340 pixels	2.469097	0.952524
		EW+NS	340 pixels	2.460292	0.971027
		NW-SE	198 pixels	2.505632	0.984508
		NE-SW	62 pixels	2.440013	0.975462
		combined	340 pixels	2.492268	0.969877
	Plum Grove, VA	E-W	62 pixels	2.407000	0.973629
		N-S	32 pixels	2.346909	0.967395
		EW+NS	75 pixels	2.528612	0.889745
		NW-SE	21 pixels	2.350549	0.971142
		NE-SW	65 pixels	2.493130	0.973831
		combined	56 pixels	2.523866	0.909874
	Rio, WV	E-W	119 pixels	2.379131	0.973926
		N-S	233 pixels	2.399764	0.985068
		EW+NS	159 pixels	2.409142	0.971121
		NW-SE	75 pixels	2.362912	0.980608

Appendix I continued

PHYSIOGRAPHIC PROVINCE	NAME OF TOPO QUAD	DIRECTION	SCALE RANGE	FRACTAL DIMENSION	R-SQUARED
Valley & Ridge		NE-SW	238 pixels	2.478532	0.982785
		combined	173 pixels	2.496607	0.929766
	Stickleyville, VA	E-W	173 pixels	2.451538	0.959330
		N-S	77 pixels	2.441429	0.909700
		EW+NS	183 pixels	2.559569	0.892811
		NW-SE	55 pixels	2.437019	0.928905
		NE-SW	145 pixels	2.490468	0.947507
		combined	176 pixels	2.590249	0.882634
	Stony Point, TN	E-W	67 pixels	2.401638	0.940281
		N-S	91 pixels	2.526380	0.882259
		EW+NS	124 pixels	2.564928	0.862999
		NW-SE	53 pixels	2.535767	0.885704
		NE-SW	91 pixels	2.483774	0.982421
		combined	56 pixels	2.463589	0.935202
	Wardensville, WV	E-W	231 pixels	2.478457	0.926292
		N-S	340 pixels	2.423500	0.971344
		EW+NS	295 pixels	2.464702	0.951448
		NW-SE	167 pixels	2.422396	0.966273
		NE-SW	88 pixels	2.457161	0.974875
		combined	275 pixels	2.489025	0.959023
	Yellow Springs, WV	E-W	115 pixels	2.429823	0.959396
		N-S	186 pixels	2.450904	0.960059
		EW+NS	132 pixels	2.431438	0.962614
		NW-SE	82 pixels	2.460747	0.954211
		NE-SW	217 pixels	2.403937	0.994082
		combined	145 pixels	2.488072	0.952132
Appalachian Plateaus	Arena, NY	E-W	262 pixels	2.515230	0.949763
		N-S	89 pixels	2.303323	0.957792
		EW+NS	215 pixels	2.505850	0.908580
		NW-SE	259 pixels	2.395975	0.969836
		NE-SW	63 pixels	2.347351	0.946597
		combined	241 pixels	2.543905	0.910480
	Broad Bottom, KY	E-W	35 pixels	2.476893	0.903439
		N-S	46 pixels	2.521064	0.875500
		EW+NS	37 pixels	2.478128	0.902758
		NW-SE	27 pixels	2.535222	0.876822
		NE-SW	125 pixels	2.734069	0.794276
		combined	50 pixels	2.610431	0.823306
	Cameron, PA	E-W	117 pixels	2.500232	0.905078
		N-S	60 pixels	2.477758	0.892133
		EW+NS	134 pixels	2.576728	0.866735
		NW-SE	163 pixels	2.633038	0.885277
		NE-SW	138 pixels	2.661806	0.817403
		combined	138 pixels	2.616137	0.859979
	Downsville, NY	E-W	65 pixels	2.352863	0.939845
		N-S	153 pixels	2.430144	0.935261
		EW+NS	149 pixels	2.485399	0.900472
		NW-SE	138 pixels	2.476495	0.948137
		NE-SW	138 pixels	2.515244	0.927247
		combined	140 pixels	2.494388	0.924046
	Emporium, PA	E-W	68 pixels	2.455302	0.922095
		N-S	84 pixels	2.555065	0.876178
		EW+NS	85 pixels	2.530193	0.886261
		NW-SE	59 pixels	2.557332	0.881840

Appendix I continued

PHYSIOGRAPHIC PROVINCE	NAME OF TOPO QUAD	DIRECTION	SCALE RANGE	FRACTAL DIMENSION	R-SQUARED
Appalachian Plateaus		NE-SW	42 pixels	2.474656	0.915222
		combined	125 pixels	2.638880	0.846356
	Fayetteville, WV	E-W	239 pixels	2.579559	0.919604
		N-S	84 pixels	2.457745	0.926230
		EW+NS	245 pixels	2.609877	0.892171
		NW-SE	229 pixels	2.568931	0.958768
		NE-SW	84 pixels	2.542444	0.884049
		combined	246 pixels	2.648976	0.878899
	First Fork, PA	E-W	158 pixels	2.510574	0.932847
		N-S	94 pixels	2.522579	0.895946
		EW+NS	156 pixels	2.549190	0.912193
		NW-SE	103 pixels	2.585677	0.903468
		NE-SW	116 pixels	2.522240	0.940986
		combined	155 pixels	2.579570	0.912949
	Fishs Eddy, NY	E-W	335 pixels	2.615972	0.905874
		N-S	93 pixels	2.385612	0.963186
		EW+NS	127 pixels	2.491366	0.917313
		NW-SE	95 pixels	2.513713	0.928483
		NE-SW	53 pixels	2.402293	0.957461
		combined	241 pixels	2.665083	0.811885
	Fleischmanns, NY	E-W	59 pixels	2.259963	0.968978
		N-S	86 pixels	2.310111	0.960967
		EW+NS	67 pixels	2.278830	0.965800
		NW-SE	39 pixels	2.260730	0.968506
		NE-SW	74 pixels	2.349798	0.961876
		combined	65 pixels	2.339897	0.947168
	Hancock, PA-NY	E-W	50 pixels	2.291186	0.957686
		N-S	132 pixels	2.454280	0.942873
		EW+NS	156 pixels	2.562541	0.846062
		NW-SE	97 pixels	2.521271	0.889598
		NE-SW	56 pixels	2.428288	0.897547
		combined	149 pixels	2.603619	0.817954
	Harold, KY	E-W	67 pixels	2.566292	0.876295
		N-S	108 pixels	2.691707	0.759781
		EW+NS	90 pixels	2.643500	0.809792
		NW-SE	57 pixels	2.645920	0.820615
		NE-SW	58 pixels	2.623037	0.846489
		combined	59 pixels	2.606980	0.848463
	Horton, NY	E-W	80 pixels	2.434305	0.913043
		N-S	94 pixels	2.393729	0.918160
		EW+NS	84 pixels	2.401076	0.924963
		NW-SE	107 pixels	2.546449	0.891829
		NE-SW	47 pixels	2.344949	0.946998
		combined	144 pixels	2.599280	0.802926
	Hunter, NY	E-W	271 pixels	2.448305	0.970878
		N-S	202 pixels	2.399799	0.962084
		EW+NS	219 pixels	2.424838	0.963433
		NW-SE	70 pixels	2.424372	0.933373
		NE-SW	95 pixels	2.306887	0.979545
		combined	304 pixels	2.527658	0.935178
	Keating Summit, PA	E-W	220 pixels	2.706618	0.823186
		N-S	173 pixels	2.629558	0.885169
		EW+NS	175 pixels	2.663207	0.849645
		NW-SE	80 pixels	2.640422	0.851242

Appendix I continued

PHYSIOGRAPHIC PROVINCE	NAME OF TOPO QUAD	DIRECTION	SCALE RANGE	FRACTAL DIMENSION	R-SQUARED
Appalachian Plateaus		NE-SW	34 pixels	2.451164	0.917091
		combined	183 pixels	2.706861	0.860651
	Lancer, KY	E-W	42 pixels	2.541983	0.856844
		N-S	41 pixels	2.503853	0.876936
		EW+NS	41 pixels	2.520328	0.869317
		NW-SE	34 pixels	2.584938	0.841544
		NE-SW	42 pixels	2.608346	0.828311
		combined	42 pixels	2.581317	0.842543
	Lee Fire Tower, PA	E-W	171 pixels	2.605605	0.887736
		N-S	136 pixels	2.599321	0.900913
		EW+NS	168 pixels	2.615710	0.890045
		NW-SE	90 pixels	2.583601	0.921554
		NE-SW	102 pixels	2.643914	0.844825
		combined	137 pixels	2.634604	0.878559
	Lewbeach, NY	E-W	93 pixels	2.392088	0.944011
		N-S	218 pixels	2.485238	0.925658
		EW+NS	247 pixels	2.564441	0.868368
		NW-SE	188 pixels	2.500487	0.939122
		NE-SW	39 pixels	2.289272	0.970555
		combined	217 pixels	2.572148	0.882351
	Lexington, NY	E-W	294 pixels	2.545279	0.953134
		N-S	86 pixels	2.235787	0.978876
		EW+NS	92 pixels	2.325897	0.965447
		NW-SE	128 pixels	2.391635	0.974071
		NE-SW	70 pixels	2.308310	0.966912
		combined	88 pixels	2.348463	0.962086
	Livingston Manor, NY	E-W	214 pixels	2.508964	0.950258
		N-S	110 pixels	2.405022	0.937042
		EW+NS	218 pixels	2.540811	0.908306
		NW-SE	84 pixels	2.445033	0.935361
		NE-SW	230 pixels	2.462406	0.979868
		combined	216 pixels	2.348463	0.962086
	Long Eddy, PA	E-W	50 pixels	2.333289	0.951862
		N-S	79 pixels	2.402059	0.929584
		EW+NS	147 pixels	2.569539	0.840741
		NW-SE	92 pixels	2.524329	0.902440
		NE-SW	39 pixels	2.347588	0.952658
		combined	141 pixels	2.611653	0.813663
	Margaretville, NY	E-W	70 pixels	2.295133	0.953511
		N-S	148 pixels	2.440444	0.919293
		EW+NS	147 pixels	2.469010	0.891045
		NW-SE	128 pixels	2.443887	0.933891
		NE-SW	98 pixels	2.493704	0.891308
		combined	152 pixels	2.512637	0.886815
	Marshlands, PA	E-W	118 pixels	2.592831	0.837194
		N-S	221 pixels	2.567728	0.952357
		EW+NS	188 pixels	2.611608	0.895148
		NW-SE	168 pixels	2.600940	0.948990
		NE-SW	115 pixels	2.606453	0.890722
		combined	172 pixels	2.623529	0.906503
	Martin, KY	E-W	58 pixels	2.613643	0.796425
		N-S	86 pixels	2.653530	0.781377
		EW+NS	86 pixels	2.673188	0.757502
		NW-SE	89 pixels	2.711346	0.805820

Appendix I continued

PHYSIOGRAPHIC PROVINCE	NAME OF TOPO QUAD	DIRECTION	SCALE RANGE	FRACTAL DIMENSION	R-SQUARED
Appalachian Plateaus		NE-SW	24 pixels	2.484514	0.896386
		combined	90 pixels	2.719310	0.736138
	Mc Dowell, KY	E-W	36 pixels	2.417407	0.927882
		N-S	49 pixels	2.515788	0.864816
		EW+NS	104 pixels	2.675941	0.745490
		NW-SE	27 pixels	2.468270	0.915003
		NE-SW	24 pixels	2.407318	0.942118
		combined	117 pixels	2.725795	0.726590
	Pikeville, KY	E-W	34 pixels	2.445423	0.901817
		N-S	67 pixels	2.573738	0.843108
		EW+NS	68 pixels	2.595703	0.821165
		NW-SE	52 pixels	2.641200	0.797254
		NE-SW	281 pixels	2.635580	0.895616
		combined	66 pixels	2.635445	0.808297
	Prestonburg, KY	E-W	53 pixels	2.612628	0.810926
		N-S	57 pixels	2.610044	0.800679
		EW+NS	56 pixels	2.615581	0.802663
		NW-SE	47 pixels	2.658896	0.801430
		NE-SW	58 pixels	2.688323	0.800643
		combined	55 pixels	2.654847	0.798118
	Roscoe, NY	E-W	66 pixels	2.348458	0.941199
		N-S	126 pixels	2.400272	0.946544
		EW+NS	120 pixels	2.461213	0.897831
		NW-SE	47 pixels	2.343094	0.953184
		NE-SW	140 pixels	2.538914	0.890073
		combined	158 pixels	2.560974	0.860179
	Seager, NY	E-W	113 pixels	2.342184	0.965104
		N-S	170 pixels	2.469897	0.914100
		EW+NS	139 pixels	2.408726	0.938438
		NW-SE	152 pixels	2.405986	0.981613
		NE-SW	78 pixels	2.370377	0.939043
		combined	133 pixels	2.437154	0.938119
	Thomas, KY	E-W	48 pixels	2.590596	0.822622
		N-S	151 pixels	2.757004	0.706689
		EW+NS	51 pixels	2.588797	0.827928
		NW-SE	21 pixels	2.492151	0.892865
		NE-SW	39 pixels	2.619437	0.818248
		combined	72 pixels	2.707685	0.739281
	Wayland, KY	E-W	55 pixels	2.484526	0.874279
		N-S	64 pixels	2.531012	0.859056
		EW+NS	62 pixels	2.520259	0.857755
		NW-SE	58 pixels	2.618847	0.806640
		NE-SW	44 pixels	2.526220	0.869240
		combined	66 pixels	2.590641	0.825243
	West Kill, NY	E-W	117 pixels	2.319724	0.964924
		N-S	171 pixels	2.463720	0.920651
		EW+NS	120 pixels	2.354823	0.957799
		NW-SE	113 pixels	2.455139	0.940502
		NE-SW	141 pixels	2.435510	0.929018
		combined	123 pixels	2.410167	0.945203
	Wharton, PA	E-W	93 pixels	2.510376	0.898005
		N-S	116 pixels	2.557755	0.889538
		EW+NS	101 pixels	2.531503	0.892191
		NW-SE	144 pixels	2.653876	0.869586

Appendix I continued

PHYSIOGRAPHIC PROVINCE	NAME OF TOPO QUAD	DIRECTION	SCALE RANGE	FRACTAL DIMENSION	R-SQUARED
Appalachian Plateaus	Whitwell, TN	NE-SW	62 pixels	2.519403	0.909734
		combined	139 pixels	2.637758	0.840310
		E-W	129 pixels	2.337968	0.962523
		N-S	345 pixels	2.435406	0.973701
		EW+NS	146 pixels	2.359123	0.964546
		NW-SE	149 pixels	2.409713	0.930230
		NE-SW	189 pixels	2.429331	0.976605
		combined	204 pixels	2.466179	0.920177
New England	Chatham, NJ	E-W	166 pixels	2.540143	0.929745
		N-S	91 pixels	2.485297	0.933787
		EW+NS	101 pixels	2.487774	0.938983
		NW-SE	58 pixels	2.505235	0.931170
		NE-SW	232 pixels	2.639464	0.940416
		combined	110 pixels	2.567486	0.908899
	Hancock, MA	E-W	93 pixels	2.287506	0.972018
		N-S	284 pixels	2.485500	0.963273
		EW+NS	98 pixels	2.336096	0.966303
		NW-SE	69 pixels	2.293528	0.971097
		NE-SW	127 pixels	2.388651	0.973041
		combined	89 pixels	2.341396	0.968638
	Lyndonville SE, VT	E-W	315 pixels	2.460079	0.973417
		N-S	146 pixels	2.359728	0.979396
		EW+NS	208 pixels	2.424529	0.966921
		NW-SE	291 pixels	2.351531	0.986743
		NE-SW	84 pixels	2.381633	0.969982
		combined	315 pixels	2.545858	0.934624
	Pound Ridge, CT	E-W	106 pixels	2.575955	0.911604
		N-S	301 pixels	2.498117	0.964704
		EW+NS	301 pixels	2.603318	0.937225
		NW-SE	193 pixels	2.636676	0.950720
		NE-SW	116 pixels	2.559197	0.977265
		combined	134 pixels	2.607129	0.942144
	Roselle, NJ	E-W	342 pixels	2.495613	0.969142
		N-S	325 pixels	2.464241	0.978918
		EW+NS	348 pixels	2.481237	0.976005
		NW-SE	186 pixels	2.484624	0.971089
		NE-SW	106 pixels	2.373275	0.996598
		combined	348 pixels	2.527788	0.963573
Interior Low Plateaus	Mammoth Cave, KY	E-W	50 pixels	2.540269	0.909492
		N-S	93 pixels	2.598240	0.880730
		EW+NS	101 pixels	2.636568	0.860841
		NW-SE	62 pixels	2.629873	0.880351
		NE-SW	46 pixels	2.594002	0.883748
		combined	87 pixels	2.657728	0.853100
	Park City, KY	E-W	62 pixels	2.546489	0.906119
		N-S	177 pixels	2.616731	0.918696
		EW+NS	139 pixels	2.622010	0.905287
		NW-SE	219 pixels	2.607345	0.961956
		NE-SW	120 pixels	2.611580	0.941694
		combined	221 pixels	2.673001	0.920048
	Rhoda, KY	E-W	83 pixels	2.586409	0.908287
		N-S	40 pixels	2.428249	0.934775
		EW+NS	99 pixels	2.619436	0.862919
		NW-SE	36 pixels	2.530827	0.908161

Appendix I continued

PHYSIOGRAPHIC PROVINCE	NAME OF TOPO QUAD	DIRECTION	SCALE RANGE	FRACTAL DIMENSION	R-SQUARED
Interior Low Plateaus		NE-SW	76 pixels	2.617682	0.902524
		combined	118 pixels	2.681976	0.837329
	Smiths Grove, KY	E-W	136 pixels	2.602464	0.949889
		N-S	97 pixels	2.526852	0.900164
		EW+NS	223 pixels	2.667490	0.868445
		NW-SE	65 pixels	2.521788	0.952162
		NE-SW	165 pixels	2.621404	0.923019
		combined	225 pixels	2.685213	0.865666
	Williams, IN	E-W	89 pixels	2.595615	0.898658
		N-S	122 pixels	2.632087	0.915297
		EW+NS	113 pixels	2.630756	0.894183
		NW-SE	60 pixels	2.607076	0.889285
		NE-SW	85 pixels	2.699787	0.845310
		combined	116 pixels	2.684806	0.858031
Central Lowland	Bartlett, KS-MO	E-W	130 pixels	2.565368	0.953867
		N-S	260 pixels	2.552479	0.995105
		EW+NS	186 pixels	2.584026	0.972101
		NW-SE	62 pixels	2.544479	0.975210
		NE-SW	240 pixels	2.479096	0.987985
		combined	259 pixels	2.613104	0.981975
	Chetopa, KS-MO	E-W	188 pixels	2.710999	0.978262
		N-S	21 pixels	2.641854	0.906556
		EW+NS	91 pixels	2.717874	0.953860
		NW-SE	13 pixels	2.629276	0.923696
		NE-SW	13 pixels	2.646143	0.913603
		combined	91 pixels	2.740904	0.957758
	Harvey, IA	E-W	224 pixels	2.533570	0.979574
		N-S	224 pixels	2.577960	0.942712
		EW+NS	224 pixels	2.556177	0.967909
		NW-SE	73 pixels	2.559109	0.952244
		NE-SW	101 pixels	2.500285	0.976758
		combined	224 pixels	2.618893	0.932064
	Labette, KS-MO	E-W	157 pixels	2.553156	0.991114
		N-S	45 pixels	2.639125	0.947080
		EW+NS	179 pixels	2.602003	0.990267
		NW-SE	39 pixels	2.662971	0.943866
		NE-SW	105 pixels	2.580230	0.994798
		combined	155 pixels	2.629481	0.989654
	Leighton, IA	E-W	110 pixels	2.532037	0.954022
		N-S	125 pixels	2.576550	0.923000
		EW+NS	118 pixels	2.556243	0.938569
		NW-SE	320 pixels	2.527283	0.922737
		NE-SW	78 pixels	2.574021	0.900492
		combined	263 pixels	2.649490	0.937306
	Missouri Valley NW, NE	E-W	218 pixels	2.591779	0.984593
		N-S	200 pixels	2.654795	0.931731
		EW+NS	298 pixels	2.623584	0.981651
		NW-SE	57 pixels	2.619986	0.922837
		NE-SW	190 pixels	2.535018	0.979617
		combined	219 pixels	2.618164	0.983889
	Oswego, KS-MO	E-W	151 pixels	2.594579	0.964503
		N-S	265 pixels	2.625020	0.986661
		EW+NS	287 pixels	2.642487	0.973889
		NW-SE	86 pixels	2.646545	0.957141

Appendix I continued

PHYSIOGRAPHIC PROVINCE	NAME OF TOPO QUAD	DIRECTION	SCALE RANGE	FRACTAL DIMENSION	R-SQUARED
Central Lowland		NE-SW	267 pixels	2.576624	0.980620
		combined	279 pixels	2.661159	0.977066
	Paxton NW, IL	E-W	287 pixels	2.423158	0.988084
		N-S	279 pixels	2.419292	0.993716
		EW+NS	285 pixels	2.422040	0.993423
		NW-SE	139 pixels	2.664779	0.988451
		NE-SW	153 pixels	2.412267	0.996323
		combined	286 pixels	2.471906	0.998294
	Paxton SE (Gifford), IL	E-W	226 pixels	2.475110	0.998006
		N-S	231 pixels	2.409624	0.996653
		EW+NS	229 pixels	2.440533	0.999476
		NW-SE	92 pixels	2.563825	0.986515
		NE-SW	133 pixels	2.396671	0.993083
		combined	231 pixels	2.499419	0.991180
	Paxton SW (Rantoul), IL	E-W	225 pixels	2.443505	0.992077
		N-S	166 pixels	2.449861	0.992393
		EW+NS	329 pixels	2.489126	0.991750
		NW-SE	104 pixels	2.533590	0.996127
		NE-SW	224 pixels	2.383859	0.994143
		combined	278 pixels	2.504585	0.989661
	Pella, IA	E-W	159 pixels	2.582249	0.949989
		N-S	337 pixels	2.573592	0.949405
		EW+NS	337 pixels	2.590388	0.956991
		NW-SE	85 pixels	2.547735	0.942304
		NE-SW	223 pixels	2.583319	0.974002
		combined	337 pixels	2.615499	0.953578
	Peoria, IA	E-W	186 pixels	2.527381	0.973000
		N-S	240 pixels	2.534951	0.970925
		EW+NS	202 pixels	2.529429	0.975779
		NW-SE	80 pixels	2.595265	0.912532
		NE-SW	128 pixels	2.523915	0.977611
		combined	161 pixels	2.567757	0.965263
Great Plains	Bar C Bar Ranch, NM	E-W	200 pixels	2.306003	0.991177
		N-S	384 pixels	2.403732	0.988496
		EW+NS	220 pixels	2.374888	0.996979
		NW-SE	161 pixels	2.439638	0.988323
		NE-SW	248 pixels	2.287485	0.995766
		combined	211 pixels	2.378287	0.996626
	Derrick Draw, NM	E-W	384 pixels	2.312122	0.994303
		N-S	170 pixels	2.622366	0.938550
		EW+NS	384 pixels	2.412471	0.991164
		NW-SE	314 pixels	2.415426	0.994098
		NE-SW	342 pixels	2.340087	0.973202
		combined	384 pixels	2.426480	0.995881
	Dexter East, NM	E-W	256 pixels	2.427333	0.959302
		N-S	384 pixels	2.432863	0.987273
		EW+NS	295 pixels	2.457119	0.978196
		NW-SE	69 pixels	2.393549	0.988781
		NE-SW	302 pixels	2.368936	0.993362
		combined	252 pixels	2.450439	0.982808
	Double Mill Draw NE, TX	E-W	120 pixels	2.498858	0.968990
		N-S	389 pixels	2.355714	0.991689
		EW+NS	389 pixels	2.436438	0.987305
		NW-SE	375 pixels	2.319607	0.977554

Appendix I continued

PHYSIOGRAPHIC PROVINCE	NAME OF TOPO QUAD	DIRECTION	SCALE RANGE	FRACTAL DIMENSION	R-SQUARED
Great Plains		NE-SW	211 pixels	2.569332	0.974148
		combined	386 pixels	2.462423	0.993720
	Double Mill Draw NW, TX	E-W	388 pixels	2.493771	0.983995
		N-S	219 pixels	2.476209	0.989593
		EW+NS	244 pixels	2.496707	0.989853
		NW-SE	244 pixels	2.378263	0.985199
		NE-SW	104 pixels	2.503881	0.981575
		combined	240 pixels	2.509666	0.991203
	Double Mill Draw SE, TX	E-W	390 pixels	2.333472	0.988474
		N-S	235 pixels	2.539329	0.981609
		EW+NS	380 pixels	2.416048	0.991961
		NW-SE	261 pixels	2.549858	0.980669
		NE-SW	333 pixels	2.416490	0.988163
		combined	378 pixels	2.451954	0.993202
	Forks Ranch, MT	E-W	198 pixels	2.529760	0.983756
		N-S	117 pixels	2.505247	0.972767
		EW+NS	200 pixels	2.564329	0.959795
		NW-SE	74 pixels	2.481740	0.992876
		NE-SW	103 pixels	2.509767	0.989296
		combined	107 pixels	2.514480	0.979825
	Fort Hood, TX	E-W	277 pixels	2.561943	0.982484
		N-S	173 pixels	2.496961	0.970008
		EW+NS	375 pixels	2.627091	0.917706
		NW-SE	123 pixels	2.551482	0.974514
		NE-SW	118 pixels	2.544159	0.972436
		combined	242 pixels	2.603376	0.950393
	Holmes Ranch, MT	E-W	318 pixels	2.427298	0.986715
		N-S	206 pixels	2.519385	0.975241
		EW+NS	295 pixels	2.502043	0.986272
		NW-SE	81 pixels	2.534459	0.960126
		NE-SW	188 pixels	2.374512	0.988991
		combined	204 pixels	2.485863	0.992045
	Hot Springs, SD	E-W	128 pixels	2.431667	0.976654
		N-S	307 pixels	2.495995	0.991097
		EW+NS	169 pixels	2.484985	0.971693
		NW-SE	120 pixels	2.406639	0.989072
		NE-SW	166 pixels	2.480034	0.990582
		combined	134 pixels	2.460450	0.984878
	Indio Hill, TX	E-W	166 pixels	2.493078	0.966250
		N-S	366 pixels	2.453567	0.972870
		EW+NS	207 pixels	2.523858	0.971218
		NW-SE	211 pixels	2.458986	0.990443
		NE-SW	175 pixels	2.600702	0.944798
		combined	180 pixels	2.526394	0.977323
	North Fort Hood, TX	E-W	298 pixels	2.529219	0.983652
		N-S	247 pixels	2.457162	0.984514
		EW+NS	271 pixels	2.491175	0.985592
		NW-SE	136 pixels	2.589784	0.939903
		NE-SW	238 pixels	2.396247	0.986768
		combined	264 pixels	2.496723	0.988354
	North Loup Hord, NE	E-W	142 pixels	2.667163	0.952862
		N-S	169 pixels	2.494430	0.988237
		EW+NS	344 pixels	2.623890	0.971360
		NW-SE	120 pixels	2.557718	0.993508

Appendix I continued

PHYSIOGRAPHIC PROVINCE	NAME OF TOPO QUAD	DIRECTION	SCALE RANGE	FRACTAL DIMENSION	R-SQUARED
Great Plains		NE-SW	247 pixels	2.502298	0.990668
		combined	159 pixels	2.561730	0.991393
	Pine Butte School, MT	E-W	310 pixels	2.363880	0.977697
		N-S	87 pixels	2.543938	0.949353
		EW+NS	289 pixels	2.495631	0.985773
		NW-SE	188 pixels	2.488092	0.989796
		NE-SW	166 pixels	2.544271	0.983446
		combined	259 pixels	2.519580	0.990973
	Post Oak Mountain, TX	E-W	140 pixels	2.576128	0.937213
		N-S	231 pixels	2.475031	0.978278
		EW+NS	223 pixels	2.537530	0.963132
		NW-SE	219 pixels	2.561193	0.969344
		NE-SW	232 pixels	2.547778	0.970961
		combined	224 pixels	2.555372	0.967537
	Shell Mountains, TX	E-W	243 pixels	2.547014	0.960225
		N-S	214 pixels	2.558547	0.947777
		EW+NS	253 pixels	2.526163	0.976945
		NW-SE	260 pixels	2.624361	0.947762
		NE-SW	138 pixels	2.490195	0.974100
		combined	260 pixels	2.595952	0.945151
Southern Rocky Mtns.	Bowen Mountain, CO	E-W	149 pixels	2.299518	0.981410
		N-S	120 pixels	2.357059	0.969631
		EW+NS	148 pixels	2.342403	0.971972
		NW-SE	168 pixels	2.376732	0.981805
		NE-SW	156 pixels	2.438291	0.938664
		combined	153 pixels	2.387559	0.964583
	Granby, CO	E-W	212 pixels	2.507475	0.962586
		N-S	208 pixels	2.456373	0.973371
		EW+NS	210 pixels	2.484130	0.969440
		NW-SE	279 pixels	2.510031	0.982078
		NE-SW	232 pixels	2.542087	0.949838
		combined	223 pixels	2.522750	0.963371
	Grand Lake, CO	E-W	287 pixels	2.300062	0.990896
		N-S	190 pixels	2.450807	0.941400
		EW+NS	303 pixels	2.358322	0.985438
		NW-SE	73 pixels	2.374296	0.957074
		NE-SW	280 pixels	2.251248	0.994202
		combined	291 pixels	2.369784	0.989027
	Isolation Peak, CO	E-W	123 pixels	2.425960	0.935176
		N-S	78 pixels	2.369368	0.952064
		EW+NS	94 pixels	2.391567	0.946678
		NW-SE	202 pixels	2.552350	0.926335
		NE-SW	52 pixels	2.333660	0.968060
		combined	119 pixels	2.495841	0.901051
	Mc Henrys Peak, CO	E-W	263 pixels	2.396754	0.970891
		N-S	241 pixels	2.495160	0.924909
		EW+NS	248 pixels	2.436514	0.962398
		NW-SE	70 pixels	2.405844	0.946916
		NE-SW	173 pixels	2.392137	0.974019
		combined	237 pixels	2.479144	0.953197
	Monarch Lake, CO	E-W	317 pixels	2.454958	0.961536
		N-S	126 pixels	2.409808	0.926443
		EW+NS	319 pixels	2.511075	0.934985
		NW-SE	249 pixels	2.363739	0.988002

Appendix I continued

PHYSIOGRAPHIC PROVINCE	NAME OF TOPO QUAD	DIRECTION	SCALE RANGE	FRACTAL DIMENSION	R-SQUARED
Southern Rocky Mtns.	Shadow Mountain, CO	NE-SW	48 pixels	2.283208	0.969699
		combined	254 pixels	2.517214	0.939708
		E-W	350 pixels	2.285123	0.998581
		N-S	83 pixels	2.325479	0.968748
		EW+NS	350 pixels	2.315689	0.994729
		NW-SE	309 pixels	2.276676	0.995659
		NE-SW	185 pixels	2.437375	0.965787
		combined	321 pixels	2.412638	0.989486
	Strawberry Lake, CO	E-W	350 pixels	2.398526	0.984252
		N-S	350 pixels	2.509639	0.963170
		EW+NS	350 pixels	2.444696	0.978034
		NW-SE	350 pixels	2.444696	0.978034
		NE-SW	97 pixels	2.481835	0.929579
		combined	350 pixels	2.462722	0.983947
	Trail Mountain, CO	E-W	67 pixels	2.399839	0.934870
		N-S	349 pixels	2.276435	0.985405
		EW+NS	349 pixels	2.385363	0.968731
		NW-SE	349 pixels	2.277532	0.967953
		NE-SW	149 pixels	2.517178	0.945173
		combined	349 pixels	2.404131	0.977740
Middle Rocky Mtns.	Big Horn, WY	E-W	181 pixels	2.581674	0.959533
		N-S	318 pixels	2.263950	0.994374
		EW+NS	228 pixels	2.591693	0.990391
		NW-SE	237 pixels	2.378241	0.993186
		NE-SW	139 pixels	2.467620	0.990015
		combined	318 pixels	2.435285	0.994908
	Flaming Gorge, UT	E-W	185 pixels	2.457362	0.950612
		N-S	251 pixels	2.443007	0.988570
		EW+NS	200 pixels	2.448633	0.979481
		NW-SE	197 pixels	2.489427	0.959122
		NE-SW	208 pixels	2.482339	0.980437
		combined	200 pixels	2.477397	0.979598
	Pat O'Hara Mountain, WY	E-W	320 pixels	2.204837	0.995943
		N-S	95 pixels	2.323851	0.982835
		EW+NS	320 pixels	2.277310	0.993931
		NW-SE	278 pixels	2.407949	0.994475
		NE-SW	317 pixels	2.213530	0.995118
		combined	320 pixels	2.310963	0.997502
Northern Rocky Mtns.	Atlanta West, ID	E-W	151 pixels	2.471400	0.950249
		N-S	132 pixels	2.407307	0.974760
		EW+NS	136 pixels	2.447783	0.941332
		NW-SE	85 pixels	2.479541	0.945319
		NE-SW	70 pixels	2.374574	0.979361
		combined	89 pixels	2.419224	0.967494
	Bata Mountain, MT	E-W	303 pixels	2.379085	0.994049
		N-S	303 pixels	2.420389	0.976528
		EW+NS	303 pixels	2.393474	0.994423
		NW-SE	303 pixels	2.268502	0.986238
		NE-SW	301 pixels	2.574531	0.926725
		combined	303 pixels	2.415374	0.992951
	Belmont Point, MT	E-W	292 pixels	2.436037	0.978314
		N-S	257 pixels	2.309536	0.996073
		EW+NS	288 pixels	2.366713	0.992019
		NW-SE	291 pixels	2.636240	0.788482

Appendix I continued

PHYSIOGRAPHIC PROVINCE	NAME OF TOPO QUAD	DIRECTION	SCALE RANGE	FRACTAL DIMENSION	R-SQUARED
Northern Rocky Mtns.		NE-SW	284 pixels	2.352782	0.954013
		combined	289 pixels	2.399204	0.989541
	Belmore Sloughs, MT	E-W	299 pixels	2.476494	0.924314
		N-S	70 pixels	2.269109	0.970406
		EW+NS	202 pixels	2.495999	0.886392
		NW-SE	49 pixels	2.298831	0.966840
		NE-SW	74 pixels	2.301676	0.974759
		combined	147 pixels	2.483535	0.893568
	Cedar Lake, MT	E-W	197 pixels	2.392548	0.953052
		N-S	70 pixels	2.376425	0.964842
		EW+NS	201 pixels	2.454076	0.943020
		NW-SE	141 pixels	2.436214	0.932991
		NE-SW	200 pixels	2.411117	0.977463
		combined	200 pixels	2.471417	0.940197
	Chief Mountain, MT	E-W	251 pixels	2.225237	0.998004
		N-S	213 pixels	2.256224	0.997349
		EW+NS	226 pixels	2.243934	0.997774
		NW-SE	73 pixels	2.312400	0.970697
		NE-SW	228 pixels	2.107213	0.993689
		combined	224 pixels	2.268736	0.997854
	Condon, MT	E-W	298 pixels	2.159518	0.993429
		N-S	192 pixels	2.452168	0.953656
		EW+NS	298 pixels	2.233106	0.996066
		NW-SE	247 pixels	2.301819	0.993114
		NE-SW	217 pixels	2.178658	0.995205
		combined	298 pixels	2.279109	0.987880
	Crimson Peak, MT	E-W	83 pixels	2.268917	0.975583
		N-S	86 pixels	2.309695	0.961626
		EW+NS	84 pixels	2.290468	0.968688
		NW-SE	68 pixels	2.306617	0.967295
		NE-SW	94 pixels	2.288755	0.985925
		combined	81 pixels	2.307828	0.970054
	Elevation Mountain, MT	E-W	288 pixels	2.460176	0.968053
		N-S	304 pixels	2.638988	0.645529
		EW+NS	293 pixels	2.524600	0.907153
		NW-SE	304 pixels	2.442897	0.988064
		NE-SW	295 pixels	2.607188	0.753765
		combined	275 pixels	2.546545	0.916122
	Gold Creek Peak, MT	E-W	249 pixels	2.505442	0.909035
		N-S	285 pixels	2.608040	0.735921
		EW+NS	276 pixels	2.567558	0.836703
		NW-SE	254 pixels	2.510996	0.938816
		NE-SW	156 pixels	2.470758	0.929301
		combined	280 pixels	2.442938	0.972162
	Gray Wolf Lake, MT	E-W	298 pixels	2.400612	0.974588
		N-S	111 pixels	2.395904	0.924029
		EW+NS	298 pixels	2.543317	0.878909
		NW-SE	96 pixels	2.393961	0.943705
		NE-SW	119 pixels	2.370574	0.975583
		combined	122 pixels	2.406512	0.945817
	Hemlock Lake, MT	E-W	263 pixels	2.267884	0.994813
		N-S	253 pixels	2.447418	0.962921
		EW+NS	277 pixels	2.343243	0.989885
		NW-SE	122 pixels	2.404176	0.972936

Appendix I continued

PHYSIOGRAPHIC PROVINCE	NAME OF TOPO QUAD	DIRECTION	SCALE RANGE	FRACTAL DIMENSION	R-SQUARED
Northern Rocky Mtns.		NE-SW	242 pixels	2.206675	0.998293
		combined	248 pixels	2.355826	0.990728
	Holland Peak, MT	E-W	201 pixels	2.452733	0.934825
		N-S	239 pixels	2.484133	0.923737
		EW+NS	206 pixels	2.461474	0.929774
		NW-SE	163 pixels	2.488092	0.928005
		NE-SW	61 pixels	2.313919	0.972869
		combined	177 pixels	2.497253	0.911989
	Lake Inez, CO	E-W	300 pixels	2.281142	0.994344
		N-S	90 pixels	2.414639	0.952211
		EW+NS	300 pixels	2.360167	0.991776
		NW-SE	204 pixels	2.301738	0.992367
		NE-SW	179 pixels	2.317436	0.995503
		combined	291 pixels	2.380705	0.987245
	Lake Marshall, MT	E-W	163 pixels	2.400579	0.979398
		N-S	192 pixels	2.373560	0.979204
		EW+NS	193 pixels	2.396570	0.978762
		NW-SE	115 pixels	2.394945	0.966259
		NE-SW	300 pixels	2.329054	0.977114
		combined	300 pixels	2.482852	0.965480
	Morrell Lake, MT	E-W	232 pixels	2.511134	0.935545
		N-S	253 pixels	2.498948	0.943285
		EW+NS	245 pixels	2.507283	0.940965
		NW-SE	48 pixels	2.329617	0.969998
		NE-SW	159 pixels	2.543037	0.902850
		combined	251 pixels	2.573926	0.910381
	Morrell Mountain, MT	E-W	57 pixels	2.290904	0.968030
		N-S	201 pixels	2.484125	0.931510
		EW+NS	281 pixels	2.579307	0.886962
		NW-SE	122 pixels	2.462822	0.954751
		NE-SW	36 pixels	2.271755	0.975927
		combined	149 pixels	2.539601	0.888376
	Peck Lake, MT	E-W	296 pixels	2.153760	0.997883
		N-S	97 pixels	2.518804	0.909338
		EW+NS	296 pixels	2.225447	0.998996
		NW-SE	241 pixels	2.191382	0.998209
		NE-SW	259 pixels	2.228203	0.995653
		combined	289 pixels	2.256518	0.995110
	Porcupine Creek, MT	E-W	236 pixels	2.350267	0.983988
		N-S	182 pixels	2.550775	0.928010
		EW+NS	229 pixels	2.430459	0.977578
		NW-SE	239 pixels	2.494730	0.959489
		NE-SW	177 pixels	2.389073	0.981817
		combined	229 pixels	2.463873	0.973192
	Priest Lake NE, ID	E-W	257 pixels	2.127926	0.996715
		N-S	92 pixels	2.232881	0.986110
		EW+NS	305 pixels	2.300423	0.983041
		NW-SE	299 pixels	2.251934	0.973142
		NE-SW	186 pixels	2.182918	0.997032
		combined	280 pixels	2.313819	0.984096
	Salmon Lake, MT	E-W	242 pixels	2.509201	0.930371
		N-S	85 pixels	2.330754	0.971322
		EW+NS	99 pixels	2.368590	0.960757
		NW-SE	158 pixels	2.423527	0.961240

Appendix I continued

PHYSIOGRAPHIC PROVINCE	NAME OF TOPO QUAD	DIRECTION	SCALE RANGE	FRACTAL DIMENSION	R-SQUARED
Northern Rocky Mtns.	Seeley Lake East, MT	NE-SW	75 pixels	2.434177	0.924912
		combined	91 pixels	2.392741	0.958991
		E-W	138 pixels	2.315221	0.972092
		N-S	301 pixels	2.347997	0.990105
		EW+NS	301 pixels	2.385777	0.976334
		NW-SE	146 pixels	2.370997	0.974221
		NE-SW	301 pixels	2.283076	0.963035
		combined	301 pixels	2.415589	0.975939
	Seeley Lake West, MT	E-W	223 pixels	2.296608	0.998304
		N-S	301 pixels	2.453697	0.983720
		EW+NS	301 pixels	2.375319	0.991379
		NW-SE	301 pixels	2.262943	0.939569
		NE-SW	147 pixels	2.324430	0.995268
		combined	301 pixels	2.413147	0.986905
	Upper Jocko Lake, MT	E-W	275 pixels	2.407675	0.988615
		N-S	300 pixels	2.544011	0.900830
		EW+NS	277 pixels	2.467464	0.963289
		NW-SE	245 pixels	2.258617	0.985989
		NE-SW	53 pixels	2.324265	0.978404
		combined	245 pixels	2.458406	0.978302
	Wapiti Lake, MT	E-W	299 pixels	2.443146	0.956833
		N-S	300 pixels	2.598491	0.837660
		EW+NS	300 pixels	2.511966	0.933827
		NW-SE	70 pixels	2.369148	0.958032
		NE-SW	89 pixels	2.406340	0.941058
		combined	199 pixels	2.528481	0.905159
	Woodworth, MT	E-W	192 pixels	2.289370	0.995669
		N-S	114 pixels	2.337979	0.977478
		EW+NS	160 pixels	2.348775	0.980858
		NW-SE	141 pixels	2.409714	0.964391
		NE-SW	121 pixels	2.339937	0.988835
		combined	145 pixels	2.371398	0.977848
	Yew Creek, MT	E-W	231 pixels	2.213526	0.991157
		N-S	294 pixels	2.244193	0.997951
		EW+NS	266 pixels	2.242587	0.992864
		NW-SE	260 pixels	2.362756	0.948455
		NE-SW	149 pixels	2.186340	0.997662
		combined	285 pixels	2.317661	0.977373
Columbia Plateaus	Wilcox, WA	E-W	136 pixels	2.587632	0.954043
		N-S	72 pixels	2.522785	0.945279
		EW+NS	84 pixels	2.545073	0.948142
		NW-SE	76 pixels	2.607378	0.967268
		NE-SW	81 pixels	2.567678	0.944549
		combined	80 pixels	2.569132	0.953833
	Yakima East, WA	E-W	287 pixels	2.238863	0.987162
		N-S	304 pixels	2.237195	0.994854
		EW+NS	304 pixels	2.239105	0.994907
		NW-SE	113 pixels	2.603243	0.987169
		NE-SW	287 pixels	2.188817	0.992264
		combined	304 pixels	2.271701	0.997118
Colorado Plateaus	Anvil Points, CO	E-W	259 pixels	2.443140	0.979190
		N-S	343 pixels	2.426712	0.979988
		EW+NS	343 pixels	2.447350	0.978557
		NW-SE	331 pixels	2.414190	0.984506
		NE-SW	151 pixels	2.598427	0.912910
		combined	343 pixels	2.478822	0.978751

Appendix I continued

PHYSIOGRAPHIC PROVINCE	NAME OF TOPO QUAD	DIRECTION	SCALE RANGE	FRACTAL DIMENSION	R-SQUARED
Colorado Plateaus	Greasewood Canyon, CO	E-W	250 pixels	2.585173	0.941582
		N-S	51 pixels	2.425781	0.944124
		EW+NS	256 pixels	2.660979	0.876463
		NW-SE	70 pixels	2.570466	0.866306
		NE-SW	192 pixels	2.614863	0.948335
		combined	86 pixels	2.567185	0.890724
	Moccasin Mesa, CO	E-W	29 pixels	2.379315	0.940080
		N-S	357 pixels	2.409541	0.978519
		EW+NS	77 pixels	2.557822	0.876723
		NW-SE	54 pixels	2.576200	0.858697
		NE-SW	234 pixels	2.569862	0.931766
		combined	279 pixels	2.580319	0.931969
	Moqui Canyon, CO	E-W	74 pixels	2.441552	0.937530
		N-S	134 pixels	2.457612	0.958275
		EW+NS	137 pixels	2.523906	0.911337
		NW-SE	130 pixels	2.519070	0.965460
		NE-SW	115 pixels	2.593869	0.861480
		combined	122 pixels	2.536751	0.923949
	Wetherill Mesa, CO	E-W	28 pixels	2.368726	0.945677
		N-S	358 pixels	2.432781	0.966820
		EW+NS	101 pixels	2.596726	0.867554
		NW-SE	244 pixels	2.554535	0.953862
		NE-SW	23 pixels	2.403993	0.942396
		combined	358 pixels	2.584850	0.937745
	Zion National Park NE, UT	E-W	119 pixels	2.561971	0.946723
		N-S	137 pixels	2.604133	0.894597
		EW+NS	125 pixels	2.577152	0.929414
		NW-SE	121 pixels	2.298864	0.986610
		NE-SW	106 pixels	2.598263	0.947662
		combined	114 pixels	2.291849	0.984432
Basin & Range	Adel, OR	E-W	202 pixels	2.288409	0.966255
		N-S	328 pixels	2.378247	0.976457
		EW+NS	328 pixels	2.398252	0.948792
		NW-SE	116 pixels	2.276243	0.972871
		NE-SW	219 pixels	2.346904	0.980793
		combined	328 pixels	2.450906	0.929796
	Buffalo Springs NW, NV	E-W	329 pixels	2.162897	0.998749
		N-S	70 pixels	2.497799	0.874740
		EW+NS	329 pixels	2.229702	0.998333
		NW-SE	308 pixels	2.222753	0.994856
		NE-SW	324 pixels	2.243559	0.996798
		combined	326 pixels	2.262451	0.997870
	Buffalo Springs SW, NV	E-W	336 pixels	2.232208	0.992600
		N-S	148 pixels	2.384138	0.966410
		EW+NS	351 pixels	2.265412	0.991783
		NW-SE	261 pixels	2.261721	0.993385
		NE-SW	197 pixels	2.343834	0.982810
		combined	351 pixels	2.318101	0.990787
	Cain Mountain NE, NV	E-W	230 pixels	2.267591	0.996975
		N-S	351 pixels	2.220647	0.990061
		EW+NS	267 pixels	2.276207	0.997842
		NW-SE	228 pixels	2.176935	0.998744
		NE-SW	104 pixels	2.365496	0.974967
		combined	235 pixels	2.287675	0.997597
	Cain Mountain NW, NV	E-W	199 pixels	2.366290	0.958506
		N-S	342 pixels	2.299896	0.985876
		EW+NS	282 pixels	2.417817	0.958248

Appendix I continued

PHYSIOGRAPHIC PROVINCE	NAME OF TOPO QUAD	DIRECTION	SCALE RANGE	FRACTAL DIMENSION	R-SQUARED
Basin & Range		NW-SE	194 pixels	2.426839	0.971709
		NE-SW	160 pixels	2.293472	0.992414
		combined	213 pixels	2.396938	0.966292
	Cain Mountain SE, NV	E-W	290 pixels	2.209198	0.997713
		N-S	351 pixels	2.194825	0.997712
		EW+NS	351 pixels	2.223878	0.996846
		NW-SE	255 pixels	2.197114	0.994930
		NE-SW	295 pixels	2.558583	0.968375
		combined	351 pixels	2.275967	0.992596
	Cain Mountain SW, NV	E-W	307 pixels	2.284658	0.990214
		N-S	351 pixels	2.197554	0.996928
		EW+NS	351 pixels	2.235960	0.999068
		NW-SE	313 pixels	2.164981	0.987482
		NE-SW	210 pixels	2.534644	0.953365
		combined	316 pixels	2.263043	0.997856
	Calderwood Resevoir, OR	E-W	283 pixels	2.396450	0.989488
		N-S	196 pixels	2.372511	0.974332
		EW+NS	285 pixels	2.411135	0.985441
		NW-SE	182 pixels	2.506006	0.966818
		NE-SW	197 pixels	2.350909	0.993697
		combined	286 pixels	2.447516	0.978123
	Coleman Lake, OR	E-W	222 pixels	2.392950	0.963911
		N-S	330 pixels	2.260045	0.994757
		EW+NS	230 pixels	2.375453	0.975920
		NW-SE	204 pixels	2.471677	0.932055
		NE-SW	259 pixels	2.357261	0.979459
		combined	231 pixels	2.409806	0.964661
	Collins Rim, OR	E-W	327 pixels	2.188949	0.998960
		N-S	281 pixels	2.241292	0.998397
		EW+NS	310 pixels	2.207549	0.998905
		NW-SE	211 pixels	2.361525	0.982036
		NE-SW	289 pixels	2.166601	0.992723
		combined	295 pixels	2.240491	0.998761
	Cortez NE, NV	E-W	315 pixels	2.365190	0.989485
		N-S	320 pixels	2.274771	0.998470
		EW+NS	319 pixels	2.321859	0.996417
		NW-SE	210 pixels	2.230130	0.997771
		NE-SW	51 pixels	2.377259	0.967431
		combined	319 pixels	2.366342	0.992494
	Cortez NW, NV	E-W	352 pixels	2.460687	0.970856
		N-S	347 pixels	2.364767	0.990070
		EW+NS	352 pixels	2.406388	0.989056
		NW-SE	215 pixels	2.394793	0.993494
		NE-SW	305 pixels	2.475222	0.952977
		combined	352 pixels	2.444881	0.987990
	Cortez SE, NV	E-W	156 pixels	2.219374	0.995440
		N-S	315 pixels	2.237406	0.998193
		EW+NS	310 pixels	2.348979	0.967406
		NW-SE	155 pixels	2.314043	0.996985
		NE-SW	167 pixels	2.245072	0.998745
		combined	165 pixels	2.265211	0.997859
	Cortez SW, NV	E-W	213 pixels	2.314481	0.994823
		N-S	251 pixels	2.343296	0.994676
		EW+NS	235 pixels	2.334532	0.996458
		NW-SE	117 pixels	2.307303	0.991574
		NE-SW	210 pixels	2.339988	0.996500
		combined	216 pixels	2.377142	0.991013

Appendix I continued

PHYSIOGRAPHIC PROVINCE	NAME OF TOPO QUAD	DIRECTION	SCALE RANGE	FRACTAL DIMENSION	R-SQUARED
Basin & Range	Crump Lake, OR	E-W	327 pixels	2.432649	0.948143
		N-S	265 pixels	2.383837	0.987614
		EW+NS	328 pixels	2.427924	0.966335
		NW-SE	97 pixels	2.287901	0.989397
		NE-SW	260 pixels	2.366357	0.983442
		combined	316 pixels	2.454752	0.963646
	Drake Peak, OR	E-W	324 pixels	2.303754	0.993708
		N-S	138 pixels	2.371700	0.952747
		EW+NS	324 pixels	2.409228	0.971645
		NW-SE	182 pixels	2.351138	0.986656
		NE-SW	137 pixels	2.368680	0.985504
		combined	325 pixels	2.454669	0.958483
	Fencemaker NE, NV	E-W	152 pixels	2.239165	0.994634
		N-S	230 pixels	2.398113	0.981692
		EW+NS	158 pixels	2.278471	0.993349
		NW-SE	135 pixels	2.305195	0.984376
		NE-SW	176 pixels	2.285365	0.998092
		combined	157 pixels	2.305493	0.990988
	Fencemaker SE, NV	E-W	218 pixels	2.199990	0.993449
		N-S	350 pixels	2.312106	0.993420
		EW+NS	225 pixels	2.232705	0.993591
		NW-SE	204 pixels	2.257391	0.985394
		NE-SW	241 pixels	2.241061	0.998864
		combined	218 pixels	2.260948	0.990758
	Glamis SE, CA	E-W	376 pixels	2.422965	0.981887
		N-S	373 pixels	2.444744	0.981010
		EW+NS	374 pixels	2.434065	0.981479
		NW-SE	16 pixels	2.545731	0.900197
		NE-SW	326 pixels	2.384872	0.986620
		combined	374 pixels	2.444263	0.982172
	Kyle Hot Springs NE, NV	E-W	244 pixels	2.222877	0.998226
		N-S	301 pixels	2.502749	0.960785
		EW+NS	249 pixels	2.286389	0.996554
		NW-SE	220 pixels	2.246461	0.998548
		NE-SW	348 pixels	2.268128	0.977863
		combined	239 pixels	2.301898	0.996538
	Kyle Hot Springs SE, NV	E-W	304 pixels	2.204818	0.998898
		N-S	343 pixels	2.388046	0.975139
		EW+NS	337 pixels	2.283931	0.997378
		NW-SE	259 pixels	2.294748	0.985702
		NE-SW	269 pixels	2.412771	0.980611
		combined	343 pixels	2.340237	0.992317
	May Lake, OR	E-W	227 pixels	2.424866	0.981769
		N-S	313 pixels	2.302753	0.996368
		EW+NS	297 pixels	2.365200	0.994168
		NW-SE	213 pixels	2.433269	0.978929
		NE-SW	95 pixels	2.422920	0.980466
		combined	302 pixels	2.415114	0.990875
	Mt. Moses NW, NV	E-W	266 pixels	2.204601	0.997443
		N-S	201 pixels	2.378621	0.984073
		EW+NS	265 pixels	2.264200	0.996671
		NW-SE	243 pixels	2.199823	0.998788
		NE-SW	307 pixels	2.437791	0.971684
		combined	257 pixels	2.288155	0.996849
	Mt. Moses SW, NV	E-W	232 pixels	2.284271	0.995271
		N-S	345 pixels	2.187104	0.999094
		EW+NS	352 pixels	2.269456	0.994785

Appendix I continued

PHYSIOGRAPHIC PROVINCE	NAME OF TOPO QUAD	DIRECTION	SCALE RANGE	FRACTAL DIMENSION	R-SQUARED
Basin & Range		NW-SE	109 pixels	2.305367	0.995411
		NE-SW	205 pixels	2.329712	0.989918
		combined	352 pixels	2.335543	0.990674
	Mt. Tobin NE, NV	E-W	349 pixels	2.161576	0.998067
		N-S	313 pixels	2.323881	0.996287
		EW+NS	349 pixels	2.199202	0.997960
		NW-SE	313 pixels	2.152927	0.994593
		NE-SW	349 pixels	2.205324	0.976702
		combined	302 pixels	2.223540	0.998441
	Mt. Tobin NW, NV	E-W	349 pixels	2.204680	0.996327
		N-S	349 pixels	2.292395	0.996826
		EW+NS	349 pixels	2.232633	0.996896
		NW-SE	349 pixels	2.107672	0.995272
		NE-SW	180 pixels	2.499405	0.962542
		combined	349 pixels	2.252051	0.998413
	Mt. Tobin SW, NV	E-W	349 pixels	2.240253	0.995194
		N-S	148 pixels	2.406151	0.954925
		EW+NS	349 pixels	2.306573	0.991705
		NW-SE	248 pixels	2.268689	0.991266
		NE-SW	220 pixels	2.271157	0.994955
		combined	349 pixels	2.351586	0.976097
	Priday Resevoir, OR	E-W	251 pixels	2.477245	0.894807
		N-S	319 pixels	2.275500	0.989457
		EW+NS	328 pixels	2.419498	0.956092
		NW-SE	244 pixels	2.383131	0.967855
		NE-SW	259 pixels	2.468086	0.924713
		combined	328 pixels	2.419498	0.956092
	Sage Hen Butte, OR	E-W	89 pixels	2.432688	0.936563
		N-S	224 pixels	2.546820	0.914004
		EW+NS	223 pixels	2.580000	0.885662
		NW-SE	37 pixels	2.328384	0.965510
		NE-SW	205 pixels	2.463211	0.966489
		combined	207 pixels	2.595594	0.894139
Cascade-Sierra Mtns.	Mt. Langley, CA	E-W	367 pixels	2.157425	0.999016
		N-S	367 pixels	2.325882	0.986757
		EW+NS	367 pixels	2.227448	0.997900
		NW-SE	68 pixels	2.442396	0.941292
		NE-SW	331 pixels	2.161848	0.997210
		combined	367 pixels	2.265470	0.998261
	Mount Tom, CA	E-W	143 pixels	2.370316	0.943195
		N-S	325 pixels	2.462878	0.944843
		EW+NS	360 pixels	2.517499	0.912289
		NW-SE	87 pixels	2.341740	0.963282
		NE-SW	135 pixels	2.371923	0.972207
		combined	113 pixels	2.359803	0.962369
	Yosemite NW, CA	E-W	271 pixels	2.334687	0.996388
		N-S	90 pixels	2.227692	0.988195
		EW+NS	237 pixels	2.417885	0.952131
		NW-SE	98 pixels	2.270638	0.989405
		NE-SW	96 pixels	2.298864	0.986610
		combined	102 pixels	2.291849	0.984432
Pacific Border	Pacifico Mountain, CA	E-W	163 pixels	2.442306	0.970245
		N-S	351 pixels	2.353665	0.997115
		EW+NS	353 pixels	2.456254	0.983345
		NW-SE	284 pixels	2.345757	0.989815
		NE-SW	161 pixels	2.446638	0.987404
		combined	291 pixels	2.443909	0.990321

BIBLIOGRAPHY

Aharony, Amnon, and Feder, Jens, (editors), 1990 **Fractals in Physics: Essays in Honour of Benoit B. Mandelbrot,** North Holland Physics Publishing, Amsterdam, The Netherlands, 398p.

Ahnert, Frank, 1984 Local Relief and the Height Limits of Mountain Ranges, *American Journal of Science,* vol. 284, no. 9, p.1035-1055.

Aki, Keiiti, 1981 A Probabilistic Synthesis of Precursory Phenomena, In David W. Simpson and Paul G. Richards, (editors), **Earthquake Prediction: An International Review,** Maurice Ewing Series vol. 4, American Geophysical Union, Washington, D. C., p.566-574.

Albers, Donald J., and Alexanderson, Gerald L., (editors), 1985 **Mathematical People: Profiles and Interviews,** Birkhauser, Boston, Massachusetts, 372p.

Andrews, D. J., 1980 A Stochastic Fault Model: 1. Static Case, *Journal of Geophysical Research,* vol. 85, no. B7, p.3867-3877.

Andrle, Robert, 1992 Estimating Fractal Dimension with the Divider Method in Geomorphology, *Geomorphology,* vol. 5, nos. 1/2, p.131-141.

------, and Abrahams, Athol D., 1989 Fractal Techniques and the Surface Roughness of Talus Slopes, *Earth Surface Processes and Landforms,* vol. 14, p.197-209.

------, and ------, 1990 Fractal Techniques and the Surface Roughness of Talus Slopes: Reply, *Earth Surface Processes and Landforms,* vol. 15, p.287-290.

Arlinghaus, Sandra L., 1985 Fractals Take a Central Place, *Geografiska Annaler,* vol. 67B, p.83-88.

------, and Arlinghaus, William C., 1989 The Fractal Theory of Central Place Geometry: A Diophantine Analysis of Fractal Generators for Arbitrary Loschian Numbers, *Geographic Analysis,* vol. 21, no. 2, p.103-121.

Armstrong, A. C., 1986 On the Fractal Dimensions of Some Transient Soil Properties, *Journal of Soil Science,* vol. 37, p.641-652.

Armstrong, Marc P., and Hopkins, Lewis D., 1983 Fractal Enhancement for Thematic Display of Topologically Stored Data, In **Proceedings of the Sixth International Symposium on Automated Cartography,** (Auto-Carto 6), Ottawa, Canada, October 16-21, 1983, vol. 2, p.309-318.

Atwood, Wallace W., 1940 **The Physiographic Provinces of North America,** Blaisdell, New York, 536p.

Aviles, C. A., Scholz, Christopher H., and Boatwright, John, 1987 Fractal Analysis Applied to Characteristic Segments of the San Andreas Fault, *Journal of Geophysical Research,* vol. 92, no. B1, p.331-344.

Avnir, David, (editor), 1989 **The Fractal Approach to Heterogeneous Chemistry: Surfaces, Colloids, Polymers,** John Wiley & Sons, Chichester, Great Britain, 441p.

------, Farin, Dina, and Pfeifer, Peter, 1984 Molecular Fractal Surfaces, *Nature,* vol. 308, p.261-263.

------, ------, and ------, 1985 Surface Geometric Irregularity of Particulate Materials: The Fractal Approach, *Journal of Colloid and Interface Science,* vol. 103, no. 1, p.112-123.

Bachelier, Louis, 1900 **Theorie de la Speculation,** A Thesis Presented to the Faculty of Sciences of the Academy of Paris on March 29, 1900, for the degree, Docteur es Sciences Mathematiques, Originally Published in *Annales Scientifiques de l'Ecole Normale Superieure,* III-17, Gauthier-Villars, Paris, p.21-86, Translated into English by A. James Boness and Included in Paul H. Cootner, (editor), 1964 **The Random Character of Stock Market Prices,** The MIT Press, Cambridge, Massachusetts, p.17-78.

Balmino, Georges, Lambeck, Kurt, and Kaula, William M., 1973 A Spherical Harmonic Analysis of the Earth's Topography, *Journal of Geophysical Research,* vol. 78, p.478-481.

------, Moynot, B., and Vales, N., 1982 Gravity Field Model of Mars in Spherical Harmonics up to Degree and Order Eighteen, *Journal of Geophysical Research,* vol. 87, p.9735-9746.

Barenblatt, G. I., and Monin, A. S., 1983 Similarity Principles for the Biology of Pelagic Animals, *Proceedings of the National Academy of Science, U. S. A.,* vol. 80, p.3540-3542.

------, Zhivago, A. V., Neprochnov, Yu. P., and Ostrovskiy, A. A., 1984 The Fractal Dimension: A Quantitative Characteristic of Ocean-Bottom Relief, *Oceanology,* vol. 24, no. 6, p.695-697.

Barnsley, Michael F., 1988 **Fractals Everywhere,** Academic Press, Inc., San Diego, California, 394p.

------, 1989 **The Desktop Fractal Design Handbook,** Academic Press, Inc., San Diego, California, 38p.

------, and Demko, Stephen, (editors), 1986 **Chaotic Dynamics and Fractals,** Academic Press, Inc., Orlando, Florida, 292p.

Bartoli, F., Philippy, R., Doirisse, M., Niquet, S., and Dubuit, M., 1991 Structure and Self-Similarity in Silty and Sand Soils: The Fractal Approach, *Journal of Soil Science,* vol. 42, no. 2, p.167-185.

Barton, Christopher C., and LaPointe, P. R., (editors), 1992 **Fractals and Their Use in the Petroleum Industry,** American Association of Petroleum Geologists.

Bates, Robert L., and Jackson, Julia A., (editors), 1987 **Glossary of Geology,** 3rd edition, American Geological Institute, Alexandria, Virginia, 788p.

Batty, Michael, 1985 Fractals ---- Geometry between Dimensions, *New Scientist,* vol. 105, no. 1450, p.31-35.

------, 1991a Generating Urban Forms from Diffusive Growth, *Environment and Planning A,* vol. 23, no. 4, p.511-544.

------, 1991b Cities as Fractals: Simulating Growth and Form, In Anthony J. Crilly, Rae A. Earnshaw and Huw Jones, (editors), **Fractals and Chaos,** Springer-Verlag, New York, p.43-69.

------, and Longley, Paul A., 1986 The Fractal Simulation of Urban Structure, *Environment and Planning A,* vol. 18, p.1143-1179.

------, and ------, 1987a Fractal-Based Description of Urban Form, *Environment and Planning B: Planning and Design,* vol. 14, p.123-134.

------, and ------, 1987b Urban Shapes as Fractals, *Area,* vol. 19, no. 3, p.215-221.

------, and ------, 1988 The Morphology of Urban Land Use, *Environment and Planning B: Planning and Design,* vol. 15, p.461-488.

------, ------, and Fotheringham, A. Stewart, 1989 Urban Growth and Form: Scaling, Fractal Geometry and Diffusion-Limited Aggregation, *Environment and Planning A,* vol. 21, p.1447-1472.

Becker, Karl-Heinz, and Dorfler, Michael, 1989 **Dynamical Systems and Fractals: Computer Graphics Experiments in Pascal,** Originally Published in German as **Computergrafische Experimente mit Pascal: Chaos und Ordnung in Dynamischen Systemen** in 1986 by Friedr. Vieweg & Sohn, Braunschweig, 1988, 2nd edition, Translated into English by Ian Stewart, Cambridge University Press, Cambridge, Great Britain, 398p.

Bell, T. H., Jr., 1975 Statistical Features of Sea-Floor Topography, *Deep-Sea Research,* vol. 22, p.883-892.

------, 1979 Mesoscale Sea Floor Roughness, *Deep Sea Research,* vol. 26A, p.65-76.

Benzer, William B., Jr., 1989 **On the Use of the Variogram for the Estimation of Rock Surface Profile Fractal Dimension,** Master's Thesis, Department of Geological Engineering, University of Nevada, Reno, Nevada, 170p.

Berger, J. M., and Mandelbrot, Benoit B., 1963 A New Model for the Clustering of Errors on Telephone Circuits, *IBM Journal of Research and Development,* vol. 7, p.224-236.

Berkson, J. M., and Mathews, J. E., 1983 Statistical Properties of Sea-Floor Roughness, In N. G. Pace, (editor), **Acoustics and the Sea-Bed,** Bath University Press, Bath, Great Britain, p.215-223.

Berry, M. V., and Hannay, J. H., 1978 Topography of Random Surfaces, *Nature,* vol. 273, no. 5663, p.573.

Besicovitch, Abram S., 1929 On Linear Sets of Points of Fractional Dimension, *Mathematische Annalen,* vol. 101, p.161-193.

------, 1934a On the Sum of Digits of Real Numbers Represented in the Dyadic System (On Sets of Fractional Dimensions II), *Mathematische Annalen,* vol. 110, p.321-330.

------, 1934b Sets of Points of Non-differentiability of Absolutely Continuous Functions and of Divergence of Fejer Sums (On Linear Sets of Fractional Dimensions III),

Mathematische Annalen, vol. 110, p.331-335.

------, 1934c Sets of Fractional Dimensions (IV): On Rational Approximation to Real Numbers, *Journal of the London Mathematical Society,* vol. 9, p.126-131.

------, 1937 Sets of Fractional Dimensions (V): On Dimensional Numbers of Some Continuous Curves, *Journal of the London Mathematical Society,* vol. 12, p.18-25.

------, 1968 On Linear Sets of Points of Fractional Dimension ---- II, *Journal of the London Mathematical Society,* vol. 43, part 3, no. 171, p.548-550.

Bibby, John, 1972 Infinite Rivers and Steinhaus' Paradox, *Area,* vol. 4, no. 4, p.214.

Bills, Bruce G., and Ferrari, A. J., 1977 A Harmonic Analysis of Lunar Topography, *Icarus,* vol. 31, p.244-259.

------, and ------, 1978 Mars Topography Harmonics and Geophysical Implications, *Journal of Geophysical Research,* vol. 83, p.3497-3508.

------, and ------, 1980 A Harmonic Analysis of Lunar Gravity, *Journal of Geophysical Research,* vol. 85, p.1013-1025.

------, and Kobrick, Michael, 1985 Venus Topography: A Harmonic Analysis, *Journal of Geophysical Research,* vol. 90, p.827-836.

Birot, Pierre, 1960 **Le cycle d'erosion sous les differents climats,** (in Portuguese), Curso de Altos Estudos Geograficos 1, Centro de Pesquisas de Geografia do Brasil, Universidade do Brasil, Rio de Janeiro, Brazil, 137p.; Translated into English by C. Ian Jackson and Keith M. Clayton, 1968 **The Cycle of Erosion in Different Climates,** University of California Press, Berkeley, California, 144p.

Block, A., Von Bloh, W., Klenke, T., and Schellnhuber, H. J., 1991 Multifractal Analysis of the Microdistribution of Elements in Sedimentary Structures Using Images from Scanning Electron Microscopy and Energy Dispersive X Ray Spectrometry, *Journal of Geophysical Research,* vol. 96, no. B10, p.16223-16230.

Bolviken, B., Stokke, P. R., Feder, J., and Jossang, T., 1992 The Fractal Nature of Geochemical Landscapes, *Journal of Geochemical Exploration,* vol. 43, p.91-109.

Bowman, Isaiah, 1911 **Forest Physiography: Physiography of the United States and Principles of Soils in Relation to Forestry,** Wiley and Sons, New York, 759p.

Bradbury, R. J., and Reichelt, R. E., 1983 Fractal Dimension of a Coral Reef at Ecological Scales, *Marine Ecology Progress Series,* vol. 10, p.169-171.

------, ------, and Green, D. G., 1984 Fractals in Ecology: Methods and Interpretation, *Marine Ecology Progress Series,* vol. 14, p.295-296.

Breyer, Sean P., and Snow, R. Scott, 1992 Drainage Basin Perimeters: A Fractal Significance, *Geomorphology,* vol. 5, nos. 1/2, p.143-157.

Brooks, William Frank, 1985 **Use of the Fractal Dimension to Characterize Landforms and Their Drainage Networks,** Master's Thesis, Cornell University, Ithaca, New York, 103p.

Brown, Stephen, R., 1987a Fluid Flow through Rock Joints: The Effect of Surface Roughness, *Journal of Geophysical Research,* vol. 92, no. B2, p.1337-1347.

------, 1987b A Note on the Description of Surface Roughness Using Fractal Dimension, *Geophysical Research Letters,* vol. 14, no. 11, p.1095-1098.

------, and Scholz, Christopher H., 1985 Broad Bandwidth Study of the Topography of Natural Rock Surfaces, *Journal of Geophysical Research,* vol. 90, no. B14, p.12575-12582.

Budel, Julius, 1948 Das Systems der klimatischen Geomorphologie, *Verhandlungen Deutscher Geographentag,* vol. 27, p.65-100.

------, 1977 **Klima-Geomorphologie,** Gebruder Borntraeger, Berlin, 304p.; Translated into English by Lenore Fischer and Detlef Busche, 1982 **Climatic Geomorphology,** Princeton University Press, Princeton, New Jersey, 443p.

Bunde, Armin, and Havlin, Shlomo, (editors), 1991 **Fractals and Disordered Systems,** Springer-Verlag, Berlin, 350p.

Burgess, T. M., and Webster, R., 1980 Optimal Interpolation and Isarithmic Mapping of Soil Properties (I): The Semi-Variogram and Punctual Kriging, *Journal of Soil Science,* vol. 31, p.315-331.

Burrough, Peter A., 1981 Fractal Dimensions of Landscape and Other Environmental Data, *Nature,* vol. 294, p.240-242.

------, 1983a Multiscale Sources of Spatial Variation in Soil: I. The Application of Fractal Concepts to Nested Levels of Soil Variation, *Journal of Soil Science,* vol. 34, p.577-597.

------, 1983b Multiscale Sources of Spatial Variation in Soil: II. A Non-Brownian Fractal Model and Its Application in Soil Survey, *Journal of Soil Science,* vol. 34, p.599-620.

------, 1984 The Application of Fractal Ideas to Geophysical Phenomena, *Bulletin, the Institute of Mathematics and Its Applications,* vol. 20, nos. 3/4, p.36-42.

------, 1985 Fakes, Facsimiles and Facts: Fractal Models of Geophysical Phenomena, In Sara Nash, (editor), **Science and Uncertainty,** Proceedings of a Conference Held under the Auspices of IBM United Kingdom Ltd., London, March 1984, Science Reviews Ltd., Northwood, Great Britain, p.150-169.

------, 1989 Fractals and Geochemistry, In David Avnir, (editor), **The Fractal Approach to Heterogeneous Chemistry: Surfaces, Colloids, Polymers,** John Wiley & Sons, Chichester, Great Britain, p.383-406.

Buttenfield, Barbara, 1985 Treatment of the Cartographic Line, *Cartographica,* vol. 22, p.1-26.

Campbell, James B., 1978 Spatial Variation of Sand Content and pH within Single Contiguous Delineations of Two Soil Mapping Units, *Soil Science Society of America Journal,* vol. 42, no. 3, p.460-464.

Cannon, James W., 1984 Additional Perspectives on Fractals, *The College*

Mathematics Journal, vol. 15, no. 2, p.118-119.

Cantor, Georg, 1883 Grundlagen einer allgemeinen Mannichfaltigkeitslehre, *Mathematische Annalen,* vol. 21, p.545-591.

Carlson, Carl A., 1991 Spatial Distribution of Ore Deposits, *Geology,* vol. 19, p.111-114.

Carpenter, Loren C., 1980 Computer Rendering of Fractal Curves and Surfaces, *Computer Graphics,* vol. 14, no. 3, **SIGGRAPH'80 Conference Proceedings,** Seattle, Washington, July 14-18, 1980, Edited by James J. Thomas, p.109.

Cesaro, Ernest, 1905 Remarques sur la courbe de von Koch, *Atti della Reale Accademia delle Scienze Fisiche e Matematiche di Napoli,* vol. 12, p.1-12.

Chase, Clement G., 1992 Fluvial Landsculpting and the Fractal Dimension of Topography, *Geomorphology,* vol. 5, nos. 1/2, p.39-57.

Cherbit, Guy, (editor), 1991a **Fractals: Non-Integral Dimensions and Applications,** Originally Published in French as **Fractals: Dimensions non-entieres et applications** by Masson, Paris in 1987 and Translated into English by F. Jellett, John Wiley & Sons, Chichester, West Sussex, Great Britain, 249p.

------, 1991b Disorder, Chance and Fractals in Biology, In Guy Cherbit, (editor), **Fractals: Non-Integral Dimensions and Applications,** John Wiley & Sons, Chichester, West Sussex, Great Britain, p.145-150.

Chorley, Richard J., Schumm, Stanley A., and Sugden, David E., 1984 **Geomorphology,** Methuen & Co. Ltd., London, 605p.

Clarke, Keith C., 1986 Computation of the Fractal Dimension of Topographic Surfaces Using the Triangular Prism Surface Area Method, *Computers & Geosciences,* vol. 12, no. 5, p.713-722.

------, 1988 Scale-based Simulation of Topographic Relief, *The American Cartographer,* vol. 15, no. 2, p.173-181.

------, 1992 One Thousand Mount Everests? In Nina Siu-Ngan Lam and Lee DeCola, (editors), **Fractals in Geography,** Prentice-Hall, Englewood Cliffs, New Jersey.

------, and Schweizer, Diane M., 1991 Measuring the Fractal Dimension of Natural Surfaces Using a Robust Fractal Estimator, *Cartography and Geographic Information Systems,* vol. 18, no. 1, p.37-47.

Coleman, Paul H., 1989 The Fractal Nature of the Galaxy Distribution, In Luciano Pietronero, (editor), **Fractals' Physical Origin and Properties,** Plenum Press, New York, p.349-363.

------, and Pietronero, Luciano, 1992 The Fractal Structure of the Universe, *Physics Reports (A Review Section of Physics Letters),* vol. 231, no. 6, p.311-389.

Costa, John E., and Cleaves, Emery T., 1984 The Piedmont Landscape of Maryland: A New Look at an Old Problem, *Earth Surface Processes and Landforms,* vol. 9, p.59-74.

Crilly, Anthony J., Earnshaw, Rae A., and Jones, Huw, (editors), 1991 **Fractals and Chaos,** Springer-Verlag, New York, 277p.

Culling, W. Edward H., 1960 Analytical Theory of Erosion, *Journal of Geology,* vol. 68, p.336-344.

------, 1963 Soil Creep and the Development of Hillside Slopes, *Journal of Geology,* vol. 71, no. 2, p.127-161.

------, 1965 Theory of Erosion on Soil-Covered Slopes, *Journal of Geology,* vol. 73, p.230-254.

------, 1986a Highly Erratic Spatial Variability of Soil-pH on Iping Common, West Sussex, *Catena,* vol. 13, p.81-98.

------, 1986b On Hurst Phenomena in the Landscape, *Transactions, the Japanese Geomorphological Union,* vol. 7, no. 4, p.221-243.

------, 1987 Ergodicity, Entropy and Dimension in the Soil Covered Landscape, *Transactions, the Japanese Geomorphological Union,* vol. 8, no. 3, p.157-174.

------, 1988 Dimension and Entropy in the Soil Covered Landscape, *Earth Surface Processes and Landforms,* vol. 13, no. 7, p.619-648.

------, 1989 The Characterization of Regular/Irregular Surfaces in the Soil-Covered Landscape by Gaussian Random Fields, *Computers & Geosciences,* vol. 15, no. 2, p.219-226.

------, and Datko, Mark, 1987 The Fractal Geometry of the Soil-covered Landscape, *Earth Surface Processes and Landforms,* vol. 12, no. 4, p.369-385.

Curl, Rane L., 1960 Stochastic Models of Cavern Development, *Bulletin of the National Speleological Society,* vol. 22, part I, p.66-76.

------, 1966 Caves as a Measure of Karst, *Journal of Geology,* vol. 74, no. 5, part 2, p.798-830.

------, 1986 Fractal Dimensions and Geometries of Caves, *Mathematical Geology,* vol. 18, no. 8, p.765-784.

Davis, William Morris, 1899 The Geographic Cycle, *Geographic Journal,* vol. 14, p.481-504.

------, 1905 The Geographic Cycle in an Arid Climate, *Journal of Geology,* vol. 13, p.381-407.

Dell'Orco, Pietro, and Ghiron, Marco, 1983 Shape Representation by Rectangles Preserving Fractality, In **Proceedings of the Sixth International Symposium on Automated Cartography,** (Auto-Carto 6), Ottawa, Canada, October 16-21, 1983, vol. 2, p.299-308.

Demko, Stephen, Hodges, Laurie, and Naylor, Bruce, 1985 construction of Fractal Objects with Iterated Function Systems, *Computer Graphics,* vol. 19, no. 3, p271-278.

Derbyshire, Edward D., (editor), 1973 **Climatic Geomorphology,** Barnes & Noble,

New York, 296p.

------, (editor), 1976 **Geomorphology and Climate,** John Wiley & Sons, London, 512p.

Devaney, Robert L., 1986 **An Introduction to Chaotic Dynamical Systems,** Benjamin/Cumming, Menlo Park, California, 320p.; 1989, 2nd edition, Addison-Wesley Publishing Company, Inc., Redwood City, California, 336p.

------, 1990 **Chaos, Fractals, and Dynamics: Computer Experiments in Mathematics,** Addison-Wesley Publishing Company, Inc., Menlo Park, California, 181p.

------, and Keen, Linda, (editors), 1989 **Chaos and Fractals: The Mathematics behind the Computer Graphics,** American Mathematical Society Short Course Notes, vol. 39, American Mathematical Society, Providence, Rhode Island, 148p.

Dewdney, A. K., 1986 Computer Recreations: Of Fractal Mountains, Graftal Plants and Other Computer Graphics at Pixar, *Scientific American,* vol. 255, no. 6, p.14-20.

Drewry, David J., 1975 Terrain Units in Eastern Antarctica, *Nature,* vol. 256, no. 5514, p.194-195.

Dubois, Jacques, and Cheminee, Jean Louis, 1991 Fractal Analysis of Eruptive Activity of Some Basaltic Volcanoes, *Journal of Volcanology and Geothermal Research,* vol. 45, p.197-208.

Dubois Reymond, Paul, 1875 Versuch einer Classification der willkurlichen Functionen reeller Argument nach ihren Anderungen in den kleinsten Intervallen, *J. fur die reine und angewandte Mathematik (Crelle),* vol. 79, p.21-37.

Dutton, Geoffrey H., 1981 Fractal Enhancement of Cartographic Line Detail, *The American Cartographer,* vol. 8, no. 1, p.23-40.

Dyson, Freeman, 1978 Characterizing Irregularity, *Science,* vol. 200, no. 4342, p.677-678.

Eastman, J. Ronald, 1985 Single-Pass Measurement of the Fractal Dimension of Digitized Cartographic Lines, Presented at the Annual Meeting of the Canadian Cartographic Association, June, 1985, at Fredericton, New Brunswick, Canada, 26p.

Edgar, Gerald A., 1990 **Measure, Topology, and Fractal Geometry,** Springer-Verlag, New York, 230p.

Efstathiou, G., 1984 Fractals and Cosmology, *Bulletin, The Institute of Mathematics and Its Applications,* vol. 20, nos. 3/4, p.43-46.

Ehlen, J., 1981 The Identification of Rock Types in an Arid Region by Air Photo Patterns: U. S. Army Engineer Topographic Laboratories, Fort Belvoir, Virginia, ETL-0261.

Einstein, Albert, 1905 On the Movement of Small Particles Suspended in a Stationary Liquid Demanded by the Molecular-Kinetic Theory of Heat, *Annalen der Physik,* series 4, vol. 17, p.549-560.

Elliot, Joanne K., 1989 An Investigation of the Change in Surface Roughness

through Time on the Foreland of Austre Okstindbreen, North Norway, *Computers & Geosciences,* vol. 15, no. 2, p.209-217.

Esbenshade, Donald H., Jr., 1991 Fractal Bread, *The Physics Teacher,* vol. 29, no. 4, p.236.

Evans, Ian S., 1980 An Integrated System of Terrain Analysis and Slope Mapping, *Zeitschrift fur Geomorphologie,* Supplementband 36, p.274-295.

Evertsz, Carl J. G., and Mandelbrot, Benoit B., 1992 Multifractal Measures, in Heinz-Otto Peitgen, Hartmut Jurgens, and Dietmar Saupe, **Chaos and Fractals: New Frontiers of Science,** Springer-Verlag, New York, p.921-953.

Eyles, R. J., 1971 A Classification of West Malaysian Drainage Basins, *Annals of the Association of American Geographers,* vol. 61, no. 3, p.460-467.

Falconer, Kenneth J., 1985 **The Geometry of Fractal Sets,** Cambridge University Press, Cambridge, Great Britain, 162p.

------, 1990 **Fractal Geometry: Mathematical Foundations and Applications,** John Wiley & Sons Ltd., Chichester, Great Britain, 288p.

Feder, Jens, 1988 **Fractals,** Plenum Press, New York, 283p.

Feller, William, 1950 **An Introduction to Probability Theory and Its Applications,** Volume One, John Wiley & Sons, Inc., New York, 419p.

Fenneman, Nevin M., 1914 Physiographic Boundaries within the United States, *Annals of the Association of American Geographers,* vol. 4, p.84-134.

------, 1916 Physiographic Divisions of the United States, *Annals of the Association of American Geographers,* vol. 6, p.19-98.

------, 1928 Physiographic Divisions of the United States, *Annals of the Association of American Geographers,* vol. 18, p.261-353.

------, 1931 **Physiography of Western United States,** McGraw-Hill Book Company, Inc., New York, 534p.

------, 1938 **Physiography of Eastern United States,** McGraw-Hill Book Company, Inc., New York, 714p.

------, 1946 **Physical Divisions of the United States,** (Map), United States Geological Survey, 1 sheet.

Fischer, P., and Smith, William R., (editors), 1985 **Chaos, Fractals and Dynamics,** Lecture Notes in Pure and Applied Mathematics, vol. 98, Marcel Dekker, Inc., New York, 261p.

Fleischmann, M., Tildesley, D. J., and Ball, R. C., (editors), 1990 **Fractals in the Natural Sciences: A Discussion,** Princeton University Press, Princeton, New Jersey, 200p.

Flint, Richard Foster, 1963 Altitude and Lithology and the Fall Zone in Connecticut, *Journal of Geology,* vol. 71, p.683-697.

Foster, Allan D., 1985 **Sentenced to Prism,** Ballantine Books, New York.

Fournier, Alain, and Fussell, Don, 1980 Stochastic Modelling in Computer Graphics, *Computer Graphics,* vol. 14, no. 3, **SIGGRAPH'80 Conference Proceedings,** Seattle, Washington, July 14-18, 1980, Edited by James J. Thomas, p.108.

------, ------, and Carpenter, Loren, 1982a Computer Rendering of Stochastic Models, *Communications of the ACM,* vol. 25, no. 6, p.371-384.

------, ------, and ------, 1982b Authors' Reply, *Communications of the ACM,* vol. 25, no. 8, p.583-584.

Fowler, Anthony D., 1990 Self-Organized Mineral Textures of Igneous Rocks: The Fractal Approach, *Earth-Science Reviews,* vol. 29, p.47-55.

------, Stanley, H. Eugene, and Daccord, Gerard, 1989 Disequilibrium Silicate Mineral Textures: Fractal and Non-Fractal Features, *Nature,* vol. 341, no. 6238, p.134-138.

Fox, Christopher G., and Hayes, Dennis E., 1985 Quantitative Methods for Analyzing the Roughness of the Seafloor, *Reviews of Geophysics,* vol. 23, no. 1, p.1-48.

Frederiksen, Poul, Jacobi, Ole, and Kubik, Kurt, 1985 A Review of Current Trends in Terrain Modelling, *ITC Journal,* no. 2, p.101-106.

Freiberger, Walter, and Grenander, Ulf, 1977 Surface Patterns in Theoretical Geography, *Computers & Geosciences,* vol. 3, no. 4, p.547-578.

Frisch, U., and Parisi, G., 1985 On the Singularity Structure of Fully Developed Turbulence, In Michael Ghil, Roberto Benzi and Giorgio Parisi, (editors), **Turbulence and Predictability in Geophysical Fluid Dynamics and Climate Dynamics,** Proceedings of the International School of Physics "Enrico Fermi," Course 88, Varenna, Italy, June 14-24, 1983, North Holland, Amsterdam, p.84-88.

Gardner, Martin, 1976 Mathematical Games: In Which "Monster" Curves Force Redefinition of the Word "Curve", *Scientific American,* vol. 235, no. 6, p.124-133.

Geilikman, M. B., Golubeva, T. V., and Pisarenko, V. F., 1990 Multifractal Patterns of Seismicity, *Earth and Planetary Science Letters,* vol. 99, p.127-132.

Gerard, A. John, 1988 **Rocks and Landforms,** Unwin Hyman, London, 319p.

Gierhart, John W., 1954 Evaluation of Methods of Area Measurement, *Surveying and Mapping,* vol. 14, p.460-465.

Gilbert, Lewis E., 1989 Are Topographic Data Sets Fractal? *Pure and Applied Geophysics,* vol. 131, nos. 1/2, p.241-254.

------, and Malinverno, Alberto, 1988 A Characterization of the Spectral Density of Residual Ocean Floor Topography, *Geophysical Research Letters,* vol. 15, no. 12, p.1401-1404.

Gleick, James, 1987 **Chaos: Making a New Science,** Penguin Books, New York, 352p.

Goff, John A., 1990 Comment on "Fractal Mapping of Digital Images: Application to the Topography of Arizona and Comparison with Synthetic Images" by J. Huang and D. L. Turcotte, *Journal of Geophysical Research,* vol. 95, no. B4, p.5159.

Goodchild, Michael F., 1980 Fractals and the Accuracy of Geographical Measures, *Mathematical Geology,* vol. 12, no. 2, p.85-98.

------, 1982 The Fractional Brownian Process as a Terrain Simulation Model, *Modelling and Simulation,* vol. 13, p.1133-1137.

------, 1988 Lakes on Fractal Surfaces: A Null Hypothesis for Lake-Rich Landscapes, *Mathematical Geology,* vol. 20, no. 6, p.615-630.

------, and Grandfield, Andrew W., 1983 Optimizing Raster Storage: An Examination of Four Alternatives, In **Proceedings of the Sixth International Symposium on Automated Cartography,** (Auto-Carto 6), Ottawa, Canada, October 16-21, 1983, vol. 1, p.400-407.

------, and Mark, David M., 1987 The Fractal Nature of Geographic Phenomena: *Annals of the Association of American Geographers,* vol. 77, no. 2, p.265-278.

Graf, William L., (editor), 1987 **Geomorphic Systems of North America,** Centennial Special Volume 2, The Geological Society of America, Inc., Boulder, Colorado, 643p.

Hack, John T., 1957 **Studies of Longitudinal Streams in Virginia and Maryland,** U. S. Geological Survey Professional Papers, No. 294B, 97p.

Hahn, Hans, 1956 The Crisis in Intuition, in James R. Newman, (editor), **The World of Mathematics,** Simon and Schuster, New York, vol. III, p.1956-1976.

Hakanson, Lars, 1978 The Length of Closed Geomorphic Lines, *Mathematical Geology,* vol. 10, no. 2, p.141-167.

------, 1981 The Length of Open Geomorphic Lines: *Zeitschrift fur Geomorphologie,* vol. 25, no. 4, p.369-382.

Hallet, Bernard, 1990 Spatial Self-Organization in Geomorphology: From Periodic Bedforms and Patterned Ground to Scale-Invariant Topography, *Earth-Science Reviews,* vol. 29, p.57-75.

Hammond, Edwin H., 1954 Small-Scale Continental Landform Maps, *Annals of the Association of American Geographers,* vol. 44, no. 1, p.33-42.

------, 1964 Analysis of Properties in Land Form Geography: An Application to Broad-Scale Land Form Mapping, *Annals of the Association of American Geographers,* vol. 54, no. 1, p.11-19.

Hansen, Jan Peter, McCauley, J. L., Muller, Jiri, and Skjeltorp, A. T., 1988 Multifractal Analysis of Sedimentary Rocks, In H. Eugene Stanley and Nicole Ostrowsky, (editors), **Random Fluctuations and Pattern Growth: Experiments and Models,** Kluwer Academic Publishers, Dordrecht, The Netherlands, p.310.

Harrington, Steven, 1987 **Computer Graphics ---- A Programming Approach,** McGraw Hill, New York, 448p.

Hausdorff, Felix, 1919 Dimension und ausseres Mass, *Mathematische Annalen,* vol. 79, p.157-179.

Hearn, Donald, and Baker, M. Pauline, 1986 **Computer Graphics,** Prentice-Hall, Englewood Cliffs, New Jersey, 352p.

Heck, Andre, and Perdang, Jean M., (editors), 1991 **Applying Fractals in Astronomy,** Lecture Notes in Physics, New Series m: Monographs, vol. m3, Springer-Verlag, Berlin, 210p.

Hermite, Charles, and Stieltjes, Thomas J., 1905 **Correspondence d'Hermite et de Stieltjes,** Edited by B. Baillaud and H. Bourget, Gauthier-Villars, Paris, vol. II, p.318.

Hewett, T. A., 1986 Fractal Distributions of Reservoir Heterogeneity and Their Influence on Fluid Transport, *Society of Petroleum Engineers Paper 15386,* 16p.

Hilbert, David, 1891 Ueber die stetige Abbildung einer Linie auf ein Flachenstuck, *Mathematische Annalen,* vol. 38, p.459-460.

Hill, F., Jr., and Walker, S. E., Jr., 1982 On the Use of Fractals for Efficient Map Generation, **Proceedings of Graphics Interface'82,** Toronto, Ontario, May 17-21, 1982, p.283-289.

Hirata, Takayuri, and Imoto, Masajiro, 1991 Multifractal Analysis of Spatial Distribution of Microearthquakes in the Kanto Region, *Geophysical Journal International,* vol. 107, p.155-162.

Hjelmfelt, Allen T., Jr., 1988 Fractals and the River-Length Catchment-Area Ratio, *Water Resources Bulletin,* vol. 24, no. 2, p.455-459.

Houck, Dewey Rush II, 1983 **Use of the Fractal Dimension in Characterization of Terrestrial Surfaces,** Master's Thesis, Department of Civil Engineering, Virginia Polytechnic Institute and State University, 128p.

Hough, Sue E., 1990 Estimating the Fractal Dimension of Topographic Profiles, *EOS (Transactions, American Geophysical Union),* vol. 71, no. 17, p.466.

Huang, Jie, and Turcotte, Donald L., 1988 Fractal Distribution of Stress and Strength and Variations of b-Value, *Earth and Planetary Science Letters,* vol. 91, p.223-230.

------, and ------, 1989 Fractal Mapping of Digitized Images: Application to the Topography of Arizona and Comparisons with Synthetic Images, *Journal of Geophysical Research,* vol. 94, no. B6, p.7491-7495.

------, and ------, 1990 Reply, *Journal of Geophysical Research,* vol. 95, no. B4, p.5161.

Hugus, Mark K., and Mark, David M., 1985 Digital Simulation of Three-Dimensional Landscape Evolution, *Modelling and Simulation,* vol. 16, part I, p.305-309.

Hunt, Charles B., 1967 **Physiography of the United States,** W. H. Freeman and Company, San Francisco, 480p.

------, 1974 **Natural Regions of the United States and Canada,** W. H. Freeman and

Company, San Francisco, 725p.

Hurd, Alan J., Weitz, David A., and Mandelbrot, Benoit B., (editors), 1987 **Fractal Aspects of Materials: Extended Abstracts of the 1987 Fall Meeting of the Materials Research Society,** Boston, Massachusetts, December 1-4, 1987, Materials Research Society, Pittsburgh, Pennsylvania, 208p.

Hurst, Harold Edwin, 1951 Long-Term Storage Capacity of Reservoirs, *Transactions of the American Society of Civil Engineers,* vol. 116, p.770-808.

------, 1955 Methods of Using Long-Term Storage in Reservoirs, *Proceedings of the Institution of Civil Engineers,* Part I, p.519-577.

Ito, Keisuke, and Matsuzaki, Mitsuhiro, 1990 Earthquakes as Self-Organized Critical Phenomena, *Journal of Geophysical Research,* vol. 95, no. B5, p.6853-6860.

Jeffery, Tom, 1987 Mimicking Mountains, *Byte,* vol. 12, no. 14, p.337-344.

Jennings, Joseph Newell, 1985 **Karst Geomorphology,** 2nd edition, Basil Blackwell, Oxford, Great Britain, 293p.

Joerg, Wolfgang L. G., 1914 The Subdivision of North America into Natural Regions: A Preliminary Inquiry, *Annals of the Association of American Geographers,* vol. 4, p.55-83.

Jones, Huw, 1991 Fractals before Mandelbrot, In Anthony J. Crilly, Rae A. Earnshaw and Huw Jones, (editors), **Fractals and Chaos,** Springer-Verlag, New York, p.7-33.

Journel, Andre G., and Huijbregts, Charles J., 1978 **Mining Geostatistics,** Academic Press, Inc., London, 600p.

Jullien, R., and Botet, R., 1987 **Aggregation and Fractal Aggregates,** World Scientific, Singapore, 120p.

Jurdy, Donna M., and Stefanick, Michael, 1990 Models for the Hotspot Distribution, *Geophysical Research Letters,* vol. 17, no. 11, p.1965-1968.

Kadanoff, Leo P., 1986 Fractals: Where's the Physics? *Physics Today,* February issue, p.6-7.

Kagan, Yan Y., 1981 Spatial Distribution of Earthquakes: The Three-Point Moment Function, *Geophysical Journal of the Royal Astronomical Society,* vol. 67, no. 3, p.697-717.

------, and Knopoff, L., 1980 Spatial Distribution of Earthquakes: The Two-Point Correlation Function, *Geophysical Journal of the Royal Astronomical Society,* vol. 62, p.303-320.

------, and ------, 1981 Stochastic Synthesis of Earthquake Catalogs, *Journal of Geophysical Research,* vol. 86, no. B4, p.2853-2862.

------, and Jackson, David D., 1991 Long-Term Earthquake Clustering, *Geophysical Journal International,* vol. 104, p.117-133.

Katz, A. J., and Thompson, A. H., 1985 Fractal Sandstone Pores: Implications for

Conductivity and Pore Formation, *Physical Review Letters,* vol. 54, no. 12, p.1325-1328.

Kaufman, J. H., Martin, James E., and Schmidt, P. W., (editors), 1989 **Fractal Aspects of Materials: Extended Abstracts of the 1989 Fall Meeting of the Materials Research Society,** Boston, Massachusetts, November 28 - December 1, 1989, Materials Research Society, Pittsburgh, Pennsylvania, 288p.

Kaye, Brian H., 1989 **A Random Walk through Fractal Dimensions,** VCH Verlagsgesellschaft, Weinheim, Federal Republic of Germany, and VCH Publishers, New York, 421p.

------, and Clark, Garry G., 1985 Fractal Description of Extra Terrestrial Fineparticles, *Particle Characterization,* vol. 2, p.143-148.

Kent, Clement, and Wong, Jonathan, 1982 An Index of Littoral Zone Complexity and Its Measurement, *Canadian Journal of Fisheries and Aquatic Sciences,* vol. 39, p.847-853.

King, Geoffrey C. P., 1983 The Accommodation of Large Strains in the Upper Lithosphere of the Earth and Other Solids by Self-Similar Fault Systems: The Geometric Origin of b-Value, *Pure and Applied Geophysics,* vol. 121, nos. 5/6, p.761-815.

Kirkby, Michael J., 1987 The Hurst Effect and Its Implications for Extrapolating Process Rates, *Earth Surface Processes and Landforms,* vol. 12, p.57-67.

Klemes, V., 1974 The Hurst Phenomenon: A Puzzle? *Water Resources Research,* vol. 10, no. 4, p.675-688.

Kline, S. A., 1945 On Curves of Fractional Dimensions, *The Journal of the London Mathematical Society,* vol. 20, part 2, no. 78, p.79-86.

Klinkenberg, Brian, 1988 **Tests of a Fractal Model of Topography,** Ph. D. Dissertation, University of Western Ontario, Canada.

------, 1992 Fractals and Morphometric Measures: Is There a Relationship? *Geomorphology,* vol. 5, nos. 1/2, p.5-20.

------, and Goodchild, Michael F., 1992 The Fractal Properties of Topography: A Comparison of Methods, *Earth Surface Processes and Landforms,* vol. 17, p.217-234.

------, and Clarke, Keith C., 1992 Exploring the Fractal Mountains, In I. Palaz and S. Sengupta, (editors), **Automated Pattern Recognition in Geophysical Exploration,** Society of Exploration Geophysics.

Krantz, Steven G., 1989 Fractal Geometry, *The Mathematical Intelligencer,* vol. 11, no. 4, p.12-16.

Krohn, C. E., 1988 Fractal Measurements of Sandstones, Shales and Carbonates, *Journal of Geophysical Research,* vol. 93, p.3297-3305.

Kukuk, Penelope F., 1980 **How Vertebrates Search for Small Prey?** Ph. D. Dissertation, University of Kansas, Lawrence, Kansas, 186p.

La Barbera, Paolo, and Rosso, Renzo, 1989 On the Fractal Dimension of Stream

Networks, *Water Resources Research,* vol. 25, no. 4, p.735-741.

------, and ------, 1990 Reply, *Water Resources Research,* vol. 26, no. 9, p.2245-2248.

La Brecque, Mort, 1986/7 Fractal Applications, *Mosaic,* vol. 17, no. 4, p.34-48.

Laibowitz, Robert B., Mandelbrot, Benoit B., and Passoja, Dann E., (editors), 1985 **Extended Abstracts: Fractal Aspects of Materials, Proceedings of Symposium N 1985 Fall Meeting of the Materials Research Society,** Boston, Massachusetts, December 2-4, 1985, Materials Research Society, Pittsburgh, Pennsylvania, 127p.

Lam, Nina Siu-Ngan, and DeCola, Lee, (editors), 1992 **Fractals in Geography,** Prentice-Hall, Englewood Cliffs, New Jersey.

Lauwerier, Hans, 1991 **Fractals: Endlessly Repeated Geometrical Figures,** Originally Published in Dutch as **Fractals: Meetkundige figuren in eindeloze herhaling,** in 1987 and Translated into English by Sophia Gill-Hoffstadt, Princeton University Press, Princeton, New Jersey, 209p.

Laverty, Martin, 1987 Fractals in Karst, *Earth Surface Processes and Landforms,* vol. 12, p.475-480.

Le Mehaute, Alain, 1991 **Fractal Geometries: Theory and Applications,** Originally Published in French as **Les Geometries Fractales: L'espace-temps brise** by Hermes, Paris in 1990 and Translated into English by Jack Howlett, CRC Press Inc., Boca Raton, Florida, 181p.

Leary, Peter, 1991 Deep Borehole Log Evidence for Fractal Distribution of Fractures in Crystalline Rock, *Geophysical Journal International,* vol. 107, p.615-627.

Lebesgue, Henri Leon, 1903-1905 Sur le probleme des aires, *Bulletin de la Societe Mathematique de France,* vol. 31, p.197-203; vol. 33, p.273-274.

Lefevre, Jacques, 1983 Teleonomical Optimization of a Fractal Model of the Pulmonary Arterial Bed, *Journal of Theoretical Biology,* vol. 102, p.225-248.

------, and Barreto, J., 1983 Reduced and Teleonomical Models in Cardiovascular Physiology, In Ghislain C. Vansteenkiste and Peter C. Young, (editors), **Modelling and Data Analysis in Biotechnology and Medical Engineering,** Proceedings of the IFIP (International Federation for Information Processing) WG 7.1 (Working Group on Modelling and Simulation) Working Conference on Modelling and Data Analysis in Biotechnology and Medical Engineering Held in Ghent, Belgium, August 31 - September 2, 1982, North-Holland Publishing Company, Amsterdam, The Netherlands, p.27-37.

------, ------, and Gonze, P., 1982 Teleonomical Representation of Arterial Beds by Fractal Symmetric and Asymmetric Trees, In A. Ballester, D. Cardus and E. Trillas, (editors), **Proceedings of the 2nd World Conference on Maths at the Service of Man,** Las Palmas, p.435-443.

------, ------, ------, Dawant, B., and Alexandre, X., 1983 Optimal Features of Arterial Systems: Input Impedance, in **Proceedings of the 36th ACEMB,** Columbus, 40.4, p.205.

Lemaitre, R., and Adler, P. M., 1990 Fractal Porous Media IV: Three-Dimensional

Stokes Flow through Random Media and Regular Fractals, *Transport in Porous Media,* vol. 5, p.325-340.

Levy, Paul, 1939 Sur Certains Processus Stochastiques Homogenes, *Compositio Mathematica,* vol. 7, p.283-339.

------, 1948 **Processus Stochastiques et Mouvement Brownien,** Gauthier-Villars, Paris, 365p.

------, 1959 Le mouvement brownien fonction d'un point de la sphere de Riemann, *Rendiconti del Circolo matematico di Palermo,* Serie II, Tomo VIII, Fascicolo III, p.297-310.

Lifton, Nathaniel A., and Chase, Clement G., 1992 Tectonic, Climatic and Lithologic Influences on Landscape Fractal Dimension and Hypsometry: Implications for Landscape Evolution in the San Gabriel Mountains, California, *Geomorphology,* vol. 5, nos. 1/2, p.77-114.

Linton, D. L., 1951 The Delimitation of Morphological Regions: In L. D. Stamp and S. W. Wooldridge, (editors), **London Essays in Geography,** Longman, London, p.199-217.

Liu, Tanzhuo, 1992 Fractal Structure and Properties of Stream Networks, *Water Resources Research,* vol. 28, no. 11, p.2981-2988.

Lloyd, E. H., 1967 Stochastic Reservoir Theory, *Advanced Hydroscience,* vol. 4, p.281-339.

Loehle, Craig, 1983 The Fractal Dimension and Ecology, *Speculations in Science Technology,* vol. 6, p.131-142.

Longley, Paul A., and Batty, Michael, 1989a Fractal Measurement and Line Generalization, *Computers & Geosciences,* vol. 15, p.167-183.

------, and ------, 1989b On the Fractal Measurement of Geographic Boundaries, *Geographic Analysis,* vol. 21, no. 1, p.47-67.

------, ------, and Shepherd, John, 1990 The Size, Shape and Dimension of Urban Settlements: Presented at the Annual Meeting of the Association of American Geographers Held in Toronto, Canada, April 19-22, 1990, 43p.

Loomis, F. K., 1937 **Physiography of the United States,** Doran and Company, Doubleday, 350p.

Lovejoy, S., 1982 Area-Perimeter Relation for Rain and Cloud Areas, *Science,* vol. 216, p.185-187.

------, and Mandelbrot, Benoit, 1985 Fractal Properties of Rain, and a Fractal Model, *Tellus,* vol. 37A, p.209-232.

------, and Schertzer, D., 1986 Scale Invariance, Symmetries, Fractals, and Stochastic Simulations of Atmospheric Phenomena, *Bulletin of American Meteorological Society,* vol. 67, p.21-32.

Maling, Derek H., 1968 How Long is a Piece of String? *The Cartographic Journal,*

vol. 5, p.147-156.

Malinverno, Alberto, 1989a Testing Linear Models of Sea-Floor Topography, *Pure and Applied Geophysics,* vol. 131, nos. 1/2, p.139-155.

------, 1989b Fractals and Ocean Floor Topography, In **Annual Report of Lamont-Doherty Geological Observatory of Columbia University,** Palisades, New York, p.39-43.

------, 1990 A Simple Method to Estimate the Fractal Dimension of a Self-Affine Series, *Geophysical Research Letters,* vol. 17, no. 11, p.1953-1956.

Mandelbrot, Benoit B., 1960 The Pareto-Levy Law and the Distribution of Income, *International Economic Review,* vol. 1, p.79-106.

------, 1961 Stable Paretian Random Functions and the Multiplicative Variation of Income, *Econometrica,* vol. 29, p.517-543.

------, 1962 Paretian Distributions and Income Maximization, *Quarterly Journal of Economics of Harvard University,* vol. 76, p.57-85.

------, 1963a The Stable Paretian Income Distribution, When the Apparent Exponent Is near Two, *International Economic Review,* vol. 4, p.111-115.

------, 1963b The Variation of Certain Speculative Prices, *Journal of Business,* vol. 36, p.394-419.

------, 1963c New Methods in Statistical Economics, *The Journal of Political Economy,* vol. 71, no. 5, p.421-440.

------, 1965a Self Similar Error Cluster in Communications Systems and the Concept of Conditional Stationarity, *IEEE Transactions on Communications Technology,* vol. 13, p.71-90.

------, 1965b Une classe de processus stochastiques homothetiques a soi: application a la loi climatologique de H. E. Hurst, *Comptes Rendus* (Paris), vol. 260, p.3274-3277.

------, 1966 Forecasts of Future Prices, Unbiased Markets, and 'Martingale' Models, *Journal of Business,* vol. 39, p.242-255.

------, 1967a The Variation of Some Other Speculative Prices, *Journal of Business,* vol. 40, p.393-413.

------, 1967b How Long Is the Coast of Britain? *Science,* vol. 156, no. 3775, p.636-638.

------, 1971 A Fast Fractional Gaussian Noise Generator, *Water Resources Research,* vol. 7, p.543-553.

------, 1972 Possible Refinement of the Lognormal Hypothesis Concerning the Distribution of Energy Dissipation in Intermittent Turbulence, In M. Rosenblatt and C. Van Atta, (editors), **Statistical Models and Turbulence,** Lecture Notes in Physics, Springer-Verlag, New York, vol. 12, p.333-351.

------, 1974 Intermittent Turbulence in Self-Similar Cascades: Divergence of High

Moments and Dimension of the Carrier, *Journal of Fluid Mechanics,* vol. 62, p.331-358.

------, 1975a On the Geometry of Homogeneous Turbulence, With Stress on the Fractal Dimension of the Iso-Surfaces of Scalars, *Journal of Fluid Mechanics,* vol. 72, p.401-416.

------, 1975b **Les Objets Fractals: Forme, Hasard et Dimension,** Flammarion, Paris, 190p.

------, 1975c Stochastic Models for the Earth's Relief, the Shape and Fractal Dimension of the Coastlines, and the Number-area Rule for Islands, *Proceedings of National Academy of Science, USA,* vol. 72, no. 10, p.3825-3828.

------, 1976 Intermittent Turbulence & Fractal Dimension: Kurtosis and the Spectral Exponent 5/3+B, In R. Teman, (editor), **Turbulence and Navier-Stokes Equations,** Lecture Notes in Mathematics, Springer-Verlag, New York, vol. 565, p.121-145.

------, 1977 **Fractals: Form, Chance, and Dimension,** W. H. Freeman and Company, San Francisco, 365p.

------, 1982 Comment on Computer Rendering of Fractal Stochastic Models, *Communications of the ACM,* vol. 25, no. 8, p.581-583.

------, 1983 **The Fractal Geometry of Nature,** W. H. Freeman and Company, New York, 468p.

------, 1985 Self-Affine Fractals and Fractal Dimension, *Physica Scripta,* vol. 32, p.257-260.

------; 1986a Self-Affine Fractal Sets I: The Basic Fractal Dimensions, In Luciano Pietronero and Erio Tosatti, (editors), **Fractals in Physics,** North-Holland Physics Publishing, Amsterdam, The Netherlands, p.3-15.

------; 1986b Self-Affine Fractal Sets II: Length and Surface Dimensions, In Luciano Pietronero and Erio Tosatti, (editors), **Fractals in Physics,** North-Holland Physics Publishing, Amsterdam, The Netherlands, p.17-20.

------; 1986c Self-Affine Fractal Sets III: Hausdorff Dimension Anomalies and Their Implications, in Luciano Pietronero and Erio Tosatti, (editors), **Fractals in Physics,** North-Holland Physics Publishing, Amsterdam, The Netherlands, p.21-28.

------; 1986d Multifractals and Fractals, *Physics Today,* September issue, p.11-13.

------, 1987 Fractals, In Robert A. Meyers, (editor), **Encyclopedia of Physical Science and Technology,** Academic Press, Inc., Orlando, Florida, vol. 5, p.579-593.

------, 1988a, People and Events behind the "Science of Fractal Images," In Heinz-Otto Peitgen and Dietmar Saupe, (editors), **The Science of Fractal Images,** Springer-Verlag, New York, p.1-19.

------, 1988b Fractal Landscapes without Creases and With Rivers, In Heinz-Otto Peitgen and Dietmar Saupe, (editors), **The Science of Fractal Images,** Springer-Verlag, New York, p.243-260.

------, 1989a An Introduction to Multifractal Distribution Functions, In H. Eugene Stanley and Nicole Ostrowsky, (editors), **Random Fluctuations and Pattern Growth: Experiments and Models,** Proceedings of the NATO Advanced Study Institute on Random Fluctuations and Pattern Growth: Experiments and Models, Cargese, Corsica, France, July 18-31, 1988, NATO ASI Series E: Applied Sciences, vol. 157, Kluwer Academic Publishers, Dordrecht, The Netherlands, p.279-291.

------, 1989b Multifractal Measures, Especially for the Geophysicist, *Pure and Applied Geophysics,* vol. 131, nos. 1/2, p.5-42.

------, 1989c Some "Facts" that Evaporate upon Examination, *The Mathematical Intelligencer,* vol. 11, no. 4, p.17-19.

------, 1991 Sundry Observations, In Guy Cherbit, (editor), **Fractals: Non-Integral Dimensions and Applications,** John Wiley & Sons, Chichester, West Sussex, Great Britain, p.3-9.

------, 1992 Fractals and the Rebirth of Experimental Mathematics, In Heinz-Otto Peitgen, Hartmut Jurgens and Dietmar Saupe, **Fractals for the Classroom, Part One: Introduction to Fractals and Chaos,** Springer-Verlag, New York, p.1-16.

------, and Passoja, Dann E., (editors), 1984 **Extended Abstracts: Fractal Aspects of Materials ---- Metal and Catalyst Surfaces, Powders and Aggregates, Proceedings of Symposium P 1984 Fall Meeting of the Materials Research Society,** Boston, Massachusetts, November 26-27, 1984, Materials Research Society, Pittsburgh, Pennsylvania, 47p.

------, and Van Ness, John W., 1968 Fractional Brownian Motions, Fractional Noises and Applications, *Siam Review,* vol. 10, no. 4, p.422-437.

------, and Wallis, James R., 1968 Noah, Joseph and Operational Hydrology, *Water Resources Research,* vol. 4, p.909-918.

------, and ------, 1969a Computer Experiments with Fractional Gaussian Noises: (three parts), *Water Resources Research,* vol. 5, p.228-267.

------, and ------, 1969b Some Long-Run Properties of Geophysical Records, *Water Resources Research,* vol. 5, p.321-340.

------, and ------, 1969c Robustness of the Rescaled Range R/S in the Measurement of Noncyclic Long Run Statistical Dependence, *Water Resources Research,* vol. 5, p.967-988.

Mareschal, Jean-Claude, 1989 Fractal Reconstruction of Sea-Floor Topography, *Pure and Applied Geophysics,* vol. 131, nos. 1/2, p.197-210.

Mark, David M., 1975 Geomorphometric Parameters: A Review and Evaluation, *Geografiska Annaler,* vol. 57A, p.165-177.

------, 1978 Comments on Freiberger and Grenander's "Surface Patterns in Theoretical Geography", *Computers & Geosciences,* vol. 4, p.371-372.

------, 1979 A Review of "Fractals: Form, Chance and Dimension" by Benoit Mandelbrot, *Geo-Processing,* vol. 1, no. 2, p.202-204.

------, 1980 On Scales of Investigation in Geomorphology, *The Canadian Geographer,* vol. 24, no. 1, p.81-82.

------, 1984 Fractal Dimension of a Coral Reef at Ecological Scales: A Discussion, *Marine Ecology Progress Series,* vol. 14, p.293-294.

------, and Aronson, Peter B., 1984 Scale-Dependent Fractal Dimensions of Topographic Surfaces: An Empirical Investigation, with Applications in Geomorphology and Computer Mapping, *Mathematical Geology,* vol. 16, no. 7, p.671-683.

Marrett, Randall, and Allmendinger, Richard W., 1992 Amount of Extension on "Small" Faults: An Example from the Viking Graben, *Geology,* vol. 20, p.47-50.

Matheron, Georges, 1963 Principles of Geostatistics, *Economic Geology,* vol. 58, no. 8, p.1246-1266.

Matsumoto, Naoko, Yomogida, Kiyoshi, and Honda, Satoru, 1992 Fractal Analysis of Fault Systems in Japan and the Philippines, *Geophysical Research Letters,* vol. 19, no. 4, p.357-360.

Matsushita, Mitsugu, and Ouchi, Shunji, 1989 On the Self-Affinity of Various Curves, *Physica D,* vol. 38, p.246-251.

Mayer, Larry, 1992 Fractal Characteristics of Desert Storm Sequences and Implications for Geomorphic Studies, *Geomorphology,* vol. 5, nos. 1/2, p.167-183.

McClelland, Steven, 1985 Using Fractals to Measure the Progress of Erosion, *Proceedings of the West Virginia Academy of Science,* vol. 57, p.91-95.

McClure, Matthew, 1985 Computer Illusions: Fractals Make Mathematical Magic in the Movies, *Popular Computing,* p.49-52.

McDermott, Jeanne, 1983 Geometrical Forms Known as Fractals Find Sense in Chaos, *Smithsonian,* vol. 14, no. 9, p.110-117.

McKee, Edwin D., (editor), 1979 **A Study of Global Sand Seas,** U. S. Geological Survey Professional Paper 1052, United States Government Printing Office, Washington, D. C., 429p.

Mckinney, Michael L., and Frederick, Daniel, 1992 Extinction and Population Dynamics: New Methods and Evidence from Paleogene Foraminifera, *Geology,* vol. 20, p.343-346.

Merceron, Thierry, and Velde, Bruce, 1991 Application of Cantor's Method for Fractal Analysis of Fractures in the Toyoha Mine, Hokkaido, Japan, *Journal of Geophysical Research,* vol. 96, no. B10, p.16641-16650.

Middleton, Gerard V., (editor), 1991 **Nonlinear Dynamics, Chaos and Fractals with Applications to Geological Systems,** Geological Association of Canada Short Course Notes, vol. 9, Geological Association of Canada, St. John's, Newfoundland, 235p.

Miller, Gavin S. P., 1986 The Definition and Rendering of Terrain Maps, *Computer Graphics,* vol. 20, no. 4, p.39-48.

Milne, Bruce T., 1988 Measuring the Fractal Geometry of Landscapes, *Applied*

Mathematics and Computation, vol. 27, p.67-79.

Moon, Francis C., 1987 **Chaotic Vibrations: An Introduction for Applied Scientists and Engineers,** John Wiley & Sons, New York, 309p.

Moore, Eliakim Hastings, 1900 On Certain Crinkly Curves, *Transactions of the American Mathematical Society,* vol. 1, p.72-90.

Moore, I. D., Grayson, R. B., and Ladson, A. R., 1991 Digital Terrain Modelling: A Review of Hydrological, Geomorphological, and Biological Applications, *Hydrological Processes,* vol. 5, p.3-30.

Morse, David R., Lawton, J. H., Dodson, M. M., and Williamson, M. H., 1985 Fractal Dimension of Vegetation and the Distribution of Arthropod Body Lengths, *Nature,* vol. 314, p.731-733.

Mottinger, N. A., Sjogren, W. L., and Bills, Bruce G., 1985 Venus Gravity: A Harmonic Analysis and Geophysical Implications, In Graham Ryder, (editor), **Proceedings of the Fifteenth Lunar and Planetary Science Conference,** Houston, Texas, March 12-16, 1984, *Journal of Geophysical Research,* vol. B90, Supplement, p.C739-C756.

Muller, Jean-Claude, 1986 Fractal Dimension and Inconsistencies in Cartographic Line Representations, *The Cartographic Journal,* vol. 23, p.123-130.

------, 1987 Fractal and Automated Line Generalization, *The Cartographic Journal,* vol. 24, p.27-34.

Nakano, Takanori, 1983 A "Fractal" Study of Some Rias Coastline in Japan, In **Annual Report, Institute of Geoscience, The University of Tsukuba, for the Academic Year 1982,** No. 9, p.75-80.

------, 1984 A Systematics of "Transient Fractals" of Rias Coastlines: An Example of Rias Coast from Kamaishi to Shizugawa, Northeastern Japan, In **Annual Report, Institute of Geoscience, The University of Tsukuba,** No. 10, p.66-68.

Newman, W. I., and Turcotte, Donald L., 1990 Cascade Model for Fluvial Geomorphology, *Geophysical Journal International,* vol. 100, p.433-439.

Nikora, Vladimir I., 1991 Fractal Structures of River Plan Forms, *Water Resources Research,* vol. 27, no. 6, p.1327-1333.

Norton, Alan, 1982 Generation and Display of Geometric Fractals in 3-D, *Computer Graphics,* vol. 16, no. 3, p.61-67.

Norton, Denis, and Sorenson, Steve, 1989 Variations in Geometric Measures of Topographic Surfaces Underlain by Fractured Granitic Plutons, *Pure and Applied Geophysics,* vol. 131, nos. 1/2, p.77-97.

Ogievsky, A. V., 1951 **Dry Land Hydrology,** Selkhozgiz, Moscow.

Okubo, Paul G., and Aki, Keiiti, 1987 Fractal Geometry in the San Andreas Fault System, *Journal of Geophysical Research,* vol. 92, no. B1, p.345-355.

Oliver, Margaret A., and Webster, R., 1986 Semi-Variograms for Modelling the Spatial Pattern of Landform and Soil Properties, *Earth Surface Processes and Landforms,*

vol. 11, p.491-504.

Oppenheimer, Peter E., 1986 Real Time Design and Animation of Fractal Plants and Trees, *Computer Graphics,* vol. 20, no. 4, p.55-64.

Orey, Steven, 1970 Gaussian Sample Functions and the Hausdorff Dimension of Level Crossings, *Zeitschrift fur Wahrscheinlichkeitstheorie und verwandte Gebiete,* vol. 15, no. 3, p.249-256.

Orford, Julian D., and Whalley, W. Brian, 1983 The Use of the Fractal Dimension to Quantify the Morphology of Irregular-Shaped Particles, *Sedimentology,* vol. 30, p.655-668.

Osgood, William F., 1903 A Jordan Curve of Positive Area, *Transactions of the American Mathematical Society,* vol. 4, p.107-112.

Ouchi, Shunji, 1990 Self-Affinity of Landform and Its Measurement, In **Geographical Reports of Tokyo Metropolitan University,** No. 25, p.67-80.

------, and Matsushita, Mitsugu, 1992 Measurement of Self-Affinity on Surfaces as a Trial Application of Fractal Geometry to Landform Analysis, *Geomorphology,* vol. 5, nos. 1/2, p.115-130.

Palaz, I., and Sengupta, S., (editors), 1992 **Automated Pattern Recognition in Geophysical Exploration,** Society of Exploration Geophysicists.

Paumgartner, D., Losa G., and Weibel, E. R., 1981 Resolution Effect on the Stereological Estimation of Surface and Volume and Its Interpretation in Terms of Fractal Dimensions, *Journal of Microscopy,* vol. 121, p.51-63.

Peano, Giuseppe, 1890 Sur une courbe, qui remplit toute une aire plane, *Mathematische Annalen,* vol. 36, p.157-160, Translated into English by Hubert C. Kennedy and Included in Hubert C. Kennedy, (editor), 1973 **Selected Works of Giuseppe Peano,** University of Toronto Press, Toronto, Canada, p.143-148.

Peitgen, Heinz-Otto, and Richter, Peter H., 1986 **The Beauty of Fractals: Images of Complex Dynamical Systems,** Springer-Verlag, Berlin, 199p.

------, and Saupe, Dietmar, (editors), 1988 **The Science of Fractal Images,** Springer-Verlag, New York, 312p.

------, Jurgens, Hartmut, and Saupe, Dietmar, 1992a **Fractals for the Classroom, Part One: Introduction to Fractals and Chaos,** Springer-Verlag, New York, 450p.

------, ------, and ------, 1992b **Chaos and Fractals: New Frontiers of Science,** Springer-Verlag, New York, 984p.

------, ------, ------, Maletsky, Evan, Perciante, Terry, and Yunker, Lee, 1991 **Fractals for the Classroom: Strategic Activities,** vol. 1, 128p.

Peleg, M., and Normand, M. D., 1985 Characterisation of the Ruggedness of Instant Coffee Particle-Shape by Natural Fractals, *Journal of Food Science,* vol. 50, no. 3, p.829-831.

Penck, Walther, 1924 **Die morphologische Analyse: ein Kapitel der physikalischen**

Geologie, J. Engelhorns Nachf, Stuttgart, 283p; Translated into English by Hella Czech and Katharine Cumming Boswell, 1953 **Morphological Analysis of Landforms: A Contribution to Physical Geology,** Macmillan and Co., Limited, London, 429p.

Peng, Zhizhong, 1986a The Deduction of Quasicrystal Lattice and the Fractal Structure Model of Quasicrystal, *Scientia Geologica Sinica,* no. 2, p.134-137.

------, 1986b The Discovery of Fractal-Dimension Structure in Quasicrystal and Its Significance in the Outlook on Nature, *Scientia Geologica Sinica,* no. 4, p.323-329.

Pepper, Echo D., 1928 On Continuous Functions without a Derivative, *Fundamenta Mathematicae,* vol. 12, p.244-253.

Perkal, Julian, 1958a O Dlugosci Krzywych Empirycznych, *Zastosowania Matematyki,* III, 3-4, p.257-286, the English Title Is: "On the Length of Empirical Curves," Translated by R. Jackowski in 1966 under the Direction of Professor Waldo R. Tobler and Included in Michigan Inter-University Community of Mathematical Geographers Discussion Paper No: 10, 34p.

------, 1958b Proba obiektywnej generalizacji, *Geodezjz i Kartografia,* Tom VII, Zeszyt 2, p.130-142, the English Title Is: "An Attempt at Objective Generalization," Translated by R. Jackowski in 1966 under the Direction of Professor Waldo R. Tobler and Included in Michigan Inter-University Community of Mathematical Geographers Discussion Paper No: 10, 17p.

Perrin, Jean Baptiste, 1906 La Discontinuite de la Matiere, *Revue du Mois,* vol. 1, p.323-344.

------, 1909 Mouvement Brownien et Realite Moleculaire, *Annales de Chimie et de Physique,* series VIII, vol. 18, p.5-114.

------, 1923 **Atoms,** Authorized Translation of **Les Atomes** by Dalziel Llewellyn Hammick, 2nd revised English edition, Constable & Company Ltd., London, 231p.

Phillips, Jonathan D., 1986 Spatial Analysis of Shoreline Erosion, Delaware Bay, New Jersey, *Annals of the Association of American Geographers,* vol. 76, no. 1, p.50-62.

------, 1989 Erosion and Planform Irregularity of an Estuarine Shoreline, *Zeitschrift fur Geomorphologie,* Supplement, vol. 73, p.59-71.

Piech, M. Ann, and Piech, Kenneth R., 1990 Fingerprints and Fractal Terrain, *Mathematical Geology,* vol. 22, no. 4, p.457-485.

Pietronero, Luciano, (editor), 1989 **Fractals' Physical Origin and Properties,** Proceedings of the Special Seminar on Fractals Held in Erice, Sicily, Italy, October 9-15, 1988, Plenum Press, New York, 370p.

------, and Tosatti, Erio, (editors), 1986 **Fractals in Physics,** Proceedings of the Sixth International Symposium on Fractals in Physics, ICTP, Trieste, Italy, July 9-12, 1985, North-Holland Physics Publishing, Amsterdam, The Netherlands, 476p.

Pike, Edward Roy, and Lugiato, Luigi A., (editors), 1987 **Chaos, Noise & Fractals,** Adam Hilger, Bristol, Great Britain, 249p.

Pitty, Alistair F., 1971 **Introduction to Geomorphology,** Methuen & Co. Ltd., London, 526p.

Plotnick, Roy E., 1986 A Fractal Model for the Distribution of Stratigraphic Hiatuses, *Journal of Geology,* vol. 94, p.885-890.

Polidori, Laurent, Choriwicz, Jean, and Guillande, Richard, 1991 Description of Terrain as a Fractal Surface, and Application to Digital Elevation Model Quality Assessment, *Photogrammetric Engineering & Remote Sensing,* vol. 57, no. 10, p.1329-1332.

Potter, Kenneth W., 1975 Comment on 'The Hurst Phenomenon: A Puzzle?' by V. Klemes, *Water Resources Research,* vol. 11, no. 2, p.373-374.

------, 1976 **A Stochastic Model of the Hurst Phenomenon: Non-Stationarity in Hydrologic Processes,** Ph. D. Dissertation, The Johns Hopkins University, Baltimore, Maryland, 104p.

Powell, John W., 1895 Physiographic Regions of the United States: *National Geographical Society Monograph, No. 3, American Book Company, New York,* p.65-100.

Power, William L., Tullis, Terry E., 1991 Euclidean and Fractal Models for the Description of Rock Surface Roughness, *Journal of Geophysical Research,* vol. 96, no. B1, p.415-424.

------, ------, Brown, Stephen R., Boitnott, G. N., and Scholz, Christopher H., 1987 Roughness of Natural Fault Surfaces, *Geophysical Research Letters,* vol. 14, no. 1, p.29-32.

Prusinkiewicz, Przemyslaw, and Hanan, James, 1989 **Lindenmayer Systems, Fractals, and Plants,** Lecture Notes in Biomathematics, No. 79, Springer-Verlag, New York, 120p.

Pynn, Roger, and Riste, Tormod, (editors), 1987 **Time-Dependent Effects in Disordered Materials,** Proceedings of a NATO Advanced Study Institute on Time-Dependent Effects in Disordered Materials Held in Geilo, Norway, March 29 - April 9, 1987, NATO ASI Series B: Physics, vol. 167, Plenum Press, New York, 504p.

------, and Skjeltorp, Arne, (editors), 1985 **Scaling Phenomena in Disordered Systems,** Proceedings of a NATO Advanced Study Institute Held April 8-19, 1985, in Geilo, Norway, NATO ASI Series B: Physics, vol. 133, Plenum Press, New York, 580p.

Qiu, Hong-Lie, 1988 Measuring the Louisiana Coastline ---- An Application of Fractals, **The Association of American Geographers Cartography Specialty Group Occasional Paper,** No. 1, p.33-40.

Reams, Max W., 1992 Fractal Dimensions of Sinkholes, *Geomorphology,* vol. 5, nos. 1/2, p.159-165.

Reigber, C., Balmino, G., Muller, H., Bosch, W., and Moynot, B., 1985 GRIM Gravity Model Improvement Using LAGEOS (GRIM 3-L1), *Journal of Geophysical Research,* vol. 90, p.9285-9299.

Richardson, Lewis F., 1961 The Problem of Contiguity: An Appendix to Statistics of Deadly Quarrels, In **General Systems: Yearbook of the Society for General Systems**

Research, vol. VI, p.139-187.

Rieu, Michel, and Sposito, Garrison, 1991a Fractal Fragmentation, Soil Porosity, and Soil Water Properties I: Theory, *Soil Science Society of America Journal,* vol. 55, no. 5, p.1231-1238.

------, and ------, 1991b Fractal Fragmentation, Soil Porosity, and Soil Water Properties II: Applications, *Soil Science Society of America Journal,* vol. 55, no. 5, p.1239-1244.

Rigaut, Jean-Paul, 1984 An Empirical Formulation Relating Boundary Lengths to Resolution in Specimens Showing 'Non-Ideally Fractal' Dimensions, *Journal of Microscopy,* vol. 133, part 1, p.41-54.

------, 1991 Fractals, Semi-Fractals and Biometry, In Guy Cherbit, (editor), **Fractals: Non-Integral Dimensions and Applications,** John Wiley & Sons, Chichester, West Sussex, Great Britain, p.151-187.

------, Berggren, P., and Robertson, B., 1983a Automated Techniques for the Study of Lung Alveolar Stereological Parameters with the IBAS Image Analyser on Optical Microscopy Sections, *Journal of Microscopy,* vol. 130, part 1, p.53-61.

------, ------, and ------, 1983b Resolution-Dependence of Stereological Estimations: Interpretation, with a New Fractal Concept, of Automated Image Analyser-Obtained Results on Lung Sections, In **Proceedings of the 6th International Congress on Stereology,** Gainesville, Acta Stereologica, vol. 2, supplement 1, p.121-124.

Robert, Andre, 1988 Statistical Properties of Sediment Bed Profiles in Alluvial Channels, *Mathematical Geology,* vol. 20, no. 3, p.205-225.

------, and Roy, Andre G., 1990 On the Fractal Interpretation of the Mainstream Length-Drainage Area Relationship, *Water Resources Research,* vol. 26, no. 5, p.839-842.

Roy, Andre G., and Robert, Andre, 1990 Fractal Techniques and the Surface Roughness of Talus Slopes: A Comment, *Earth Surface Processes and Landforms,* vol. 15, p.283-285.

------, Gravel, Ginette, and Gauthier, Celine, 1987 Measuring the Dimension of Surfaces: A Review and Appraisal of Different Methods, **Auto-Carto 8 Proceedings,** Baltimore, Maryland, March 29 - April 3, 1987, p.68-77.

Ruffet, C., Gueguen, Y., and Darot, M., 1991 Complex Conductivity Measurements and Fractal Nature of Porosity, *Geophysics,* vol. 56, no. 6, p.758-768.

Sammis, Charles G., Osborne, Robert H., Anderson, J. Lawford, Banerdt, Mavonwe, and White, Patricia, 1986 Self-Similar Cataclasis in the Formation of Fault Gauge, *Pure and Applied Geophysics,* vol. 123, p.53-78.

Saupe, Dietmar, 1988 Algorithms for Random Fractals, In Heinz-Otto Peitgen and Dietmar Saupe, (editors), **The Science of Fractal Images,** Springer-Verlag, New York, p.71-136.

------, 1991 Random Fractals in Image Synthesis, In Anthony J. Crilly, Rae A. Earnshaw and Huw Jones, (editors), **Fractals and Chaos,** Springer-Verlag, New York,

p.89-118.

Sayles, R. S., and Thomas, T. R., 1978a Surface Topography as a Nonstationary Random Process, *Nature,* vol. 271, no. 5644, p.431-434.

------, and ------, 1978b Reply, *Nature,* vol. 273, no. 5663, p.573.

Schaefer, Dale W., Laibowitz, Robert B., Mandelbrot, Benoit B., and Liu, Sam H., (editors), 1986 **Fractal Aspects of Materials: Extended Abstract of the 1986 Fall Meeting of the Materials Research Society,** Boston, Massachusetts, December 2-4, 1986, Materials Research Society, Pittsburgh, Pennsylvania, 148p.

Scheidegger, Adrian E., 1970 **Theoretical Geomorphology,** 2nd edition, Springer-Verlag, Berlin, 435p.; 1991, 3rd edition, 434p.

------, 1983 Instability Principle in Geomorphic Equilibrium, *Zeitschrift fur Geomorphologie,* vol. 27, p.1-19.

Schertzer, Daniel, and Lovejoy, Shaun, (editors), 1991 **Non-Linear Variability in Geophysics: Scaling and Fractals,** Kluwer Academic Publishers, Dordrecht, The Netherlands, 318p.

Scholz, Christopher H., and Mandelbrot, Benoit B., 1989 **Fractals in Geophysics,** Birkhauser Verlag, Basel, 313p.

Schramm, David, and Luo, Xiaochun, 1992 Universal Pancakes, *University of Chicago Magazine,* (the August issue), p.9.

Schroeder, Manfred R., 1991 **Fractals, Chaos, Power Laws: Minutes from an Infinite Paradise,** W. H. Freeman and Company, New York, 429p.

Scott, R. M., and Austin, M. P., 1971 Numerical Classification of Land Systems Using Geomorphological Attributes, *Australian Geographical Studies,* vol. 9, no. 1, p.33-40.

Seginer, Ido, 1969 Random Walk and Random Roughness Models of Drainage Networks, *Water Resources Research,* vol. 5, no. 5, p.591-607.

Sen, P. N., Scala, C., and Cohen, M. H., 1981 A Self-Similar Model for Sedimentary Rocks with Application to the Dielectric Constant of Fused Glass Beads, *Geophysics,* vol. 46, no. 5, p.781-795.

Shapiro, S. A., and Faizullin, I. S., 1992 Fractal Properties of Fault Systems by Scattering of Body Seismic Waves, *Tectonophysics,* vol. 202, p.177-181.

Shelberg, Mark C., and Moellering, Harold, and Lam, Nina, 1982 Measuring the Fractal Dimensions of Empirical Cartographic Curves, in **Proceedings of the Fifth International Symposium on Computer-Assisted Cartography,** (Auto-Carto 5), Crystal City, Virginia, August 22-28, 1982, p.481-490.

------, Lam, Nina, and Moellering, Harold, 1983 Measuring the Fractal Dimensions of Surfaces, **Proceedings of the Sixth International Symposium on Computer-Assisted Cartography,** (Auto-Carto 6), Ottawa, Canada, October 16-21, 1983, p.319-328.

Shimer, John A., 1972 **Field Guide to Landforms in the United States,** Macmillan

Publishing Co., Inc., New York, 272p.

Shlesinger, Michael F., Mandelbrot, Benoit B., and Rubin, Robert J., (editors), 1984 **Proceedings of a Symposium on Fractals in the Physical Sciences,** Held at the U. S. Bureau of Standards, Gaithersburg, Maryland, November 21-23, 1983, *Journal of Statistical Physics,* vol. 36, nos. 5/6, p.519-921.

Sierpinski, Waclaw, 1915 Sur une courbe dont tout point est un point de ramification, *Comptes Rendus* (Paris), vol. 160, p.302.

------, 1916 Sur une courbe cantorienne qui contient une image biunivoque et continue de toute courbe donnee, *Comptes Rendus* (Paris), vol. 162, p.629.

Skoda, G., 1987 Fractal Dimension of Rainbands over Hilly Terrain, *Meteorology and Atmospheric Physics,* vol. 36, nos. 1-4, p.74-82.

Smalley, Robert F., Jr., Chatelain, J. L., Turcotte, Donald L., and Prevot, R., 1987 A Fractal Approach to the Clustering of Earthquakes: Applications to the Seismicity of the New Hebridges, *Bulletin of the Seismological Society of America,* vol. 77, no. 4, p.1368-1381.

Smith, Alvy Ray, 1984 Plants, Fractals, and Formal Languages, *Computer Graphics,* vol. 18, no. 3, p.1-10.

Snow, R. Scott, 1989 Fractal Sinuosity of Stream Channels, *Pure and Applied Geophysics,* vol. 131, nos. 1/2, p.99-109.

------, 1992 The Cantor Dust Model for Discontinuity in Geomorphic Process, *Geomorphology,* vol. 5, nos. 1/2, p.185-194.

------, and Mayer, Larry, (editors), 1992 **Fractals in Geomorphology,** *Geomorphology,* (Special Issue), vol. 5, nos. 1/2, 194p.

Sorensen, Peter R., 1984 Fractals: Exploring the Rough Edges between Dimensions, *Byte,* vol. 9, no. 10, p.157-172.

Sornette, A., Dubois, J., and Cheminee, D., 1991 Are Sequences of Volcanic Eruptions Deterministically Chaotic? *Journal of Geophysical Research,* vol. 96, no. B7, p.11931-11945.

Sparks, B. W., 1971 **Rocks and Relief,** St. Martin's Press, New York, 404p.

Sprunt, B., 1972 Digital Simulation of Drainage Basin Development, In Richard J. Chorley, (editor), **Spatial Analysis in Geomorphology,** Methuen & Co. Ltd., London, p.371-389.

Stanley, Harry Eugene, and Ostrowsky, Nicole, (editors), 1986 **On Growth and Form: Fractal and Non-Fractal Patterns in Physics,** Proceedings of a Course Offered as Part of the NATO Advanced Study Institute Series, at the Cargese Summer School in Cargese, Corsica, France, June 27 - July 6, 1985, NATO ASI Series E: Applied Sciences, No. 100, Martinus Nijhoff Publishers, Dordrecht, The Netherlands, 308p.

------, and ------, (editors), 1989 **Random Fluctuations and Pattern Growth: Experiments and Models,** Proceedings of the NATO Advanced Study Institute on Random

Fluctuations and Pattern Growth: Experiments and Models, Held in Cargese, Corsica, France, July 18-31, 1988, NATO ASI Series E: Applied Sciences, No. 157, Kluwer Academic Publishers, Dordrecht, The Netherlands, 355p.

Stauffer, Dietrich, and Stanley, Harry E., 1990 **From Newton to Mandelbrot: A Primer in Theoretical Physics,** Springer-Verlag, Berlin, 191p.

Steinhaus, Hugo, 1954 Length, Shape and Area, *Colloquium Mathematicum,* vol. III, p.1-13.

Stewart, Ian, 1989 **Does God Play Dice? The Mathematics of Chaos,** Basil Blackwell, Oxford, United Kingdom, 317p.

------, and Golubitsky, Martin, 1992 **Fearful Symmetry: Is God a Geometer?** Basil Blackwell, Oxford, United Kingdom, 287p.

Stoddart, David Ross, 1969 Climatic Geomorphology: Review and Re-Assessment, *Progress in Geography,* vol. 1, p.159-222.

Sweeting, Marjorie Mary, 1972 **Karst Landforms,** Macmillan, London, 362p.

Taggart, I. J., and Salisch, H. A., 1991 Fractal Geometry, Reservoir Characterisation and Oil Recovery, *The APEA Journal,* vol. 31, p.377-385.

Takayasu, Hideki, 1990 **Fractals in the Physical Sciences,** Manchester University Press, Manchester, United Kingdom, 170p.

Tanner, William F., 1961 An Alternate Approach to Morphogenetic Climates, *Southeastern Geologist,* vol. 2, p.251-257.

Tarboton, David G., Bras, Rafael L., and Rodriguez-Iturbe, Ignacio, 1988 The Fractal Nature of River Networks, *Water Resources Research,* vol. 24, no. 8, p.1317-1322.

------, ------, and ------, 1990 Comment on "On the Fractal Dimension of Stream Networks" by Paolo La Barbera and Renzo Rosso, *Water Resources Research,* vol. 26, no. 9, p.2243-2244.

Thompson, A. H., 1991 Fractals in Rock Physics, *Annual Review in Earth and Planetary Sciences,* vol. 19, p.237-262.

------, Katz, A. J., and Krohn, C. E., 1987 The Microgeometry and Transport Properties of Sedimentary Rock, *Advances in Physics,* vol. 36, p.625-694.

Thornbury, William D., 1965 **Regional Geomorphology of the United States,** John Wiley & Sons, Inc., New York, 609p.

Tricart, Jean, 1974 **Structural Geomorphology,** Longman, Inc., New York, 305p.

------, and Cailleux, Andre, 1972 **Introduction to Climatic Geomorphology,** Longman, London, 295p.

Troll, C., 1958 Climatic Seasons and Climatic Classification, *Oriental Geographer,* vol. 2, p.141-165.

Trudgill, Stephen Thomas, 1985 **Limestone Geomorphology,** Longman, London,

196p.

Turcotte, Donald L., 1986a A Fractal Model for Crustal Deformation, *Tectonophysics,* vol. 132, p.261-269.

------, 1986b Fractals and Fragmentation, *Journal of Geophysical Research,* vol. 91, no. B2, p.1921-1926.

------, 1986c A Fractal Approach to the Relationship between Ore Grade and Tonnage, *Economic Geology,* vol. 81, p.1528-1532.

------, 1987 A Fractal Interpretation of Topography and Geoid Spectra on the Earth, Moon, Venus, and Mars, In **Proceedings of the Seventeenth Lunar and Planetary Science,** part 2, *Journal of Geophysical Research,* vol. 92, no. B4, p.E597-E601.

------, 1989 Fractals in Geology and Geophysics, *Pure and Applied Geophysics,* vol. 131, nos. 1/2, p.171-196.

------, 1992 **Fractals and Chaos in Geology and Geophysics,** Cambridge University Press, Cambridge, Great Britain, 221p.

Turner, Daniel S., 1969 **Applied Earth Science,** Wm. C. Brown Company Publishers, Dubuque, Iowa, 125p.

Twidale, Charles Rowland, 1971 **Structural Landforms: Landforms Associated with Granitic Rocks, Faults, and Folded Strata,** The MIT Press, Cambridge, Massachusetts, 247p.

------, 1982 **Granite Landforms,** Elsevier Scientific Publishing Company, Amsterdam, The Netherlands, 372p.

Tyler, Scott W., and Wheatcraft, Stephen W., 1990a Fractal Processes in Soil Water Retention, *Water Resources Research,* vol. 26, no. 5, p.1047-1054.

------, and ------, 1990b The Consequences of Fractal Scaling in Heterogeneous Soils and Porous Media, In Daniel Hillel and David E. Elrick, (editors), **Scaling in Soil Physics: Principles and Applications,** Soil Science Society of America Special Publication No. 25, Soil Science Society of America, Inc., Madison, Wisconsin, p.109-122.

Unwin, David, (editor), 1989 **Fractals and the Geosciences,** *Computers & Geosciences,* (Special Issue), vol. 15, no. 2, p.163-235.

Upton, William B., Jr., 1955 **A Set of One Hundred Topographic Maps Illustrating Specified Physiographic Features,** U. S. Geological Survey.

Velde, B., Dubois, J., Touchard, G., and Badri, A., 1990 Fractal Analysis of Fractures in Rocks: The Cantor's Dust Method, *Tectonophysics,* vol. 179, p.345-352.

Viczek, Tamas, 1989 **Fractal Growth Phenomena,** World Scientific, Singapore, 355p.

Vignes-Adler, Michele, Le Page, Alain, and Adler, Pierre M., 1991 Fractal Analysis of Fracturing in Two African Regions, From Satellite Imagery to Ground Scale, *Tectonophysics,* vol. 196, p.69-86.

Von Koch, Helge, 1904 Sur une courbe continue sans tangente, obtenue par une

construction geometrique elementaire, *Arkiv for Matematik, Astronomi och Fysik,* vol. 1, p.681-704.

Voss, Richard F., 1975 '1/f Noise' in Music and Speech, *Nature,* vol. 258, p.317-318.

------, 1985a Random Fractal Forgeries: From Mountains to Music, In Sara Nash, (editor), **Science and Uncertainty,** Proceedings of a Conference Held under the Auspices of IBM United Kingdom Ltd., London, March 1984, Science Reviews Ltd., Northwood, Great Britain, p.68-85.

------, 1985b Random Fractal Forgeries, In Rae A. Earnshaw, (editor), **Fundamental Algorithms for Computer Graphics,** NATO ASI Series F: Computer and Systems Sciences, vol. 17, Springer-Verlag, Berlin, p.805-835.

------, 1986 Characterization and Measurement of Random Fractals, *Physica Scripta,* vol. T13, p.27-32, also Published in Roger Pynn and Arne Skjeltorp, (editors), 1985 **Scaling Phenomena in Disordered Systems,** NATO ASI Series B: Physics, vol. 133, Proceedings of a NATO Advanced Study Institute Held in Geilo, Norway, April 8-19, 1985, under the Title "Random Fractals: Characterization and Measurement," Plenum Press, New York, p.1-11.

------, 1988 Fractals in Nature: From Characterization to Simulation, in Hein-Otto Peitgen and Dietmar Saupe, (editors), **The Science of Fractal Images,** Springer-Verlag, New York, p.21-70.

------, and Clarke, John, 1978 "1/f Noise" in Music: Music from 1/f Noise, *Journal of the Acoustic Society of America,* vol. 63, no. 1, p.258-263.

Walsh, Joseph L., 1949 Another Contribution to the Rapidly Growing Literature of Mathematics and Human Behavior, *Scientific American,* vol. 181, no. 2, p.56-58.

Waschka, R., II, 1990 **Let Me Make It Simple for You,** Doctor of Musical Arts Dissertation, University of North Texas, Denton, Texas, 101p.

Weibel, Ewald R., 1979 **Stereological Methods,** Volume One: **Practical Methods for Biological Morphometry,** Academic Press, Inc., London, Great Britain.

Weitz, David A., Sander, Leonard M., and Mandelbrot, Benoit B., (editors), 1988 **Fractal Aspects of Materials: Disordered Systems, Extended Abstract of the 1988 Fall Meeting of the Materials Research Society,** Boston, Massachusetts, November 29 - December 2, 1988, Materials Research Society, Pittsburgh, Pennsylvania, 356p.

West, Bruce J., 1990 **Fractal Physiology & Chaos in Medicine,** World Scientific Publishing Co., Singapore, 380p.

Wicks, Keith R., 1991 **Fractals and Hyperspaces,** Lecture Notes in Mathematics, vol. 1492, Springer-Verlag, Berlin, Germany, 168p.

Wiener, Norbert, 1923 Differential Space, *Journal of Mathematics and Physics,* vol. 2, no. 3, p.131-174.

------, 1924 Un Probleme de Probabilites Denombrables, *Bulletin de la Societe Mathematique de France,* vol. 52, p.569-578.

------, 1956 **I Am a Mathematician: The Later Life of Prodigy,** The MIT Press, Cambridge, Massachusetts, 309p.

Williams, John K., and Dawe, Richard A., 1986 Fractals ---- An Overview of Potential Applications to Transport in Porous Media, *Transport in Porous Media,* vol. 1, p.201-209.

Wilson, L., 1969 Relationship between Geomorphic Processes and Modern Climates as a Method in Paleoclimatology, *Revue de Geographie physique et de Geologie dynamique,* vol. 11, p.303-314.

Wong, Po-Zen, 1987 Fractal Surfaces in Porous Media, In Jayanth R. Banavar, Joel Koplik and Kenneth W. Winkler, (editors), **Physics and Chemistry of Porous Media II,** American Institute of Physics Conference Proceedings, No. 154, American Institute of Physics, New York, p.304-318.

------, Howard, James, and Lin, Jar-Shyong, 1986 Surface Roughening and the Fractal Nature of Rocks, *Physical Review Letters,* vol. 57, no. 5, p.637-640.

Wood, W. F., and Snell, J. B., 1960 A Quantitative System for Classifying Landforms, Quartermaster Research and Engineering Command, U. S. Army (Natick, Massachusetts), Technical Report EP-124, 20p.

Woronow, Alexander, 1981 Morphometric Consistency with the Hausdorff-Besicovitch Dimension, *Mathematical Geology,* vol. 13, no. 3, p.201-216.

Wu, Ru-Shan, and Aki, Keiiti, 1985 The Fractal Nature of the Inhomogeneities in the Lithosphere Evidenced from Seismic Wave Scattering, *Pure and Applied Geophysics,* vol. 123, p.805-818.

Yatsu, Eiju, 1966 **Rock Control in Geomorphology,** Sozosha, Tokyo, 135p.

Yfantis, E. A., Flatman, G. T., and Englund, E. J., 1988 Simulation of Geological Surfaces Using Fractals, *Mathematical Geology,* vol. 20, no. 6, p.667-672.

Yokoya, Naokazu, and Yamamoto, Kazuhiko, 1989 Fractal-Based Analysis and Interpolation of 3D Natural Surface Shapes and Their Application to Terrain Modelling, *Computer Vision, Graphics, and Image Processing,* vol. 46, no. 3, p.284-302.

Young, I. M., and Crawford, J. W., 1991 The Fractal Structure of Soil Aggregates: Its Measurement and Interpretation, *Journal of Soil Science,* vol. 42, no. 2, p.187-192.

Zevenbergen, Lyle W., and Thorne, Colin R., 1987 Quantitative Analysis of Land Surface Topography, *Earth Surface Processes and Landforms,* vol. 12, p.47-56.

Zhao, Zhong-Yan, Wang, Yi, and Liu, Xiao-Han, 1990 Fractal Analysis Applied to Cataclastic Rocks, *Tectonophysics,* vol. 178, p.373-377.

Zipf, George Kingsley, 1949 **Human Behavior and the Principle of Least-Effort: An Introduction to Human Ecology,** Addison-Wesley Press, Inc., Boston, Massachusetts, 573p.